The gravitational field produced by extreme-mass-ratio orbits on Schwarzschild spacetime

by
Seth Hopper

A dissertation submitted to the faculty of the University of North Carolina at Chapel Hill in partial fulfillment of the requirements for the degree of Doctor of Philosophy in the Department of Physics and Astronomy.

Chapel Hill
2011

Approved by:

Charles R. Evans, Advisor

J. Christopher Clemens, Reader

Y. Jack Ng, Reader

Paul Anderson, Committee Member

Reyco Henning, Committee Member

Abstract

SETH HOPPER: The gravitational field produced by extreme-mass-ratio orbits on Schwarzschild spacetime.
(Under the direction of Charles R. Evans.)

A stellar-mass compact object orbiting a supermassive black hole will radiate energy and angular momentum in the form of gravitational waves, causing it to spiral inward. Such an *extreme-mass-ratio inspiral* (EMRI) is an important potential source for a direct gravity wave detection. It will require sufficiently accurate source modeling for such detections to be made and analyzed. In this thesis I present original research that has furthered the collective goal of accurate numerical EMRI simulations.

I begin by giving an overview of the extensive work that has been done in this field, with an eye toward significant headway that has been made in the last decade. I then lay the groundwork for my own work by reviewing the mathematical foundations for gravity waves and black hole perturbation theory. Before attacking the subject of gravity waves on a curved background, I examine the model problem of the scalar field that is induced by an orbiting charge. This problem, while idealized, introduces many of the mathematical and numerical techniques which are necessary to solve the perturbed Einstein equations. At this point, with the foundation laid, I present new work on eccentric orbits of point masses about a Schwarzschild black hole. I show how the method of extended homogeneous solutions is generalized to find the radiative part of the first-order metric perturbation in Regge-Wheeler (RW) gauge using frequency domain techniques. Additionally, for the first time we computed the local point-singular nature of the metric perturbation in RW gauge. Due mostly to such gauge artifacts, RW gauge is not ideal of performing a local self-force calculation. Thus, I then present work on transforming the metric perturbation to Lorenz gauge. This will allow for the direct calculation of the self-force. I end this thesis by summarizing the potential and necessary areas of EMRI research in the near future.

Acknowledgments

My family has been exceptionally generous as I have worked toward my degree. In particular, I'm grateful for all the kindness shown to me by my sister Marie and my brother-in-law Joseph, who allowed me to partake of their hospitality on countless occasions.

And most of all, I'd like to thank my advisor Charles Evans for his boundless patience and unwavering support. This would not have been possible without him.

Table of Contents

List of Figures

List of Tables

List of Abbreviations and Symbols

$\alpha, \beta, \gamma, \ldots$	Spacetime coordinates indices running from 0 to 3
$i, j, k, \ldots$	Spatial coordinates indices running from 1 to 3
$a, b, c, \ldots$	Schwarzschild coordinates indices on the $\mathcal{M}^2$ submanifold, $\{t, r\}$
$A, B, C, \ldots$	Standard two-sphere coordinate indices on the $\mathcal{S}^2$ submanifold, $\{\theta, \phi\}$
$\mathsf{g}, \mathsf{\Gamma}, \mathsf{R}, \ldots$	Sans-serif symbols indicate perturbed versions of their serifed counterparts
μ	Mass of the orbiting particle
M	Mass of the central supermassive black hole
$\eta_{\mu\nu}$	Minkowski metric
$g_{\mu\nu}$	Background metric
g_{ab}	Schwarzschild metric on submanifold $\mathcal{M}^2$
Ω_{AB}	Metric on the unit two-sphere
g_{AB}	Metric on submanifold $\mathcal{S}^2$, $g_{AB} = r^2\Omega_{AB}$
$G_{\mu\nu}$	Einstein tensor
$R_{\alpha\mu\beta\nu}$	Riemann tensor
$R_{\mu\nu}$	Ricci tensor
R	Ricci scalar
$\Gamma^{\alpha}{}_{\beta\gamma}$	Connection coefficients
∂_μ or $_{,\mu}$	Partial derivative
${}^4\nabla_\mu$, ∇_μ, or $_{\|\mu}$	Four-dimensional covariant derivative of the background manifold
∇_a	Two-dimensional covariant derivative on submanifold $\mathcal{M}^2$
D_A	Two-dimensional covariant derivative on submanifold $\mathcal{S}^2$
$\doteq$	Tensor components in a specific set of coordinates
$\overset{*}{=}$	Equality holds in a locally Lorentz frame
GW	Gravity wave
EMRI	Extreme-mass-ratio inspiral
SMBH	Supermassive black hole
FD	Frequency domain
TD	Time domain
RW	Regge-Wheeler
EHS	Extended homogeneous solutions
EPS	Extended particular solutions
MiSaTaQuWa	Mino, Sasaki, Tanaka, Quinn and Wald
BOS	Barack, Ori, and Sago
SNS	Sago, Nakano, and Sasaki

Chapter 1

Introduction

1.1 The two-body problem in general relativity

The two-body problem stands as one of the classic unsolved problems of general relativity. The challenge is to take two gravitationally interacting objects with arbitrary initial positions and velocities (and potentially spins) and solve for their positions and the gravitational field at all future times. Given the complexity of the nonlinear, coupled Einstein equations, it is impossible to solve such a problem, in general, through analytical approaches. Researchers have therefore turned to numerical methods to provide solutions. Early work involved post-Newtonian theory—work that goes back to Einstein at the dawn of general relativity and Einstein, Infeld, and Hoffmann [4]. The first numerical relativity simulation of a two-body system was made by Hahn and Lindquist, who attempted to collide two non-rotating black holes head on [5] in 1964. Their code only ran for a brief time, and was not able to model the merger of the two holes. Still, it was the first step in what has become an active and mature field. In recent years, interest in such simulations has increased dramatically with the prospect of detecting gravitational waves.

1.1.1 Observational interest

Even beyond the inherent theoretical motivation for solving the two-body problem, there exists a strong observational need to study this system. The detection of gravitational radiation appears close at hand. Though other types of detectors (most notably resonant

bars) have been designed and built, interferometers have reached the most promising levels of sensitivity. Gravity waves (GWs) produce slight time-dependent changes in the distances between objects. Interferometers can detect these changes by measuring the time it takes for photons to travel down to a mirror and back. Due to the extremely weak nature of GWs, these detectors must be unprecedentedly sensitive. Detected GWs are anticipated to cause fractional distance shifts of no more than one part in 10^{21} [6].

Detections will most likely be made by the Laser Interferometer Gravity-Wave Observatory LIGO [7]. LIGO is currently offline, as it is being upgraded with new components. When the upgrade is complete it will enter its third stage, dubbed Advanced LIGO. Researchers are hoping the first gravity waves will be detected shortly after Advanced LIGO goes online in 2014. If detected at LIGO's two sites, and at the VIRGO [8] and GEO600 [9] detectors, a source of GW will be identified, localized and analyzed. These detections will not happen, however, without sufficiently accurate theoretical models of GW sources.

Even the strongest astrophysical sources will produce GW signals that are buried deeply in the noise of a detector's data stream. Therefore, accurate theoretical models of a large number of waveforms will be necessary in order to correlate with detector output. Processes such as matched filtering can be used to extract a signal that has been masked by the various noise sources in a detector (e.g., seismic, thermal, and shot noise) [10].

In addition to their use in GW detection, accurate waveforms are also needed for source parameter estimation. Black hole binaries produce complicated wave forms with as many as fifteen parameters. For the case where the black holes have comparable mass, the field of numerical relativity (NR) has been quite successful at modeling late-time waveforms. As the mass-ratio becomes smaller NR calculations become progressively more challenging. At this point, mass-ratios of 1:100 appear to be the outside limit of what is possible [11], and even then the accuracy leaves much to be desired.

1.1.2 Extreme-mass-ratio inspirals

The GWs that LIGO detects will likely come from the merger of comparable mass compact objects (black holes or neutron stars). This is because LIGO has a frequency band of ~ 10

Hz -1 kHz, a range ideal for detection of binaries with comparable mass ($\sim 1 - 10 M_\odot$) companions. Another likely astrophysical source of GWs are *extreme-mass-ratio inspirals* (EMRIs) where solar-mass objects ($\sim 1 - 10 M_\odot$) orbit supermassive black holes (SMBHs, $\sim 10^5 - 10^7 M_\odot$). These sources are thought to exist in the centers of all major galaxies. For instance, the SMBH at the center of the Milky Way, Sagittarius A*, has a mass of $\sim 4.3 \times 10^6\ M_\odot$. M31 (the Andromeda Galaxy) has a SMBH of $\sim 10^8\ M_\odot$ at its center. Small ($\mu \lesssim 100\ M_\odot$) compact objects orbiting such SMBH will radiate GWs at lower frequencies outside the LIGO passband.

In order to detect them, the European Space Agency (ESA) is planning a space based interferometer detector. Until recently, this was to be a joint NASA-ESA mission named the Laser Interferometer Space Antenna (LISA) [12]. NASA funding issues led to their backing out [13]. At this point, ESA is reworking the mission to fit within a tighter budget. It is not yet clear how the revised mission will change in specifications (or even name) from the original joint plan. For the purposes of this discussion I will continue to call the mission LISA and use the old specifications.

LISA will have a passband of $\sim 10^{-4} - 10^{-2}$ Hz, several orders of magnitude below LIGO. An EMRI is expected to stay in LISA's passband for up to one million orbits as it spirals toward the SMBH and eventually plunges. The final stages of the inspiral will be marked by an increase in frequency and amplitude until the small body plunges toward the event horizon and a last burst of radiation is released. This increase in frequency and in amplitude of the signal is called a chirp. The SMBH will then ring down exponentially as it settles back to its usual stationary state.

As with ground based detectors, LISA's detections will have to be pulled out of the noise of its data stream. Therefore, tables of simulated waveforms will be needed for matched filtering and parameter estimation. Given the types of different orbits that can exist and the number of parameters, this is a formidable task. Astrophysical SMBHs are thought to be Kerr black holes, probably spinning at near maximal rates. In general, bound orbits in the Kerr spacetime will be eccentric and out of the plane of the black hole's rotation. The orbital plane, as well as the line of apses will precess. Additionally unknown will be the

distance to the source and its orientation relative to the detector. Finally, the small body itself may be spinning, which can give rise to spin-orbit effects.

The previously mentioned method of general relativity simulations, numerical relativity (NR), is not suited to the challenge of the EMRI problem. First there is a prohibitive computational cost of such an approach. NR codes run on thousands of nodes, often for months in order to compute 10's of orbits. They work well for comparable mass systems because of the similar length scales involved in the problem. The EMRI problem has two distinct length scales: the background curvature associated with the SMBH, and the radius of the small body. The ratio of these two scales will be on the order of the mass-ratio, which can be as small as 10^{-7}. Even if one could resolve the different length scales, NR codes could not run with accuracy for the $\sim 10^6$ orbits (as encountered with EMRIs) before plunge. It is for these reasons that researchers have turned to perturbative approaches.

1.2 Black hole perturbation theory

In black hole perturbation theory one takes a known solution to the Einstein equations (typically that of a Schwarzschild or Kerr black hole) as a lowest order solution to the gravitational field. Then, at lowest order in the equations of motion the small body, or particle, moves on a geodesic of the background spacetime. This particle pulls up a first-order perturbation to the gravitational field. Far away in the wave zone, it is evident that this perturbation carries energy and angular momentum away from the system in the form of gravitational waves. The energy loss comes at the expense of the particle's orbit. Locally, the inspiral that results can be viewed as the result of a "self-force." In order to compute the self-force at the location of the particle, one must remove the singular part of the particle's field that does not contribute to radiation reaction. This procedure is called "regularization." One then seeks to find the way the orbit changes by solving the first-order corrected equations of motion. This updated trajectory sources changes in the second-order field, which in turn sources second-order corrections to the particle's trajectory, and so on. In theory, following this process through an infinite number of orders produces the true

motion of the particle and gives the complete gravitational field. I go into the details of first-order perturbation theory in detail in Chapter 2.

History

Black hole perturbation theory has a history going back to Regge and Wheeler [14] in 1957. They considered first-order perturbations to the Schwarzschild metric. In so doing, they divided the metric perturbation into its even and odd-parity components and derived their eponymous equation for the odd-parity perturbations. Their work was extended to include a radial wave equation for the even-parity perturbations by Zerilli [15] in 1970. Moncrief [16] re-derived both the Regge-Wheeler and Zerilli equations from a variational principle without choosing a specific gauge. He also introduced gauge-invariant functions of the metric perturbation amplitudes. Working with Cunningham and Price [17, 18], he also introduced a more useful variable than Regge and Wheeler's original odd-parity master function. Theirs is essentially the time integral of the Regge-Wheeler function and allows for easier reconstruction of the odd-parity metric perturbation.

Important work was also done in 1975 in the field of quasi-normal modes by Chandrasekhar and Detweiler [19]. These modes describe how black holes ring down when they are perturbed without a source. The least rapidly decaying such modes are of particular interest for the time just after a particle plunges into a black hole.

Work on perturbations of the Kerr background was pioneered by Teukolsky [20] when he presented the equation which now shares his name. The Teukolsky equation describes the dynamics of the Weyl scalars (e.g., ψ_4, ψ_0), which are tetrad projections of the Weyl curvature tensor. There is a long history of results of computing solutions to the Teukolsky equation for a small mass in order about a Kerr black hole. More difficult is determining the metric from the computed curvature perturbations (see Chrzanowski [21], Cohen and Kegeles [22, 23] (CCK), Stewart [24] and Wald [25]). The so-called CCK formalism is powerful, yet only works for homogeneous solutions to the Teukolsky equation. Recent work by Keidl, Wiseman, and Friedman [26] and others [27, 28] appears to have broken through this barrier. They use the Detweiler-Whiting scheme (discussed below) to remove

the singular contribution to the Weyl scalars and then apply the CCK formalism to the homogeneous solution which remains.

1.3 Flat space self-force

Before diving into self-force calculations in general relativity we start by discussing some simpler systems, which nonetheless contain many features in common with gravitational self-force. I draw from many sources here, most notably Detweiler [29].

1.3.1 Newtonian self-force

Consider a simple two-body system described by Newtonian gravity. Let the first body have a mass M and second body (or particle) of mass μ, which we initially take to be vanishingly small. At this lowest-order approximation the particle will travel in an ellipse with the center of the large body at one focus, obeying Kepler's laws. Let us consider the special case of circular motion at radius r, where Kepler's third law says the angular frequency of the motion is

$$\Omega^2 = \frac{M}{r^3}. \tag{1.3.1}$$

If we allow the particle to have a mass, then Kepler's third law is [30]

$$\Omega^2 = \frac{M}{r^3 \left(1 + \mu/M\right)^2}. \tag{1.3.2}$$

When $\mu \to 0$, the small body travels in a circle of radius r, but when we allow it to have a mass, the two bodies orbit the common barycenter with a separation $r(1 + \mu/M)$. Now, expanding in the small mass-ratio parameter μ/M, we find

$$\Omega^2 = \frac{M}{r^3}\left[1 - 2\frac{\mu}{M} + \mathcal{O}\left(\frac{\mu^2}{M^2}\right)\right]. \tag{1.3.3}$$

The first term is just the $\mu \to 0$ limit. The second term is a first-order correction, a Newtonian example of a self-force. Note, of course that this is a non-radiative correction. It is a conservative shift in the fundamental frequency in the system.

1.3.2 Radiation reaction in electromagnetism

Consider an accelerating, non-relativistic charge in flat space. It will radiate energy via electromagnetic waves with a power calculable from Larmour's formula (in Gaussian units) [31]

$$P = \frac{2e^2}{3c^3}a^2. \tag{1.3.4}$$

This can be used to derive the Abraham-Lorentz force

$$\mathbf{F} = \frac{2e^2}{3c^3}\dot{\mathbf{a}}, \tag{1.3.5}$$

from which one can compute the acceleration due to radiated energy loss. With careful allowance for spurious solutions, this formula is useful for computing a particle's change in motion due to its own radiation reaction. However, it falls short in providing an explanation for why the particle radiates. Indeed, it is at odds with the Lorentz force law which states that acceleration is caused by an external electromagnetic field.

Consider, for concreteness, a non-relativistic electron in circular motion about a much more massive positive charge, which we take to be immovable. To an observer far away in the wave zone, the electron will clearly pull up a $1/r$ radiation field which has a Poynting flux that describes the energy lost by the system. On the other hand, an observer much closer to the electron will measure the local electromagnetic field to be changing, but will not be able to identify within it any hallmarks of radiation. Therefore, this second observer will see the electron spiraling into the center, as predicted by Eq. (1.3.5), but will not be able to describe this phenomenon as radiation reaction. Nor will he be able to explain the inspiral as a result of some external field that sources the Lorentz force law.

Upon generalizing the Abraham-Lorentz force, Dirac [32] rectified this problem of observer dependent descriptions of this system. Dirac generalized the system to include relativistic charges. He used a conservation of energy-momentum argument to show that the local, symmetric Coulomb field $F_S^{\mu\nu} = \frac{1}{2}\left(F_{\text{ret}}^{\mu\nu} + F_{\text{adv}}^{\mu\nu}\right)$ exerts no force on the charge. Here S stands for singular or symmetric. The singular field $F_S^{\mu\nu}$ satisfies the inhomogeneous

Maxwell equations: $F_S^{\mu\nu}{}_{,\nu} = 4\pi j^\mu$. However, because of the relation between the retarded and advanced Green functions $G_{\rm ret}(x,x') = G_{\rm adv}(x',x)$, the field $F_S^{\mu\nu}$ is invariant under time-reversal. Therefore, it cannot be responsible for the radiation reaction. The remainder, which *is* responsible for the radiation reaction is

$$F_R^{\mu\nu} = F_{\rm ret}^{\mu\nu} - F_S^{\mu\nu} = \frac{1}{2}\left(F_{\rm ret}^{\mu\nu} - F_{\rm adv}^{\mu\nu}\right), \tag{1.3.6}$$

where R stands for regular or remainder. The regular field is nonsingular everywhere and a is homogeneous solution to the Maxwell equations. Furthermore, it produces the correct acceleration when used with the Lorentz force law. Since Dirac's initial work, others have confirmed his results through different means. For a good summary see [33].

1.4 Curved space self-force

In curved space the problem of self-force becomes much more complicated. This is primarily due to the fact that the retarded Green function no longer only has support *on* the past light cone. Since radiation (both electromagnetic and gravitational) can scatter off of a curved background (and even off itself in the case of gravity), the Green function also has support in the entire causally connected region inside the past light cone.

1.4.1 Electromagnetic self-force

Consider a particle with charge q in free fall in curved space. Here we are only concerned with the electromagnetic (and not gravitational) radiation that is released as the charge accelerates. In their work on electromagnetic radiation reaction, Dewitt and Brehme [34] separated the Green function into a direct part, which only has support on the light cone, and a tail part, which has support inside the light cone. They follow Dirac's conservation approach and find that only the tail field contributes to radiation reaction. Their final result is that the four-force on the charge due to radiation reaction is

$$F_{\rm rr}^\mu = q g^{\mu\nu}\left(\nabla_\nu A_\alpha^{\rm tail} - \nabla_\alpha A_\nu^{\rm tail}\right) u^\alpha. \tag{1.4.1}$$

This force is directly analogous to the Abraham-Lorentz force. It has great utility in that one can compute the particle's acceleration from it, but it is not consistent with the generalized Lorentz force law $F^\mu = ma^\mu = qF^{\mu\nu}u_\nu$. That is, the force in Eq. (1.4.1) does not result from an external electromagnetic field. Indeed, an observer close to the particle would notice its changing field, but being so close, would not be able to identify radiation. Therefore, this near-observer would see no explanation for the particle's motion as it deviates from a background geodesic. Furthermore, the field $A_\mu^{\rm tail}$ is not a solution to the curved space electromagnetic field equations.

Detweiler and Whiting [35] circumvented these conceptual obstacles by introducing a different decomposition of the potential. They looked at the Green functions as follows. We know the retarded Green function has support on and inside the past light cone while the advanced Green function has support on and inside the future light cone. Define the singular (S) Green function to have support in the spacelike area between the retarded and advanced Green functions. Then, the regular (R) field will be the remainder $A_\mu^R = A_\mu^{\rm ret} - A_\mu^S$. I will not go into the details here, but the singular field is constructed specifically to remove the Coulomb part of the particle's field, which produces no force. The field $F_{\mu\nu}^S$, constructed from A_μ^S, is a solution to the inhomogeneous curved space Maxwell equations. The regular remainder $F_{\mu\nu}^R$, constructed from A_μ^R, is a homogeneous solution to those equations. Furthermore, $F_{\mu\nu}^R$ appears to a local observer to be responsible for the entire self-force as computed from the Lorentz force law.

1.4.2 Gravitational self-force

Here I consider the self-force on a small object moving in a curved spacetime. I sketch out some of the most important results in this field. For a more thorough treatment see [36], from which I draw heavily.

Historical perspective

A major milestone for the EMRI problem came in 1997 when Mino, Sasaki, and Tanaka [37] and subsequently Quinn and Wald [38] derived the equations of motion of a particle moving

on a curved background. The so-called *MiSaTaQuWa equations* are first-order equations of motion which (at least in theory) can be solved to give the deviation of a particle's motion off the background geodesic.

Mino et al. gave two derivations of the equations. The first was from a point particle formulation. Point particles are useful, but their physical validity is questionable in certain circumstances. For instance, a point particle pulls up a divergent $1/r$ local field which, close enough to the particle, violates the fundamental assumption of perturbation theory (that the particle's field be small compared to the background). Their second derivation considered the more physical scenario of a small black hole moving on a curved background. They used matched asymptotic expansions to show that the equations of motion of the two systems were the same. This is an important discovery, as it justifies all the work that has been done where the small black hole is modeled as a point particle, at least up to a certain order in perturbation theory. Although a black hole is not a point particle, we are able to treat it as such when $\mu/M \ll 1$.

Detweiler and Whiting [35] provided a powerful reinterpretation of the self-force problem. In the Detweiler-Whiting scheme, the particle's retarded field is separated into regular R and singular S parts. The former is a smooth field and a homogeneous solution to the field equations. The latter is a solution to the inhomogeneous field equations, but gives no contribution to the self-force. Therefore, the self-force can be found by substituting in the regular field in for the retarded field in the equations of motion.

Mathematical formalism

Let a particle with mass μ move in a spacetime dominated by a much larger body of mass M. For the large body alone, take a known solution to the Einstein equations, with the metric $g_{\mu\nu}$ to be given. Black hole perturbation theory is an expansion around $g_{\mu\nu}$ with a small expansion parameter taken to be μ/M. In our work we expand around the Schwarzschild metric in Schwarzschild coordinates, but in principle it could be any solution. At lowest order the particle will move on a geodesic γ_0 of $g_{\mu\nu}$, found by solving the geodesic equation $u^\alpha \nabla_\alpha u^\beta = 0$ on the background. This geodesic of the background goes into computing the

stress-energy tensor, which serves as a source to the first-order field equations. We define the difference between the true metric $\mathsf{g}_{\mu\nu}$ and the background metric $g_{\mu\nu}$ to be the metric perturbation $p_{\mu\nu}$. To first-order, we find its solution by solving the field equations in Lorenz gauge (see Chapter 2),

$$\Box\bar{p}_{\mu\nu} + 2R^{\alpha}{}_{\mu}{}^{\beta}{}_{\nu}\bar{p}_{\alpha\beta} = -16\pi T_{\mu\nu}, \qquad (\nabla^{\nu}\bar{p}_{\mu\nu} = 0). \tag{1.4.2}$$

Here, $\Box \equiv \nabla_{\alpha}\nabla^{\alpha}$ and we use an overbar to indicate a trace-reverse. $T_{\mu\nu}$ is the stress-energy tensor of a point particle. The retarded solution is

$$\bar{p}^{\mu\nu}_{\rm ret}(x) = 4\mu \int_{\gamma_0} G^{\mu\nu}_{{\rm ret}\ \alpha\beta}(x,z)u^{\alpha}u^{\beta}d\tau. \tag{1.4.3}$$

Here $G^{\mu\nu}_{{\rm ret}\ \alpha\beta}(x,z)$ is the retarded Green function associated with Eq. (1.4.2) The parameter z represents the four spacetime coordinates being integrated over along the past geodesic.

The solution to these equations contains all the information about the first-order gravitational field. At this point, the first-order field leads to a natural correction to the zeroth-order motion of the particle. By demanding the motion be geodesic in the perturbed spacetime $\mathsf{g}_{\mu\nu}$ we obtain the correction to the equations of motion

$$a^{\mu} = -\frac{1}{2}\left(g^{\mu\nu} + u^{\mu}u^{\nu}\right)\left(2p^{\rm ret}_{\nu\alpha;\beta} - p^{\rm ret}_{\alpha\beta;\nu}\right)u^{\alpha}u^{\beta}. \tag{1.4.4}$$

This much appears straightforward enough, but a problem arises due to the local field of the particle. The gravitational field of a point particle diverges like $1/r$ along the particle's worldline, and therefore the force as calculated from the retarded metric perturbation is divergent.

Yet, there clearly is a self-force. To the distant observer, the retarded metric perturbation is plainly evident as radiation which falls off with the inverse of distance. This is seen in the form of the gravitational waveform, which is a gauge-invariant observable. But, close to the particle, while the local gravitational field is changing, the particle is inspiralling,

and yet there is no evidence for radiation. This paradox is once again resolved by the separation of $p^{\rm ret}_{\mu\nu}$ into singular ($p^S_{\mu\nu}$) and regular ($p^R_{\mu\nu}$) parts. The former is a solution to the inhomogeneous equation 1.4.2, but provides no contribution to the self-force. The latter is a smooth, homogeneous solution to Eq. (1.4.2), and fully responsible for the self-force. The covariant derivative of $p^R_{\mu\nu}$ is

$$p^R_{\mu\nu;\alpha} = -4\mu\Big(u_{(\mu}R_{\nu)\beta\alpha\gamma} + R_{\mu\beta\nu\gamma}u_\alpha\Big)u^\beta u^\gamma + p^{\rm tail}_{\mu\nu\alpha}, \tag{1.4.5}$$

where

$$p^{\rm tail}_{\mu\nu\alpha} = \int_{-\infty}^{\tau^-} \nabla_\alpha \left(G_{\rm ret}{}_{\mu\nu\mu'\nu'}\left[z(\tau), z(\tau')\right] - \frac{1}{2}g_{\mu\nu}G_{\rm ret}{}^{\beta}{}_{\beta\mu'\nu'}\left[z(\tau), z(\tau')\right]\right) u^{\mu'}u^{\nu'}d\tau'. \tag{1.4.6}$$

When we substitute in $p^R_{\mu\nu}$ for $p^{\rm ret}_{\mu\nu}$ we obtain

$$a^\mu = -\frac{1}{2}\left(g^{\mu\nu} + u^\mu u^\nu\right)\left(2p^{\rm tail}_{\nu\alpha\beta} - p^{\rm tail}_{\alpha\beta\nu}\right)u^\alpha u^\beta, \tag{1.4.7}$$

which are the *MiSaTaQuWa equations*. They are first-order equations of motion which give the particle's acceleration off its background geodesic due to its own acceleration. An important feature of these equations is that *they are not generally covariant*, but rather are derived specifically in Lorenz gauge. Indeed the self-force is not a gauge-invariant; its change under a gauge transformation was computed by Barack and Ori [39]. One could even choose a gauge where it vanishes at first-order [40]. This all serves to emphasize a crucial point: in the end, we must calculate physically observable gauge-invariant quantities. Later in this section we discuss this further.

The Detweiler-Whiting axiom and the conservative/dissipative split

The regular/singular split of the retarded field is very convenient, but not altogether obvious. Detweiler and Whiting made their derivations from an axiomatic standpoint. Their axiom is: *The singular field does not contribute at all to the self-force. The self-force is entirely due to the regular field.* Their axiom is based on the symmetric nature of the singular field.

This is analogous to the time-reversal symmetry of Dirac's Coulomb field $\frac{1}{2}\left(F^{\mu\nu}_{\rm ret} + F^{\mu\nu}_{\rm adv}\right)$, which is clearly not responsible for radiation. However, the gravitational case is more subtle because the gravitational self-force is responsible for more than just radiation reaction. The gravitational self-force separates into two distinct pieces: conservative and dissipative.

The conservative piece is a consequence of the time-symmetric portion of the gravitational field. It creates discrete shifts in the physical observables of the system. For example (see Sec. 1.3.1), by adding a finite mass to the particle, one will naturally measure the system to be that much more massive. Furthermore, the two objects will orbit around their common barycenter. Even beyond these Newtonian corrections, there will be changes to the shape of the particle's orbit, with contributions at every multipole order. The symmetric, singular part is non-radiative and does not contribute to the dissipative piece of the self-force. The conservative part of the self-force is

$$F^{\rm cons}_\mu = \frac{1}{2}\left(F^{\rm ret}_\mu + F^{\rm adv}_\mu\right) - F^S_\mu. \tag{1.4.8}$$

The dissipative piece of the self-force is the part responsible for radiation reaction, and therefore only receives contributions from all modes $\ell \geq 2$. As mentioned, the singular part of the perturbed metric is strictly conservative. Therefore, we can write the dissipative part of the self-force as

$$F^{\rm diss}_\mu = \frac{1}{2}\left(F^{\rm ret}_\mu - F^{\rm adv}_\mu\right). \tag{1.4.9}$$

Note that adding these two pieces together gives the regular field,

$$F^R_\mu = F^{\rm cons}_\mu + F^{\rm diss}_\mu = F^{\rm ret}_\mu - F^S_\mu. \tag{1.4.10}$$

Mode-sum-regularization

The separation of the gravitational field into regular and singular parts is quite useful in numerical calculations. It provides two general paths forward toward computing the self-force.

The first and more common approach is called *mode-sum regularization*. In order to see

the general idea behind mode-sum regularization, consider a scalar field ψ which is pulled up by a particle with charge q orbiting a Schwarzschild black hole. (There is an exact parallel to the gravitational case, just with more tedious equations) The scalar field will satisfy the equation

$$\Box\psi(x) = q\ \delta^4\left(x, x_p(\tau)\right). \tag{1.4.11}$$

Here $\Box \equiv \nabla^\alpha\nabla_\alpha$, x, represents all four spacetime variables, and the particle travels on a geodesic x_p parametrized by its proper time τ. The field can be decomposed in spherical harmonics, as shown in Chapter 3, which yields a radial wave equation for each ℓ, m mode. By imposing outgoing wave boundary conditions at spatial infinity, downgoing conditions at the event horizon, and the correct internal jump conditions at the particle's location, one finds the retarded field at each mode, $\psi^{\rm ret}_{\ell m}(x)$.

The idea, pioneered by Barack and Ori [41], is to then subtract off the singular part of the self-force mode-by-mode. This subtraction is possible because, although the full field is divergent, it is finite at each order. For a given ℓ, taking the divergence of $\psi^{\rm ret}_{\ell m}$ and summing over m yields

$$\nabla_\alpha\psi^{\rm ret}_\ell = \sum_m \nabla_\alpha\psi^{\rm ret}_{\ell m}. \tag{1.4.12}$$

Given this, we compute the self-force ℓ-by-ℓ from

$$F^\ell_\alpha = \nabla_\alpha\psi^{\rm ret}_\ell - A_\alpha\left(\ell + 1/2\right) - B_\alpha - \frac{C_\alpha}{\ell + 1/2} + \cdots \tag{1.4.13}$$

The full self-force F_α is then a convergent sum over the F^ℓ_α. The coefficients $A_\alpha, B_\alpha, \ldots$ are called the *regularization coefficients*. They are independent of ℓ (though they depend in general on the physical parameters of the problem) and are computed analytically.

Mode-sum regularization has been used successfully by numerous groups to compute self-forces due to scalar, electromagnetic, and gravitational fields from particles moving on Schwarzschild and Kerr backgrounds, in radial, circular, and eccentric orbits.

Effective sources

As an alternative to mode-sum regularization, there is the effective-source approach. This was developed independently by Vega and Detweiler [42] and Barack and Golbourn [43]. Here, one computes $p^S_{\mu\nu}$ analytically, and then, the field is regularized by subtracting $p^S_{\mu\nu}$ from $p^{\rm ret}_{\mu\nu}$ and forming $p^R_{\mu\nu}$, which is formally smooth along the worldline (though in practice will have a discontinuity at some order of differentiability). Having formed $p^R_{\mu\nu}$, one can then solve the first-order field equations, typically in the time-domain. Having already removed the singular part, the self-force is trivial to compute at any stage in the integration. This is a nice conceptual idea, though it does have several practical challenges. Foremost among these is the analytic computation of $p^S_{\mu\nu}$. The divergent, singular field can only be found approximately, and even this is a tedious and lengthy task. An additional challenge arises because far from the particle one wishes to have the retarded field, which contains relevant information such as the gravitational waveform. Therefore, one typically uses a "window function" which transitions from the locally used regular field to the retarded field used further away. Choosing an appropriate window function is a subtle task. For more details see [44].

The gauge problem

As I have emphasized, the self-force is not a gauge-invariant quantity. The MiSaTaQuWa equations are formulated in Lorenz gauge, and the regularization procedure is also Lorenz gauge dependent. However, it is not always convenient to solve the field equation in Lorenz gauge. As discussed in Chapter 2, significant simplification can be achieved on Schwarzschild by choosing Regge-Wheeler gauge. And, until about seven years ago [45] nearly all work on Schwarzschild was done in Regge-Wheeler gauge. The challenges entailed in transforming from Regge-Wheeler to Lorenz gauge are covered in depth in Chapter 5.

One method of avoiding the gauge problem is to compute gauge-invariant quantities. Physically measurable values such as the waveform are gauge-invariant. The mass and angular momentum of an orbiting body are gauge-invariants. Of particular interest is a quantity introduced by Detweiler [46], commonly referred to as the Detweiler redshift invariant. It

was introduced for circular orbits on Schwarzschild and has since been generalized to eccentric orbits [47]. For a small body in orbit about a Schwarzschild black hole the local observer will measure one value for the period of radial motion (local total proper time). A distant observer will measure a different value for the period of the orbit. The ratio of these two periods is Detweiler's gauge-invariant quantity. Having such a quantity is useful because one can compute the way it changes under a self-force correction in any gauge. This is not only computationally convenient, but also good for checking results by taking different routes to the same solution.

1.5 Original work: eccentric orbits on Schwarzschild

The previous sections of this introduction should give an overview of the current state of research into the EMRI problem. Here I will give an overview of the contributions that I have made to the field. My research has centered on eccentric orbits on a Schwarzschild background. I will present some background on that specific problem and then summarize the new pieces I have added. For more detail, see Chapters 4 and 5.

1.5.1 Background

Generic eccentric orbits on Schwarzschild were first studied numerically by Tanaka, Shibata, Sasaki, Tagoshi, and Nakamura [48] and subsequently by Cutler, Kennefick, and Poisson [49]. They used frequency domain (FD) methods to compute energy and angular momentum fluxes from particles in a variety of orbits. FD codes have the benefit of converging very quickly for mildly eccentric orbits, but as eccentricities grow they get less and less efficient. Spurred largely by the work of Martel [50] and Haas [51], time domain (TD) codes have gained great popularity in recent years. Additionally, until recently (see below) it was impossible to accurately represent the gravitational field of a point particle in eccentric orbit through FD calculations. This is due to the Gibbs phenomenon, which crops up because of the singular nature of the source. A standard Fourier synthesis of the gravitational field will lead to slow (algebraic as opposed to exponential) convergence, if it converges at all.

Therefore, TD codes seemed necessary for local self-force calculations.

An additional change has taken place in recent years. Traditionally, most work on Schwarzschild has been done in Regge-Wheeler (RW) gauge. RW gauge is attractive mainly because it reduces the number of equations that must be solved for each mode from ten to two. (This equation counting is a bit of a simplification, but the point is that RW gauge makes it efficient to solve the Einstein equations.) The problem with RW gauge, as discussed above, is that it is not ideal for self-force calculations. The MiSaTaQuWa equations, and the mode-sum regularization scheme, are both formulated in Lorenz gauge.

There are two ways around the gauge problem. One is to solve the Einstein equations directly in Lorenz gauge, as proposed by Barack and Lousto [45]. This adds its own complications, but does have the benefit that it gives the gravitational field in the desired gauge. The other option is to solve the Einstein equations in RW gauge, as done usually, but then transform the solution into Lorenz gauge, by solving the gauge transformation equations.

We have chosen the second option. We work in the FD and in RW gauge. Then, we perform the gauge transformation to find the metric in Lorenz gauge.

1.5.2 Contributions of this thesis project

As mentioned, a major problem with FD work on eccentric orbits was the Gibbs phenomenon. In 2008, Barack, Ori and Sago [1] showed how to circumvent the Gibbs phenomenon with the *method of extended homogeneous solutions* (EHS). They demonstrated the method using the monopole term in a scalar field model problem. The standard Fourier synthesis provides algebraic convergence for this field, and its derivative does not converge at all. The EHS method allows exponential convergence of both the field and its derivative, including right up to the particle's location.

In our 2010 paper [52], we showed how to extend the EHS method to all radiative gravitational modes. Working in RW gauge, the source term has not only a delta function, but also a derivative of a delta function term. We found that the EHS method was applicable even with this more singular source term. From this we were able to reconstruct the metric perturbation in RW gauge at all locations, including the very location of the particle.

In finding the metric perturbation, we also examined the singular nature of RW gauge in depth for the first time. We found the spherical harmonic amplitudes of the metric perturbation to be discontinuous (C^{-1}) in all cases and in some cases to contain time-dependent delta function contributions. We were able to compute the time dependent magnitudes of these jumps and the time dependent coefficients of the delta functions for the first time.

Our work in the FD is noteworthy for two practical reasons. First, our results are far more accurate (relative errors of $\sim 10^{-12}$) than those of standard TD codes (relative errors of $\sim 10^{-7}$). Given the subtraction that takes place during the regularization procedure, one wishes to have as much accuracy as possible when computing the retarded field. Secondly, our code is very fast, especially for low eccentricities. Simulations which could take days on TD codes run in hours or minutes. Further, even relatively high eccentricities ($e \sim .9$) appear to give competitive runtimes to TD codes, especially when the benefit of the FD accuracy is taken into account. Lastly, all this is based on single processor calculations. Yet, our FD-based computations are easily ported to run on parallel computers.

Following this, we have begun work moving from RW to Lorenz gauge. Formally, the gauge transformation is clear. The infinitesimal coordinate transformation is presented in standard relativity texts (e.g. [53]), and is only a few lines. However, the specifics are far more subtle. Moving from RW to Lorenz gauge involves solving a set of coupled wave equations for each harmonic mode. This is further complicated by the singular nature of the source (which in this case is the divergence of the trace-reversed metric perturbation). The problem was examined in some detail by Sago, Nakano, and Sasaki [54]. We have decided to use their decomposition as a starting point and perform the transformation numerically for the first time. Though we have not completed the entire task, there are a few details worth noting here.

First, a FD solution to the gauge transformation equations is not a straightforward application of the EHS method. We have had to develop new techniques to treat the types of differential equations we encounter in this gauge transformation. The first technique is called the *method of partial annihilators* and the second is the *method of extended particular*

solutions. Both are covered in depth in Chapter 5. We have completed the odd-parity part of the gauge transformation, and have seen that as expected the C^{-1} behavior in the amplitudes is transformed to C^0 behavior at $r = r_p(t)$ in Lorenz gauge. Also, the RW metric is non-asymptotically flat. In Lorenz gauge, we find that proper asymptotic flatness is recovered.

The completion of the gauge transformation will leave us in an ideal situation for computing the self-force. We will have a highly accurate computation of the retarded metric perturbation in Lorenz gauge at all locations, including the location of the particle. This last part is key, as it is there where we must take the divergence and perform the regularization. There are several paths forward from this point, as discussed in Chapter 6.

1.6 Thesis organization

This thesis is organized into five additional chapters. In Chapter 2, I provide an overview of first-order black hole perturbation theory. I start with linearizing the Einstein equations around a Minkowski background and then generalize to a curved background. Finally, I present the $\mathcal{M}^2 \times \mathcal{S}^2$ decomposition of Martel and Poisson [55], lay out the techniques of tensor spherical harmonics, and give the field equations for the metric perturbation amplitudes in both Regge-Wheeler and Lorenz gauge.

Chapter 3 contains work on a scalar field model problem. The scalar field is an excellent testing ground for work before jumping into gravity. Here I present the multipole decomposition of a scalar field produced by a charged particle moving in flat space and show how this is equivalent to an exact solution to that problem. Finally, I move to curved space and derive the field equations that must be solved for a scalar charge in eccentric orbit about a Schwarzschild black hole.

Chapter 4 is taken from our first paper, Ref. [52]. It shows how we solved for the radiative parts of a first-order metric perturbation due to a small mass in eccentric orbit about a Schwarzschild black hole. In so doing we computed the metric perturbation to high accuracy all the way up to the location of the particle and presented the exact local singular

nature of the metric in Regge-Wheeler gauge.

Chapter 5 is a thorough discussion of subsequent results that will appear in a second paper. It goes into the details of performing the first-order gauge transformation to take the metric perturbation from Regge-Wheeler to Lorenz gauge. We give results there showing the completed odd-parity transformation, as well as a significant component of the even-parity part of the transformation.

Chapter 6 is a conclusion. I summarize the work presented in this thesis and give potential future directions for research on the EMRI problem.

Chapter 2

Mathematical preliminaries: gravitational waves and black hole perturbation theory

The nonlinearity of general relativity makes finding exact solutions to the Einstein equations formidable and often impossible. Therefore, perturbative approaches are important for finding approximate solutions of all but the simplest physical systems. One approach is post-Newtonian (PN) theory, wherein one expands the Einstein equations in powers of v/c. PN has been very successful in checking the predictions of general relativity through solar system [56] and binary pulsar experiments [57]. However, it fails in the strong field, fast motion regime, which is where other perturbative methods must be employed. As an alternative, one can consider a system wherein the mass-ratio μ/M of a two-body system is very small. An expansion of the Einstein equations in this parameter yields equations which are valid even as the small body is deep in the gravitational field of a black hole, and traveling at speeds $v \lesssim c$.

Along with Chapter 3, this chapter sets the stage for my original research in Chapters 4 and 5. I start by reviewing how perturbing a flat metric leads to gravitational wave equations in the context of linearized gravity. Using this as a model, I expand the Einstein equations on a curved background and find wave equations for the first-order metric perturbation. This expansion sets the theoretical foundation for finding the gravitational radiation emitted by a small body in motion around a black hole. At this point I specialize to a Schwarzschild spacetime, and use a decomposition introduced by Martel and Poisson [55] to separate the metric into two submanifolds. This allows for a convenient way to decompose the

first-order Einstein equations in spherical harmonics. Further, I examine how those field equations change under a gauge transformation. I end by giving the field equations for the metric perturbation amplitudes in both Regge-Wheeler and Lorenz gauge, both of which will be useful in subsequent chapters.

2.1 Linearized gravity

The presentation here follows closely that of [58, 53]. In the linearized theory of gravity, we define our metric as

$$\mathsf{g}_{\mu\nu} = \eta_{\mu\nu} + p_{\mu\nu}, \qquad |p_{\mu\nu}| \ll |\eta_{\mu\nu}|, \tag{2.1.1}$$

and assume that space is asymptotically flat. All our work will be to first-order in $p_{\mu\nu}$. Using the Minkowski metric and its inverse to raise and lower indices, we define the inverse of the metric perturbation as $p^{\mu\nu} \equiv \eta^{\mu\alpha}\eta^{\nu\beta}p_{\alpha\beta}$. A natural assumption is that the inverse metric will vary from flat space by only a small amount, $\mathsf{g}^{\mu\nu} = \eta^{\mu\nu} + k^{\mu\nu}, |k^{\mu\nu}| \ll |\eta^{\mu\nu}|$. Then, we demand that $\mathsf{g}_{\mu\alpha}\mathsf{g}^{\alpha\nu} = \delta_\mu{}^\nu$, and find

$$\delta_\mu{}^\nu = \mathsf{g}_{\mu\alpha}\mathsf{g}^{\alpha\nu} = (\eta_{\mu\alpha} + p_{\mu\alpha})\,(\eta^{\alpha\nu} + k^{\alpha\nu}) = \delta_\mu{}^\nu + k_\mu{}^\nu + p_\mu{}^\nu. \tag{2.1.2}$$

(Note that the $p_{\mu\alpha}k^{\alpha\nu}$ is dropped for being second-order.) So, evidently $k_{\mu\nu} = -p_{\mu\nu}$, and the inverse metric is $\mathsf{g}^{\mu\nu} = \eta^{\mu\nu} - p^{\mu\nu}$.

In a coordinate basis, the connection coefficients are, to first-order

$$\Gamma^\alpha{}_{\beta\gamma} = \frac{1}{2}\eta^{\alpha\delta}\left(p_{\delta\gamma,\beta} + p_{\delta\beta,\gamma} - p_{\beta\gamma,\delta}\right). \tag{2.1.3}$$

We form the linearized Riemann tensor in the standard way. After dropping terms quadratic in the connection coefficients, this is

$$\mathsf{R}_{\alpha\mu\beta\nu} = \frac{1}{2}\left(p_{\alpha\nu,\mu\beta} + p_{\mu\beta,\nu\alpha} - p_{\mu\nu,\alpha\beta} - p_{\alpha\beta,\mu\nu}\right). \tag{2.1.4}$$

Now we move on and consider gauge transformations of the form $x^\mu \to x'^\mu = x^\mu + \Xi^\mu, |\Xi^\mu| \sim |p_{\mu\nu}| \ll 1$. Note that Ξ^μ is on the same order as the metric perturbation, so

we will drop any second-order terms. In order to transform geometric objects we need the Jacobian matrix,

$$\frac{\partial x'^{\mu}}{\partial x^{\nu}} = \frac{\partial x^{\mu}}{\partial x^{\nu}} + \frac{\partial \Xi^{\mu}}{\partial x^{\nu}} = \delta^{\mu}{}_{\nu} + \Xi^{\mu}{}_{,\nu}. \tag{2.1.5}$$

The inverse transformation is also needed. We use the same logic that got us the inverse metric perturbation. Demanding

$$\frac{\partial x^{\mu}}{\partial x'^{\alpha}} \frac{\partial x'^{\alpha}}{\partial x^{\nu}} = \delta^{\mu}{}_{\nu} \tag{2.1.6}$$

and assuming the inverse transformation has a similar form to Eq. (2.1.5) we get

$$\delta^{\mu}{}_{\nu} = \frac{\partial x^{\mu}}{\partial x'^{\alpha}} \frac{\partial x'^{\alpha}}{\partial x^{\nu}} = \left(\delta^{\mu}{}_{\alpha} + f^{\mu}{}_{\alpha}\right)\left(\delta^{\alpha}{}_{\nu} + \Xi^{\alpha}{}_{,\nu}\right). \tag{2.1.7}$$

This defines $f_{\mu\nu}$ which is on the same order as $\Xi^{\mu}{}_{,\nu}$. Expanding out the product, we find $f^{\mu}{}_{\nu} = -\Xi^{\mu}{}_{,\nu}$, and so the inverse gauge transformation is

$$\frac{\partial x^{\mu}}{\partial x'^{\nu}} = \delta^{\mu}{}_{\nu} - \Xi^{\mu}{}_{,\nu}. \tag{2.1.8}$$

From this we can compute the transformation law for the metric (to first-order):

$$\mathsf{g}'_{\mu\nu} = \eta'_{\mu\nu} + p'_{\mu\nu} = \left(\delta^{\alpha}{}_{\mu} - \Xi^{\alpha}{}_{,\mu}\right)\left(\delta^{\beta}{}_{\nu} - \Xi^{\beta}{}_{,\nu}\right)\left(\eta_{\alpha\beta} + p_{\alpha\beta}\right) \tag{2.1.9}$$

$$= \eta_{\mu\nu} + p_{\mu\nu} - \Xi_{\nu,\mu} - \Xi_{\mu,\nu} \tag{2.1.10}$$

$$p'_{\mu\nu} = p_{\mu\nu} - 2\Xi_{(\mu,\nu)}. \tag{2.1.11}$$

Note that this works because the Minkowski metric is gauge-invariant ($\eta_{\mu\nu} = \eta'_{\mu\nu}$). The Riemann tensor changes under a gauge transformation as

$$\mathsf{R}'_{\alpha\mu\beta\nu} = \left(\delta^{\gamma}{}_{\alpha} - \Xi^{\gamma}{}_{,\alpha}\right)\left(\delta^{\rho}{}_{\mu} - \Xi^{\rho}{}_{,\mu}\right)\left(\delta^{\delta}{}_{\beta} - \Xi^{\delta}{}_{,\beta}\right)\left(\delta^{\sigma}{}_{\nu} - \Xi^{\sigma}{}_{,\nu}\right)\mathsf{R}_{\gamma\rho\delta\sigma}. \tag{2.1.12}$$

Once again, we discard terms of higher than linear-order, so

$$\mathsf{R}'_{\alpha\mu\beta\nu} = \mathsf{R}_{\alpha\mu\beta\nu} - \Big(\delta^{\gamma}{}_{\alpha}\delta^{\rho}{}_{\mu}\delta^{\delta}{}_{\beta}\Xi^{\sigma}{}_{,\nu} + \delta^{\gamma}{}_{\alpha}\delta^{\rho}{}_{\mu}\delta^{\sigma}{}_{\nu}\Xi^{\delta}{}_{,\beta} + \delta^{\gamma}{}_{\alpha}\delta^{\delta}{}_{\beta}\delta^{\sigma}{}_{\nu}\Xi^{\rho}{}_{,\mu} + \delta^{\rho}{}_{\mu}\delta^{\sigma}{}_{\nu}\delta^{\delta}{}_{\beta}\Xi^{\gamma}{}_{,\alpha}\Big)\mathsf{R}_{\gamma\rho\delta\sigma} \tag{2.1.13}$$

$$= \mathsf{R}_{\alpha\mu\beta\nu} - \Big(\mathsf{R}_{\alpha\mu\beta\sigma}\Xi^{\sigma}{}_{,\nu} + \mathsf{R}_{\alpha\mu\delta\nu}\Xi^{\delta}{}_{,\beta} + \mathsf{R}_{\alpha\rho\beta\nu}\Xi^{\rho}{}_{,\mu} + \mathsf{R}_{\gamma\mu\beta\nu}\Xi^{\gamma}{}_{,\alpha}\Big) \tag{2.1.14}$$

Up to now, we have considered a general, first-order gauge transformation for any form of the Riemann tensor. Now, looking at Eq. (2.1.4) we see that this specific form of the Riemann tensor has *no zeroth-order terms* (because we are using flat space as our background). Each term in it is linear in derivatives of the metric perturbation. Therefore, the terms in Eq. (2.1.14) that involve products of $\mathsf{R}_{\alpha\mu\beta\nu}$ and $\Xi^{\mu}{}_{,\nu}$ are *all second-order*. Hence, to first-order the Riemann tensor (and therefore, each of its contractions) is gauge-invariant: $\mathsf{R}'_{\alpha\mu\beta\nu} = \mathsf{R}_{\alpha\mu\beta\nu}$.

The Ricci tensor (which, as a contraction of the Riemann tensor, is also a gauge-invariant) is

$$\mathsf{R}_{\mu\nu} \equiv \mathsf{g}^{\alpha\beta}\mathsf{R}_{\alpha\mu\beta\nu} = \frac{1}{2}\left(p_{\alpha\nu,\mu}{}^{\alpha} + p_{\mu}{}^{\alpha}{}_{,\nu\alpha} - p_{\mu\nu,\alpha}{}^{\alpha} - p^{\alpha}{}_{\alpha,\mu\nu}\right). \tag{2.1.15}$$

The Ricci scalar is

$$\mathsf{R} = \frac{1}{2}\left(\eta^{\mu\nu} - p^{\mu\nu}\right)\left(p_{\alpha\nu,\mu}{}^{\alpha} + p_{\mu}{}^{\alpha}{}_{,\nu\alpha} - p_{\mu\nu,\alpha}{}^{\alpha} - p^{\alpha}{}_{\alpha,\mu\nu}\right) = p_{\alpha\mu,}{}^{\alpha\mu} - p^{\mu}{}_{\mu,}{}^{\alpha}{}_{\alpha}. \tag{2.1.16}$$

Defining $p \equiv p_{\alpha}{}^{\alpha}$, we now form the Einstein tensor

$$\mathsf{G}_{\mu\nu} \equiv \mathsf{R}_{\mu\nu} - \frac{1}{2}\mathsf{g}_{\mu\nu}\mathsf{R} \tag{2.1.17}$$

$$= \frac{1}{2}\left(p_{\alpha\nu,\mu}{}^{\alpha} + p_{\alpha\mu,\nu}{}^{\alpha} - p_{\mu\nu,\alpha}{}^{\alpha} - p_{,\mu\nu}\right) - \frac{1}{2}\left(\eta_{\mu\nu} + p_{\mu\nu}\right)\Big(p_{\alpha\beta,}{}^{\alpha\beta} - p_{,\alpha}{}^{\alpha}\Big). \tag{2.1.18}$$

Then, the linearized field equations are (from $G_{\mu\nu} = 8\pi T_{\mu\nu}$)

$$p_{\alpha\nu,\mu}{}^{\alpha} + p_{\alpha\mu,\nu}{}^{\alpha} - p_{\mu\nu,\alpha}{}^{\alpha} - p_{,\mu\nu} - \eta_{\mu\nu}\Big(p_{\alpha\beta,}{}^{\alpha\beta} - p_{,\alpha}{}^{\alpha}\Big) = 16\pi T_{\mu\nu}. \tag{2.1.19}$$

This simplifies if we express the metric perturbation in its trace-reversed form

$$\bar{p}_{\mu\nu} \equiv p_{\mu\nu} - \frac{1}{2}\eta_{\mu\nu}p \qquad \Rightarrow \qquad p = -\bar{p} \equiv \bar{p}^{\alpha}{}_{\alpha}. \tag{2.1.20}$$

We use the overbar to represent a trace reversal in any tensor. Therefore $\mathsf{G}_{\mu\nu} = \bar{\mathsf{R}}_{\mu\nu}$ and $p_{\mu\nu} = \bar{\bar{p}}_{\mu\nu}$. Plugging in $p_{\mu\nu} = \bar{p}_{\mu\nu} - \frac{1}{2}\eta_{\mu\nu}\bar{p}$ we have

$$\begin{aligned}\bar{p}_{\alpha\nu,\mu}{}^{\alpha} - \frac{1}{2}\eta_{\alpha\nu}\bar{p}_{,\mu}{}^{\alpha} + \bar{p}_{\alpha\mu,\nu}{}^{\alpha} - \frac{1}{2}\eta_{\alpha\mu}\bar{p}_{,\nu}{}^{\alpha} - \bar{p}_{\mu\nu,\alpha}{}^{\alpha} \\ + \frac{1}{2}\eta_{\mu\nu}\bar{p}_{,\alpha}{}^{\alpha} + \bar{p}_{,\mu\nu} - \eta_{\mu\nu}\left(\bar{p}_{\alpha\beta,}{}^{\alpha\beta} - \frac{1}{2}\eta_{\alpha\beta}\bar{p}_{,}{}^{\alpha\beta} + \bar{p}_{,\alpha}{}^{\alpha}\right) = 16\pi T_{\mu\nu} \qquad (2.1.21)\end{aligned}$$

$$\bar{p}_{\alpha\nu,\mu}{}^{\alpha} + \bar{p}_{\alpha\mu,\nu}{}^{\alpha} - \bar{p}_{\mu\nu,\alpha}{}^{\alpha} - \eta_{\mu\nu}\bar{p}_{\alpha\beta,}{}^{\alpha\beta} = 16\pi T_{\mu\nu}. \tag{2.1.22}$$

From here it is standard [53] to choose the Lorenz gauge condition $\bar{p}^{\mu\nu}{}_{,\nu} = 0$. Three of the four terms on the left side vanish and we get the linearized Einstein equations in Lorenz gauge,

$$\Box\bar{p}_{\mu\nu} = -16\pi T_{\mu\nu}. \tag{2.1.23}$$

It is instructive to show that one can always find a gauge that satisfies the Lorenz gauge condition. First, the trace of the metric perturbation transform as $p'^{\mu}{}_{\mu} = p^{\mu}{}_{\mu} - \Xi^{\mu}{}_{,\mu} - \Xi_{\mu,}{}^{\mu} \Rightarrow p' = p - 2\Xi^{\mu}{}_{,\mu}$. From this we can compute the transformation of the trace-reverse of the metric perturbation,

$$\bar{p}'_{\mu\nu} = p'_{\mu\nu} - \frac{1}{2}\eta_{\mu\nu}p' = p_{\mu\nu} - 2\Xi_{(\mu,\nu)} - \frac{1}{2}\eta_{\mu\nu}\left(p - 2\Xi^{\alpha}{}_{,\alpha}\right) = \bar{p}_{\mu\nu} - 2\Xi_{(\mu,\nu)} + \eta_{\mu\nu}\Xi^{\alpha}{}_{,\alpha} \tag{2.1.24}$$

Now, suppose that $\partial^{\nu}\bar{p}_{\mu\nu} \neq 0$. Perform a gauge transformation as described by Eq. (2.1.24), and take the divergence of both sides:

$$\partial^{\nu}\bar{p}'_{\mu\nu} = \partial^{\nu}\left(\bar{p}_{\mu\nu} - 2\Xi_{(\mu,\nu)} + \eta_{\mu\nu}\Xi^{\alpha}{}_{,\alpha}\right). \tag{2.1.25}$$

Demand that the left side equal zero, so that the Lorenz gauge is satisfied in our new

coordinates

$$0 = \bar{p}_{\mu\nu,}{}^{\nu} - \Xi_{\mu,\nu}{}^{\nu} - \Xi_{\nu,\mu}{}^{\nu} + \eta_{\mu\nu}\Xi_{\alpha,}{}^{\alpha\nu}. \tag{2.1.26}$$

The last two terms cancel because partial derivatives commute and we are left with an inhomogeneous wave equation,

$$\Box\Xi_{\mu} = \bar{p}_{\mu\nu,}{}^{\nu}. \tag{2.1.27}$$

We can reduce the full linear field equations (2.1.22) to the form of Eq. (2.1.23) by finding any 4-vector Ξ^{μ} that satisfies Eq. (2.1.27). While this puts restrictions on the form of Ξ^{μ}, there is still residual gauge freedom because Eq. (2.1.27) is *inhomogeneous*. Given a solution to an inhomogeneous differential equation, we can add any *homogeneous* solution to it and get another inhomogeneous solution. To see this, assume the Lorenz gauge is already satisfied. Then consider another linear-order gauge transformation

$$\bar{p}'_{\mu\nu} \rightarrow \bar{p}''_{\mu\nu} = \bar{p}'_{\mu\nu} - 2\Xi'_{(\mu,\nu)} + \eta_{\mu\nu}\Xi'^{\alpha}{}_{,\alpha}. \tag{2.1.28}$$

Again, take the divergence of both sides and demand the left side vanish:

$$\bar{p}''_{\mu\nu,}{}^{\nu} = 0 = \bar{p}'_{\mu\nu,}{}^{\nu} - \Xi'_{\mu,\nu}{}^{\nu} - \Xi'_{\nu,\mu}{}^{\nu} + \eta_{\mu\nu}\Xi'_{\alpha,}{}^{\alpha\nu}. \tag{2.1.29}$$

Again the last two terms cancel. Now, recall that we've already demanded that the Lorenz gauge be satisfied, so the first term on the right side vanishes also. Therefore, we are left with the following source-free wave equation that expresses the residual gauge freedom $\Box\Xi'_{\mu} = 0$.

Relation of the Lorenz gauge to the Bianchi identities

There are 10 algebraically independent Einstein field equations. Conservation of energy-momentum is expressed by the Bianchi identities,

$$\nabla^{\nu}\mathsf{G}_{\mu\nu} = 8\pi\nabla^{\nu}T_{\mu\nu} = 0. \tag{2.1.30}$$

This is a set of four equations that limits the degrees of freedom inherent in the theory down from 10 to 6. Consider now the linearized field equations in the Lorenz gauge (2.1.23). Taking the divergence of both sides gives (note that in linearized gravity we take derivatives with respect to the flat spacetime: $\nabla_\mu \to \partial_\mu$)

$$\partial^\nu \Box \bar{p}_{\mu\nu} = \Box \left(\bar{p}_{\mu\nu,}{}^{\nu} \right) = 0 = -16\pi T_{\mu\nu,}{}^{\nu} = 0. \tag{2.1.31}$$

This equation is satisfied identically. The left side is an expression of the gauge condition, while the right is conservation of energy-momentum. Therefore, using the freedom of a linear-order gauge transformation to remove four of the degrees of freedom from the full equations of linear gravity is equivalent to removing the same four degrees of freedom by imposing the Bianchi identities.

2.2 Perturbed Einstein equations in curved space

This section also draws heavily upon [53]. As an extension of the previous section, we now consider small changes from a curved background. Consider a known, background solution to the Einstein equations $g_{\mu\nu}$. A first-order perturbation to that metric, $p_{\mu\nu}$ yields

$$\mathsf{g}_{\mu\nu} = g_{\mu\nu} + p_{\mu\nu} \qquad |p_{\mu\nu}| \ll |g_{\mu\nu}|. \tag{2.2.1}$$

We denote covariant derivatives with respect to the background metric $g_{\mu\nu}$ with ∇_μ or $_{|\mu}$. At first-order we raise and lower indices with the background metric. For the inverse metric we find

$$\delta^\mu{}_\nu = \left(g^{\mu\alpha} + k^{\mu\alpha}\right)\left(g_{\alpha\nu} + p_{\alpha\nu}\right) = \delta^\mu{}_\nu + k^\mu{}_\nu + p^\mu{}_\nu + \mathcal{O}(p^2), \tag{2.2.2}$$

and so as in flat space $k^\mu{}_\nu = -p^\mu{}_\nu$, implying $\mathsf{g}^{\mu\nu} = g^{\mu\nu} - p^{\mu\nu}$.

Now, consider the transformation law for the connection coefficients,

$$\Gamma'^{\alpha}{}_{\beta\gamma} = \frac{\partial x^\mu}{\partial x'^\beta}\frac{\partial x^\nu}{\partial x'^\gamma}\frac{\partial x'^\alpha}{\partial x^\sigma}\Gamma^\sigma{}_{\mu\nu} - \frac{\partial x^\mu}{\partial x'^\beta}\frac{\partial x^\nu}{\partial x'^\gamma}\frac{\partial^2 x'^\alpha}{\partial x^\mu \partial x^\nu}. \tag{2.2.3}$$

The first term is the standard tensor transformation law, but the second term breaks the tensor relation. However, notice that this term only depends on the coordinates (it is not traced over any geometrical objects). So, if we take the difference between two covariant derivatives, these terms cancel out and we find

$$S'^{\alpha}{}_{\beta\gamma} = \Gamma'^{\alpha}{}_{\beta\gamma} - \Gamma'^{\alpha}{}_{\beta\gamma} = \frac{\partial x^{\mu}}{\partial x'^{\beta}} \frac{\partial x^{\nu}}{\partial x'^{\gamma}} \frac{\partial x'^{\alpha}}{\partial x^{\sigma}} \left(\Gamma^{\sigma}{}_{\mu\nu} - \Gamma^{\sigma}{}_{\mu\nu}\right) = \frac{\partial x^{\mu}}{\partial x'^{\beta}} \frac{\partial x^{\nu}}{\partial x'^{\gamma}} \frac{\partial x'^{\alpha}}{\partial x^{\sigma}} S^{\sigma}{}_{\mu\nu}, \tag{2.2.4}$$

where we use a sans-serif $\mathsf{\Gamma}^{\alpha}{}_{\beta\gamma}$ to represent the connection coefficient of the perturbed spacetime Therefore, $S^{\alpha}{}_{\beta\gamma}$ obeys the tensor transformation law and is indeed a tensor.

We now compute $S^{\alpha}{}_{\beta\gamma}$ by using the standard connection coefficient expression to get

$$\begin{aligned} S^{\alpha}{}_{\beta\gamma} = \frac{1}{2}\mathsf{g}^{\alpha\mu} \left(g_{\mu\gamma,\beta} + g_{\beta\mu,\gamma} - g_{\beta\gamma,\mu} + p_{\mu\gamma,\beta} + p_{\beta\mu,\gamma} - p_{\beta\gamma,\mu}\right) \\ - \frac{1}{2} g^{\alpha\mu} \left(g_{\mu\gamma,\beta} + g_{\beta\mu,\gamma} - g_{\beta\gamma,\mu}\right). \end{aligned} \tag{2.2.5}$$

Now, if we are in a locally Lorentz frame the background metric $g_{\mu\nu} = \eta_{\mu\nu}$ and its derivative vanishes. Also, in that frame since connection terms (though not their derivatives) vanish partial derivatives can be written as covariant derivatives ($_{,\mu} =_{|\mu}$). Therefore we have in the locally Lorentz frame (we indicate an equality in a locally Lorentz frame with the symbol $\overset{*}{=}$)

$$S^{\alpha}{}_{\beta\gamma} \overset{*}{=} \frac{1}{2}\mathsf{g}^{\alpha\mu} \left(p_{\mu\gamma|\beta} + p_{\beta\mu|\gamma} - p_{\beta\gamma|\mu}\right). \tag{2.2.6}$$

At this point, recognize that this is a tensor equation (note the importance of proving the tensor nature of $S^{\alpha}{}_{\beta\gamma}$), and thus it must be true in all frames, so

$$S^{\alpha}{}_{\beta\gamma} = \frac{1}{2}\mathsf{g}^{\alpha\mu} \left(p_{\mu\gamma|\beta} + p_{\beta\mu|\gamma} - p_{\beta\gamma|\mu}\right). \tag{2.2.7}$$

Using the standard Riemann tensor formula, we write down the difference between the

perturbed Riemann tensor ($\mathsf{R}^{\alpha}{}_{\beta\gamma\delta}$) and the background Riemann tensor,

$$\mathsf{R}^{\alpha}{}_{\beta\gamma\delta} - R^{\alpha}{}_{\beta\gamma\delta} = \left[\partial_\gamma \mathsf{\Gamma}^{\alpha}{}_{\beta\delta} - \partial_\delta \mathsf{\Gamma}^{\alpha}{}_{\beta\gamma} + \mathsf{\Gamma}^{\mu}{}_{\beta\delta}\mathsf{\Gamma}^{\alpha}{}_{\mu\gamma} - \mathsf{\Gamma}^{\mu}{}_{\beta\gamma}\mathsf{\Gamma}^{\alpha}{}_{\mu\delta}\right] - \left[\partial_\gamma \Gamma^{\alpha}{}_{\beta\delta} - \partial_\delta \Gamma^{\alpha}{}_{\beta\gamma} + \Gamma^{\mu}{}_{\beta\delta}\Gamma^{\alpha}{}_{\mu\gamma} - \Gamma^{\mu}{}_{\beta\gamma}\Gamma^{\alpha}{}_{\mu\delta}\right]. \quad (2.2.8)$$

Again consider a locally Lorentz frame where the background connection terms vanish. There, grouping terms we have

$$\mathsf{R}^{\alpha}{}_{\beta\gamma\delta} - R^{\alpha}{}_{\beta\gamma\delta} \overset{*}{=} \partial_\gamma\left(\mathsf{\Gamma}^{\alpha}{}_{\beta\delta} - \Gamma^{\alpha}{}_{\beta\delta}\right) - \partial_\delta\left(\mathsf{\Gamma}^{\alpha}{}_{\beta\gamma} - \Gamma^{\alpha}{}_{\beta\gamma}\right) + \mathsf{\Gamma}^{\mu}{}_{\beta\delta}\mathsf{\Gamma}^{\alpha}{}_{\mu\gamma} - \mathsf{\Gamma}^{\mu}{}_{\beta\gamma}\mathsf{\Gamma}^{\alpha}{}_{\mu\delta}. \quad (2.2.9)$$

Because the background connections vanish, in this Lorentz frame we have $S^{\alpha}{}_{\beta\gamma} = \mathsf{\Gamma}^{\alpha}{}_{\beta\gamma}$. Also, as before ${}_{,\mu} =_{|\mu}$, and so

$$\mathsf{R}^{\alpha}{}_{\beta\gamma\delta} - R^{\alpha}{}_{\beta\gamma\delta} \overset{*}{=} \nabla_\gamma S^{\alpha}{}_{\beta\delta} - \nabla_\delta S^{\alpha}{}_{\beta\gamma} + S^{\mu}{}_{\beta\delta}S^{\alpha}{}_{\mu\gamma} - S^{\mu}{}_{\beta\gamma}S^{\alpha}{}_{\mu\delta}. \quad (2.2.10)$$

Again, we notice that this is a tensor equation, and so it must be true in all frames,

$$\mathsf{R}^{\alpha}{}_{\beta\gamma\delta} - R^{\alpha}{}_{\beta\gamma\delta} = S^{\alpha}{}_{\beta\delta|\gamma} - S^{\alpha}{}_{\beta\gamma|\delta} + S^{\mu}{}_{\beta\delta}S^{\alpha}{}_{\mu\gamma} - S^{\mu}{}_{\beta\gamma}S^{\alpha}{}_{\mu\delta}. \quad (2.2.11)$$

Contracting over the first and third indices gives the difference in the Ricci tensors

$$\mathsf{R}_{\beta\delta} - R_{\beta\delta} = S^{\alpha}{}_{\beta\delta|\alpha} - S^{\alpha}{}_{\beta\alpha|\delta} + S^{\mu}{}_{\beta\delta}S^{\alpha}{}_{\mu\alpha} - S^{\mu}{}_{\beta\alpha}S^{\alpha}{}_{\mu\delta}. \quad (2.2.12)$$

Direct calculations from Eqs. (2.2.7) and (2.2.12) give

$$\begin{aligned}\mathsf{R}_{\beta\delta} - R_{\beta\delta} = {} & \nabla_\alpha\left[\frac{1}{2}\mathsf{g}^{\alpha\mu}\left(p_{\mu\delta|\beta} + p_{\beta\mu|\delta} - p_{\beta\delta|\mu}\right)\right] - \nabla_\delta\left[\frac{1}{2}\mathsf{g}^{\alpha\mu}\left(p_{\mu\alpha|\beta} + p_{\beta\mu|\alpha} - p_{\beta\alpha|\mu}\right)\right] \\ & + \frac{1}{4}\mathsf{g}^{\mu\nu}\mathsf{g}^{\alpha\lambda}\left(p_{\nu\delta|\beta} + p_{\beta\nu|\delta} - p_{\beta\delta|\nu}\right)\left(p_{\lambda\alpha|\mu} + p_{\mu\lambda|\alpha} - p_{\mu\alpha|\lambda}\right) \\ & - \frac{1}{4}\mathsf{g}^{\mu\zeta}\mathsf{g}^{\alpha\sigma}\left(p_{\zeta\alpha|\beta} + p_{\beta\zeta|\alpha} - p_{\beta\alpha|\zeta}\right)\left(p_{\sigma\delta|\mu} + p_{\mu\sigma|\delta} - p_{\mu\delta|\sigma}\right). \quad (2.2.13)\end{aligned}$$

Keeping terms up to linear-order (noting that they will be multiplying other factors of $p_{\alpha\beta}$)

in $p_{\alpha\beta}$, we plug in for $\mathsf{g}^{\alpha\beta}$, and get (neglecting terms of order p^3)

$$\begin{aligned}
\mathsf{R}_{\beta\delta} - R_{\beta\delta} = \nabla_\alpha &\left[\frac{1}{2}\left(g^{\alpha\mu} - p^{\alpha\mu}\right)\left(p_{\mu\delta|\beta} + p_{\beta\mu|\delta} - p_{\beta\delta|\mu}\right)\right] \\
&- \nabla_\delta \left[\frac{1}{2}\left(g^{\alpha\mu} - p^{\alpha\mu}\right)\left(p_{\mu\alpha|\beta} + p_{\beta\mu|\alpha} - p_{\beta\alpha|\mu}\right)\right] \\
&+ \frac{1}{4}\left(g^{\mu\nu} - p^{\mu\nu}\right)\left(g^{\alpha\lambda} - p^{\alpha\lambda}\right)\left(p_{\nu\delta|\beta} + p_{\beta\nu|\delta} - p_{\beta\delta|\nu}\right)\left(p_{\lambda\alpha|\mu} + p_{\mu\lambda|\alpha} - p_{\mu\alpha|\lambda}\right) \\
&- \frac{1}{4}\left(g^{\mu\zeta} - p^{\mu\zeta}\right)\left(g^{\alpha\sigma} - p^{\alpha\sigma}\right)\left(p_{\zeta\alpha|\beta} + p_{\beta\zeta|\alpha} - p_{\beta\alpha|\zeta}\right)\left(p_{\sigma\delta|\mu} + p_{\mu\sigma|\delta} - p_{\mu\delta|\sigma}\right). \quad (2.2.14)
\end{aligned}$$

The first-order contribution is (defining $\Box \equiv {}_{|\alpha}{}^{\alpha}$ and $p \equiv p^{\alpha}{}_{\alpha}$)

$${}^1R_{\mu\nu} = \frac{1}{2}\left(-\Box p_{\mu\nu} - p_{|\mu\nu} + p^{\alpha}{}_{\nu|\mu\alpha} + p_{\mu}{}^{\alpha}{}_{|\nu\alpha}\right) = 8\pi T_{\mu\nu}. \quad (2.2.15)$$

As in flat space, it is convenient to introduce the trace-reverse of the metric perturbation $\bar{p}_{\mu\nu} = p_{\mu\nu} - \frac{1}{2}g_{\mu\nu}p$. Then Eq. (2.2.15) are written

$$\Box\bar{p}_{\mu\nu} + g_{\mu\nu}\bar{p}^{\alpha\beta}{}_{|\alpha\beta} - 2\bar{p}_{\alpha(\mu|}{}^{\alpha}{}_{\nu)} + 2R_{\alpha\mu\beta\nu}\bar{p}^{\alpha\beta} - 2R_{\alpha(\mu}\bar{p}_{\nu)}{}^{\alpha} = -16\pi T_{\mu\nu}, \quad (2.2.16)$$

where the Riemann and Ricci tensor terms result from commuting covariant derivatives. This seems to have only complicated matters, but if we impose the Lorenz gauge condition, $\bar{p}_{\mu\nu|}{}^{\nu} = 0$, we see a vast simplification. The second and third terms vanish due to the gauge condition. In addition, the last term also vanishes because $R_{\mu\nu} = 0$. Thus, the first-order Einstein equations, in Lorenz gauge are

$$\Box\bar{p}_{\mu\nu} + 2R_{\alpha\mu\beta\nu}\bar{p}^{\alpha\beta} = -16\pi T_{\mu\nu}. \quad (2.2.17)$$

2.3 The $\mathcal{M}^2 \times \mathcal{S}^2$ decomposition in a spherically symmetric spacetime

Now we specialize to a spherically symmetric background. In this section we introduce formalism from [55] for doing a harmonic decomposition of scalar, vectors, and tensors in such a spacetime. We specialize to Schwarzschild spacetime with Schwarzschild coordinates

and decompose its metric $g_{\mu\nu}$ on two submanifolds, yielding g_{ab} and $g_{AB} = r^2\Omega_{AB}$. Here $a, b, \ldots \in \{0, 1\}$ and $A, B, \ldots \in \{\theta, \phi\}$. The x^a coordinates span the "(t, r) plane" while x^A are the standard two-sphere polar and azimuthal coordinates. In matrix form we have

$$g_{\mu\nu} \doteq \begin{bmatrix} g_{00} & g_{01} & 0 & 0 \\ g_{10} & g_{11} & 0 & 0 \\ 0 & 0 & r^2\Omega_{\theta\theta} & r^2\Omega_{\theta\phi} \\ 0 & 0 & r^2\Omega_{\phi\theta} & r^2\Omega_{\phi\phi} \end{bmatrix} = \begin{bmatrix} g_{00} & g_{01} & 0 & 0 \\ g_{10} & g_{11} & 0 & 0 \\ 0 & 0 & r^2 & 0 \\ 0 & 0 & 0 & r^2\sin^2\theta \end{bmatrix}. \tag{2.3.1}$$

Specifically, we are interested in an expression of the Schwarzschild metric that is covariant under two-dimensional transformations: $x^a \to x'^a$. The line element can be written as

$$ds^2 = g_{ab}\, dx^a dx^b + r^2\Omega_{AB}\, dx^A dx^B. \tag{2.3.2}$$

In Schwarzschild coordinates, the submanifold $\mathcal{M}^2$ has a metric and inverse

$$g_{ab} \doteq \begin{bmatrix} -f & 0 \\ 0 & 1/f \end{bmatrix}, \qquad g^{ab} \doteq \begin{bmatrix} -1/f & 0 \\ 0 & f \end{bmatrix}, \qquad f \equiv 1 - \frac{2M}{r}. \tag{2.3.3}$$

The unit two-sphere has a metric and inverse

$$\Omega_{AB} \doteq \begin{bmatrix} 1 & 0 \\ 0 & \sin^2\theta \end{bmatrix}, \qquad \Omega^{AB} \doteq \begin{bmatrix} 1 & 0 \\ 0 & 1/\sin^2\theta \end{bmatrix}. \tag{2.3.4}$$

Note that in general (off the *unit* two-sphere) we use the metric $g_{AB} \equiv r^2\Omega_{AB}$.

2.3.1 The Submanifold $\mathcal{M}^2$

The connection coefficients on $\mathcal{M}^2$ are computed in the standard way

$$\Gamma^a{}_{bc} = \frac{1}{2} g^{ad} \left(g_{cd,b} + g_{db,c} - g_{bc,d} \right). \tag{2.3.5}$$

In Schwarzschild coordinates, the submanifold $\mathcal{M}^2$ has a metric and inverse given by Eq. (2.3.3). From these expressions, we see that the only derivatives of the metric that survive are

$$\partial_r g_{tt} = -\partial_r f = -\frac{2M}{r^2}, \quad \partial_r g_{rr} = \partial_r \left(f^{-1}\right) = -f^{-2}\partial_r f = -\frac{1}{f^2}\frac{2M}{r^2} = -\frac{2M}{(r-2M)^2}. \tag{2.3.6}$$

Then, the non-vanishing connection coefficients are

$$\Gamma^r{}_{rr} = \frac{1}{2}g^{rr}\left(g_{rr,r} + g_{rr,r} - g_{rr,r}\right) = \frac{1}{2}\frac{r-2M}{r}\frac{-2M}{(r-2M)^2} = -\frac{1}{f}\frac{M}{r^2}, \tag{2.3.7}$$

$$\Gamma^r{}_{tt} = \frac{1}{2}g^{rr}\left(g_{tr,t} + g_{rt,t} - g_{tt,r}\right) = \frac{1}{2}\frac{r-2M}{r}\frac{2M}{r^2} = f\frac{M}{r^2}, \tag{2.3.8}$$

$$\Gamma^t{}_{rt} = \Gamma^t{}_{tr} = \frac{1}{2}g^{tt}\left(g_{rt,t} + g_{tt,r} - g_{tr,t}\right) = \frac{1}{2}\frac{-r}{r-2M}\frac{-2M}{r^2} = \frac{1}{f}\frac{M}{r^2}. \tag{2.3.9}$$

With the connection coefficients calculated, we can compute the form of the wave operator on this submanifold. Use $h(x^a)$ to represent a scalar test function on which the box operator will act. Then, we have

$$\Box h \equiv g^{ab}\nabla_a\nabla_b h = g^{ab}\nabla_a\partial_b h = -\frac{1}{f}\partial_t^2 h + f\partial_r^2 h + 2\frac{M}{r^2}\partial_r h. \tag{2.3.10}$$

Introducing the tortoise coordinate, defined through the differential equation $dr/dr_* = f$, we change this expression to

$$\Box h = -\frac{1}{f}\partial_t^2 h + f\partial_r\left[\frac{dr_*}{dr}\partial_{r_*}h\right] + 2\frac{M}{r^2}\frac{dr_*}{dr}\partial_{r_*}h = \frac{1}{f}\left(-\partial_t^2 + \partial_{r_*}^2\right)h. \tag{2.3.11}$$

Additionally, we will need the Levi-Civta tensor on $\mathcal{M}^2$, which is

$$\varepsilon_{ab} \doteq \begin{bmatrix} 0 & 1 \\ -1 & 0 \end{bmatrix} \qquad \varepsilon^{ab} \doteq \begin{bmatrix} 0 & -1 \\ 1 & 0 \end{bmatrix} \tag{2.3.12}$$

in Schwarzschild coordinates. Also, we define

$$r_a \equiv \frac{\partial r}{\partial x^a} \doteq \begin{bmatrix} 0 \\ 1 \end{bmatrix} \qquad \text{and} \qquad t^a \equiv -\varepsilon^{ab} r_b \doteq \begin{bmatrix} 1 \\ 0 \end{bmatrix}, \tag{2.3.13}$$

which serve as a basis for vectors on $\mathcal{M}^2$.

2.3.2 The Submanifold $\mathcal{S}^2$

We define a compatible covariant derivative from $D_A g_{BC} = r^2 D_A \Omega_{BC} \equiv 0$. Note the r^2 which connects the definitions of Ω_{AB} and g_{AB} pulls through the covariant derivative, as r is constant on any given two-sphere. In order to use the covariant derivative we will need connection coefficients, found in the standard way

$$\Gamma^A{}_{BC} = \frac{1}{2r^2} \Omega^{AD} r^2 \left(\Omega_{CD,B} + \Omega_{DB,C} - \Omega_{BC,D} \right). \tag{2.3.14}$$

Clearly, the only partial derivative of the metric that will not vanish is $\Omega_{\phi\phi,\theta} = 2 \sin\theta \cos\theta$. With this in mind, we find that the only non-vanishing coefficients are

$$\Gamma^\theta{}_{\phi\phi} = \frac{1}{2} \Omega^{\theta\theta} \left(\Omega_{\phi\theta,\phi} + \Omega_{\theta\phi,\phi} - \Omega_{\phi\phi,\theta} \right) = -\sin\theta \cos\theta \tag{2.3.15}$$

$$\Gamma^\phi{}_{\phi\theta} = \Gamma^\phi{}_{\theta\phi} = \frac{1}{2} \Omega^{\phi\phi} \left(\Omega_{\phi\theta,\phi} + \Omega_{\theta\phi,\phi} - \Omega_{\phi\phi,\theta} \right) = \frac{\cos\theta}{\sin\theta}. \tag{2.3.16}$$

The Riemann tensor is computed in the normal way, through

$$R^A{}_{BCD} = \partial_C \Gamma^A{}_{BD} - \partial_D \Gamma^A{}_{BC} + \Gamma^E{}_{BD} \Gamma^A{}_{EC} - \Gamma^E{}_{BC} \Gamma^A{}_{ED}. \tag{2.3.17}$$

We contract over the first and third indices to find the Ricci tensor

$$R_{BD} = R^A{}_{BAD} = \partial_A \Gamma^A{}_{BD} - \partial_D \Gamma^A{}_{BA} + \Gamma^E{}_{BD} \Gamma^A{}_{EA} - \Gamma^E{}_{BA} \Gamma^A{}_{ED}. \tag{2.3.18}$$

Finally, the Ricci scalar is found by contracting over the two remaining indices,

$$R = g^{BD} R_{BD} = \frac{1}{r^2} \Omega^{BD} \left(\partial_A \Gamma^A{}_{BD} - \partial_D \Gamma^A{}_{BA} + \Gamma^E{}_{BD} \Gamma^A{}_{EA} - \Gamma^E{}_{BA} \Gamma^A{}_{ED} \right). \tag{2.3.19}$$

Now, we plug in the non-vanishing connection coefficients to find

$$R = \frac{2}{r^2}. \tag{2.3.20}$$

Recall, finally that the Riemann tensor on a maximally symmetric two-dimensional space is written as [59]

$$R_{ABCD} = \frac{R}{2} \left(g_{AC} g_{BD} - g_{AD} g_{BC} \right), \tag{2.3.21}$$

which means for our case that

$$R_{ABCD} = \frac{1}{r^2} \left(g_{AC} g_{BD} - g_{AD} g_{BC} \right) = r^2 \left(\Omega_{AC} \Omega_{BD} - \Omega_{AD} \Omega_{BC} \right), \tag{2.3.22}$$

and the Ricci tensor is

$$R_{BD} = \frac{1}{r^2} \Omega^{AC} R_{ABCD} = \frac{1}{r^2} \Omega^{AC} r^2 \left(\Omega_{AC} \Omega_{BD} - \Omega_{AD} \Omega_{BC} \right) = \Omega_{BD}. \tag{2.3.23}$$

Now, consider spherical harmonics, starting with the scalar case. They are eigenfunctions, satisfying the equation

$$\left[\frac{1}{\sin\theta} \partial_\theta \left(\sin\theta \cdot \partial_\theta \right) + \frac{1}{\sin^2\theta} \partial_\phi^2 + \ell \left(\ell + 1 \right) \right] Y_{\ell m}(\theta, \phi) = 0. \tag{2.3.24}$$

Acting on a test scalar function f we have

$$\Omega^{AB} D_A D_B f = \Omega^{AB} \left(\partial_A \partial_B - \Gamma^C{}_{AB} \partial_C \right) f \tag{2.3.25}$$

$$= \partial_\theta^2 f - \Gamma^C{}_{\theta\theta} \partial_C f + \frac{1}{\sin^2\theta} \partial_\phi^2 f - \frac{1}{\sin^2\theta} \Gamma^C{}_{\phi\phi} \partial_C f \tag{2.3.26}$$

$$= \left(\frac{1}{\sin\theta} \partial_\theta \left(\sin\theta \cdot \partial_\theta \right) + \frac{1}{\sin^2\theta} \partial_\phi^2 \right) f. \tag{2.3.27}$$

So, we can write Eq. (2.3.24) in the compact form

$$\left[\Omega^{AB} D_A D_B + \ell\,(\ell+1)\right] Y_{\ell m}(\theta,\phi) = 0. \tag{2.3.28}$$

The solution to this equation with standard normalization [31] is

$$Y_{\ell m} = \sqrt{\frac{2\ell+1}{4\pi}\frac{(\ell-m)!}{(\ell+m)!}}\; P_\ell^m(\cos\theta) e^{im\phi} \tag{2.3.29}$$

where P_ℓ^m are the associated Legendre functions. These are an orthonormal set of functions,

$$\int Y_{\ell m}(\theta,\phi)\bar{Y}_{\ell' m'}(\theta,\phi) d\Omega = \delta_{\ell\ell'}\delta_{mm'}. \tag{2.3.30}$$

Here $d\Omega = \sin\theta\; d\theta\; d\phi$ and the overbar represents complex conjugation.

We can use the covariant derivative D_A to take derivatives of this scalar function to define vector and tensor spherical harmonics. There are even- and odd-parity vector spherical harmonics. We define the even ones as the covariant derivative of the scalar harmonics:

$$Y_A^{\ell m}(\theta,\phi) \equiv D_A Y^{\ell m}(\theta,\phi) \doteq \begin{bmatrix} \partial_\theta Y_{\ell m} \\ \partial_\phi Y_{\ell m} \end{bmatrix}. \tag{2.3.31}$$

In order to create the odd-parity vectorial harmonics we need to define the Levi-Civita tensor on the two-sphere:

$$\varepsilon_{AB} \doteq \begin{bmatrix} 0 & \sin\theta \\ -\sin\theta & 0 \end{bmatrix}. \tag{2.3.32}$$

Using this, the odd-parity harmonics are

$$X_A^{\ell m}(\theta,\phi) \equiv -\varepsilon_A{}^B D_B Y^{\ell m}(\theta,\phi) = -\Omega^{CB}\varepsilon_{AC} Y_B^{\ell m}(\theta,\phi). \tag{2.3.33}$$

Switching to matrices we can calculate the components:

$$X_A^{\ell m}(\theta,\phi) \doteq -\begin{bmatrix} 0 & \sin\theta \\ -\sin\theta & 0 \end{bmatrix}\begin{bmatrix} 1 & 0 \\ 0 & 1/\sin^2\theta \end{bmatrix}\begin{bmatrix} \partial_\theta Y_{\ell m} \\ \partial_\phi Y_{\ell m} \end{bmatrix} \tag{2.3.34}$$

$$\doteq \begin{bmatrix} -\partial_\phi Y_{\ell m}/\sin\theta \\ \sin\theta\ \partial_\theta Y_{\ell m} \end{bmatrix}. \tag{2.3.35}$$

The tensor spherical harmonics also are either even- and odd-parity. There are two even-parity ones,

$$Y_{\ell m}\Omega_{AB} \doteq \begin{bmatrix} Y_{\ell m} & 0 \\ 0 & \sin^2\theta Y_{\ell m} \end{bmatrix} \tag{2.3.36}$$

and the more complicated

$$Y_{AB}^{\ell m} \equiv \left[D_A D_B + \frac{1}{2}\ell(\ell+1)\,\Omega_{AB}\right] Y_{\ell m} \tag{2.3.37}$$

$$= \partial_A\partial_B Y_{\ell m} - \Gamma^C{}_{AB}\partial_C Y_{\ell m} + \frac{1}{2}\ell(\ell+1)\,\Omega_{AB}Y_{\ell m}. \tag{2.3.38}$$

We've already calculated the connection coefficients, so evaluating this is straightforward, leaving us with the components

$$Y_{AB}^{\ell m} \doteq \begin{bmatrix} \left(\partial_\theta^2 + \frac{\ell(\ell+1)}{2}\right) Y_{\ell m} & \left(\partial_\theta\partial_\phi - \cot\theta\ \partial_\phi\right) Y_{\ell m} \\ \left(\partial_\theta\partial_\phi - \cot\theta\ \partial_\phi\right) Y_{\ell m} & \left(\partial_\phi^2 + \sin\theta\cos\theta\ \partial_\theta + \frac{\ell(\ell+1)}{2}\sin^2\theta\right) Y_{\ell m} \end{bmatrix}. \tag{2.3.39}$$

The odd-parity tensor harmonics are

$$X_{AB}^{\ell m} = -\frac{1}{2}\left[\varepsilon_A{}^C D_B + \varepsilon_B{}^C D_A\right] D_C Y_{\ell m} \tag{2.3.40}$$

$$= -\frac{1}{2}\left[\varepsilon_A{}^\theta D_B D_\theta + \varepsilon_A{}^\phi D_B D_\phi + \varepsilon_B{}^\phi D_A D_\theta + \varepsilon_B{}^\phi D_A D_\phi\right] Y_{\ell m}. \tag{2.3.41}$$

In matrix form we have

$$X^{\ell m}_{AB} \doteq \begin{bmatrix} \left(-\frac{1}{\sin\theta}\partial_\theta\partial_\phi + \frac{\cos\theta}{\sin^2\theta}\partial_\phi\right) Y_{\ell m} & -\frac{1}{2}\left(\frac{\partial^2_\phi}{\sin\theta} + \cos\theta\ \partial_\theta - \sin\theta\ \partial^2_\theta\right) Y_{\ell m} \\ -\frac{1}{2}\left(\frac{\partial^2_\phi}{\sin\theta} + \cos\theta\ \partial_\theta - \sin\theta\ \partial^2_\theta\right) Y_{\ell m} & \left(\sin\theta\ \partial_\phi\partial_\theta - \cos\theta\ \partial_\phi\right) Y_{\ell m} \end{bmatrix}. \tag{2.3.42}$$

Now we look at some identities involving these spherical harmonics. We have already seen in Eq. (2.3.30) that the scalar spherical harmonics are orthonormal. Now consider

$$\int Y^A_{\ell m} \bar{Y}^{\ell' m'}_A d\Omega = \frac{1}{r^2}\int \Omega^{AB} D_A Y_{\ell m} D_B \bar{Y}_{\ell' m'} d\Omega \tag{2.3.43}$$

$$= \frac{1}{r^2}\int \left(\partial_\theta Y_{\ell m}\partial_\theta \bar{Y}_{\ell' m'} + \frac{1}{\sin^2\theta}\partial_\phi Y_{\ell m}\partial_\phi \bar{Y}_{\ell' m'}\right)\sin\theta\ d\theta\ d\phi. \tag{2.3.44}$$

We integrate by parts (note that surface terms vanish by periodicity as we integrate of the full 4π steradians) and find

$$\int Y^A_{\ell m} \bar{Y}^{\ell' m'}_A d\Omega = \frac{1}{r^2}\int \Bigg[-\frac{1}{\sin\theta}\partial_\theta\left(\sin\theta\ \partial_\theta Y_{\ell m}\right)\bar{Y}_{\ell' m'} - \frac{1}{\sin^2\theta}\partial^2_\phi Y_{\ell m}\bar{Y}_{\ell' m'}\Bigg]\sin\theta\ d\theta\ d\phi \tag{2.3.45}$$

$$= \frac{1}{r^2}\ell(\ell+1)\delta_{\ell\ell'}\delta_{mm'}. \tag{2.3.46}$$

The odd-parity equivalent is

$$\int X^A_{\ell m} \bar{X}^{\ell' m'}_A d\Omega = \int \varepsilon^A{}_C Y^C_{\ell m} \varepsilon_A{}^B \bar{Y}^{\ell' m'}_B d\Omega. \tag{2.3.47}$$

This 2D contraction of the Levi-Civita tensor gives the negative of the Kronecker delta, and therefore

$$\int X^A_{\ell m} \bar{X}^{\ell' m'}_A d\Omega = \int \delta^B{}_C Y^C_{\ell m} \bar{Y}^{\ell' m'}_B d\Omega = \int Y^A_{\ell m} \bar{Y}^{\ell' m'}_A d\Omega = \frac{1}{r^2}\ell(\ell+1)\delta_{\ell\ell'}\delta_{mm'}. \tag{2.3.48}$$

Now, when we contract the even and odd-parity vector harmonics we get

$$\int Y^A_{\ell m}\bar{X}^{\ell' m'}_A d\Omega = -\int D_A Y^{\ell m}\varepsilon^{AB} D_B \bar{Y}^{\ell' m'} d\Omega. \tag{2.3.49}$$

By parts integration we have

$$\int Y^A_{\ell m}\bar{X}^{\ell' m'}_A d\Omega = \int \varepsilon^{AB} D_A D_B Y^{\ell m}\bar{Y}^{\ell' m'} d\Omega = 0 = \int \bar{Y}^A_{\ell m} X^{\ell' m'}_A d\Omega, \tag{2.3.50}$$

because of the derivatives commute while the Levi-Civita tensor is antisymmetric. Consider now$\Omega^{AB} D_A D_B Y^{\ell m}_C = \Omega^{AB} D_A D_B D_C Y^{\ell m}$. The two closest covariant derivatives commute, but we have to use the rule

$$[D_A, D_B]\, V^C = R^C{}_{DAB} V^D \qquad \Rightarrow \qquad [D_A, D_B]\, V_C = R_C{}^D{}_{AB} V_D \tag{2.3.51}$$

to commute the outer two, and therefore

$$\Omega^{AB} D_A D_B Y^{\ell m}_C = \Omega^{AB} D_A D_C D_B Y^{\ell m} \tag{2.3.52}$$

$$= \Omega^{AB}\left(D_C D_A D_B + R_B{}^D{}_{AC} D_D\right) Y^{\ell m}. \tag{2.3.53}$$

Using the differential equation for the scalar harmonics, we get

$$\Omega^{AB} D_A D_B Y^{\ell m}_C = -\ell(\ell+1) Y^{\ell m}_C + \Omega^{AB}\frac{1}{r^2}\Omega^{DE}\left(\Omega_{BA}\Omega_{EC} - \Omega_{BC}\Omega_{EA}\right) Y^{\ell m}_D \tag{2.3.54}$$

$$= \Big[1 - \ell(\ell+1)\Big] Y^{\ell m}_C. \tag{2.3.55}$$

Additionally, we have

$$\Omega^{AB} D_A D_B X^{\ell m}_C = -\varepsilon_C{}^D \Omega^{AB} D_A D_B Y^{\ell m}_D = \Big[1 - \ell(\ell+1)\Big] X^{\ell m}_C. \tag{2.3.56}$$

Taking the divergence $Y^A_{\ell m}$ and $X^A_{\ell m}$ gives

$$D_A Y^A_{\ell m} = \frac{1}{r^2}\Omega^{AB} D_A D_B Y_{\ell m} = -\frac{\ell(\ell+1)}{r^2} Y_{\ell m} \tag{2.3.57}$$

$$D_A X^A_{\ell m} = -\frac{1}{r^2}\Omega^{AB} D_A \varepsilon_B{}^C D_C Y_{\ell m} = -\frac{1}{r^2}\varepsilon^{AC} D_A D_C Y_{\ell m} = 0. \tag{2.3.58}$$

Now we consider contractions of the tensor harmonics. First of all, because they are each trace free, we have

$$\Omega^{AB} Y^{\ell m}_{AB} = \Omega^{AB} X^{\ell m}_{AB} = 0. \tag{2.3.59}$$

This is clear from inspecting the matrix forms of these harmonics above. Note that this implies that both $Y^{\ell m}_{AB}$ and $X^{\ell m}_{AB}$ are orthogonal to $\Omega_{AB} Y_{\ell m}$. Now, we consider

$$\int Y^{AB}_{\ell m} \bar{Y}^{\ell' m'}_{AB} d\Omega$$

$$= \int g^{AC} g^{BD} \left[D_C D_D + \frac{\ell\,(\ell+1)}{2}\Omega_{DC} \right] Y_{\ell m} \left[D_A D_B + \frac{\ell'\,(\ell'+1)}{2}\Omega_{AB} \right] \bar{Y}^{\ell' m'} d\Omega \tag{2.3.60}$$

$$= \frac{1}{r^4} \int \left[-\Omega^{AC}\Omega^{BD} D_A D_C D_D Y_{\ell m} D_B \bar{Y}^{\ell' m'} - \frac{1}{2}\ell'\left(\ell'+1\right)\ell\,(\ell+1)\, Y_{\ell m} \bar{Y}^{\ell' m'} \right] d\Omega \tag{2.3.61}$$

So, in order to evaluate this we need the harmonic operator $(\Omega^{AB} D_A D_B)$ acting on Y_C, which we calculated above. Using it and the completeness of the scalar harmonics gives

$$\int Y^{AB}_{\ell m} \bar{Y}^{\ell' m'}_{AB} d\Omega$$

$$= \frac{1}{r^4} \int \left[-\Omega^{BD} \Big[1 - \ell(\ell+1) \Big] D_D Y_{\ell m} D_B \bar{Y}^{\ell' m'} \right] d\Omega - \frac{1}{2r^4}\ell^2\,(\ell+1)^2\,\delta_{\ell\ell'}\delta_{mm'} \tag{2.3.62}$$

$$= \frac{1}{2r^4}(\ell-1)\ell\,(\ell+1)\,(\ell+2)\delta_{\ell\ell'}\delta_{mm'}. \tag{2.3.63}$$

A similar, though slightly longer calculation for the odd-parity case gives

$$\int X^{AB}_{\ell m} \bar{X}^{\ell' m'}_{AB} d\Omega = \frac{1}{2r^4}(\ell-1)\ell\,(\ell+1)\,(\ell+2)\delta_{\ell\ell'}\delta_{mm'}. \tag{2.3.64}$$

For the divergence of the tensor harmonics we first consider the even-parity case,

$$D^B Y^{\ell m}_{AB} = \frac{1}{r^2}\Omega^{BC} D_C \left[D_A D_B Y^{\ell m} + \frac{1}{2}\ell\left(\ell+1\right)\Omega_{AB} Y^{\ell m}\right], \tag{2.3.65}$$

$$= \frac{1}{r^2}\Omega^{BC}\left(D_A D_C D_B Y^{\ell m} + R_B{}^D{}_{CA} D_D Y^{\ell m}\right) + \frac{1}{2r^2}\ell\left(\ell+1\right) D_A Y^{\ell m}, \tag{2.3.66}$$

$$= \frac{1}{r^2}\left[1 - \frac{1}{2}\ell\left(\ell+1\right)\right] Y^{\ell m}_A. \tag{2.3.67}$$

For the odd-parity harmonics we have

$$D^B X^{\ell m}_{AB} = \frac{1}{2}\frac{1}{r^2}\Omega^{BD} D_D \left[D_B X^{\ell m}_A + D_A X^{\ell m}_B\right], \tag{2.3.68}$$

$$= \frac{1}{2r^2}\Big[1 - \ell(\ell+1)\Big] X^{\ell m}_A + \frac{1}{2r^2}\Omega^{BD}\left(D_A D_D X^{\ell m}_B + R_{BCDA} X^C_{\ell m}\right). \tag{2.3.69}$$

The divergence of $X^{\ell m}_B$ vanishes, so we are left with

$$D^B X^{\ell m}_{AB} = \frac{1}{2r^2}\Big[1 - \ell(\ell+1)\Big] X^{\ell m}_A + \frac{1}{2r^2}\Omega^{BD} r^2\left(\Omega_{BD}\Omega_{CA} - \Omega_{BA}\Omega_{CD}\right) X^C_{\ell m}, \tag{2.3.70}$$

$$= \frac{1}{r^2}\left[1 - \frac{1}{2}\ell\left(\ell+1\right)\right] X^{\ell m}_A. \tag{2.3.71}$$

Recurrence relation

Here we present a recurrence relation for the harmonics, which is useful when doing numerical calculations. First, we separate them into functions of θ and ϕ alone

$$Y_{\ell m}(\theta,\phi) = A^m_\ell(x) e^{im\phi}, \qquad x \equiv \cos\theta \tag{2.3.72}$$

with

$$A^m_\ell(x) = \sqrt{\frac{2\ell+1}{4\pi}\frac{(\ell-m)!}{(\ell+m)!}}\; P^m_\ell(x). \tag{2.3.73}$$

Next, consider the recursion relation for the associated Legendre functions

$$(\ell - m)\, P^m_\ell(x) = (2\ell-1) x P^m_{\ell-1}(x) - (\ell+m-1) P^m_{\ell-2}(x). \tag{2.3.74}$$

We'll use this to develop a recursion relation for our functions A_ℓ^m, and then extend that to the spherical harmonics. Now, using Eq. (2.3.73) to express the associated Legendre functions in terms of A_ℓ^m, we have

$$P_\ell^m(x) = \sqrt{\frac{4\pi}{2\ell+1}\frac{(\ell+m)!}{(\ell-m)!}}A_\ell^m(x) \tag{2.3.75}$$

$$P_{\ell-1}^m(x) = \sqrt{\frac{4\pi}{2\ell-1}\frac{(\ell+m-1)!}{(\ell-m-1)!}}A_{\ell-1}^m(x) \tag{2.3.76}$$

$$P_{\ell-2}^m(x) = \sqrt{\frac{4\pi}{2\ell-3}\frac{(\ell+m-2)!}{(\ell-m-2)!}}A_{\ell-2}^m(x). \tag{2.3.77}$$

Plugging into Eq. (2.3.74) we get

$$A_\ell^m(x) = x\sqrt{\frac{(2\ell+1)(2\ell-1)}{(\ell+m)(\ell-m)}}A_{\ell-1}^m(x) - \sqrt{\frac{2\ell+1}{2\ell-3}\frac{(\ell+m-1)(\ell-m-1)}{(\ell+m)(\ell-m)}}A_{\ell-2}^m(x). \tag{2.3.78}$$

Then, multiplying through by $e^{im\phi}$ and recalling that $x \equiv \cos\theta$ we have our recursion relation

$$Y_{\ell m} = \cos\theta\sqrt{\frac{(2\ell+1)(2\ell-1)}{(\ell+m)(\ell-m)}}Y_{\ell-1,m} - \sqrt{\frac{2\ell+1}{2\ell-3}\frac{(\ell+m-1)(\ell-m-1)}{(\ell+m)(\ell-m)}}Y_{\ell-2,m}. \tag{2.3.79}$$

This is a bit strange as recursion relations go. One might expect for a given ℓ, to start with $Y_{\ell 0}$ and then calculate $Y_{\ell 1}$, then $Y_{\ell 2}$, up to $Y_{\ell\ell}$, but this is not what we have found. Rather, for a given value of m, we can calculate the next value of ℓ.

In order to use the recursion relation, we need a way to get started. This is provided by the identity

$$P_m^m(x) = (-1)^m(2m-1)!!\left(1-x^2\right)^{m/2}. \tag{2.3.80}$$

Absorbing the coefficient from Eq. (2.3.72) this becomes

$$A_m^m(x) = (-1)^m\sqrt{\frac{2m+1}{4\pi}\frac{(m-m)!}{(m+m)!}}(2m-1)!!\left(1-x^2\right)^{m/2}. \tag{2.3.81}$$

This is a perfectly valid expression, but if we manipulate it, we can put it in a form that will

be much easier to use numerically. Expanding out the factorials and multiplying through by $\exp(im\phi)$.

$$Y_{mm} = \frac{(-1)^m}{\sqrt{4\pi}} \sqrt{\left(\frac{2m+1}{2m}\right)\left(\frac{2m-1}{2m-2}\right)\cdots\left(\frac{5}{4}\right)\left(\frac{3}{2}\right)} \,(\sin\theta)^m \, e^{im\phi}. \tag{2.3.82}$$

This is a useful form of this equation because each of the terms under the radical is on the order of one.

To calculate the derivatives of the spherical harmonics we need another recursion relation. The ϕ derivatives are easy. From Eq. (2.3.72) we see

$$\frac{\partial Y_{\ell m}}{\partial \phi} = imY_{\ell m}. \tag{2.3.83}$$

For the θ derivatives, we return to Eq. (2.3.79), giving

$$\begin{aligned}\frac{\partial Y_{\ell m}}{\partial \theta} = \sqrt{\frac{(2\ell+1)(2\ell-1)}{(\ell+m)(\ell-m)}} \,(\cos\theta \;\partial_\theta \,(Y_{\ell-1,m}) - \sin\theta \; Y_{\ell-1,m}) \\ - \sqrt{\frac{2\ell+1}{2\ell-3}\frac{(\ell+m-1)(\ell-m-1)}{(\ell+m)(\ell-m)}}\partial_\theta \,(Y_{\ell-2,m})\end{aligned} \tag{2.3.84}$$

If we want to use these recursion relations, we need somewhere to start. Returning to look at Eq. (2.3.82), we see that

$$\frac{\partial Y_{mm}}{\partial \theta} = \frac{(-1)^m}{\sqrt{4\pi}} \sqrt{\left(\frac{2m+1}{2m}\right)\left(\frac{2m-1}{2m-2}\right)\cdots\left(\frac{5}{4}\right)\left(\frac{3}{2}\right)} \,(m\cdot\sin^m\theta\cdot\cos\theta)\, e^{im\phi}. \tag{2.3.85}$$

The benefit of this expression is that, although the *total* numerator and the *total* denominator under the radical can be very large numbers, if we group the terms wisely, the quotient can be computed with no numerical trouble.

Now, let's consider second derivatives. The ϕ derivatives are simpler again. First, we have

$$\frac{\partial^2 Y_{\ell m}}{\partial \phi^2} = -m^2 \; Y_{\ell m}. \tag{2.3.86}$$

Also, we have, for both of the mixed partials

$$\frac{\partial^2 Y_{\ell m}}{\partial\phi\,\partial\theta} = \frac{\partial^2 Y_{\ell m}}{\partial\theta\,\partial\phi} = im\frac{\partial Y_{\ell m}}{\partial\theta} \tag{2.3.87}$$

The plot gets more interesting with the second θ derivative of $Y_{\ell m}$. Returning to Eq. (2.3.84), we directly differentiate to get

$$\begin{aligned}\frac{\partial^2 Y_{\ell m}}{\partial\theta^2} = \sqrt{\frac{(2\ell+1)(2\ell-1)}{(\ell+m)(\ell-m)}}\left(\cos\theta\;\partial_\theta^2\left(Y_{\ell-1,m}\right) - 2\sin\theta\;\partial_\theta Y_{\ell-1,m} - \cos\theta\;Y_{\ell-1,m}\right)\\ - \sqrt{\frac{2\ell+1}{2\ell-3}\frac{(\ell+m-1)(\ell-m-1)}{(\ell+m)(\ell-m)}}\partial_\theta^2\left(Y_{\ell-2,m}\right).\end{aligned} \tag{2.3.88}$$

This section has provided a practical way of computing spherical harmonics for arbitrarily high ℓ, m values. The recurrence relation is useful because the standard textbook expressions (e.g. [31]) are not practical numerically, as the factorial terms grow inconveniently large.

2.4 First-order field equations

2.4.1 Harmonic decomposition

Martel and Poisson [55] give covariant and gauge-invariant field equations. Following their lead, we decompose the metric perturbation $p_{\mu\nu}$ as

$$\begin{aligned}p_{ab}\left(x^\mu\right) &= \sum_{\ell,m} h_{ab}^{\ell m} Y^{\ell m},\\ p_{aB}\left(x^\mu\right) &= \sum_{\ell,m}\left[j_a^{\ell m} Y_B^{\ell m} + h_a^{\ell m} X_B^{\ell m}\right],\\ p_{AB}\left(x^\mu\right) &= \sum_{\ell,m}\left[r^2\left(K^{\ell m}\Omega_{AB}Y^{\ell m} + G^{\ell m}Y_{AB}^{\ell m}\right) + h_2^{\ell m}X_{AB}^{\ell m}\right].\end{aligned} \tag{2.4.1}$$

We refer to the coefficients of the spherical harmonics $(h_{ab}^{\ell m}, j_a^{\ell m}, h_a^{\ell m}, K^{\ell m}, G^{\ell m}, h_2^{\ell m})$ as the metric perturbation amplitudes (or just amplitudes for short). They are functions of only t and r. Inserting Eq. (2.4.1) into the first-order Einstein equations (2.2.17), yields field

equations for the amplitudes. Martel and Poisson give the details of how the equations are derived. We follow their lead and start by writing the field equations for gauge-invariant quantities in Schwarzschild coordinates. We show how this is equivalent to writing the field equations in Regge-Wheeler gauge. We then write them in a gauge-undefined way and eventually Lorenz gauge. Through the rest of this section we suppress ℓ and m indices for brevity.

Even-parity sector

In the even-parity sector there are four gauge-invariant fields, formed from linear combinations of the metric perturbation amplitudes and their first derivatives [55]

$$\begin{aligned}
\tilde{h}_{tt} &= h_{tt} - 2\partial_t j_t + \frac{2Mf}{r^2} j_r + r^2 \partial_t^2 G - Mf\partial_r G \\
\tilde{h}_{tr} &= h_{tr} - \partial_r j_t - \partial_t j_r + \frac{2M}{fr^2} j_t + r^2 \partial_t \partial_r G + \frac{r-3M}{f}\partial_t G \\
\tilde{h}_{rr} &= h_{rr} - 2\partial_r j_r - \frac{2M}{fr^2} j_r + r^2 \partial_r^2 G + \frac{2r-3M}{f}\partial_r G \\
\tilde{K} &= K - \frac{2f}{r} j_r + rf\partial_r G + (\lambda+1)G.
\end{aligned} \tag{2.4.2}$$

Written in terms of those gauge-invariant fields, the seven field equations are

$$-\partial_r^2 \tilde{K} - \frac{3r-5M}{r^2 f}\partial_r \tilde{K} + \frac{f}{r}\partial_r \tilde{h}_{rr} + \frac{(\lambda+2)\,r+2M}{r^3}\tilde{h}_{rr} + \frac{\lambda}{r^2 f}\tilde{K} = Q^{tt}, \tag{2.4.3}$$

$$\partial_t \partial_r \tilde{K} + \frac{r-3M}{r^2 f}\partial_t \tilde{K} - \frac{f}{r}\partial_t \tilde{h}_{rr} - \frac{\lambda+1}{r^2}\tilde{h}_{tr} = Q^{tr}, \tag{2.4.4}$$

$$\begin{aligned}
-\partial_t^2 \tilde{K} + \frac{(r-M)f}{r^2}\partial_r \tilde{K} + \frac{2f}{r}\partial_t \tilde{h}_{tr} - \frac{f}{r}\partial_r \tilde{h}_{tt} \\
+ \frac{(\lambda+1)r+2M}{r^3}\tilde{h}_{tt} - \frac{f^2}{r^2}\tilde{h}_{rr} - \frac{\lambda f}{r^2}\tilde{K} = Q^{rr},
\end{aligned} \tag{2.4.5}$$

$$\partial_t \tilde{h}_{rr} - \partial_r \tilde{h}_{tr} + \frac{1}{f}\partial_t \tilde{K} - \frac{2M}{r^2 f}\tilde{h}_{tr} = Q^{t}, \tag{2.4.6}$$

$$-\partial_t \tilde{h}_{tr} + \partial_r \tilde{h}_{tt} - f\partial_r \tilde{K} - \frac{r-M}{r^2 f}\tilde{h}_{tt} + \frac{(r-M)f}{r^2}\tilde{h}_{rr} = Q^{r}, \tag{2.4.7}$$

$$
\begin{aligned}
&-\partial_t^2\tilde{h}_{rr} + 2\partial_t\partial_r\tilde{h}_{tr} - \partial_r^2\tilde{h}_{tt} - \frac{1}{f}\partial_t^2\tilde{K} + f\partial_r^2\tilde{K} \\
&+\frac{2(r-M)}{r^2 f}\partial_t\tilde{h}_{tr} - \frac{r-3M}{r^2 f}\partial_r\tilde{h}_{tt} - \frac{(r-M)f}{r^2}\partial_r\tilde{h}_{rr} + \frac{2(r-M)}{r^2}\partial_r\tilde{K} \\
&\quad+\frac{(\lambda+1)r^2 - 2(\lambda+2)Mr + 2M^2}{r^4 f^2}\tilde{h}_{tt} - \frac{(\lambda+1)r^2 - 2\lambda Mr - 2M^2}{r^4}\tilde{h}_{rr} = Q^\flat,
\end{aligned}
\tag{2.4.8}
$$

$$
\frac{1}{f}\tilde{h}_{tt} - f\tilde{h}_{rr} = Q^\sharp, \tag{2.4.9}
$$

which have source terms

$$
\begin{aligned}
Q^{ab}(t,r) &\equiv 8\pi\int T^{ab}Y^*\,d\Omega, \qquad Q^a(t,r) \equiv \frac{16\pi r^2}{\ell(\ell+1)}\int T^{aB}Y^*_B\,d\Omega, \\
Q^\flat(t,r) &\equiv 8\pi r^2\int T^{AB}\Omega_{AB}Y^*\,d\Omega, \qquad Q^\sharp(t,r) \equiv 32\pi r^4\frac{(\ell-2)!}{(\ell+2)!}\int T^{AB}Y^*_{AB}\,d\Omega.
\end{aligned}
\tag{2.4.10}
$$

Odd-parity sector

In the odd-parity sector there are two gauge-invariant fields, formed from linear combinations of the metric perturbation amplitudes and their first derivatives [55]

$$
\tilde{h}_t \equiv h_t - \frac{1}{2}\frac{\partial h_2}{\partial t}, \qquad \tilde{h}_r \equiv h_r - \frac{1}{2}\frac{\partial h_2}{\partial r} + \frac{h_2}{r}. \tag{2.4.11}
$$

Written in terms of those gauge-invariant fields, the three field equations are

$$
-\partial_t\partial_r\tilde{h}_r + \partial_r^2\tilde{h}_t - \frac{2}{r}\partial_t\tilde{h}_r - \frac{2(\lambda+1)r - 4M}{r^3 f}\tilde{h}_t = P^t, \tag{2.4.12}
$$

$$
\partial_t^2\tilde{h}_r - \partial_t\partial_r\tilde{h}_t + \frac{2}{r}\partial_t\tilde{h}_t + \frac{2\lambda f}{r^2}\tilde{h}_r = P^r, \tag{2.4.13}
$$

$$
-\frac{1}{f}\partial_t\tilde{h}_t + f\partial_r\tilde{h}_r + \frac{2M}{r^2}\tilde{h}_r = P, \tag{2.4.14}
$$

which have source terms

$$
P^a(t,r) \equiv \frac{16\pi r^2}{\ell(\ell+1)}\int T^{aB}X^*_B\,d\Omega, \qquad P(t,r) \equiv 16\pi r^4\frac{(\ell-2)!}{(\ell+2)!}\int T^{AB}X^*_{AB}\,d\Omega. \tag{2.4.15}
$$

2.4.2 Regge-Wheeler gauge

Regge-Wheeler is an algebraic gauge in which four of the ten components of the metric perturbation are set to zero. This leads to a dramatic simplification of the field equations, but introduces some gauge artifacts which must be dealt with carefully (see Chapter 5).

Even-parity sector

We use our gauge freedom to set $G = j^t = j^r = 0$. Examining the gauge invariant quantities, we find

$$\tilde{h}_{tt} = h_{tt}, \qquad \tilde{h}_{tr} = h_{tr}, \qquad \tilde{h}_{rr} = h_{rr}, \qquad \tilde{K} = K. \tag{2.4.16}$$

Therefore, the fields in RW gauge are the gauge-invariant fields themselves, and the field equations in RW gauge are simply those given above with all the tildes removed. Incidentally, note that if one has the metric perturbation in another gauge, it is trivial to obtain it in RW: simply form the gauge-invariant fields; those are the fields in RW gauge. This is a powerful and straightforward way of checking if two first-order answers to the Einstein equations, computed in different gauges, are indeed the same solutions.

At this point, it is common to reduce the even-parity field equations to one master equation. After solving the master equation, the metric perturbation can be reconstructed. Details of this can be found in Chapter 4.

Odd-parity sector

We use our gauge freedom to set h_2. Examining the gauge invariant quantities, we find

$$\tilde{h}_t = h_t, \qquad \tilde{h}_r = h_r. \tag{2.4.17}$$

Therefore, the fields in RW gauge are the gauge-invariant fields themselves, and the field equations in RW gauge are simply those given above with all the tildes removed. Again, if one has the metric perturbation in another gauge, it is trivial to obtain it in RW: simply form the gauge-invariant fields; those are the fields in RW gauge.

At this point, it is also common to reduce the odd-parity field equations to one master equation. After solving the master equation, the metric perturbation can be reconstructed. Details of this can also be found in Chapter 4.

2.4.3 Lorenz gauge

We now form the Lorenz gauge field equations in a number of steps. We start by deriving the four Lorenz gauge conditions for each mode. Three of these are in the even-parity sector and one is odd. Then, we insert the gauge-invariant equations above into the gauge-invariant fields. This gives a set of "gauge-undefined" equations. Finally, we impose the Lorenz gauge condition and obtain the field equations in Lorenz gauge.

The Lorenz gauge condition is $\bar{p}^{\mu\nu}{}_{|\nu} = 0$, which we expand as

$$\bar{p}^{\mu\nu}{}_{|\nu} = \bar{p}^{\mu\nu}{}_{,\nu} + {}^4\Gamma^{\mu}{}_{\alpha\beta}\bar{p}^{\alpha\beta} + {}^4\Gamma^{\alpha}{}_{\beta\alpha}\bar{p}^{\mu\beta} = 0. \tag{2.4.18}$$

Now, after the divergence is taken we are left with a vector. The part on the $\mathcal{M}^2$ sector is

$$\begin{aligned}\bar{p}^{a\nu}{}_{|\nu} = \bar{p}^{ab}{}_{,b} + \bar{p}^{aB}{}_{,B} + {}^4\Gamma^{a}{}_{bc}\bar{p}^{bc} + {}^4\Gamma^{a}{}_{BC}\bar{p}^{BC} + {}^4\Gamma^{a}{}_{bC}\bar{p}^{bC} + {}^4\Gamma^{a}{}_{Bc}\bar{p}^{Bc} \\ + {}^4\Gamma^{b}{}_{cb}\bar{p}^{ac} + {}^4\Gamma^{b}{}_{Bb}\bar{p}^{aB} + {}^4\Gamma^{A}{}_{bA}\bar{p}^{ab} + {}^4\Gamma^{A}{}_{BA}\bar{p}^{aB} = 0.\end{aligned} \tag{2.4.19}$$

When we write the connection coefficients with a pre-superscript 4, it indicates that this is a connection coefficient of the full 4D spacetime. These are related to the connection terms on $\mathcal{M}^2$ and $\mathcal{S}^2$ by [recall the definition of r^a in Eq. (2.3.13)]

$$\begin{aligned} {}^4\Gamma^{a}{}_{bc} = \Gamma^{a}{}_{bc}, \qquad {}^4\Gamma^{A}{}_{BC} = \Gamma^{A}{}_{BC}, \qquad {}^4\Gamma^{a}{}_{Bc} = {}^4\Gamma^{a}{}_{cB} = 0, \\ {}^4\Gamma^{a}{}_{BC} = -rr^a\Omega_{BC}, \qquad {}^4\Gamma^{A}{}_{Bc} = {}^4\Gamma^{A}{}_{cB} = \frac{1}{r}r_c\delta^{A}{}_{B}, \qquad {}^4\Gamma^{A}{}_{bc} = 0. \end{aligned} \tag{2.4.20}$$

Then, Eq. (2.4.19) becomes

$$\bar{p}^{a\nu}{}_{|\nu} = \bar{p}^{ab}{}_{,b} + \bar{p}^{aB}{}_{,B} + \Gamma^{a}{}_{bc}\bar{p}^{bc} - rr^a\Omega_{BC}\bar{p}^{BC} + \Gamma^{b}{}_{cb}\bar{p}^{ac} + \frac{1}{r}r_b\delta^{A}{}_{A}\bar{p}^{ab} + \Gamma^{A}{}_{BA}\bar{p}^{aB}, \tag{2.4.21}$$

$$= \nabla_b\bar{p}^{ab} + D_B\bar{p}^{aB} - rr^a\Omega_{BC}\bar{p}^{BC} + \frac{2}{r}r_b\bar{p}^{ab} = 0. \tag{2.4.22}$$

Lowering indices we have

$$g_{ac}\bar{p}^{a\nu}{}_{|\nu} = g_{ac}\nabla_b\bar{p}^{ab} + g_{ac}g^{BC}D_B\bar{p}^a{}_C - g_{ac}\frac{1}{r}r^a g^{BD}g^{CE}g_{BC}\bar{p}_{DE} + g_{ac}\frac{2}{r}r^b\bar{p}^a{}_b, \tag{2.4.23}$$

$$= \nabla^b\bar{p}_{cb} + \frac{1}{r^2}\Omega^{BC}D_B\bar{p}_{cC} - r_c\frac{1}{r^3}\Omega^{DE}\bar{p}_{DE} + \frac{2}{r}r^b\bar{p}_{cb} = 0. \tag{2.4.24}$$

The part of the vector on the two-sphere is

$$\bar{p}^{A\nu}{}_{|\nu} = \bar{p}^{Ab}{}_{,b} + \bar{p}^{AB}{}_{,B} + {}^4\Gamma^A{}_{bc}\bar{p}^{bc} + {}^4\Gamma^A{}_{BC}\bar{p}^{BC} + {}^4\Gamma^A{}_{bC}\bar{p}^{bC} + {}^4\Gamma^A{}_{Bc}\bar{p}^{Bc}$$
$$+ {}^4\Gamma^b{}_{cb}\bar{p}^{Ac} + {}^4\Gamma^b{}_{Bb}\bar{p}^{AB} + {}^4\Gamma^B{}_{bB}\bar{p}^{Ab} + {}^4\Gamma^C{}_{BC}\bar{p}^{AB} = 0. \tag{2.4.25}$$

Substituting for the full, 4D connections we have

$$\bar{p}^{A\nu}{}_{|\nu} = \bar{p}^{Ab}{}_{,b} + \bar{p}^{AB}{}_{,B} + \Gamma^A{}_{BC}\bar{p}^{BC} + \frac{1}{r}r_b\bar{p}^{bA}$$
$$+ \frac{1}{r}r_c\bar{p}^{Ac} + \Gamma^b{}_{cb}\bar{p}^{Ac} + \frac{2}{r}r_b\bar{p}^{Ab} + \Gamma^C{}_{BC}\bar{p}^{AB}, \tag{2.4.26}$$

$$= \nabla_b\bar{p}^{Ab} + D_B\bar{p}^{AB} + \frac{4}{r}r_b\bar{p}^{Ab} = 0. \tag{2.4.27}$$

Again, we lower indices, giving

$$g_{AC}\bar{p}^{A\nu}{}_{|\nu} = r^2\Omega_{AC}\nabla_b\bar{p}^{Ab} + D^B\bar{p}_{CB} + \frac{4}{r}r^b\bar{p}_{Cb}, \tag{2.4.28}$$

$$= \nabla_b\Big(r^2\Omega_{AC}\bar{p}^{Ab}\Big) - \nabla_b\left(r^2\right)\Omega_{AC}\bar{p}^{Ab} + D^B\bar{p}_{CB} + \frac{4}{r}r^b\bar{p}_{Cb}, \tag{2.4.29}$$

$$= \nabla^b\bar{p}_{Cb} + D^B\bar{p}_{CB} + \frac{2}{r}r^b\bar{p}_{Cb} = 0. \tag{2.4.30}$$

The metric perturbation expands as given in Eq. (2.4.1), so its trace-reverse is

$$\bar{p}_{\mu\nu} = p_{\mu\nu} - \frac{1}{2}g_{\mu\nu}\left[g^{ab}h_{ab}Y + g^{AB}\Big(r^2\left(K\Omega_{AB}Y + GY_{AB}\right) + h_2X_{AB}\Big)\right]. \tag{2.4.31}$$

Both Y_{AB} and X_{AB} are trace-free, and therefore

$$\bar{p}_{\mu\nu} = p_{\mu\nu} - \frac{1}{2}g_{\mu\nu}\Big(g^{ab}h_{ab} + 2K\Big)Y. \tag{2.4.32}$$

The trace-reverse for the different sectors is

$$\bar{p}_{ab} = \left(h_{ab} - \frac{1}{2}g_{ab}\left(h^c{}_c + 2K\right)\right)Y, \tag{2.4.33}$$

$$\bar{p}_{aB} = j_a Y_B + h_a X_B, \tag{2.4.34}$$

$$\bar{p}_{AB} = r^2\Big(K\Omega_{AB}Y + GY_{AB}\Big) + h_2 X_{AB} - \frac{1}{2}g_{AB}\left(h^c{}_c + 2K\right)Y, \tag{2.4.35}$$

$$= r^2\left(-\frac{1}{2}h^c{}_c\Omega_{AB}Y + GY_{AB}\right) + h_2 X_{AB}. \tag{2.4.36}$$

Inserting these in Eq. (2.4.24) yields

$$\begin{aligned} g^{ab}\nabla_a\left[h_{cb} - \frac{1}{2}g_{cb}\left(h^d{}_d + 2K\right)\right]Y + \frac{1}{r^2}\Omega^{BC}D_B\left(j_c Y_C + h_c X_C\right) \\ - r_c\frac{1}{r^3}\Omega^{DE}\left[r^2\left(-\frac{1}{2}h^d{}_d\Omega_{DE}Y + GY_{DE}\right) + h_2 X_{DE}\right] \\ + \frac{2}{r}r^b\left[h_{cb} - \frac{1}{2}g_{cb}\left(h^d{}_d + 2K\right)\right]Y = 0. \end{aligned} \tag{2.4.37}$$

The tensor harmonics Y_{AB} and X_{AB} are trace-free, so (using the completeness of the scalar harmonics and simplifying)

$$g^{ab}\nabla_a\left[h_{cb} - \frac{1}{2}g_{cb}\left(h^d{}_d + 2K\right)\right] - \frac{j_c}{r^2}\ell(\ell+1) + \frac{2}{r}r^b h_{cb} - \frac{2}{r}r_c K = 0. \tag{2.4.38}$$

The part of the vector on the two-sphere is

$$\begin{aligned} \bar{p}^{A\nu}{}_{|\nu} = \left(\nabla_b + \frac{4}{r}r_b\right)\left(j^b Y^A + h^b X^A\right) \\ + D_B\left[r^2\left(-\frac{1}{2}h^c{}_c\Omega^{AB}Y + GY^{AB}\right) + h_2 X^{AB}\right] = 0. \end{aligned} \tag{2.4.39}$$

Using identities derived in Sec. 2.3.2 to rewrite the divergences of the tensor harmonics,

$$\bar{p}^{A\nu}{}_{|\nu} = \left(\nabla_b + \frac{4}{r}r_b\right)\left(j^b Y^A + h^b X^A\right) - \left(\frac{1}{2}h^c{}_c - \lambda G\right)Y^A - \frac{\lambda}{r^2}h_2 X^A = 0. \tag{2.4.40}$$

Now, we use the orthogonality of the vector harmonics. First, multiplying by the even-parity vector harmonic kills off the odd-parity terms and leaves behind an equation in only

t and r,

$$\nabla_b \left(j^b \frac{1}{r^2} \right) + \frac{4}{r} r_b j^b \frac{1}{r^2} + r^2 \left[-\frac{1}{2r^2} h^c{}_c + \frac{1}{r^2} \left(1 - \frac{1}{2} \ell \left(\ell + 1 \right) \right) G \right] \frac{1}{r^2} = 0. \tag{2.4.41}$$

Now, simplifying and defining $\lambda \equiv (\ell + 2)(\ell - 1)/2$,

$$\left(\nabla_b + \frac{2}{r} r_b \right) j^b - \frac{1}{2} h^c{}_c - \lambda G = 0. \tag{2.4.42}$$

For the odd parity we return to Eq. (2.4.40). The orthogonality condition for the X_A will create a r^{-2} term that modifies the $4r_b/r$. In the end, the scalar equation we are left with is

$$\left(\nabla_b + \frac{2}{r} r_b \right) h^b - \frac{\lambda}{r^2} h_2 = 0. \tag{2.4.43}$$

Even-parity field equations

First, for the gauge conditions on the $\mathcal{M}^2$ sector

$$g^{ab} \left(\partial_a h_{cb} - \Gamma^d{}_{ab} h_{cd} - \Gamma^d{}_{ac} h_{db} \right) - \frac{1}{2} \partial_c h^d{}_d \\ - \partial_c K - \frac{j_c}{r^2} \ell(\ell + 1) + \frac{2}{r} r^b h_{cb} - \frac{r_c}{r} 2K = 0. \tag{2.4.44}$$

Plugging in for the connection terms, we get two equations,

$$-\frac{1}{2f} \partial_t h_{tt} - \frac{f}{2} \partial_t h_{rr} + f \partial_r h_{tr} - \partial_t K + \frac{2}{r^2} \left(r - M \right) h_{rt} - \frac{\ell(\ell + 1)}{r^2} j_t = 0, \tag{2.4.45}$$

$$-\frac{1}{f} \partial_t h_{rt} + \frac{f}{2} \partial_r h_{rr} + \frac{1}{2f} \partial_r h_{tt} - \partial_r K - \frac{\ell(\ell + 1)}{r^2} j_r + \frac{2}{r^2} \left(r - M \right) h_{rr} - \frac{2}{r} K = 0. \tag{2.4.46}$$

The even-parity gauge condition on the two-sphere reduces to

$$-\frac{1}{f} \partial_t j_t + f \partial_r j_r + \frac{2}{r^2} \left(r - M \right) j_r + \frac{1}{2f} h_{tt} - \frac{f}{2} h_{rr} - \lambda G = 0. \tag{2.4.47}$$

Plugging in the gauge-invariant fields, we obtain a set of gauge-undefined Einstein equations,

$$-\partial_r^2 K - \frac{3r-5M}{r^2 f}\partial_r K + \frac{f}{r}\partial_r h_{rr} - 2\frac{(\lambda+1)}{r^2}\partial_r j_r + 2\frac{(\lambda+1)(M-r)}{r^4 f} j_r + \frac{\lambda(\lambda+1)}{r^2 f} G + \frac{(\lambda+2)\, r + 2M}{r^3} h_{rr} + \frac{\lambda}{r^2 f} K = Q^{tt}, \tag{2.4.48}$$

$$\partial_t \partial_r K + \frac{r-3M}{r^2 f}\partial_t K - \frac{f}{r}\partial_t h_{rr} + \frac{\lambda+1}{r^2}\partial_t j_r + \frac{\lambda+1}{r^2}\partial_r j_t - \frac{\lambda+1}{r^2} h_{tr} - \frac{2M(\lambda+1)}{r^4 f} j_t = Q^{tr}, \tag{2.4.49}$$

$$-\partial_t^2 K + \frac{(r-M)f}{r^2}\partial_r K + \frac{2f}{r}\partial_t h_{tr} - \frac{f}{r}\partial_r h_{tt} - 2\frac{\lambda+1}{r^2}\partial_t j_t + \frac{(\lambda+1)r+2M}{r^3} h_{tt} - \frac{f^2}{r^2} h_{rr} - \frac{\lambda f}{r^2} K - \frac{f\lambda(\lambda+1)}{r^2} G + 2\frac{f(r-M)(\lambda+1)}{r^4} j_r = Q^{rr}, \tag{2.4.50}$$

$$\partial_t h_{rr} - \partial_r h_{tr} + \frac{1}{f}\partial_t K + \frac{\lambda}{f}\partial_t G - \partial_t \partial_r j_r + \partial_r^2 j_t - \frac{2}{r}\partial_t j_r - \frac{2M}{r^2 f} h_{tr} + \frac{4M}{r^3 f} j_t = Q^t, \tag{2.4.51}$$

$$-\partial_t h_{tr} + \partial_r h_{tt} - f\partial_r K + \partial_t^2 j_r - \partial_t \partial_r j_t + \frac{2}{r}\partial_t j_t - \lambda f \partial_r G - \frac{r-M}{r^2 f} h_{tt} + \frac{(r-M)f}{r^2} h_{rr} - 2\frac{f}{r^2} j_r = Q^r, \tag{2.4.52}$$

$$-\partial_t^2 h_{rr} + 2\partial_t \partial_r h_{tr} - \partial_r^2 h_{tt} - \frac{1}{f}\partial_t^2 K + f\partial_r^2 K - \frac{r-3M}{r^2 f}\partial_r h_{tt} + \frac{2(r-M)}{r^2 f}\partial_t h_{tr} - \frac{(r-M)f}{r^2}\partial_r h_{rr} + \frac{2(r-M)}{r^2}\partial_r K + 2\frac{(\lambda+1)f}{r^2}\partial_r j_r - 2\frac{(\lambda+1)}{r^2 f}\partial_t j_t + 4\frac{(\lambda+1)M}{r^4} j_r + \frac{(\lambda+1)r^2 - 2(\lambda+2)Mr + 2M^2}{r^4 f^2} h_{tt} - \frac{(\lambda+1)r^2 - 2\lambda M r - 2M^2}{r^4} h_{rr} = Q^\flat, \tag{2.4.53}$$

$$\frac{r^2}{f}\partial_t^2 G - r^2 f \partial_r^2 G - 2(r-M)\partial_r G - \frac{2}{f}\partial_t j_t + 2f\partial_r j_r + \frac{4M}{r^2} j_r + \frac{h_{tt}}{f} - f h_{rr} = Q^\sharp. \tag{2.4.54}$$

We can then impose the Lorenz gauge condition by incorporating Eqs. (2.4.45 - 2.4.47) equations into these field equations (2.4.48 - 2.4.54). There are many ways to do this.

Indeed, one could simply solve these seven field equations in parallel with the gauge equations. However, we find it more efficient to plug those conditions in and manipulate the field equations to put them into a simpler form. In the end, we leave the equations on the $\mathcal{M}^2$ sector untouched, and rewrite the other four equations. Those four Lorenz gauge field equations are

$$-\frac{1}{f^2}\partial_t^2 j_t + \partial_r^2 j_t + \frac{1}{2f^2}\partial_t h_{tt} + \frac{1}{2}\partial_t h_{rr} - \partial_r h_{tr} + \frac{1}{f}\partial_t K + \frac{2M}{r^2 f}\partial_t j_r - \frac{2M}{r^2 f}h_{tr} + \frac{4M}{r^3 f}j_t = Q^t, \quad (2.4.55)$$

$$\partial_t^2 j_r - f^2\partial_r^2 j_r - \frac{2f}{r^2}(r+M)\partial_r j_r + \frac{2}{r}\partial_t j_t - \partial_t h_{tr} + \frac{1}{2}\partial_r h_{tt} + \frac{f^2}{2}\partial_r h_{rr} - f\partial_r K - \frac{r-M}{r^2 f}h_{tt} + \frac{f}{r^2}(r+M)h_{rr} - \frac{4M}{r^4}(2r-3M)\, j_r + \lambda\frac{2M}{r^2}G = Q^r, \quad (2.4.56)$$

$$\frac{r^2}{f}\partial_t^2 G - r^2 f\partial_r^2 G - 2(r-M)\partial_r G + 2\lambda G - \frac{4f}{r}j_r = Q^\sharp, \quad (2.4.57)$$

$$-\frac{1}{f}\partial_t^2 K + f\partial_r^2 K - \partial_t^2 h_{rr} + 2\partial_t\partial_r h_{tr} - \partial_r^2 h_{tt} + \frac{2M}{r^2 f}\partial_r h_{tt} + 2\frac{(2r-3M)(r-M)}{r^4}h_{rr} + 2M\frac{M-2r}{r^4 f^2}h_{tt} + 4\frac{(\lambda+1)}{r^4}(3M-2r)\, j_r + 2\frac{\lambda(\lambda+1)}{r^2}G - \frac{4(r-M)}{r^3}K = Q^\flat. \quad (2.4.58)$$

Odd-parity field equation

The one odd-parity gauge condition reduces to

$$-\frac{1}{f}\partial_t h_t + f\partial_r h_r + \frac{2M}{r^2}h_r + \frac{2f}{r}h_r - \frac{\lambda}{r^2}h_2 = 0. \quad (2.4.59)$$

The gauge-undefined field equations are

$$-\partial_t\partial_r h_r + \partial_r^2 h_t - \frac{2}{r}\partial_t h_r - \frac{1}{r^2}\partial_t h_2 - \frac{2(\lambda+1)r - 4M}{r^3 f}\left(h_t - \frac{1}{2}\partial_t h_2\right) = P^t, \tag{2.4.60}$$

$$\partial_t^2 h_r - \partial_t\partial_r h_t + \frac{2}{r}\partial_t h_t + \frac{2\lambda f}{r^2}h_r - \frac{\lambda f}{r^2}\partial_r h_2 + \frac{2\lambda f}{r^3}h_2 = P^r, \tag{2.4.61}$$

$$\frac{1}{2f}\partial_t^2 h_2 - \frac{f}{2}\partial_r^2 h_2 - \frac{1}{f}\partial_t h_t + \partial_r\left(f h_r\right) + \partial_r\left(\frac{f}{r}h_2\right) - \frac{M}{r^2}\partial_r h_2 = P. \tag{2.4.62}$$

Imposing the Lorenz gauge condition in Eq. (2.4.59), we get the Lorenz gauge field equations

$$-\partial_t^2 h_t + \partial_{r_*}^2 h_t - f\frac{2M}{r^2}\partial_r h_t + f\frac{2M}{r^2}\partial_t h_r + \frac{f}{r^2}\partial_t h_2 - f\frac{2(\lambda+1)r - 4M}{r^3}h_t = f^2 P^t, \tag{2.4.63}$$

$$-\partial_t^2 h_r + \partial_{r_*}^2 h_r + \frac{2f}{r}\partial_r h_r - \frac{2}{r^4}\Big[r^2 - 6M(r-M)\Big]h_r - \frac{2M\lambda}{r^4}h_2 - \frac{2}{r}\partial_t h_t - \frac{2\lambda f}{r^2}h_r = -P^r, \tag{2.4.64}$$

$$-\partial_t^2 h_2 + \partial_{r_*}^2 h_2 - f\frac{\ell(\ell+1)}{r^2}h_2 + 4\frac{f^2}{r}\left(h_r - \frac{1}{2}\partial_r h_2 + \frac{h_2}{r}\right) = -2fP. \tag{2.4.65}$$

2.5 Chapter summary

In this chapter I have introduced much of the theoretical foundation for the original work that follows in Chapters 4 and 5. Starting from the full Einstein equations, I have shown how the first-order field equations are derived. Then, I used the spherical symmetry of the Schwarzschild spacetime to decompose the field equations into equations for spherical harmonic amplitudes. I have given these equations in both Regge-Wheeler gauge and Lorenz gauge (in addition to a gauge-undefined form). These field equations will be important in the chapters to come.

Chapter 3

A scalar field model problem

In our attempt to understand gravitational waves, it is instructive to study first a simpler problem: the dynamics of a scalar field. The purpose of this model problem is to is to introduce many of the concepts that will be important in Chapters 4 and 5. I start by examining the scalar field sourced by a charged particle in circular motion in flat space. The charge will radiate scalar waves which can be analyzed in multipolar form. After performing the multipole expansion, I show how this model problem can be solved exactly, by introducing a spherical harmonic decomposition of the field. Getting the solution for each harmonic mode requires appropriate inner and outer boundary conditions, which I explain how to choose. I expand the exact solutions and show that in the slow motion, far field limit, they agree with the multipole expansion.

I then extend this to circular orbits around a Schwarzschild black hole. I show how the source term is chosen in curved space, and then show how the field and source decompose into harmonics. This leads to an introduction of the Regge-Wheeler equation for the first time. At this point I show how the inner boundary condition must be changed to a horizon boundary condition to account for radiation that falls into the black hole. For the outer boundary condition I introduce the asymptotic expansion which must be used to achieve accurate numerical results. Finally, I extend my analysis to include eccentric orbits on Schwarzschild. Moving to the frequency domain, this allows me to introduce extended sources and the method of homogeneous solutions, both of which will be important in later chapters.

3.1 The multipole expansion

Here we will consider a model problem, just to show how the multipolar field manifests itself, without being encumbered by the mathematics of curved space. For a thorough presentation of the multipole expansion of the gravitational field in relativity see [10].

A moving charged particle will pull up a scalar field around it that is found by solving the wave equation with a source,

$$\Box\Psi\left(x^{\mu}\right)=\left(-\partial_{t}^{2}+\nabla^{2}\right)\Psi\left(x^{\mu}\right)=-4\pi\rho\left(x^{\mu}\right). \tag{3.1.1}$$

For the moment, we will leave the orbit (which is determined by ρ) undefined, and solve Eq. (3.1.1) in general. The Green function for this equation [31] on flat space is

$$G\left(t,\boldsymbol{x},t',\boldsymbol{x'}\right)=\frac{\delta\left(t'-\left[t-\left|\boldsymbol{x}-\boldsymbol{x'}\right|\right]\right)}{\left|\boldsymbol{x}-\boldsymbol{x'}\right|}. \tag{3.1.2}$$

The delta function demands retarded time causality. Integrating the Green function over the source provides a solution to Eq. (3.1.1):

$$\Psi\left(x^{\mu}\right)=\int d^{3}x'\int dt'G\left(t,\boldsymbol{x},t',\boldsymbol{x'}\right)\rho\left(t',\boldsymbol{x'}\right) \tag{3.1.3}$$

$$=\int d^{3}x'\int dt'\frac{\delta\left(t'-\left[t-\left|\boldsymbol{x}-\boldsymbol{x'}\right|\right]\right)}{\left|\boldsymbol{x}-\boldsymbol{x'}\right|}\rho\left(t',\boldsymbol{x'}\right) \tag{3.1.4}$$

$$=\int d^{3}x'\frac{\rho\left(t-\left|\boldsymbol{x}-\boldsymbol{x'}\right|,\boldsymbol{x'}\right)}{\left|\boldsymbol{x}-\boldsymbol{x'}\right|} \tag{3.1.5}$$

Even for a known function ρ, we cannot perform integral in Eq. (3.1.5) in general. But, we can perform a far field expansion of $1/\left|\boldsymbol{x}-\boldsymbol{x'}\right|$ and $\left|\boldsymbol{x}-\boldsymbol{x'}\right|$ and find Ψ in terms of its multipoles. We start with the definition (we will be switching back and forth between component x_i and vector $\boldsymbol{x}$ notation)

$$f(x_{i},x_{i}')\equiv\left|\boldsymbol{x}-\boldsymbol{x'}\right|=\left[\left(x_{i}-x_{i}'\right)\left(x_{i}-x_{i}'\right)\right]^{1/2}. \tag{3.1.6}$$

Note that $f(x_i,x_i')$ is a function of both x_i and x_i'. We are performing our expansion around

$x_i' = 0$, which is

$$f(x_i, x_i') = f\left(x_i, 0\right) + \frac{\partial f}{\partial x_j'}\left(x_i, 0\right) \cdot x_j' + \frac{1}{2!}\frac{\partial^2 f}{\partial x_j' \partial x_k'}\left(x_i, 0\right) \cdot x_j' x_k' + \frac{1}{3!}\frac{\partial^3 f}{\partial x_j' \partial x_k' \partial x_\ell'}\left(x_i, 0\right) \cdot x_j' x_k' x_\ell' + \cdots . \quad (3.1.7)$$

We define

$$r \equiv \sqrt{x_i x_i}, \qquad r' \equiv \sqrt{x_i' x_i'} \qquad n_i \equiv \frac{x_i}{r} \qquad n_i' \equiv \frac{x_i'}{r'}. \quad (3.1.8)$$

The coefficients we will need are

$$\begin{aligned} f\left(x_i, 0\right) = r, \qquad \frac{\partial f}{\partial x_j'}\left(x_i, 0\right) = -\frac{x_j}{r}, \qquad \frac{\partial^2 f}{\partial x_j' \partial x_k'}\left(x_i, 0\right) = -\frac{x_j x_k}{r^3} + \frac{\delta_{jk}}{r}, \\ \frac{\partial^3 f}{\partial x_j' \partial x_k' \partial x_\ell'}\left(x_i, 0\right) = -3\frac{x_j x_k x_m}{r^5} + \frac{x_j \delta_{km} + x_k \delta_{jm} + x_m \delta_{jk}}{r^3}. \end{aligned} \quad (3.1.9)$$

Putting these different expressions together, we get the expansion

$$\left|\boldsymbol{x} - \boldsymbol{x'}\right| = r - \boldsymbol{n} \cdot \boldsymbol{x'} - \frac{1}{2r}\left[\left(\boldsymbol{n} \cdot \boldsymbol{x'}\right)^2 - r'^2\right] - \frac{\left(\boldsymbol{n} \cdot \boldsymbol{x'}\right)}{2r^2}\left[\left(\boldsymbol{n} \cdot \boldsymbol{x'}\right)^2 - r'^2\right] + \mathcal{O}\left(\frac{r'^4}{r^3}\right) \quad (3.1.10)$$

We also need the expansion of the inverse,

$$g(x_i, x_i') \equiv \frac{1}{|\boldsymbol{x} - \boldsymbol{x'}|} = \left[\left(x_i - x_i'\right)\left(x_i - x_i'\right)\right]^{-1/2}, \quad (3.1.11)$$

which is

$$g\left(x_i, x_i'\right) = g\left(x_i, 0\right) + \frac{\partial g}{\partial x_j'}\left(x_i, 0\right) \cdot x_j' + \frac{1}{2!}\frac{\partial^2 g}{\partial x_j' \partial x_k'}\left(x_i, 0\right) \cdot x_j' x_k' + \frac{1}{3!}\frac{\partial^3 g}{\partial x_j' \partial x_k' \partial x_\ell'}\left(x_i, 0\right) \cdot x_j' x_k' x_\ell' + \cdots . \quad (3.1.12)$$

This will require

$$g\left(x_i,0\right)=\frac{1}{r},\qquad \frac{\partial g}{\partial x'_j}\left(x_i,0\right)=\frac{x_j}{r^3},\qquad \frac{\partial^2 g}{\partial x'_j\partial x'_k}\left(x_i,0\right)=3\frac{x_jx_k}{r^5}-\frac{\delta_{jk}}{r^3},$$
$$\frac{\partial^3 g}{\partial x'_j\partial x'_k\partial x'_\ell}\left(x_i,0\right)=15\frac{x_jx_kx_\ell}{r^7}+3\frac{x_j\delta_{kl}+x_k\delta_{jl}+x_\ell\delta_{jk}}{r^5}, \tag{3.1.13}$$

which allows us to write down the expansion

$$\frac{1}{|\boldsymbol{x}-\boldsymbol{x'}|}=\frac{1}{r}+\frac{\boldsymbol{n}\cdot\boldsymbol{x'}}{r^2}+\frac{1}{2r^3}\left[3\left(\boldsymbol{n}\cdot\boldsymbol{x'}\right)^2-r'^2\right]+$$
$$\frac{\left(\boldsymbol{n}\cdot\boldsymbol{x'}\right)}{2r^4}\left[5\left(\boldsymbol{n}\cdot\boldsymbol{x'}\right)^2-3r'^2\right]+\mathcal{O}\left(\frac{r'^4}{r^5}\right). \tag{3.1.14}$$

The last expansion we will need is ρ itself. For the sake of simplicity, let us temporarily abbreviate $t-|\boldsymbol{x}-\boldsymbol{x'}|$ as y. Then, the Taylor expansion around a point $y_\circ$ in the first slot of ρ will be

$$\rho\left(y,\boldsymbol{x'}\right)=\rho\left(y_\circ,\boldsymbol{x'}\right)+\frac{\partial\rho}{\partial y}\left(y_\circ,\boldsymbol{x'}\right)\cdot\left(y-y_\circ\right)+\frac{1}{2!}\frac{\partial^2\rho}{\partial y^2}\left(y_\circ,\boldsymbol{x'}\right)\cdot\left(y-y_\circ\right)^2$$
$$+\frac{1}{3!}\frac{\partial^3\rho}{\partial y^3}\left(y_\circ,\boldsymbol{x'}\right)\cdot\left(y-y_\circ\right)^3+\cdots \tag{3.1.15}$$

We can change the variable with which we differentiate from y to t by

$$\frac{\partial\rho}{\partial y}=\frac{dt}{dy}\frac{\partial\rho}{\partial t}=\frac{\partial\rho}{\partial t}. \tag{3.1.16}$$

So, using dots to denote differentiation with respect to time, we have

$$\rho\left(y,\boldsymbol{x'}\right)=\rho\left(y_\circ,\boldsymbol{x'}\right)+\dot\rho\left(y_\circ,\boldsymbol{x'}\right)\cdot\left(y-y_\circ\right)+\frac{1}{2}\ddot\rho\left(y_\circ,\boldsymbol{x'}\right)\cdot\left(y-y_\circ\right)^2$$
$$+\frac{1}{6}\dddot\rho\left(y_\circ,\boldsymbol{x'}\right)\cdot\left(y-y_\circ\right)^3+\cdots \tag{3.1.17}$$

Now, plugging in for y and letting $y_\circ = t - r$ gives

$$\rho\left(t - \left|\boldsymbol{x} - \boldsymbol{x'}\right|, \boldsymbol{x'}\right) = \rho\left(t - r, \boldsymbol{x'}\right) + \dot{\rho}\left(t - r, \boldsymbol{x'}\right) \cdot \left[r - \left|\boldsymbol{x} - \boldsymbol{x'}\right|\right] + \frac{1}{2}\ddot{\rho}\left(t - r, \boldsymbol{x'}\right) \cdot \left[r - \left|\boldsymbol{x} - \boldsymbol{x'}\right|\right]^2 + \frac{1}{6}\dddot{\rho}\left(t - r, \boldsymbol{x'}\right) \cdot \left[r - \left|\boldsymbol{x} - \boldsymbol{x'}\right|\right]^3 + \cdots \quad (3.1.18)$$

Using Eq. (3.1.10) to expand the $|\boldsymbol{x} - \boldsymbol{x'}|$ terms,

$$\begin{aligned}\rho\left(t - \left|\boldsymbol{x} - \boldsymbol{x'}\right|, \boldsymbol{x'}\right) &= \rho\left(t - r, \boldsymbol{x'}\right) \\ &+ \dot{\rho}\left(t - r, \boldsymbol{x'}\right) \cdot \left[\boldsymbol{n} \cdot \boldsymbol{x'} + \frac{1}{2r}\left[\left(\boldsymbol{n} \cdot \boldsymbol{x'}\right)^2 - r'^2\right] + \frac{\left(\boldsymbol{n} \cdot \boldsymbol{x'}\right)}{2r^2}\left[\left(\boldsymbol{n} \cdot \boldsymbol{x'}\right)^2 - r'^2\right] + \mathcal{O}\left(\frac{r'^4}{r^3}\right)\right] \\ &+ \frac{1}{2}\ddot{\rho}\left(t - r, \boldsymbol{x'}\right) \cdot \left[\boldsymbol{n} \cdot \boldsymbol{x'} + \frac{1}{2r}\left[\left(\boldsymbol{n} \cdot \boldsymbol{x'}\right)^2 - r'^2\right] + \mathcal{O}\left(\frac{r'^3}{r^2}\right)\right]^2 \\ &+ \frac{1}{6}\dddot{\rho}\left(t - r, \boldsymbol{x'}\right) \cdot \left[\boldsymbol{n} \cdot \boldsymbol{x'} + \mathcal{O}\left(\frac{r'^2}{r}\right)\right]^3 + \mathcal{O}\left(r'^4\right) \quad (3.1.19)\end{aligned}$$

We have kept terms with at most three powers of r', indicating that we will be performing the expansion through octupole ($\ell = 3$) order.

Now we can consider the expansion of the full Green function for the wave equation using Eqn. (3.1.14) and (3.1.19). Here, for brevity I will suppress the arguments for ρ on the right side of the equation, which are understood to be $(t - r, \boldsymbol{x'})$.

$$\begin{aligned}\frac{\rho\left(t - \left|\boldsymbol{x} - \boldsymbol{x'}\right|, \boldsymbol{x'}\right)}{\left|\boldsymbol{x} - \boldsymbol{x'}\right|} &= \left[\rho + \dot{\rho} \cdot \left[\boldsymbol{n} \cdot \boldsymbol{x'} + \frac{1}{2r}\left[\left(\boldsymbol{n} \cdot \boldsymbol{x'}\right)^2 - r'^2\right] + \frac{\left(\boldsymbol{n} \cdot \boldsymbol{x'}\right)}{2r^2}\left[\left(\boldsymbol{n} \cdot \boldsymbol{x'}\right)^2 - r'^2\right]\right]\right. \\ &\left. + \frac{1}{2}\ddot{\rho} \cdot \left[\boldsymbol{n} \cdot \boldsymbol{x'} + \frac{1}{2r}\left[\left(\boldsymbol{n} \cdot \boldsymbol{x'}\right)^2 - r'^2\right]\right]^2 + \frac{1}{6}\dddot{\rho} \cdot \left[\boldsymbol{n} \cdot \boldsymbol{x'}\right]^3\right] \\ &\times \left[\frac{1}{r} + \frac{\boldsymbol{n} \cdot \boldsymbol{x'}}{r^2} + \frac{1}{2r^3}\left[3\left(\boldsymbol{n} \cdot \boldsymbol{x'}\right)^2 - r'^2\right] + \frac{\left(\boldsymbol{n} \cdot \boldsymbol{x'}\right)}{2r^4}\left[5\left(\boldsymbol{n} \cdot \boldsymbol{x'}\right)^2 - 3r'^2\right]\right] + \cdots \quad (3.1.20)\end{aligned}$$

The multipole expansion is in powers of n. After performing some factorization, we define

terms based on the power of n, which in component notation are

$$\begin{aligned}
T_0 &= \frac{\rho}{r} + \frac{\ddot{\rho}}{6r} r'^2 \\
T_1 &= \left[\frac{\dot{\rho}}{r} + \frac{\rho}{r^2} + \frac{\dddot{\rho}}{10r} r'^2 + \frac{\ddot{\rho}}{10r^2} r'^2 \right] n_j x'_j \\
T_2 &= \frac{1}{2} \left[\frac{\ddot{\rho}}{r} + \frac{3\dot{\rho}}{r^2} + \frac{3\rho}{r^3} \right] \left[x'_j x'_k - \frac{r'^2}{3} \delta_{jk} \right] n_j n_k \\
T_3 &= \frac{1}{6} \left[\frac{\dddot{\rho}}{r} + 6\frac{\ddot{\rho}}{r^2} + 15\frac{\dot{\rho}}{r^3} + 15\frac{\rho}{r^4} \right] \left[x'_j x'_k x'_\ell - \frac{r'^2}{5} \left(x'_j \delta_{kl} + x'_k \delta_{jl} + x'_\ell \delta_{jk} \right) \right] n_j n_k n_\ell,
\end{aligned} \tag{3.1.21}$$

so up to octupole order the expansion is

$$\frac{\rho\left(t - |\boldsymbol{x} - \boldsymbol{x'}|, \boldsymbol{x'}\right)}{|\boldsymbol{x} - \boldsymbol{x'}|} = T_0 + T_1 + T_2 + T_3 + \cdots . \tag{3.1.22}$$

These terms will all go into the integral in Eq. (3.1.5). To that end, we define the various multipole moment tensors (which are in powers of x'_j), up through octupole order.

Name	Symbol	Value
Monopole	$\mathscr{M}(t-r)$	$= \int d^3x' \rho(t-r, \boldsymbol{x'})$
Moment of Inertia	$\mathscr{I}(t-r)$	$= \int d^3x' \rho(t-r, \boldsymbol{x'}) r'^2$
Dipole	$\mathscr{D}_j(t-r)$	$= \int d^3x' \rho(t-r, \boldsymbol{x'}) x'_j$
Octupole Trace	$\mathscr{O}_j(t-r)$	$= \int d^3x' \rho(t-r, \boldsymbol{x'}) r'^2 x'_j$
Traceless Quadrupole	$\mathscr{I}_{jk}(t-r)$	$= \int d^3x' \rho(t-r, \boldsymbol{x'}) \left(x'_j x'_k - \frac{r'^2}{3} \delta_{jk} \right)$
Traceless Octupole	$\mathscr{O}_{jkl}(t-r)$	$= \int d^3x' \rho(t-r, \boldsymbol{x'}) \left(x'_j x'_k x'_\ell - \frac{r'^2}{5} \left(x'_j \delta_{kl} + x'_k \delta_{jl} + x'_\ell \delta_{jk} \right) \right)$

With these definitions, we can write the expression for the field concisely as

$$\begin{aligned}
\Psi(x^\mu) = \frac{1}{r} \left(\mathscr{M} + \frac{\ddot{\mathscr{I}}}{6} \right) + \left(\frac{\dot{\mathscr{D}}_j}{r} + \frac{\mathscr{D}_j}{r^2} + \frac{\dddot{\mathscr{O}}_j}{10r} + \frac{\ddot{\mathscr{O}}_j}{10r^2} \right) n_j + \frac{1}{2} \left(\frac{\ddot{\mathscr{I}}_{jk}}{r} + 3\frac{\dot{\mathscr{I}}_{jk}}{r^2} + 3\frac{\mathscr{I}_{jk}}{r^3} \right) n_j n_k \\
+ \frac{1}{6} \left(\frac{\dddot{\mathscr{O}}_{jkl}}{r} + 6\frac{\ddot{\mathscr{O}}_{jkl}}{r^2} + 15\frac{\dot{\mathscr{O}}_{jkl}}{r^3} + 15\frac{\mathscr{O}_{jkl}}{r^4} \right) n_j n_k n_\ell + \mathcal{O}\left(n^4\right).
\end{aligned} \tag{3.1.23}$$

3.1.1 Circular motion

We are interested in a point mass with charge q traveling in a circular orbit of radius $r_\circ$. Recall that there is no gravity in this system, but special relativity does apply. For this case, the charge density ρ is

$$\rho(t, \boldsymbol{x}) = \frac{q}{\gamma r^2 \sin\theta} \delta\left(r - r_\circ\right) \delta\left(\theta - \frac{\pi}{2}\right) \delta\left(\phi - \Omega t\right). \tag{3.1.24}$$

This charge density describes circular motion in the equatorial plane with an angular frequency Ω at a radius $r_\circ$. Furthermore, γ is the Lorentz factor and q is the charge carried by the particle.

In this section we will compute the moment tensors and their derivatives for the specific case of this charge density.

Moment tensors

With the specific source in Eq. (3.1.24) we can perform these integrals to get an expression for the field. Starting with the monopole term we have the unsurprising result

$$\mathscr{M}\left(t - r\right) = \frac{q}{\gamma} \int \frac{d^3x'}{r'^2 \sin\theta'} \delta\left(r' - r_\circ\right) \delta\left(\theta' - \frac{\pi}{2}\right) \delta\left(\phi' - \Omega\left(t - r\right)\right) = \frac{q}{\gamma}. \tag{3.1.25}$$

The moment of inertia is also an expected constant:

$$\mathscr{I}\left(t - r\right) = \frac{q}{\gamma} \int \frac{d^3x'}{r'^2 \sin\theta'} \delta\left(r' - r_\circ\right) \delta\left(\theta' - \frac{\pi}{2}\right) \delta\left(\phi' - \Omega\left(t - r\right)\right) r'^2 = \frac{q\, r_\circ^2}{\gamma}. \tag{3.1.26}$$

For the dipole term, we have

$$\begin{aligned}\mathscr{D}_j\left(t - r\right) = \frac{q r_\circ}{\gamma} \int \frac{d\Omega'}{\sin\theta'} \delta\left(\theta' - \frac{\pi}{2}\right) \delta\left(\phi' - \Omega\left(t - r\right)\right) n'_j \\ = \frac{q r_\circ}{\gamma} n_j\left[\theta = \pi/2, \phi = \Omega\left(t - r\right)\right].\end{aligned} \tag{3.1.27}$$

The directional vector has components

$$n_j\left[\pi/2, \Omega\left(t-r\right)\right] \doteq \begin{bmatrix} \sin\left(\pi/2\right)\cos\left[\Omega\left(t-r\right)\right] \\ \sin\left(\pi/2\right)\sin\left[\Omega\left(t-r\right)\right] \\ \cos\left(\pi/2\right) \end{bmatrix} = \begin{bmatrix} \cos\left[\Omega\left(t-r\right)\right] \\ \sin\left[\Omega\left(t-r\right)\right] \\ 0 \end{bmatrix}, \tag{3.1.28}$$

so, in cartesian coordinates the dipole vector is

$$\mathscr{D}_j\left(t-r\right) \doteq \frac{qr_\circ}{\gamma}\begin{bmatrix} \cos\left[\Omega\left(t-r\right)\right] \\ \sin\left[\Omega\left(t-r\right)\right] \\ 0 \end{bmatrix}. \tag{3.1.29}$$

Next comes the trace of the octupole tensor, which will be exactly like the dipole vector, except with an extra factor of $r_\circ^2$:

$$\mathscr{O}_j\left(t-r\right) \doteq \frac{qr_\circ^3}{\gamma}\begin{bmatrix} \cos\left[\Omega\left(t-r\right)\right] \\ \sin\left[\Omega\left(t-r\right)\right] \\ 0 \end{bmatrix}. \tag{3.1.30}$$

The traceless quadrupole tensor is

$$\begin{aligned} &\mathscr{I}_{jk}\left(t-r\right) \\ &\quad = \frac{q}{\gamma}\int \frac{d^3x'}{r'^2\sin\theta'}\delta\left(r'-r_\circ\right)\delta\left(\theta'-\frac{\pi}{2}\right)\delta\left(\phi'-\Omega\left(t-r\right)\right)\left(x'_jx'_k-\frac{r'^2}{3}\delta_{jk}\right), \end{aligned} \tag{3.1.31}$$

which has cartesian coordinates

$$\begin{aligned} &\mathscr{I}_{jk}\left(t-r\right) \\ &\quad \doteq \frac{qr_\circ^2}{\gamma}\begin{bmatrix} \cos^2\left[\Omega\left(t-r\right)\right]-\frac{1}{3} & \cos\left[\Omega\left(t-r\right)\right]\cdot\sin\left[\Omega\left(t-r\right)\right] & 0 \\ \cos\left[\Omega\left(t-r\right)\right]\cdot\sin\left[\Omega\left(t-r\right)\right] & \sin^2\left[\Omega\left(t-r\right)\right]-\frac{1}{3} & 0 \\ 0 & 0 & -\frac{1}{3} \end{bmatrix}. \end{aligned} \tag{3.1.32}$$

Derivatives of moment tensors

In order to write down the field we need time derivatives of these moment tensors. For a circular orbit, the moment of inertia is a constant, so those derivatives vanish. The first time derivative of the dipole term is

$$\dot{\mathscr{D}}_j\left(t-r\right) \doteq \frac{qr_\circ}{\gamma}\Omega \begin{bmatrix} -\sin\left[\Omega\left(t-r\right)\right] \\ \cos\left[\Omega\left(t-r\right)\right] \\ 0 \end{bmatrix}. \tag{3.1.33}$$

The first and second time derivatives of the traceless quadrupole tensor are

$$\dot{\mathscr{I}}_{jk}\left(t-r\right) \doteq \frac{qr_\circ^2}{\gamma}\Omega \begin{bmatrix} -\sin\left[2\Omega\left(t-r\right)\right] & \cos\left[2\Omega\left(t-r\right)\right] & 0 \\ \cos\left[2\Omega\left(t-r\right)\right] & \sin\left[2\Omega\left(t-r\right)\right] & 0 \\ 0 & 0 & 0 \end{bmatrix} \tag{3.1.34}$$

$$\ddot{\mathscr{I}}_{jk}\left(t-r\right) \doteq -2\frac{qr_\circ^2\,\Omega^2}{\gamma} \begin{bmatrix} \cos\left[2\Omega\left(t-r\right)\right] & \sin\left[2\Omega\left(t-r\right)\right] & 0 \\ \sin\left[2\Omega\left(t-r\right)\right] & -\cos\left[2\Omega\left(t-r\right)\right] & 0 \\ 0 & 0 & 0 \end{bmatrix} \tag{3.1.35}$$

The Dipole Terms

Now we can compute the products between these tensors and the directional vectors.

$$\mathscr{D}_j n_j = \frac{qr_\circ}{\gamma} \begin{bmatrix} \cos\left[\Omega\left(t-r\right)\right] \\ \sin\left[\Omega\left(t-r\right)\right] \\ 0 \end{bmatrix} \cdot \begin{bmatrix} \sin\theta\cos\phi \\ \sin\theta\sin\phi \\ \cos\theta \end{bmatrix} = \frac{qr_\circ}{\gamma}\sin\theta\cos\left[\phi-\Omega\left(t-r\right)\right] \tag{3.1.36}$$

Likewise,

$$\dot{\mathscr{D}}_j n_j = \frac{qr_\circ}{\gamma}\Omega\sin\theta\sin\left[\phi-\Omega\left(t-r\right)\right] \tag{3.1.37}$$

The Quadrupole Terms

$$\mathscr{I}_{jk}n_j n_k = \frac{qr_\circ^2}{\gamma}\begin{bmatrix} \cos^2\left[\Omega\left(t-r\right)\right]-\frac{1}{3} & \cos\left[\Omega\left(t-r\right)\right]\cdot\sin\left[\Omega\left(t-r\right)\right] & 0 \\ \cos\left[\Omega\left(t-r\right)\right]\cdot\sin\left[\Omega\left(t-r\right)\right] & \sin^2\left[\Omega\left(t-r\right)\right]-\frac{1}{3} & 0 \\ 0 & 0 & -\frac{1}{3} \end{bmatrix} \cdot \begin{bmatrix} \sin\theta\cos\phi \\ \sin\theta\sin\phi \\ \cos\theta \end{bmatrix} \cdot \begin{bmatrix} \sin\theta\cos\phi \\ \sin\theta\sin\phi \\ \cos\theta \end{bmatrix} \tag{3.1.38}$$

$$\mathscr{I}_{jk}n_j n_k = \frac{qr_\circ^2}{6\gamma}\left[3\sin^2\theta\cos\left[2\left(\phi-\Omega\left(t-r\right)\right)\right]-3\cos^2\theta+1\right] \tag{3.1.39}$$

Similarly,

$$\dot{\mathscr{I}}_{jk}n_j n_k = \frac{qr_\circ^2}{\gamma}\Omega\sin^2\theta\sin\left[2\left(\phi-\Omega\left(t-r\right)\right)\right] \tag{3.1.40}$$

and

$$\ddot{\mathscr{I}}_{jk}n_j n_k = -\frac{2qr_\circ^2}{\gamma}\Omega^2\sin^2\theta\cos\left[2\left(\phi-\Omega\left(t-r\right)\right)\right] \tag{3.1.41}$$

Putting these terms together, we get, through quadrupole order, in the slow motion limit, the asymptotic field of a particle in circular orbit,

$$\begin{aligned}\Psi\left(x^\mu\right) = \frac{q}{\gamma r} &+ \frac{qr_\circ}{\gamma r}\Omega\sin\theta\sin\left[\phi-\Omega\left(t-r\right)\right] + \frac{qr_\circ}{\gamma r^2}\sin\theta\cos\left[\phi-\Omega\left(t-r\right)\right] \\ &- \frac{qr_\circ^2}{\gamma r}\Omega^2\sin^2\theta\cos\left[2\left(\phi-\Omega\left(t-r\right)\right)\right] + \frac{3qr_\circ^2}{2\gamma r^2}\Omega\sin^2\theta\sin\left[2\left(\phi-\Omega\left(t-r\right)\right)\right] \\ &+ \frac{3qr_\circ^2}{4\gamma r^3}\sin^2\theta\cos\left[2\left(\phi-\Omega\left(t-r\right)\right)\right] - \frac{qr_\circ^2}{4\gamma r^3}\left[3\cos^2\theta-1\right].\end{aligned} \tag{3.1.42}$$

3.2 Exact solution to scalar charge motion in flat space

We now look to solve the wave equation (3.1.1) exactly. Expressing the Laplacian in spherical coordinates, we have (suppressing the argument x^μ)

$$-\partial_t^2\Psi + \frac{1}{r^2}\partial_r\left(r^2\partial_r\Psi\right) + \frac{1}{r^2\sin\theta}\partial_\theta\left(\sin\theta\ \partial_\theta\Psi\right) + \frac{1}{r^2\sin^2\theta}\partial_\phi^2\Psi = -4\pi\rho. \tag{3.2.1}$$

Now we decompose Ψ in spherical harmonics as

$$\Psi\left(t,r,\theta,\phi\right) = \sum_{\ell=0}^{\infty}\sum_{m=-\ell}^{\ell}\Psi_{\ell m}\left(t,r\right)Y_{\ell m}\left(\theta,\phi\right). \tag{3.2.2}$$

Plugging this in, the left side of Eq. (3.2.1) gives

$$\Box\Psi = \frac{1}{r^2}\sum_{\ell,m}\Big[-r^2\partial_t^2 + \partial_r\left(r^2\partial_r\right) - \ell\left(\ell+1\right)\Big]\Psi_{\ell m}\left(t,r\right)Y_{\ell m}\left(\theta,\phi\right), \tag{3.2.3}$$

where we have used the fact that the spherical harmonics are eigenfunctions of the angular operator with eigenvalues $-\ell\left(\ell+1\right)$. Meanwhile, a point particle with charge q moving along a circular orbit worldline $x'^\mu(\tau)$ will produce a charge density

$$\rho = \frac{q}{\gamma r^2\sin\theta}\delta\left(r-r_\circ\right)\delta\left(\phi-\Omega t_s\right)\delta\left(\theta-\frac{\pi}{2}\right), \tag{3.2.4}$$

where γ is the Lorentz factor. Now, recall that the spherical harmonics are complete in the sense that

$$\sum_{\ell=0}^{\infty}\sum_{m=-\ell}^{\ell}Y^*_{\ell m}(\theta',\phi')\cdot Y_{\ell m}(\theta,\phi) = \delta(\phi-\phi')\delta(\cos\theta-\cos\theta') = \frac{1}{\sin\theta}\delta(\phi-\phi')\delta(\theta-\theta'), \tag{3.2.5}$$

so ρ can be written as (we drop the subscript s on the coordinate time parameter from here on)

$$\rho = \frac{q}{\gamma r^2 \sin\theta}\delta(r - r_\circ)\sin\theta \sum_{\ell,m} Y^*_{\ell m}(\pi/2, \Omega t) Y_{\ell m}(\theta, \phi), \tag{3.2.6}$$

$$= \frac{q}{\gamma r^2}\delta(r - r_\circ) \sum_{\ell,m} e^{-im\Omega t} Y_{\ell m}(\pi/2, 0) Y_{\ell m}(\theta, \phi). \tag{3.2.7}$$

In the last line we used the fact that

$$Y_{\ell m}(\theta, \phi) = e^{im\phi} Y_{\ell m}(\theta, 0) \quad \Rightarrow \quad Y^*_{\ell m}(\theta, \phi) = e^{-im\phi} Y^*_{\ell m}(\theta, 0) = e^{-im\phi} Y_{\ell m}(\theta, 0). \tag{3.2.8}$$

We define $\omega_m \equiv m\Omega$ and write

$$\frac{1}{r^2}\sum_{\ell,m}\Big[-r^2\partial_t^2 + \partial_r\left(r^2\partial_r\right) - \ell\left(\ell+1\right)\Big]\Psi_{\ell m}\left(t, r\right) Y_{\ell m}\left(\theta, \phi\right)$$

$$= -4\pi\frac{q}{\gamma r^2}\delta(r - r_\circ)\sum_{\ell,m} e^{-i\omega_m t} Y_{\ell m}(\pi/2, 0) Y_{\ell m}(\theta, \phi). \tag{3.2.9}$$

Using the spherical harmonics' orthonormality,

$$\Big[-r^2\partial_t^2 + \partial_r\left(r^2\partial_r\right) - \ell\left(\ell+1\right)\Big]\Psi_{\ell m}\left(t, r\right) = -\frac{4\pi q}{\gamma} e^{-i\omega_m t} Y_{\ell m}(\pi/2, 0)\,\delta(r - r_\circ). \tag{3.2.10}$$

The time dependence on the right side of this equation implies that we can separate the t and r pieces of $\Psi_{\ell m}$ as

$$\Psi_{\ell m}\left(t, r\right) = e^{-i\omega_m t} R_{\ell m}(r), \tag{3.2.11}$$

and therefore, in the frequency domain

$$\frac{d^2 R_{\ell m}}{dr^2}(r) + \frac{2}{r}\frac{dR_{\ell m}}{dr}\left(r\right) + \left[\omega_m^2 - \frac{\ell\left(\ell+1\right)}{r^2}\right] R_{\ell m}(r) = -\frac{4\pi q}{\gamma r^2} Y_{\ell m}(\pi/2, 0)\,\delta(r - r_\circ). \tag{3.2.12}$$

Note that for this circular case there is only one frequency mode, whereas in an elliptic orbit case, for example, there would be a countably infinite set of harmonics.

This is now an ordinary differential equation which we are capable of solving analytically

mode-by-mode. Away from $r = r_\circ$, the right side of the equation vanishes. Therefore, we look for homogeneous solutions to Eq. (3.2.12). We will enforce a causal boundary condition at $r \to \infty$ and a regular boundary condition at $r \to 0$. Finally, we apply the appropriate jump condition at $r = r_\circ$ as demanded by the singular source.

The homogeneous solutions to Eq. (3.2.12) are the *spherical Bessel functions*

$$R^h_{\ell m}(r) = C^1_{\ell m} j_\ell\left(\omega_m r\right) + C^2_{\ell m} n_\ell\left(\omega_m r\right). \tag{3.2.13}$$

As $r \to 0$, $n_\ell \to -\infty$, so $C^2_{\ell m} = 0$ for the inner solution. As $r \to \infty$, we expect to see an outward traveling wave. The correct linear combination of the two Bessel functions is the *first Hankel function*

$$h^1_\ell(x) = j_\ell(x) + i n_\ell(x), \tag{3.2.14}$$

which, to leading order at large x is

$$h^1_\ell(x) \sim \frac{e^{ix}}{x}, \tag{3.2.15}$$

for all ℓ. So, $R_{\ell m}$ and its derivative are

$$R_{\ell m}(r) = \begin{cases} A_{\ell m} j_\ell(\omega_m r) & r \le r_\circ, \\ B_{\ell m} h^1_\ell(\omega_m r) & r \ge r_\circ, \end{cases} \tag{3.2.16}$$

$$\frac{dR_{\ell m}}{dr}(r) = \begin{cases} A_{\ell m} \frac{dj_\ell}{dr}(\omega_m r) & r < r_\circ, \\ B_{\ell m} \frac{dh^1_\ell}{dr}(\omega_m r) & r > r_\circ. \end{cases} \tag{3.2.17}$$

We integrate the differential equation to get the discontinuity in the slope

$$\int_{r_\circ-\epsilon}^{r_\circ+\epsilon} \left[\frac{d^2 R_{\ell m}}{dr^2}(r) + \frac{2}{r}\frac{dR_{\ell m}}{dr}(r) + \left(\omega_m^2 - \frac{\ell\left(\ell+1\right)}{r^2}\right) R_{\ell m}(r)\right] dr = -\int_{r_\circ-\epsilon}^{r_\circ+\epsilon} \left[\frac{4\pi q}{\gamma r^2} Y_{\ell m}(\pi/2, 0)\, \delta(r - r_\circ)\right] dr, \tag{3.2.18}$$

which gives an expression for the jump in the derivative of $R_{\ell m}$,

$$\frac{dR_{\ell m}}{dr}(r)\Big|_{r_\circ-\epsilon}^{r_\circ+\epsilon} = -\frac{4\pi q}{\gamma r_\circ^2} Y_{\ell m}(\pi/2, 0). \tag{3.2.19}$$

We use this expression along with Eqs. (3.2.16) and (3.2.17) to solve for the normalization constants $A_{\ell m}$ and $B_{\ell m}$, which we find to be

$$A_{\ell m} = \frac{4\pi i \omega_m q}{\gamma} Y_{\ell m}(\pi/2, 0) h_\ell^1(\omega_m r_\circ), \tag{3.2.20}$$

$$B_{\ell m} = \frac{4\pi i \omega_m q}{\gamma} Y_{\ell m}(\pi/2, 0) j_\ell(\omega_m r_\circ). \tag{3.2.21}$$

Note that we used the fact that the Wronskian is

$$W_{\ell m}\left[j_\ell\left(\omega_m r_\circ\right), h_\ell^1\left(\omega_m r_\circ\right)\right] = -\frac{1}{i\omega_m^2 r_\circ^2}. \tag{3.2.22}$$

Now, plugging in for $\omega_m = m\Omega$, where Ω is the angular velocity and $\gamma = \left(1-\beta^2\right)^{-1/2}$, where β is the coordinate velocity (note that $c = 1$ here), we get

$$A_{\ell m} = 4\pi i m \Omega q \; Y_{\ell m}(\pi/2, 0)\sqrt{1-\beta^2}\; h_\ell^1(m\Omega r_\circ), \tag{3.2.23}$$

$$B_{\ell m} = 4\pi i m \Omega q \; Y_{\ell m}(\pi/2, 0)\sqrt{1-\beta^2}\; j_\ell(m\Omega r_\circ). \tag{3.2.24}$$

We can rewrite the angular velocity in terms of the velocity β. Note that this system does not require that we obey Kepler's third law, but we still have to obey special relativity. Setting $\Omega = \beta/r_\circ$ we get

$$A_{\ell m} = \frac{4\pi i m q}{r_\circ} Y_{\ell m}(\pi/2, 0)\beta\sqrt{1-\beta^2}\; h_\ell^1(m\beta), \tag{3.2.25}$$

$$B_{\ell m} = \frac{4\pi i m q}{r_\circ} Y_{\ell m}(\pi/2, 0)\beta\sqrt{1-\beta^2}\; j_\ell(m\beta), \tag{3.2.26}$$

which finally yields

$$R_{\ell m}(r) = \frac{4\pi i m q}{r_\circ} Y_{\ell m}(\pi/2, 0)\beta\sqrt{1-\beta^2} \begin{cases} h^1_\ell(m\beta) \cdot j_\ell\left(m\beta r/r_\circ\right) & r \leq r_\circ, \\ j_\ell(m\beta) \cdot h^1_\ell\left(m\beta r/r_\circ\right) & r \geq r_\circ. \end{cases} \tag{3.2.27}$$

If we define

$$q_{\ell m} \equiv 4\pi \frac{q}{r_\circ} Y_{\ell m}(\pi/2, 0)\sqrt{1-\beta^2}, \tag{3.2.28}$$

then this becomes

$$R_{\ell m}(r) = im\beta q_{\ell m} \begin{cases} h^1_\ell(m\beta) \cdot j_\ell\left(m\beta r/r_\circ\right) & r \leq r_\circ, \\ j_\ell(m\beta) \cdot h^1_\ell\left(m\beta r/r_\circ\right) & r \geq r_\circ. \end{cases} \tag{3.2.29}$$

Now, we can write down an expression for the full scalar field. Recalling that our decomposition was

$$\Psi\left(t, r, \theta, \phi\right) = \sum_{\ell,m} e^{-i\omega_m t} R_{\ell m}(r) Y_{\ell m}(\theta, \phi), \tag{3.2.30}$$

we have

$$\Psi\left(t, r, \theta, \phi\right) = \sum_{\ell,m} im\beta q_{\ell m} e^{-i\omega_m t} Y_{\ell m}(\theta, \phi) \begin{cases} h^1_\ell(m\beta) \cdot j_\ell\left(m\beta r/r_\circ\right) & r \leq r_\circ, \\ j_\ell(m\beta) \cdot h^1_\ell\left(m\beta r/r_\circ\right) & r \geq r_\circ. \end{cases} \tag{3.2.31}$$

3.2.1 Multipole terms

We can expand the Bessel and Hankel functions to compare the solution in Eq. (3.2.31) to that obtained with the multipole expansion in the previous section.

The monopole term

Consider first $l = 0, m = 0$. The Bessel and Hankel functions are

$$j_0(x) = \frac{\sin x}{x}, \qquad h^1_0(x) = -i\frac{e^{ix}}{x} = \frac{\sin x}{x} - i\frac{\cos x}{x}. \tag{3.2.32}$$

Evaluated in the limit as $m \to 0$ we have

$$\lim_{m\to 0}\ m\ j_\ell(m\Omega r_\circ)h_\ell^1\left(m\Omega r\right) = \lim_{m\to 0}\ m\frac{\sin(m\Omega r_\circ)}{m\Omega r_\circ}\left[\frac{\sin(m\Omega r)}{m\Omega r} - i\frac{\cos(m\Omega r)}{m\Omega r}\right], \tag{3.2.33}$$

$$= -\frac{i}{\Omega r} \tag{3.2.34}$$

Then, the full field, evaluated at $\ell = 0, m = 0$ is

$$\Psi_{00}\left(x^\mu\right) = i\frac{4\pi q\Omega}{\gamma}Y_{00}\left(\pi/2, 0\right)Y_{00}(\theta,\phi)\cdot\frac{-i}{\Omega r} = \frac{q}{\gamma r}, \tag{3.2.35}$$

in agreement with the monopole term in Eq. (3.1.42).

The dipole terms

To calculate the dipole terms, we will need the $\ell = 1$ versions of the Bessel and Hankel functions. They are

$$j_1(x) = \frac{\sin x}{x^2} - \frac{\cos x}{x}, \qquad h_1^1(x) = -\frac{e^{ix}}{x}\left[1 + \frac{i}{x}\right]. \tag{3.2.36}$$

With these, we write down the $\ell = 1, m = 1$ part of the field

$$\Psi_{11} = i\frac{4\pi q\Omega}{\gamma}e^{i\Omega t}Y_{11}\left(\pi/2, 0\right)Y_{11}\left(\theta,\phi\right)\cdot j_1\left(\Omega r_\circ\right)\cdot h_1^1\left(\Omega r\right), \tag{3.2.37}$$

$$= -i\frac{3q}{2\gamma r}\sin\theta e^{i[\phi-\Omega(t-r)]}\left[\frac{\sin\left(\Omega r_\circ\right)}{\left(\Omega r_\circ\right)^2} - \frac{\cos\left(\Omega r_\circ\right)}{\Omega r_\circ}\right]\left[1 + \frac{i}{\Omega r}\right]. \tag{3.2.38}$$

The harmonic amplitudes of the field obey the same relations as the spherical harmonics: $\Psi_{\ell,-m} = \Psi^*_{\ell m}$ for all ℓ and m. Therefore, $\Psi_{1,-1} = \Psi^*_{1,1}$. The $\ell = 1, m = 0$ mode will not contribute because $Y_{10}\left(\pi/2, 0\right) = 0$. So, the sum of the two $\ell = 1$ modes is

$$\Psi_{\ell=1} = \Psi_{1,-1} + \Psi_{11} = \Psi_{11} + \Psi^*_{11} = 2\Re\left[\Psi_{11}\right], \tag{3.2.39}$$

$$= \frac{3q}{\gamma r}\sin\theta\left[\frac{\sin\left(\Omega r_\circ\right)}{\left(\Omega r_\circ\right)^2} - \frac{\cos\left(\Omega r_\circ\right)}{\Omega r_\circ}\right]\left[\sin\left[\phi - \Omega\left(t - r\right)\right] + \frac{\cos\left[\phi - \Omega\left(t - r\right)\right]}{\Omega r}\right]. \tag{3.2.40}$$

The first term in the square brackets is a function of $\Omega r_\circ = \beta$, the speed of the particle. We can compute the Taylor expansion of this term in the slow motion limit,

$$\frac{\sin x}{x^2} - \frac{\cos x}{x} = \frac{1}{x} - \frac{x}{6} - \frac{1}{x} + \frac{x}{2} + \mathcal{O}\left(x^3\right) = \frac{x}{3} + \mathcal{O}\left(x^3\right), \tag{3.2.41}$$

Plugging this in, we get

$$\Psi_{\ell=1}\left(x^\mu\right) = \frac{3q}{\gamma r}\sin\theta\left[\frac{\Omega r_\circ}{3}\right]\left[\sin\left[\phi - \Omega\left(t-r\right)\right] + \frac{\cos\left[\phi - \Omega\left(t-r\right)\right]}{\Omega r}\right], \tag{3.2.42}$$

$$= \frac{q\Omega r_\circ}{\gamma r}\sin\theta\left[\sin\left[\phi - \Omega\left(t-r\right)\right] + \frac{\cos\left[\phi - \Omega\left(t-r\right)\right]}{\Omega r}\right], \tag{3.2.43}$$

which agrees with the dipole terms in Eq. (3.1.42) in the slow motion limit.

The quadrupole terms

The quadrupole terms will only include Ψ_{22}, Ψ_{20}, and $\Psi_{2,-2}$. The Ψ_{22} term is

$$\Psi_{22}\left(x^\mu\right) = i\frac{4\pi q\Omega}{\gamma}e^{-2i\Omega t}Y_{22}\left(\pi/2, 0\right)Y_{22}(\theta,\phi)\cdot 2\cdot j_2(2\Omega r_\circ)\cdot h_2^2\left(2\Omega r\right), \tag{3.2.44}$$

$$= i\frac{15q\Omega}{4\gamma}\sin^2\theta e^{2i(\phi-\Omega t)}j_2(2\Omega r_\circ)\cdot h_2^2\left(2\Omega r\right). \tag{3.2.45}$$

The needed special functions are

$$j_2(x) = \left[\frac{3}{x^2} - 1\right]\frac{\sin x}{x} - 3\frac{\cos x}{x^2}, \qquad h_2^1(x) = i\frac{e^{ix}}{x}\left[1 + \frac{3i}{x} - \frac{3}{x^2}\right], \tag{3.2.46}$$

so

$$\Psi_{22}\left(x^\mu\right) = -\frac{15q}{8\gamma r}\sin^2\theta e^{2i(\phi-\Omega(t-r))}\left[\left(\frac{3}{\left(2\Omega r_\circ\right)^2} - 1\right)\frac{\sin\left(2\Omega r_\circ\right)}{2\Omega r_\circ} - 3\frac{\cos\left(2\Omega r_\circ\right)}{\left(2\Omega r_\circ\right)^2}\right]$$
$$\times\left[1 + \frac{3i}{2\Omega r} - \frac{3}{\left(2\Omega r\right)^2}\right]. \tag{3.2.47}$$

Again, we expand the first term in the square brackets in the slow motion limit:

$$\left(\frac{3}{x^2}-1\right)\frac{\sin x}{x}-3\frac{\cos x}{x^2}=\frac{3}{x^2}-1-\frac{3}{6}+\frac{3x^2}{120}+\frac{x^2}{6}-3\left(\frac{1}{x^2}-\frac{1}{2}+\frac{x^2}{24}\right)+\mathcal{O}\left(x^4\right), \quad (3.2.48)$$

$$=\frac{x^2}{15}+\mathcal{O}\left(x^4\right). \quad (3.2.49)$$

Plugging this in we have, in the slow motion limit

$$\Psi_{22}\left(x^\mu\right)=-\frac{15q}{8\gamma r}\sin^2\theta e^{2i(\phi-\Omega(t-r))}\left(\frac{\left(2\Omega r_\circ\right)^2}{15}\right)\left[1+\frac{3i}{2\Omega r}-\frac{3}{\left(2\Omega r\right)^2}\right], \quad (3.2.50)$$

$$=-\frac{q\Omega^2 r_\circ^2}{2\gamma r}\sin^2\theta\Big[\cos\left[2\left(\phi-\Omega\left(t-r\right)\right)\right] + i\sin\left[2\left(\phi-\Omega\left(t-r\right)\right)\right]\Big]\left[1+\frac{3i}{2\Omega r}-\frac{3}{\left(2\Omega r\right)^2}\right], \quad (3.2.51)$$

while the real part of this is

$$\Re\left[\Psi_{22}\left(x^\mu\right)\right]=-\frac{1}{2}\frac{qr_\circ^2}{\gamma r}\Omega^2\sin^2\theta\cos\left[2\left(\phi-\Omega\left(t-r\right)\right)\right] + \frac{3}{4}\frac{qr_\circ^2}{\gamma r^2}\Omega\sin^2\theta\sin\left[2\left(\phi-\Omega\left(t-r\right)\right)\right]+\frac{3}{8}\frac{qr_\circ^2}{\gamma r^3}\sin^2\theta\cos\left[2\left(\phi-\Omega\left(t-r\right)\right)\right]. \quad (3.2.52)$$

Now, consider the Ψ_{20} mode,

$$\Psi_{20}\left(x^\mu\right)=i\frac{4\pi q\Omega}{\gamma}Y_{20}\left(\pi/2,0\right)Y_{20}\left(\theta,\phi\right)\Big[mj_2\left(m\Omega r_\circ\right)\cdot h_1^2\left(m\Omega r\right)\Big]_{m=0}. \quad (3.2.53)$$

In order to evaluate this, we must expand the special functions. We have already seen that the leading order term in $j_2(x)$ is $x^2/15$. The Hankel function expands as follows,

$$h_1^2(x)=i\frac{e^{ix}}{x}\left(1+\frac{3i}{x}-\frac{3}{x^2}\right), \quad (3.2.54)$$

$$=\frac{i}{x}\left[-\frac{3}{x^2}-\frac{1}{2}+\mathcal{O}\left(x^2\right)\right]=-\frac{3i}{x^3}-\frac{i}{2x}+\mathcal{O}\left(x\right). \quad (3.2.55)$$

Now we can use these expansions to find the $m = 0$ term.

$$\lim_{m\to 0} m j_2\left(m\Omega r_\circ\right)\cdot h_2^2\left(m\Omega\right) = \lim_{m\to 0} m\frac{\left(m\Omega r_\circ\right)^2}{15}\left(-\frac{3i}{\left(m\Omega r\right)^3}\right) + \cdots = -\frac{ir_\circ^2}{5\Omega r^3}. \tag{3.2.56}$$

This goes into Eq. (3.2.53) to give

$$\Psi_{20}\left(x^\mu\right) = i\frac{4\pi q\Omega}{\gamma}Y_{20}\left(\pi/2,0\right)Y_{20}\left(\theta,\phi\right)\left(-\frac{ir_\circ^2}{5\Omega r^3}\right), \tag{3.2.57}$$

$$= -\frac{qr_\circ^2}{4\gamma r^3}\left(3\cos^2\theta - 1\right). \tag{3.2.58}$$

Finally, we can put together all of the modes to give the quadrupole contribution to the field. Noting that $\Psi_{21} = \Psi_{2,-1} = 0$, we have $\Psi_{\ell=2} = 2\Re\left[\Psi_{22}\right] + \Psi_{20}$, and so

$$\begin{aligned}\Psi_{\ell=2}\left(x^\mu\right) = -\frac{qr_\circ^2}{\gamma r}\Omega^2\sin^2\theta\cos\left[2\left(\phi-\Omega\left(t-r\right)\right)\right] + \frac{3}{2}\frac{qr_\circ^2}{\gamma r^2}\Omega\sin^2\theta\sin\left[2\left(\phi-\Omega\left(t-r\right)\right)\right] \\ + \frac{3}{4}\frac{qr_\circ^2}{\gamma r^3}\sin^2\theta\cos\left[2\left(\phi-\Omega\left(t-r\right)\right)\right] - \frac{qr_\circ^2}{4\gamma r^3}\left[3\cos^2\theta-1\right].\end{aligned} \tag{3.2.59}$$

Once again, this agrees with the multipole expansion within the slow motion limit.

In this section we have introduced the spherical harmonic decomposition of the scalar field. This led to radial mode equations for each ℓ and m. We found exact solutions to these mode functions, and then we imposed causal interior (jump) conditions and exterior boundary conditions. We will see in the next section that many of these features extend directly to the curved space wave equation.

3.3 Scalar fields in curved space

We turn now to the wave equation in curved space

$$\Box\Psi\left(x^\mu\right) = -4\pi\rho, \tag{3.3.1}$$

with $\Box \equiv \nabla_\mu\nabla^\mu$ and Ψ as the retarded field. Let's consider a particle in circular orbit with radius $r_\circ$ and angular frequency Ω, around a Schwarzschild black hole, with θ constant at

$\pi/2$. We begin by forming the appropriate charge density to source this wave equation.

3.3.1 Current conservation and source term

Let's start with a four-current J^μ. Charge conservation demands

$$\nabla_\mu J^\mu = \partial_\mu J^\mu + \frac{1}{2}\left(g^{\mu\beta}g_{\beta\mu,\nu} + g^{\mu\beta}g_{\beta\nu,\mu} - g^{\mu\beta}g_{\mu\nu,\beta}\right) J^\nu \tag{3.3.2}$$

$$= \partial_\mu J^\mu + \frac{1}{2} g^{\mu\beta}g_{\beta\mu,\nu}J^\nu = 0. \tag{3.3.3}$$

In order to proceed further we must rewrite the term $g^{\mu\beta}g_{\beta\mu,\nu}$. We can write this as

$$g^{\mu\beta}g_{\beta\mu,\nu} = g^{\mu\beta}\partial_\nu g_{\beta\mu} = \mathrm{Tr}\left(\boldsymbol{g}^{-1}\partial_\nu \boldsymbol{g}\right), \tag{3.3.4}$$

where $\boldsymbol{g}$ is the matrix representation of the metric and $\boldsymbol{g}^{-1}$ is its inverse. In this form we can use the matrix identity[1] $\det A = e^{\mathrm{Tr}(\ln A)}$. Varying both sides gives

$$\delta \det A = e^{\mathrm{Tr}(\ln A)}\ \delta \mathrm{Tr}\left(\ln A\right) = \det A\ \mathrm{Tr}\left(A^{-1}\delta A\right), \quad \Rightarrow \quad \mathrm{Tr}\left(A^{-1}\delta A\right) = \frac{\delta \det A}{\det A}. \tag{3.3.5}$$

Hence, if we let $g \equiv \det \boldsymbol{g}$ we can rewrite the right hand side of Eq. (3.3.4) so we have

$$g^{\mu\beta}g_{\beta\mu,\nu} = \mathrm{Tr}\left(\boldsymbol{g}^{-1}\partial_\nu \boldsymbol{g}\right) = \frac{\partial_\nu\left(-g\right)}{-g} = \partial_\nu\left(\ln\left(-g\right)\right), \tag{3.3.6}$$

where the minus sign has been introduced since the determinant of the metric is negative. Plugging this back into Eq. (3.3.3) gives

$$\nabla_\mu J^\mu = \partial_\mu J^\mu + \frac{1}{2}\partial_\mu\left(\ln\left(-g\right)\right) J^\mu = \frac{1}{\sqrt{-g}}\partial_\mu\left(\sqrt{-g}\ J^\mu\right) = 0. \tag{3.3.7}$$

---

[1] For a matrix A, the exponential is defined by the power series and the ln is the inverse of that exponential.

Integrating over all spacetime we have[2]

$$\int d^4x\sqrt{-g}\nabla_\mu J^\mu = \int d^4x\sqrt{-g}\frac{1}{\sqrt{-g}}\partial_\mu\left(\sqrt{-g}\ J^\mu\right) = \int d^4x\ \partial_\mu\left(\sqrt{-g}\ J^\mu\right) = 0. \qquad (3.3.8)$$

Separating into space and time components yields

$$\int dt\ d^3x\ \partial_0\left(\sqrt{-g}\ J^0\right) = -\int dt\ d^3x\ \partial_i\left(\sqrt{-g}\ J^i\right). \qquad (3.3.9)$$

We then use the generalized Stokes' theorem, which allows us to write

$$\int d^3x\sqrt{-g}J^0\Big|_{t_0}^{t_1} = -\int dt\sqrt{-g}\ d\sigma_i J^i. \qquad (3.3.10)$$

This statement says that whatever charge is inside our volume at t_0 will also be there at t_1 unless it has passed through a surface σ, as is displayed in Fig. (3.1). If we now integrate

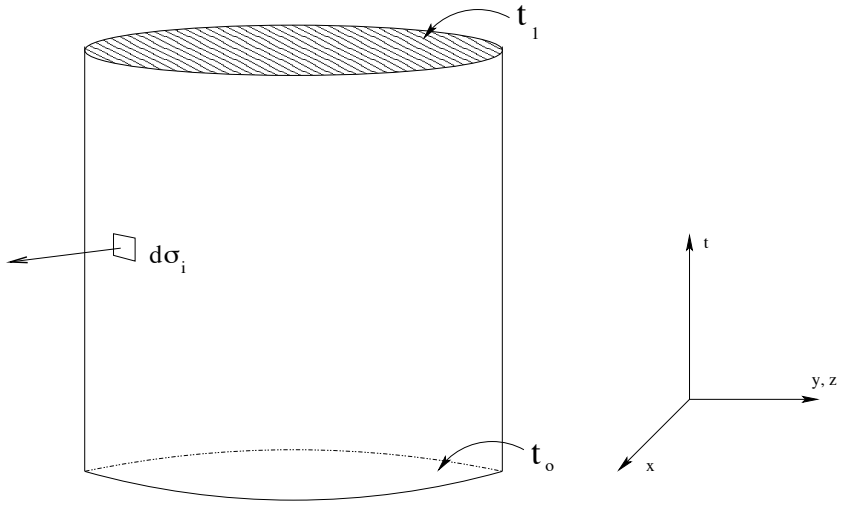

Figure 3.1: With the inclusion of time to our diagram, we must compress y and z into one dimension. Hence, each sheet of time represents a three dimensional snapshot.

over all space, there will be no flux through the surface σ, since it will be at infinity. Now,

[2]Note that $d^4x = dx^0dx^1dx^2dx^3$. Multiplying this by $\sqrt{-g}$ gives the appropriate four dimensional volume element.

the four-current is defined as $J^\mu \equiv \rho u^\mu$ for some four-velocity u^μ, so Eq. (3.3.10) becomes

$$\int d^3x\sqrt{-g}\rho u^0\Big|_{t_0}^{t_1} = 0. \tag{3.3.11}$$

Clearly this integral does not change value between any two times t_0 and t_1. At any given point t, we expect it to give us the total charge in space

$$q = \int d^3x\sqrt{-g}\rho u^0. \tag{3.3.12}$$

From this we can work backward to construct ρ, such that it will give us the correct charge. If all we have is a point charge (as we'll be considering), we will need a three dimensional delta function multiplied by the value q itself to localize the charge. We also need factors of $1/\sqrt{-g}$ and $1/u^0$ in order to cancel those factors in Eq. (3.3.12). Putting these together gives[3]

$$\rho = \frac{q\delta^3\left(x^i - x'^i\right)}{\sqrt{-g}u^0}. \tag{3.3.13}$$

In order to localize our charge in time we can introduce a temporal delta function as well. Then we have to integrate over all time. Letting the integration variable be t_s, the Schwarzschild time coordinate, we have

$$\rho = q\int \frac{\delta^3\left(x^i - x'^i\right)\delta\left(t - t_s\right)}{\sqrt{-g}u^0}dt_s. \tag{3.3.14}$$

The time portion of the four-velocity is $dt_s/d\tau$, which allows us to change our variable of integration.

$$\rho = q\int \frac{\delta^4\left(x^\mu - x'^\mu\right)}{\sqrt{-g}}d\tau. \tag{3.3.15}$$

We leave this equation with the comment that it is specifically constructed to give the charge q of a point particle when it is plugged into an integral over all space.

---

[3]Note that here $\delta^3\left(x^i - x'^i\right) \equiv \delta\left(x^1 - x'^1\right)\delta\left(x^2 - x'^2\right)\delta\left(x^3 - x'^3\right)$ with no Jacobian factor. The same is true in Cartesian or Minkowski spatial coordinates.

Plugging this source term into the wave equation in spherical coordinates gives

$$\Box\Psi = -4\pi\frac{q}{r^2\sin\theta}\left(\frac{dt_s}{d\tau}\right)^{-1}\delta\left(r-r_\circ\right)\delta\left(\phi-\Omega t_s\right)\delta\left(\theta-\frac{\pi}{2}\right). \tag{3.3.16}$$

The $1/(r^2\sin\theta)$ term comes from $1/\sqrt{-g}$ and $(dt_s/d\tau)^{-1} = u^0$. Now, if we use a dot to express differentiation with respect to proper time, then $(dt_s/d\tau)^{-1}$ is $1/\dot{t}_s$. We can calculate this value by using the variational method for geodesics.

Variational methods

The quantity K is defined by

$$2K = g_{\mu\nu}\dot{x}^\mu\dot{x}^\nu = \begin{cases} 0 & \text{lightlike geodesic,} \\ -1 & \text{timelike geodesic,} \\ +1 & \text{spacelike geodesic,} \end{cases} \tag{3.3.17}$$

and satisfies the Euler-Lagrange equations

$$\frac{\partial K}{\partial x^\mu} - \frac{d}{d\tau}\left[\frac{\partial K}{\partial \dot{x}^\mu}\right] = 0. \tag{3.3.18}$$

On Schwarzschild Eq. (3.3.17) becomes, for our timelike, massive particle

$$2K = -\left(1-\frac{2M}{r}\right)\dot{t}_s^2 + \left(1-\frac{2M}{r}\right)^{-1}\dot{r}^2 + r^2\dot{\theta}^2 + r^2\sin^2\theta\dot{\phi}^2 = -1. \tag{3.3.19}$$

In our case of a circular orbit, $\theta = \pi/2$ and $\dot{r} = \dot{\theta} = 0$, so we have

$$K = -\frac{1}{2}\left(1-\frac{2M}{r}\right)\dot{t}_s^2 + \frac{1}{2}r^2\dot{\phi}^2 = -\frac{1}{2}. \tag{3.3.20}$$

Plugging this into Eq. (3.3.18) gives

$$\frac{\partial K}{\partial t_s} - \frac{d}{d\tau}\left[\frac{\partial K}{\partial \dot{t}_s}\right] = \frac{d}{d\tau}\left[\left(1 - \frac{2M}{r}\right)\dot{t}_s\right] = 0 \tag{3.3.21}$$

$$\frac{\partial K}{\partial \phi} - \frac{d}{d\tau}\left[\frac{\partial K}{\partial \dot{\phi}}\right] = -\frac{d}{d\tau}\left[r^2\dot{\phi}\right] = 0 \tag{3.3.22}$$

$$\frac{\partial K}{\partial r} - \frac{d}{d\tau}\left[\frac{\partial K}{\partial \dot{r}}\right] = -\frac{M}{r^2}\dot{t}_s^2 + r\dot{\phi}^2 = 0, \tag{3.3.23}$$

so for constants A and B,

$$\dot{t}_s = \frac{A}{1 - \frac{2M}{r}}, \qquad \dot{\phi} = \frac{B}{r^2}, \qquad r^2\dot{\phi}^2 = \frac{M}{r}\dot{t}_s^2. \tag{3.3.24}$$

For our purposes we only need the last of these expressions. Plugging it into Eq. (3.3.20) gives

$$-\frac{1}{2}\left(1 - \frac{2M}{r}\right)\dot{t}_s^2 + \frac{1}{2}\frac{M}{r}\dot{t}_s^2 = -\frac{1}{2}, \tag{3.3.25}$$

which we can solve for $\dot{t}_s$

$$\dot{t}_s = \frac{1}{\sqrt{1 - \frac{3M}{r}}}. \tag{3.3.26}$$

Returning to Eq. (3.3.16) and, plugging in for $(dt_s/d\tau)^{-1}$ gives

$$\Box\Psi = -4\pi\frac{q}{r^2\sin\theta}\sqrt{1 - \frac{3M}{r}}\,\delta\left(r - r_\circ\right)\delta\left(\phi - \Omega t_s\right)\delta\left(\theta - \frac{\pi}{2}\right). \tag{3.3.27}$$

Harmonic decomposition of source

Now, using the completeness of the spherical harmonics, we find

$$-4\pi\rho = -4\pi\frac{q}{r^2}\sqrt{1 - \frac{3M}{r}}\delta(r - r_\circ)\sum_{\ell,m} e^{-im\Omega t_s}Y^*_{\ell m}(\pi/2, 0)\cdot Y_{\ell m}(\theta,\phi). \tag{3.3.28}$$

If we define

$$q_{\ell m} \equiv 4\pi\frac{q}{r_\circ}Y^*_{\ell m}(\pi/2,0)\sqrt{1 - \frac{3M}{r_\circ}}, \qquad \omega_m \equiv m\Omega, \tag{3.3.29}$$

then

$$-4\pi\rho = -\sum_{\ell,m} \frac{\delta(r-r_\circ)}{r_\circ}\; q_{\ell m}\; e^{-i\omega_m t_s}\; Y_{\ell m}(\theta,\phi). \tag{3.3.30}$$

3.3.2 The wave equation

Having expanded the right side of the wave equation, we now turn to the left. Looking at Eq. (3.3.7) we see that if we plug in $\nabla^\mu\Psi$ for J^μ, then

$$\Box\Psi = \nabla_\mu\nabla^\mu\Psi = \frac{1}{\sqrt{-g}}\partial_\mu\left(\sqrt{-g}\;\nabla^\mu\Psi\right). \tag{3.3.31}$$

But, for a scalar, by definition $\nabla_\mu\Psi = \partial_\mu\Psi$, so lowering the index μ with the metric, we have

$$\frac{1}{\sqrt{-g}}\partial_\mu\left(\sqrt{-g}\;g^{\mu\nu}\partial_\nu\Psi\right) = -4\pi\frac{q}{r^2\sin\theta}\sqrt{1-\frac{3M}{r}}\delta\left(r-r_\circ\right)\delta\left(\phi-\Omega t_s\right)\delta\left(\theta-\frac{\pi}{2}\right). \tag{3.3.32}$$

Expanding the wave operator,

$$\begin{aligned}\left[-\frac{1}{1-2M/r}\partial_{t_s}^2+\frac{1}{r^2}\partial_r\left[\left(r^2-2Mr\right)\partial_r\right]+\frac{1}{\sin\theta}\partial_\theta\left(\sin\theta\cdot\partial_\theta\right)+\frac{1}{r^2\sin^2\theta}\partial_\phi^2\right]\Psi \\ = -4\pi\frac{q}{r^2\sin\theta}\sqrt{1-\frac{3M}{r}}\delta\left(r-r_\circ\right)\delta\left(\phi-\Omega t_s\right)\delta\left(\theta-\frac{\pi}{2}\right).\end{aligned} \tag{3.3.33}$$

Harmonic decomposition of the retarded field

Let us now decompose the retarded field into spherical harmonics as we did with the source:

$$\Psi(t_s,r,\theta,\phi) = \sum_{\ell,m}\Psi_{\ell m}(r)e^{-i\omega_m t_s}Y_{\ell m}(\theta,\phi). \tag{3.3.34}$$

So, using the wave operator on this expansion yields

$$\Box\Psi = \sum_{\ell,m}\left[\frac{\omega_m^2}{1-2M/r}+\frac{1}{r^2}\partial_r\left(\left(r^2-2Mr\right)\partial_r\right)-\frac{\ell\left(\ell+1\right)}{r^2}\right]\Psi_{\ell m}(r)e^{-i\omega_m t_s}Y_{\ell m}. \tag{3.3.35}$$

We can combine this with the source term from the right side to get

$$\sum_{\ell,m}\left[\frac{\omega_m^2}{1-2M/r}+\frac{1}{r^2}\partial_r\left(\left(r^2-2Mr\right)\partial_r\right)-\frac{\ell\left(\ell+1\right)}{r^2}\right]\Psi_{\ell m}(r)e^{-i\omega_m t_s}Y_{\ell m}(\theta,\phi)$$
$$=-\sum_{\ell,m}\frac{\delta(r-r_\circ)}{r_\circ}\;q_{\ell m}\;e^{-i\omega_m t_s}\;Y_{\ell m}(\theta,\phi) \quad (3.3.36)$$

The orthonormality of the spherical harmonics allows us to write

$$\left[\frac{\omega_m^2}{1-2M/r}+\frac{\partial_r\left(\left(r^2-2Mr\right)\partial_r\right)}{r^2}-\frac{\ell\left(\ell+1\right)}{r^2}\right]\Psi_{\ell m}(r)=-\frac{q_{\ell m}}{r_\circ}\delta(r-r_\circ), \quad (3.3.37)$$

or

$$\frac{d^2\Psi_{\ell m}}{dr^2}+\frac{2\left(r-M\right)}{r\left(r-2M\right)}\frac{d\Psi_{\ell m}}{dr}+\left[\frac{\omega_m^2 r^2}{\left(r-2M\right)^2}-\frac{\ell\left(\ell+1\right)}{r\left(r-2M\right)}\right]\Psi_{\ell m}$$
$$=-\frac{q_{\ell m}}{r_\circ-2M}\delta(r-r_\circ). \quad (3.3.38)$$

It is common practice to switch independent variables, from the Schwarzschild radius r to the *tortoise coordinate* r_*, defined by the differential equation

$$\frac{dr}{dr_*}=1-\frac{2M}{r}. \quad (3.3.39)$$

Then, making the definitions

$$V_\ell(r)\equiv f\left(\frac{\ell\left(\ell+1\right)}{r^2}+\frac{2M}{r^3}\right),\qquad f\equiv 1-\frac{2M}{r},\qquad \psi_{\ell m}(r)\equiv r\Psi_{\ell m}(r), \quad (3.3.40)$$

Eq. (3.3.38) reduces to the Regge-Wheeler equation

$$\frac{d^2}{dr_*^2}\psi_{\ell m}\left(r\right)+\left[\omega_m^2-V_\ell\left(r\right)\right]\psi_{\ell m}\left(r\right)=-q_{\ell m}f\delta(r-r_\circ). \quad (3.3.41)$$

This equation does not admit analytic solutions for general ℓ, m modes, and therefore must solve it numerically. We begin by setting boundary conditions at the event horizon and spatial infinity. At the horizon, when r_* becomes large and negative, the potential falls off

exponentially and we can choose a traveling wave going down into the black hole, $e^{-i\omega_{mn}r_*}$. At large r_* the potential falls off only algebraically and we must use an asymptotic expansion to set an accurate boundary condition.

3.3.3 Asymptotic expansion as $r, r_* \to \infty$

Now we turn to the subject of the asymptotic expansion. Though many of the details here can be found in standard differential equations texts (e.g. [60]), we give the details here for completeness. In later chapters, though we will perform asymptotic expansions more tersely, the logic will follow that presented here.

Consider a general potential

$$V_\ell = f\left(\frac{\ell\left(\ell+1\right)}{r^2} + \frac{2M}{r^3}\left(1-j^2\right)\right), \tag{3.3.42}$$

where j determines the potential for scalar ($j=0$), vector ($j=1$), and tensor ($j=2$) waves. Now, as r and r_* tend toward infinity, the potential goes to zero, and we will have plane wave solutions

$$\psi_{\ell m} \sim e^{i\omega_m r_*} \qquad \left(r_* \to \infty\right). \tag{3.3.43}$$

As r and r_* get big, but finite, let's assume that the solutions to Eq. (3.3.41) are of the form

$$\psi_{\ell m} = e^{i\omega_m r_*} J_{\ell m}\left(r\right), \tag{3.3.44}$$

where $J_{\ell m}$ goes to 1 as r_* becomes infinite. Plugging this into Eq. (3.3.41) gives

$$\frac{d^2}{dr_*^2}\left(e^{i\omega_m r_*} J_{\ell m}\left(\omega_m, r\right)\right) + \left(\omega_m^2 - V_\ell\left(r\right)\right) e^{i\omega_m r_*} J_{\ell m} = 0, \tag{3.3.45}$$

$$\frac{d^2}{dr_*^2} J_{\ell m} + 2i\omega_m \frac{d}{dr_*} J_{\ell m} - V_\ell\left(r\right) J_{\ell m} = 0. \tag{3.3.46}$$

Changing the derivatives to be with respect to r and plugging in the potential,

$$f\frac{d^2}{dr^2} J_{\ell m} + \left(\frac{2M}{r^2} + 2i\omega_m\right)\frac{d}{dr} J_{\ell m} - \left(\frac{\ell\left(\ell+1\right)}{r^2} + \frac{2M}{r^3}\left(1-j^2\right)\right) J_{\ell m} = 0. \tag{3.3.47}$$

At this point we find it helpful to define the dimensionless variables $z \equiv \omega_m r$ and $\sigma \equiv M\omega_m$, so

$$f = 1 - \frac{2M}{r} = 1 - \frac{2\sigma}{z} \qquad \Rightarrow \qquad \frac{d}{dr} = \frac{dz}{dr}\frac{d}{dz} = \omega_m \frac{d}{dz}. \tag{3.3.48}$$

This changes the differential equation to

$$f\frac{d^2}{dz^2}J_{\ell m} + \left(\frac{2\sigma}{z^2} + 2i\right)\frac{d}{dz}J_{\ell m} - \left(\frac{\ell\left(\ell+1\right)}{z^2} + \frac{2\sigma}{z^3}\left(1-j^2\right)\right)J_{\ell m} = 0. \tag{3.3.49}$$

Now, let's assume an asymptotic series solution of $J_{\ell m}$ of the form

$$J_{\ell m} = \sum_{n=0}^{\infty} \frac{a_n}{z^n}, \tag{3.3.50}$$

Plugging this in Eq. (3.3.49) yields

$$\begin{aligned}\sum_{n=1}^{\infty} n\left(n+1\right)\frac{a_n}{z^{n-2}} - 2\sigma\sum_{n=1}^{\infty} n\left(n+1\right)\frac{a_n}{z^{n-1}} - 2\sigma\sum_{n=1}^{\infty} n\frac{a_n}{z^{n-1}} \\ - 2i\sum_{n=1}^{\infty} n\frac{a_n}{z^{n-3}} - \ell\left(\ell+1\right)\sum_{n=0}^{\infty}\frac{a_n}{z^{n-2}} - 2\sigma\left(1-j^2\right)\sum_{n=0}^{\infty}\frac{a_n}{z^{n-1}} = 0.\end{aligned} \tag{3.3.51}$$

Now, let's redefine our values of n so that all our terms scale as z^{-n}, which yields

$$\begin{aligned}\sum_{n=-1}^{\infty}\left(n+2\right)\left(n+3\right)\frac{a_{n+2}}{z^n} - 2\sigma\sum_{n=0}^{\infty}\left(n+1\right)\left(n+2\right)\frac{a_{n+1}}{z^n} - 2\sigma\sum_{n=0}^{\infty}\left(n+1\right)\frac{a_{n+1}}{z^n} \\ - 2i\sum_{n=-2}^{\infty}\left(n+3\right)\frac{a_{n+3}}{z^n} - \ell\left(\ell+1\right)\sum_{n=-2}^{\infty}\frac{a_{n+2}}{z^n} - 2\sigma\left(1-j^2\right)\sum_{n=-1}^{\infty}\frac{a_{n+1}}{z^n} = 0.\end{aligned} \tag{3.3.52}$$

In order to make this one summation, all the sums have to start at the same value of n, so we now pull out the leading terms to even things out, giving

$$\begin{aligned}&\left(-2ia_1 - \ell\left(\ell+1\right)a_0\right)z^2 + \left(2a_1 - 4ia_2 - \ell\left(\ell+1\right)a_1 - 2\sigma\left(1-j^2\right)a_0\right)z \\ &\quad + \sum_{n=0}^{\infty}\Big[\left(n+2\right)\left(n+3\right)a_{n+2} - 2\sigma\left(n+1\right)\left(n+2\right)a_{n+1} - 2\sigma\left(n+1\right)a_{n+1} \\ &\qquad - 2i\left(n+3\right)a_{n+3} - \ell\left(\ell+1\right)a_{n+2} - 2\sigma\left(1-j^2\right)a_{n+1}\Big]\frac{1}{z^n} = 0.\end{aligned} \tag{3.3.53}$$

Since this expression vanishes order-by-order, each coefficient must equal zero. The z^2 term gives us

$$a_1 = \frac{i\ell\left(\ell+1\right)}{2} a_0. \tag{3.3.54}$$

Note that we can pick the value of a_0, which corresponds to the freedom to scale homogeneous solutions. The coefficient of the z term in Eq. (3.3.53) gives us the formula for a_2 in terms of a_1 and a_0,

$$a_2 = \frac{i}{4}\left(\left(\ell\left(\ell+1\right)-2\right)a_1 + 2\sigma\left(1-j^2\right)a_0\right). \tag{3.3.55}$$

We can plug in Eq. (3.3.54) for a_1 to get this all in terms of a_0,

$$a_2 = \left(\frac{i\sigma}{2}\left(1-j^2\right) - \frac{1}{8}\ell\left(\ell+1\right)\left(\ell+2\right)\left(\ell-1\right)\right)a_0 \tag{3.3.56}$$

The same logic works for every power of z in the summation in Eq. (3.3.53). In fact, we can solve for a recursion relation for the n^{th} component as follows:

$$2nia_n = -2\sigma\Big[\left(1-j^2\right)+n\left(n-2\right)\Big]a_{n-2} - \Big[\ell\left(\ell+1\right)-n\left(n-1\right)\Big]a_{n-1}. \tag{3.3.57}$$

Note that if we define $a_n = 0$ for all $n < 0$, we can acquire the a_0 and a_1 identities given above.

3.3.4 Scalar field jump condition

We integrate the equation of motion to calculate the jump condition,

$$\int_{r_\circ-\epsilon}^{r_\circ+\epsilon}\left\{\frac{d^2\Psi_{\ell m}}{dr^2} + \frac{2\left(r-M\right)}{r\left(r-2M\right)}\frac{d\Psi_{\ell m}}{dr} + \left[\frac{\omega_m^2 r^2}{\left(r-2M\right)^2} - \frac{\ell\left(\ell+1\right)}{r\left(r-2M\right)}\right]\Psi_{\ell m}\right\}dr$$
$$= -\int_{r_\circ-\epsilon}^{r_\circ+\epsilon}\left[\frac{q_{\ell m}}{r_\circ-2M}\delta(r-r_\circ)\right]dr. \tag{3.3.58}$$

We integrate by parts, and since the field itself is continuous across the location of the particle, we see that

$$\int_{r_\circ-\epsilon}^{r_\circ+\epsilon} \frac{d}{dr}\left[\frac{d\Psi_{\ell m}}{dr}\right] dr = \left.\frac{d\Psi_{\ell m}}{dr}\right|_{r_\circ-\epsilon}^{r_\circ+\epsilon} = -\frac{q_{\ell m}}{r_\circ - 2M}. \tag{3.3.59}$$

Let the value of the field and its derivative be

$$\Psi_{\ell m}(r) = \begin{cases} A_{\ell m}\Psi^{\rm H}_{\ell m} & r \le r_\circ, \\ B_{\ell m}\Psi^{\infty}_{\ell m} & r \ge r_\circ, \end{cases} \tag{3.3.60}$$

and

$$\frac{d\Psi_{\ell m}}{dr}(r) = \begin{cases} A_{\ell m}\frac{d\Psi^{\rm H}_{\ell m}}{dr} & r < r_\circ, \\ B_{\ell m}\frac{d\Psi^{\infty}_{\ell m}}{dr} & r > r_\circ. \end{cases} \tag{3.3.61}$$

Then, from the continuity in the field and discontinuity of its derivative at the particle, we have the pair of equations

$$B_{\ell m}\Psi^{\infty}_{\ell m}(r_\circ) - A_{\ell m}\Psi^{\rm H}_{\ell m}(r_\circ) = 0, \tag{3.3.62}$$

$$B_{\ell m}\frac{d\Psi^{\infty}_{\ell m}}{dr}(r_\circ) - A_{\ell m}\frac{d\Psi^{\rm H}_{\ell m}}{dr}(r_\circ) = -\frac{q_{\ell m}}{r_\circ - 2M}. \tag{3.3.63}$$

We solve for $A_{\ell m}$ and $B_{\ell m}$, giving

$$A_{\ell m} = -\frac{q_{\ell m}}{r_\circ}\frac{\Psi^{\infty}_{\ell m}(r_\circ)}{\Psi^{\rm H}_{\ell m}(r_\circ)\frac{d\Psi^{\infty}_{\ell m}}{dr_*}(r_\circ) - \frac{d\Psi^{\rm H}_{\ell m}}{dr_*}(r_\circ)\Psi^{\infty}_{\ell m}(r_\circ)}, \tag{3.3.64}$$

$$B_{\ell m} = -\frac{q_{\ell m}}{r_\circ}\frac{\Psi^{\rm H}_{\ell m}(r_\circ)}{\Psi^{\rm H}_{\ell m}(r_\circ)\frac{d\Psi^{\infty}_{\ell m}}{dr_*}(r_\circ) - \frac{d\Psi^{\rm H}_{\ell m}}{dr_*}(r_\circ)\Psi^{\infty}_{\ell m}(r_\circ)}. \tag{3.3.65}$$

If we write this in terms of $\psi_{\ell m} = r\Psi_{\ell m}$, we get

$$A_{\ell m} = -q_{\ell m}\frac{\psi^{\infty}_{\ell m}(r_\circ)}{W_{\ell m}}, \qquad B_{\ell m} = -q_{\ell m}\frac{\psi^{\rm H}_{\ell m}(r_\circ)}{W_{\ell m}}, \tag{3.3.66}$$

where we have defined the Wronskian as

$$W_{\ell m}\left(\psi^{\mathrm{H}}_{\ell m},\psi^{\infty}_{\ell m}\right)=\psi^{\mathrm{H}}_{\ell m}\frac{d\psi^{\infty}_{\ell m}}{dr_*}-\frac{d\psi^{\mathrm{H}}_{\ell m}}{dr_*}\psi^{\infty}_{\ell m}. \tag{3.3.67}$$

Then, the field is

$$\psi_{\ell m}(r)=-\frac{q_{\ell m}}{W_{\ell m}}\begin{cases}\psi^{\infty}_{\ell m}\left(r_\circ\right)\psi^{\mathrm{H}}_{\ell m}\left(r\right) & r\leq r_\circ,\\ \psi^{\mathrm{H}}_{\ell m}\left(r_\circ\right)\psi^{\infty}_{\ell m}\left(r\right) & r\geq r_\circ.\end{cases} \tag{3.3.68}$$

Now, we can write out an explicit expression for the whole scalar field,

$$\Psi\left(t_s,r,\theta,\phi\right)=\sum_{l,m}\frac{q_{\ell m}}{W_{\ell m}}\frac{Y_{\ell m}(\theta,\phi)e^{-i\omega_m t_s}}{r}\begin{cases}\psi^{\infty}_{\ell m}\left(r_\circ\right)\psi^{\mathrm{H}}_{\ell m}\left(r\right) & r\leq r_\circ,\\ \psi^{\mathrm{H}}_{\ell m}\left(r_\circ\right)\psi^{\infty}_{\ell m}\left(r\right) & r\geq r_\circ.\end{cases} \tag{3.3.69}$$

3.4 Eccentric orbits on Schwarzschild

Next, we extend our investigation of scalar fields to include those induced by a particle in eccentric orbit. As usual, this field is found by solving the wave equation

$$\Box\Psi\left(x^\mu\right)=-4\pi\rho\left(x^\mu\right). \tag{3.4.1}$$

As we have seen, this can be decomposed in spherical harmonics. For the eccentric case we write the Regge-Wheeler equation

$$-\frac{\partial^2}{\partial t^2}\psi_{\ell m}+\frac{\partial^2}{\partial r_*^2}\psi_{\ell m}-V_\ell(r)\psi_{\ell m}=-4\pi f r\rho_{\ell m}. \tag{3.4.2}$$

Now we consider the specific form of the source term in our wave equation. We take the scalar charge density ρ to be a Dirac delta function

$$-4\pi\rho\left(x^\mu\right)=-4\pi q\int\frac{\delta^4\left(x^\mu-x_p^\mu\right)}{\sqrt{-g}}d\tau. \tag{3.4.3}$$

The determinant of the metric g, in Schwarzschild coordinates, is $-r^4\sin^2\theta$. We take the proper time τ to be the affine parameter of the orbit of our particle. With this in mind we

change the variable of integration to coordinate time t, giving

$$-4\pi\rho\left(x^{\mu}\right) = -4\pi q \int \frac{\delta^4\left(x^{\mu} - x_p^{\mu}\left(\tau\right)\right)}{r^2 \sin\theta} \frac{d\tau}{dt} dt, \tag{3.4.4}$$

$$= -\frac{4\pi q}{u^t r^2 \sin\theta} \delta\left[r - r_p(t)\right] \delta\left[\phi - \phi_p(t)\right] \delta\left[\theta - \pi/2\right]. \tag{3.4.5}$$

Here we have defined the time component of the four-velocity $u^t \equiv dt_p/d\tau$, and restricted (without loss of generality) the motion of the particle to the equatorial plane. In order to use Eq. (3.4.2) we need a specific form of $\rho_{\ell m}$. The spherical harmonic amplitudes of the source are found from

$$-4\pi\rho_{\ell m}(t,r) = -4\pi \int \rho(x^{\mu}) Y^*_{\ell m}(\theta,\phi) d\Omega. \tag{3.4.6}$$

Plugging in Eq. (3.4.5) gives

$$-4\pi\rho_{\ell m}(t,r) = -\frac{4\pi q}{u^t r^2} \int \frac{1}{\sin\theta} \delta\left[r - r_p(t)\right] \delta\left[\phi - \phi_p(t)\right] \delta\left[\theta - \pi/2\right] Y^*_{\ell m}(\theta,\phi) d\Omega, \tag{3.4.7}$$

$$= -\frac{4\pi q}{u^t r^2} \delta\left[r - r_p(t)\right] Y_{\ell m}(\pi/2, 0) e^{-im\phi_p(t)}. \tag{3.4.8}$$

3.4.1 The frequency domain

We now decompose the partial differential equations (3.4.2) into ordinary differential equations by moving from the time domain into the frequency domain. In the case of a circular orbit, this is simple. There is only one time scale that the physical problem depends on, and therefore all relevant frequencies are multiples of the fundamental: $\omega_m \equiv m \cdot 2\pi/T_{\phi}$. When our particle is in an eccentric orbit, however, the situation is more complicated. Now there are two fundamental frequencies of the motion, Ω_{ϕ} and Ω_r as the particle oscillates in ϕ and r. The Fourier transform of the radial function is

$$\psi_{\ell m}(t,r) = \int d\omega R_{lm\omega}(r) e^{-i\omega t}, \tag{3.4.9}$$

while the source term decomposes as

$$-4\pi r f \rho_{\ell m}(t,r) = \int d\omega Z_{\ell m\omega}(r) e^{-i\omega t}. \tag{3.4.10}$$

Plugging these into Eq. (3.4.2) we have

$$-\partial_t^2 \left[\int d\omega R_{\ell m\omega}(r) e^{-i\omega t}\right] + \partial_{r_*}^2 \left[\int d\omega R_{\ell m\omega}(r) e^{-i\omega t}\right]$$
$$-V_\ell(r) \int d\omega R_{\ell m\omega}(r) e^{-i\omega t} = \int d\omega Z_{\ell m\omega}(r) e^{-i\omega t}, \tag{3.4.11}$$

$$\frac{d^2 R_{\ell m\omega}}{dr_*^2}(r) - \left(V_\ell(r) - \omega^2\right) R_{\ell m\omega}(r) = Z_{\ell m\omega}. \tag{3.4.12}$$

Because the problem we are considering has two fundamental periods, the frequency dependence will be doubly periodic. That is, we will find that

$$\omega = \omega_{mn} \equiv m\Omega_\phi + n\Omega_r, \qquad m, n \in \mathbb{Z}, \tag{3.4.13}$$

where $\Omega_r \equiv 2\pi/T_r$ and

$$\Omega_\phi \equiv \frac{1}{T_r} \int_0^{T_r} \left(\frac{d\phi_p}{dt}\right) dt. \tag{3.4.14}$$

Now, in order to calculate the source term in the frequency domain we use the inverse Fourier transform:

$$Z_{\ell mn} = -\frac{4\pi}{T_r} \int_0^{T_r} f r \rho_{\ell m}(t,r) e^{i\omega_{mn} t} dt. \tag{3.4.15}$$

We can plug in for the source from Eq. (3.4.8) to get our specific form of $Z_{\ell mn}$,

$$Z_{\ell mn} = -\frac{4\pi q}{T_r} Y_{\ell m}(\pi/2, 0) \int_0^{T_r} \frac{f}{u^t r} \delta\left[r - r_p(t)\right] e^{-im\phi_p(t)} e^{i\omega_{mn} t_p} dt, \tag{3.4.16}$$

$$= -2\frac{4\pi q}{T_r} Y_{\ell m}(\pi/2, 0) \frac{f(r_p)}{u^r r_p} e^{-im\phi_p(r_p)} e^{i\omega_{mn} t(r_p)}. \tag{3.4.17}$$

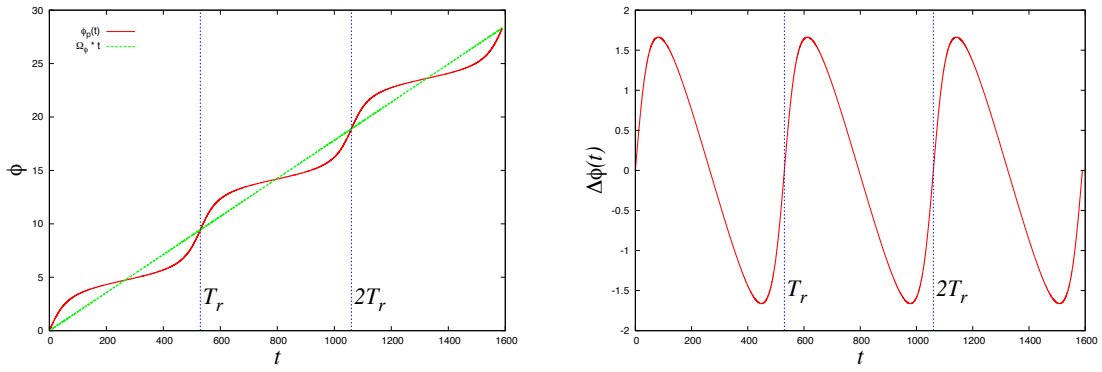

Figure 3.2: In red on the left we plot the azimuthal advance of a particle in eccentric orbit around a Schwarzschild black hole. Its average advance $\Omega_\phi t$ is plotted in green. Subtracting off this average advance leaves the right panel. Note that this oscillation about the mean value of ϕ has a period of T_r, corresponding to the radial motion of the particle.

We can decompose $\phi_p(t)$ as a part that grows linearly with time, and a part, $\Delta\phi(t)$, that has a periodicity of T_r,

$$\phi_p(t) = \Omega_\phi t + \Delta\phi(t). \tag{3.4.18}$$

Now we solve the ODE (3.4.12). We set unit normalized boundary conditions at the horizon and at infinity,

$$\hat{R}^-_{\ell mn}(r_* \to -\infty) = e^{-i\omega_{mn} r_*}, \qquad \hat{R}^+_{\ell mn}(r_* \to +\infty) = e^{i\omega_{mn} r_*}. \tag{3.4.19}$$

The method of variation of parameters gives the solution to the inhomogeneous equation,

$$R_{\ell mn}(r) = c^+_{\ell mn}(r)\hat{R}^+_{\ell mn}(r) + c^-_{\ell mn}(r)\hat{R}^-_{\ell mn}(r), \tag{3.4.20}$$

where

$$\begin{aligned} c^+_{\ell mn}(r) &\equiv \frac{1}{W_{\ell mn}} \int_{r_{\min}}^{r} dr' \frac{\hat{R}^-_{\ell mn}(r') Z_{\ell mn}(r')}{f(r')}, \\ c^-_{\ell mn}(r) &\equiv \frac{1}{W_{\ell mn}} \int_{r}^{r_{\max}} dr' \frac{\hat{R}^+_{\ell mn}(r') Z_{\ell mn}(r')}{f(r')}, \end{aligned} \tag{3.4.21}$$

and

$$W_{\ell mn} \equiv \hat{R}^{-}_{\ell mn} \frac{d\hat{R}^{+}_{\ell mn}}{dr_*} - \hat{R}^{+}_{\ell mn} \frac{d\hat{R}^{-}_{\ell mn}}{dr_*}, \tag{3.4.22}$$

is the Wronskian. Outside the source libration region, Eq. (3.4.20) reduces to the normalized homogeneous solutions that are properly connected through the source region,

$$R^{+}_{\ell mn}(r) = C^{+}_{\ell mn}\hat{R}^{+}_{\ell mn}(r), \quad r \geq r_{\max}, \quad R^{-}_{\ell mn}(r) = C^{-}_{\ell mn}\hat{R}^{-}_{\ell mn}(r), \quad r \leq r_{\min}, \tag{3.4.23}$$

where $C^{\pm}_{\ell mn}$ are the values of $c^{\pm}_{\ell mn}(r)$ evaluated at the ends of the range of the source,

$$C^{+}_{\ell mn} \equiv c^{+}_{\ell mn}\left(r_{\max}\right), \qquad C^{-}_{\ell mn} \equiv c^{-}_{\ell mn}\left(r_{\min}\right). \tag{3.4.24}$$

From here, the standard approach is to return to the time domain with the Fourier synthesis

$$\Psi_{\ell m}(t, r) = \sum_n R_{\ell mn}(r) e^{-i\omega_{mn}t}. \tag{3.4.25}$$

Because our source has a singularity, the function we are trying to reconstruct will have a lack of differentiability, and this reconstruction will therefore suffer from the Gibbs phenomenon.

3.4.2 Extended homogeneous solutions

We can regain the exponential convergence we want by turning to the method of extended homogeneous solutions (EHS) developed by Barack, Ori, and Sago [1]. We start by defining the frequency domain EHS, which are valid for all r,

$$R^{\pm}_{\ell mn}(r) \equiv C^{\pm}_{\ell mn}\hat{R}^{\pm}_{\ell mn}(r), \quad r > 2M. \tag{3.4.26}$$

Next, we define the time domain EHS, which (given that they are homogeneous solutions to the differential equation) are again formally valid everywhere,

$$\Psi^{\pm}_{\ell m}(t, r) \equiv \sum_n R^{\pm}_{\ell mn}(r) e^{-i\omega_{mn}t}. \tag{3.4.27}$$

Now, we claim that the true solution to Eq. (3.4.2) is

$$\Psi^{\rm EHS}_{\ell m}(t,r) \equiv \Psi^{+}_{\ell m}(t,r)\,\theta\left[r - r_p(t)\right] + \Psi^{-}_{\ell m}(t,r)\,\theta\left[r_p(t) - r\right]. \tag{3.4.28}$$

That this is the actual time domain scalar field is not obvious. In Chapter 4 we will discuss this method more thoroughly (including more general source terms).

3.5 Chapter summary

In the next chapter we will solve the field equations for the gravitational perturbation due to a particle in eccentric orbit about a Schwarzschild black hole. This chapter has introduced several ideas that will be important to that task. After examining scalar fields in flat space, we derived the Regge-Wheeler equation. This is the equation (with a different potential and source), that we will have to solve to find the metric perturbation amplitudes in Chapter 4. We saw how to choose causally appropriate boundary conditions, including performing the asymptotic expansion on the large r side. Then, considering a particle in eccentric orbit, we noted that the system exhibits two fundamental frequencies. Thus, upon moving to the frequency domain, we found that Regge-Wheeler equation must be solved for a doubly-infinite countable set of modes. Additionally, the source (which was point singular in the time domain) becomes a function of r, confined to the region $r_{\rm min}$ to $r_{\rm max}$. This leads to the Gibbs phenomenon, when a standard Fourier synthesis is used to return to the time domain. To circumvent this, we introduced the method of extended homogeneous solutions, which will be an important part of our work on gravitational fields in Chapters 4 and 5.

Chapter 4

Gravitational perturbations and metric reconstruction: Method of extended homogeneous solutions applied to eccentric orbits on a Schwarzschild black hole

Chapters 2 and 3 have set the stage for us to solve the perturbed Einstein equations for a particle in eccentric orbit about a Schwarzschild black hole. In Chapter 2 we saw how the first-order Einstein equations are derived on a curved background, and then subsequently how they are decomposed into equations for the spherical harmonic amplitudes when working in the Schwarzschild spacetime. We also introduced the Regge-Wheeler (RW) gauge, which we will be using in this chapter. We will see that solving the field equations in RW gauge reduces to solving a wave equation for one master function for each harmonic mode. In Chapter 3 we introduced many of the necessary concepts for solving the type of wave equation we will solve in this chapter. We saw horizon and infinity boundary conditions, eccentric orbit bi-periodicity, singular source terms, and the method of extended homogeneous solutions.

This chapter contains two noteworthy contributions to the field of EMRI research. First, we have applied the method of extended homogeneous solutions to all radiative gravitational modes. This allows for the fast and accurate frequency domain calculation of the radiative gravitational field at the point of the particle for the first time. Our second original result is the detailed analysis of the local singular nature of the metric perturbation in RW gauge.

We find that the six nonzero perturbation amplitudes are all discontinuous (C^{-1}) and three of them are additionally singular ($\sim \delta(z)$) at the location of the particle. We compute the time dependent magnitudes of these jumps and delta functions analytically.

4.1 Introduction

Considerable research on the two-body problem in general relativity has been fostered over the past decade by the prospects of detecting gravitational radiation from extreme-mass-ratio binaries. The general relativistic two-body problem is notoriously difficult, as it involves dynamics of the motion of the bodies and of the gravitational field itself. Gravitational wave emission carries away energy and angular momentum from the orbit, leading to inspiral and eventual merger. The future joint NASA-ESA LISA mission [61] is expected to detect between tens and thousands of such extreme-mass-ratio inspirals (EMRIs)–binaries composed of a compact object ($\mu \sim 1 - 50 M_\odot$) in orbit about a supermassive Kerr black hole ($M \sim 10^5 - 10^7 M_\odot$) out to cosmological distances ($z \sim 1$) [62]. The small mass ratio $10^{-7} \lesssim \mu/M \lesssim 10^{-3}$ of expected astrophysical sources [12] implies a gradual change in orbital parameters, with $\gtrsim 10^5$ wave periods as the binary evolves through the LISA passband ($10^{-4} - 10^{-2}$ Hz). Detailed theoretical calculations will aid in both detection of EMRI gravitational wave signals and in determination of the source's physical parameters.

Quite apart from the prospects of astrophysical observation, this problem is one of intrinsic interest in theoretical physics. Of the various possibilities, the physically simplest compact binary is one composed of two black holes. Such a system eliminates the complications of stellar microphysics and reduces the problem to a minimum parameter set. In approaching the problem mathematically, the extreme mass-ratio and gradual orbital evolution is of benefit theoretically, allowing black hole perturbation theory to be used. Furthermore, the small mass ratio allows even the black hole structure of the small mass to be ignored (at lowest order), restoring a point-like (particle) behavior [36] on length scales that are large compared to μ and thereby simplifying the perturbation problem.

The perturbation problem proceeds in stages. At the outset the motion of the particle

is taken as a geodesic ($\mu/M \to 0$, or zeroth order) on the background spacetime. The first-order (in μ/M) gravitational field perturbation is then computed, yielding a new metric $\mathrm{g}_{\mu\nu} = g_{\mu\nu} + p_{\mu\nu}$ that corrects the background metric $g_{\mu\nu}$. The gravitational waves in the perturbation $p_{\mu\nu}$ carry energy and angular momentum to infinity and down the black hole event horizon, giving rise to a back reaction or local self-force (SF) on the particle that has both conservative and dissipative terms. Formally, the SF depends on gradients of $p_{\mu\nu}$ and acts locally on the particle to accelerate it off its background geodesic. Once the first-order correction to the motion is successfully computed, the calculation may proceed to second order in the field perturbation (see Pound [63] for a recent background discussion and an alternative formulation).

Yet having idealized the small body as a point particle, the metric perturbation and SF are found to diverge at the location of the particle, and the formal perturbation to the equation of motion is meaningless without careful regularization. This problem is similar to the classic SF problem of an accelerating, radiating charge in electromagnetic theory in flat spacetime [32]. Two pivotal papers, by Mino, Sasaki, and Tanaka [37] and Quinn and Wald [38], showed how the metric perturbation may be separated into a divergent, direct part $p^{\mathrm{dir}}_{\mu\nu}$ and a finite tail term $p^{\mathrm{tail}}_{\mu\nu}$, with the latter providing the regularized field that makes the SF finite. As an alternative, Detweiler and Whiting [35] proposed decomposing the metric perturbation into regular $p^{R}_{\mu\nu}$ and singular $p^{S}_{\mu\nu}$ parts. Under this interpretation, $p^{R}_{\mu\nu}$ is a solution to the vacuum field equations, but gives rise to the same SF as $p^{\mathrm{tail}}_{\mu\nu}$.

Since then, SF calculations have been made in certain special cases [64, 65, 46, 66, 2]. See the review by Barack [62]. Ultimately, the theory aims to provide self-consistent SF calculations of arbitrary orbits about Kerr black holes. In this chapter, we concern ourselves with a more modest goal: demonstrating a complete computation of the radiative gravitational perturbations produced by a mass in eccentric orbit on a Schwarzschild black hole and reconstruction of the corresponding parts of the perturbed metric in Regge-Wheeler gauge. While we leave for another occasion computation of both the nonradiative perturbations and the SF, the accurate reconstruction of the radiative parts of the metric, at all locations up to and including the point mass, should serve as a starting point for a further

gauge transformation or alternative regularization technique.

We note in passing that most work to date computing EMRI evolution has not made use of local SF calculation. Sufficiently adiabatic changes in an orbit on Schwarzschild spacetime allow a *balance calculation* approach [49], where orbital energy and angular momentum are "evolved" (acausally) to match corresponding gravitational wave fluxes through bounding surfaces at large radius and near the horizon. Much effort is ongoing to extend the reach of adiabatic calculations [67, 68, 69]. Unfortunately, the approach only approximates dissipative SF terms and cannot account for conservative SF effects. In any event, the more self-consistent SF approach should serve to confirm the validity of these or other approximations.

Perturbation theory for Schwarzschild black holes has a traditional formalism pioneered by Regge and Wheeler [14], Zerilli [15], and Vishveshwara [70] that uses spherical harmonics and the Regge-Wheeler gauge to simplify algebraically the form of the metric perturbation. At each spherical harmonic order there are just two *master* functions, $\Psi^{\rm even}_{\ell m}(t,r)$ and $\Psi^{\rm odd}_{\ell m}(t,r)$, one for each parity or gravitational degree of freedom, which satisfy linear inhomogeneous wave equations in t and r. The formalism was improved by Moncrief [16] and colleagues [17, 18], making use instead of gauge-invariant master functions that satisfy similar wave equations. Recently Martel and Poisson [55] have placed the theory in both a gauge-invariant and covariant form.

For perturbations of Kerr black holes, Teukolsky [20] developed a formalism based on Newman-Penrose curvature scalars and spin-weighted spheroidal harmonics. In the frequency domain the radial part is a single (complex) master equation [71], which can, of course, be applied to a Schwarzschild hole as well [49, 72].

An alternative to the Regge-Wheeler-Zerilli (RWZ) approach has recently been advanced by Barack and Lousto [45]. They propose directly evolving the ten spherical harmonic amplitudes that describe the metric perturbation in Lorenz (or harmonic) gauge. In this direct metric perturbation approach, the equations separate into even- and odd-parity sectors, yet still involve systems of seven and three coupled equations, respectively. Barack and Sago [65, 2] have used the formalism to compute the time evolution of metric perturbations

generated by circular and eccentric orbits on Schwarzschild, along with the resulting SF components.

The RWZ and direct metric perturbation approaches each have advantages and disadvantages. The direct metric perturbation formalism yields directly what one wants as an input to a SF calculation, namely the metric itself in Lorenz gauge. In a time domain calculation, as so far employed, it has the disadvantage of requiring simultaneous solution of a large set of coupled partial differential equations (PDE's). Anticipating the subtraction involved in the SF regularization, Barack, Lousto, and Sago have built a fourth-order convergent finite difference code to compute the modes to sufficient accuracy. In contrast, the RWZ approach has the advantage that only a single uncoupled wave equation need be solved for each mode and parity. Unfortunately, an added step is required to reconstruct the metric from the mode solutions. Moreover, the reconstruction involves terms that are singular at the particle location and the simplest reconstruction yields the metric perturbation in Regge-Wheeler gauge [50, 73]. Finally, the RWZ approach provides only the radiative ($\ell \geq 2$) parts of the perturbation and the nonradiative modes ($\ell = 0, 1$) must be derived by separate means.

In this chapter we opt for using the gauge-invariant RWZ approach detailed by Martel and Poisson [55], and adopt the Zerilli-Moncrief $\Psi^{\rm ZM}_{\ell m} = \Psi^{\rm even}_{\ell m}$ and Cunningham-Price-Moncrief $\Psi^{\rm CPM}_{\ell m} = \Psi^{\rm odd}_{\ell m}$ master functions for even and odd-parity, respectively. Our use of this relatively standard method is augmented, though, by a new technique that enables accurate reconstruction of the corresponding parts of the metric in Regge-Wheeler gauge. We leave for a later occasion our own consideration of the monopole and dipole terms (which are essential to a SF calculation) and instead direct attention to discussion by Detweiler and Poisson [30] and recent successful numerical implementation by Barack and Sago [2].

The master functions can be obtained directly by numerical evolution (solution of PDE's) in the time domain (TD) (see e.g., [74, 64, 50, 51, 65, 75, 66, 2]) or by numerical integration of ordinary differential equations (ODE's) for the Fourier modes in the frequency domain (FD) (see e.g., [49, 76, 77, 1]). Each method has strengths and weaknesses. TD calculations require solving just one equation for each ℓ, m mode and time dependence of

the subsequently reconstructed metric and SF is of direct interest. Disadvantages of TD calculations include (1) modeling the discontinuous source movement through the finite difference grid [45, 2]; (2) numerical stability of PDE evolution; (3) difficulty devising numerical schemes of adequately small truncation error; and (4) challenges in posing outgoing wave boundary conditions at finite radius. In contrast, in FD calculations (1) the numerical errors tend to be much smaller (i.e., by solving ODE's); (2) outgoing wave boundary conditions are handled mode-by-mode and extrapolated to infinity and to the black hole event horizon; and (3) the discontinuous source presents few difficulties in computing (at least) the Fourier mode functions $R_{\ell mn}(r)$. However, FD methods require, for eccentric orbits, computing and summing over numerous harmonics n of the radial libration frequency Ω_r for each ℓ, m and transformation to the TD is nontrivial given the singular source terms.

Barack, Ori, and Sago (BOS) [1] highlighted the latter difficulty. They used the model problem of a scalar field $\Phi(t, r, \theta, \varphi)$ generated by a scalar point charge in eccentric orbit on Schwarzschild. The spherical harmonic modes $\phi_{\ell m}(t, r) = r\Phi_{\ell m}(t, r)$ satisfy a wave equation with a singular source, $S^{\rm scalar}_{\ell m}(t, r) = C_{\ell m}(t, r)\, \delta[r - r_p(t)]$. Here $C_{\ell m}(t, r)$ is some smooth function and $r = r_p(t)$ describes the radial libration of the particle's worldline between two turning points. In the FD, ODE's are solved for the Fourier-harmonic modes $R_{\ell mn}(r)$. These mode functions are, at each point r, Fourier series coefficients. The resulting Fourier series converges for the piecewise continuous (C^0) $\phi_{\ell m}(t, r)$ but the singular nature of the source S makes $\phi_{\ell m}(t, r)$ converge slowly in the region traversed by the point charge. The radial derivative $\partial_r \phi_{\ell m}$ is however discontinuous at $r = r_p(t)$ and its Fourier series only converges, in the usual sense [78], almost everywhere. The attempt to assemble the radial derivative from the Fourier series is plagued by the Gibbs phenomenon; the series converges to the mean value at the discontinuity and the series "overshoots" and fails to converge properly in the limit as both $n \to \infty$ and $r \to r_p(t)^{\pm}$.

BOS circumvented the difficulty with a new *method of extended homogeneous solutions*. In brief, they use FD analysis to find Fourier-harmonic mode solutions to the homogeneous equation, valid outside and on either side of the source libration region. The associated

Fourier series converge exponentially fast to homogeneous solutions of the TD wave equation. They then analytically extend both homogeneous TD solutions into the source libration region up to the instantaneous position of the point charge. Summed to adequately high order, the two homogeneous solutions match in value at $r_p(t)$, as expected. With the field represented in this way, the left and right derivatives can be accurately determined. BOS argued that the method should work for other problems with similar wave equations, including the Teukolsky equation.

We show in this chapter that the method can indeed be extended to the case of gravitational perturbations computed in the RWZ formalism, and apply the method to a large set of Fourier-harmonic modes stemming from a mass in eccentric orbit on Schwarzschild. (Note that Barack and Sago [2] previously implemented this method in the gravitational case but only for the $\ell = 0, 1$ modes in Lorenz gauge.) An important distinction arises: in the gravitational case the source distribution in the Regge-Wheeler gauge contains both delta function and derivative-of-delta function terms,

$$S_{\ell m}(t,r) = G_{\ell m}(t,r)\,\delta[r - r_p(t)] + F_{\ell m}(t,r)\,\delta'[r - r_p(t)], \tag{4.1.1}$$

with $G_{\ell m}(t,r)$ and $F_{\ell m}(t,r)$ being smooth functions. As a consequence the master functions have a jump discontinuity at $r = r_p(t)$ (referred to sometimes as a C^{-1} function). The resulting extension of the homogeneous solutions, $\Psi^{+}_{\ell m}$ and $\Psi^{-}_{\ell m}$, written as

$$\Psi_{\ell m}(t,r) = \Psi^{+}_{\ell m}(t,r)\,\theta[r - r_p(t)] + \Psi^{-}_{\ell m}(t,r)\,\theta[r_p(t) - r], \tag{4.1.2}$$

where $\theta[r - r_p(t)]$ is the Heaviside function, is a type of *weak solution* to the inhomogeneous master equation. Thus in the gravitational case in RWZ gauge the difficulty with local convergence occurs with the master function itself. We show that the use of distributions, or generalized functions [79], makes possible separate analytic calculation of the expected jumps in value and slope of $\Psi_{\ell m}$. We further demonstrate that the metric perturbation can be accurately numerically computed, including the time dependent magnitudes of delta function terms that appear in some of the metric amplitudes in Regge-Wheeler gauge.

This chapter is organized as follows. In Sec. 4.2 we briefly outline the general mathematical problem of using FD techniques to solve for perturbations in the RWZ formalism. We also review the standard parameterization of eccentric orbits. Sec. 4.3 concerns the method of extended homogeneous solutions. We first review BOS's solution for the scalar field case. We show then our treatment of more general source terms and extension of the method to gravitational perturbations. Sec. 4.4 provides numerical results on the computed Fourier-harmonic mode functions, including convergence tests and calculation of radiated gravitational wave energy and angular momentum. In particular, the energy and angular momentum fluxes are shown to agree with past published values. More importantly, the method is shown to provide a solution to the field and its derivatives that is convergent exponentially fast everywhere. Then in Sec. 4.5, we show that the equations which allow the metric to be obtained from the master functions, along with an understanding of the form of the weak solutions for $\Psi^{\rm even}_{\ell m}$ and $\Psi^{\rm odd}_{\ell m}$, can be used to determine both the smooth and distributional parts of the metric. App. 4.A discusses fully evaluated forms of distributional source terms. App. 4.B gives the details of such source terms for our case of eccentric orbits on Schwarzschild. In App. 4.C we concisely summarize the metric perturbation formalism in the Regge-Wheeler gauge. We show the construction of gauge-invariant master functions of each parity, and provide the spherical harmonic decomposition of the Einstein equations and Bianchi identities. App. 4.D concludes this chapter with a brief discussion of asymptotic expansions used to set boundary conditions on the mode functions at large r.

Throughout this chapter we use the sign conventions and notation of Misner, Thorne, and Wheeler [53] and use units in which $c = G = 1$. We use Schwarzschild coordinates $x^\mu = (t, r, \theta, \varphi)$ except as otherwise indicated.

4.2 Background on the standard RWZ approach to gravitational perturbations in the frequency domain

In this section we briefly summarize both the standard notation for parameterizing bound orbits on Schwarzschild and the usual approach to computing gravitational perturbations

using the Regge-Wheeler-Zerilli (RWZ) formalism in the frequency domain (FD). The description of the geodesic motion on the background, in terms of various curve functions, is used throughout the rest of the chapter. The standard FD analysis provides the notation for describing the Fourier-harmonic modes, and their normalization, and sets the stage for discussion in Sec. 4.3 of how gravitational perturbations can be returned successfully to the time domain (TD). Here, and throughout this chapter, we use a subscript p to indicate evaluation along the worldline of the particle.

4.2.1 Bound orbits on a Schwarzschild black hole

Consider bound timelike geodesic motion around a Schwarzschild black hole (i.e., $\mu \to 0$). We may for the nonce use proper time τ to parameterize the geodesic, $x^\mu_p(\tau) = [t_p(\tau), r_p(\tau), \theta_p(\tau), \varphi_p(\tau)]$, with the associated four-velocity $u^\mu = dx^\mu_p/d\tau$. On Schwarzschild we take $\theta_p(\tau) = \pi/2$ without loss of generality. The geodesic equations yield immediate first integrals and allow the trajectory to be described by the conserved energy $\mathcal{E}$ and angular momentum $\mathcal{L}$ per unit mass. Alternatively, we can choose the (dimensionless) semi-latus rectum p and the eccentricity e as orbital parameters (c.f., [49, 2]). A third choice would be use of the periapsis and apapsis, $r_{\rm min}$ and $r_{\rm max}$. We will find all of these useful in what follows. The latter two parameter pairs are related to each other by

$$p \equiv \frac{2 r_{\rm max} r_{\rm min}}{M(r_{\rm max} + r_{\rm min})}, \qquad e \equiv \frac{r_{\rm max} - r_{\rm min}}{r_{\rm max} + r_{\rm min}}, \tag{4.2.1}$$

or inversely

$$r_{\rm max} = \frac{pM}{1-e}, \qquad r_{\rm min} = \frac{pM}{1+e}. \tag{4.2.2}$$

The specific energy and angular momentum are related to p and e by [49]

$$\mathcal{E}^2 = \frac{(p-2-2e)(p-2+2e)}{p(p-3-e^2)}, \qquad \mathcal{L}^2 = \frac{p^2 M^2}{p-3-e^2}. \tag{4.2.3}$$

The geodesic equations provide the following differential equations for the orbital motion and for the time dependence of the four-velocity,

$$\frac{dt_p}{d\tau} = u^t = \frac{\mathcal{E}}{f_p}, \qquad \frac{d\varphi_p}{d\tau} = u^\varphi = \frac{\mathcal{L}}{r_p^2}, \qquad \left(\frac{dr_p}{d\tau}\right)^2 = (u^r)^2 = \mathcal{E}^2 - U_p^2, \tag{4.2.4}$$

where

$$f(r) \equiv 1 - \frac{2M}{r}, \qquad U^2(r, \mathcal{L}^2) \equiv f\left(1 + \frac{\mathcal{L}^2}{r^2}\right). \tag{4.2.5}$$

For purposes of numerical integration there is another curve parameter, originally devised by Darwin [80], that proves useful. Here one introduces a phase angle χ that is related to the radial position on the orbit by the Keplerian-appearing form

$$r_p(\chi) = \frac{pM}{1 + e\cos\chi}. \tag{4.2.6}$$

Of course, in the relativistic case χ differs from the true anomaly φ. The orbit goes through one radial libration for each change $\Delta\chi = 2\pi$. The use of χ eliminates singularities in the differential equations at the turning points [49]. Note that at $\chi = 0$, $r_p = r_{\min}$ and at $\chi = \pi$, $r_p = r_{\max}$. (Also note that in this section we are content with making a slight abuse of notation in jumping from $r_p(\tau)$ to $r_p(\chi)$, before ultimately settling on $r_p(t)$.) In terms of χ the equations are

$$\frac{dt_p}{d\chi} = \frac{p^2 M}{(p - 2 - 2e\cos\chi)(1 + e\cos\chi)^2}\left[\frac{(p-2)^2 - 4e^2}{p - 6 - 2e\cos\chi}\right]^{1/2}, \tag{4.2.7}$$

$$\frac{d\varphi_p}{d\chi} = \left[\frac{p}{p - 6 - 2e\cos\chi}\right]^{1/2}, \tag{4.2.8}$$

and

$$\frac{d\tau_p}{d\chi} = \frac{Mp^{3/2}}{(1 + e\cos\chi)^2}\left[\frac{p - 3 - e^2}{p - 6 - 2e\cos\chi}\right]^{1/2}. \tag{4.2.9}$$

We use Eq. (4.2.7) to derive the fundamental frequency and period of radial motion,

$$\Omega_r \equiv \frac{2\pi}{T_r}, \qquad T_r \equiv \int_0^{2\pi}\left(\frac{dt_p}{d\chi}\right)d\chi. \tag{4.2.10}$$

It is also of importance to have the average rate at which the azimuthal angle advances, found by averaging the angular frequency $d\varphi_p/dt$ over a radial libration via

$$\Omega_\varphi \equiv \frac{1}{T_r}\int_0^{T_r}\left(\frac{d\varphi_p}{dt}\right)dt. \tag{4.2.11}$$

While T_r represents the lapse of coordinate time in a radial libration, the time $T_\varphi = 2\pi/\Omega_\varphi$ has no particular physical significance [81]. Finally, because wave equation source functions contain terms like $\delta[r - r_p(t)]$ and $\delta'[r - r_p(t)]$, we have need of derivatives of $r_p(t)$,

$$\dot{r}_p^2(t) = f_p^2 - \frac{f_p^2}{\mathcal{E}^2}U_p^2, \qquad \ddot{r}_p(t) = \frac{2Mf_p}{r_p^2} - \frac{f_p^2}{\mathcal{E}^2 r_p^2}\left[3M - \frac{\mathcal{L}^2}{r_p} + \frac{5M\mathcal{L}^2}{r_p^2}\right], \tag{4.2.12}$$

where we let a dot signify differentiation with respect to coordinate time.

4.2.2 The Regge-Wheeler-Zerilli formalism in the frequency domain

As discussed in the Introduction, we use the RWZ approach to gravitational perturbations and use specifically the even-parity Zerilli-Moncrief function $\Psi^{\rm even}_{\ell m}$ [16] and the odd-parity Cunningham-Price-Moncrief function $\Psi^{\rm odd}_{\ell m}$ [18]. See Martel and Poisson [55] for recent discussion and references therein. Both of these functions satisfy wave equations of the form

$$\left[-\frac{\partial^2}{\partial t^2} + \frac{\partial^2}{\partial r_*^2} - V_\ell(r)\right]\Psi_{\ell m}(t,r) = S_{\ell m}(t,r), \tag{4.2.13}$$

where $r_* = r + 2M\ln(r/2M - 1)$ is the usual tortoise coordinate. The potential used in Eq. (4.2.13) is either the Zerilli or Regge-Wheeler potential depending on whether the parity is even or odd, respectively.

The source terms also depend upon parity but further depend on which specific master functions are chosen. Martel and Poisson gave the covariant form of $S^{\rm even}_{\ell m}$ and $S^{\rm odd}_{\ell m}$ (see App. 4.C for these in Schwarzschild coordinates) that are associated with the Zerilli-Moncrief and Cunningham-Price-Moncrief functions. Martel [50] derived the detailed form of $S^{\rm even}_{\ell m}$ for a point mass in eccentric orbit. Sopuerta and Laguna [75] derived the detailed form of $S^{\rm odd}_{\ell m}$ for eccentric orbits (see also Field et al. [82]). We give in App. 4.B detailed

expressions for these sources in a form that is useful for both mode integrations and metric reconstruction.

In each case the source term has the following general form

$$S_{\ell m}(t,r) = \tilde{G}_{\ell m}(t)\,\delta[r - r_p(t)] + \tilde{F}_{\ell m}(t)\,\delta'[r - r_p(t)], \tag{4.2.14}$$

where $\tilde{G}_{\ell m}(t)$ and $\tilde{F}_{\ell m}(t)$ are smooth (differentiable) functions. Note that the source, as written here, differs from notation originally used by Martel [50] (who retained smooth functions of r and t, as in Eq. (4.1.1)). Our expression uses the delta function, and parts integration, to yield a *fully evaluated form* along the worldline of the particle (see App. 4.A), making $\tilde{G}_{\ell m}(t)$ and $\tilde{F}_{\ell m}(t)$ unique functions of time only.

Eq. (4.2.13) can be solved directly in the TD–an approach that has received much attention lately. In this chapter we are interested instead in extending the reach of FD analysis, and the balance of this section provides a brief review of the standard FD solution. We note in passing that a hybrid approach is possible–using FD analysis for low ℓ and m modes while using TD calculation for high order modes [83].

On Schwarzschild, eccentric orbits are typically not closed and therefore the motion is not simply periodic as seen by an asymptotic static observer. The radial libration is periodic (but not typically sinusoidal) with fundamental frequency Ω_r. The smooth functions $\tilde{G}_{\ell m}(t)$ and $\tilde{F}_{\ell m}(t)$, which depend upon the particle's radial and angular motion, have terms that are periodic with fundamental frequency Ω_r, but also involve a term that is proportional to $\exp[-im\varphi_p(t)]$. This latter term comes from restricting the spherical harmonics $Y^*_{\ell m}(\theta,\varphi)$ with $\delta[\varphi - \varphi_p(t)]$. The function $\varphi_p(t)$ advances with an average rate Ω_φ, but is modulated (in an eccentric orbit) by a function $\Delta\varphi(t)$ that is periodic with fundamental frequency Ω_r. Hence, the source $S_{\ell m}(t,r)$, and therefore the field $\Psi_{\ell m}(t,r)$, can be represented by a Fourier series with fundamental frequency Ω_r, but multiplied by a phase factor that advances linearly with rate Ω_φ. These fields *would* appear simply periodic to an observer whose frame rotates at rate Ω_φ [49]. To a static observer, a given mode ℓ and m will have a spectrum of harmonics offset by $m\Omega_\varphi$; taken together the full field will have a two-fold

countably infinite frequency spectrum,

$$\omega = \omega_{mn} \equiv m\Omega_\varphi + n\Omega_r, \qquad m, n \in \mathbb{Z}. \tag{4.2.15}$$

Accordingly, the wave equation (4.2.13) Fourier transforms into a set of ODE's,

$$\left[\frac{d^2}{dr_*^2} - V_\ell(r) + \omega_{mn}^2\right] R_{\ell mn}(r) = Z_{\ell mn}(r), \tag{4.2.16}$$

where $R_{\ell mn}(r)$ and $Z_{\ell mn}(r)$ are Fourier harmonic amplitudes

$$R_{\ell mn}(r) \equiv \frac{1}{T_r}\int_0^{T_r} dt\ \Psi_{\ell m}(t,r)\, e^{i\omega_{mn}t}, \qquad Z_{\ell mn}(r) \equiv \frac{1}{T_r}\int_0^{T_r} dt\ S_{\ell m}(t,r)\, e^{i\omega_{mn}t}. \tag{4.2.17}$$

The series representations of $\Psi_{\ell m}(t,r)$ and $S_{\ell m}(t,r)$ are

$$\Psi_{\ell m}(t,r) = \sum_{n=-\infty}^{\infty} R_{\ell mn}(r)\, e^{-i\omega_{mn}t}, \qquad S_{\ell m}(t,r) = \sum_{n=-\infty}^{\infty} Z_{\ell mn}(r)\, e^{-i\omega_{mn}t}, \tag{4.2.18}$$

and are subject to the usual provisos of Fourier theory regarding for what r Eqs. (4.2.18) converge to the original functions.

In order to find the solution to Eq. (4.2.16), we start by solving the homogeneous version of that equation, obtaining two independent solutions. Using the terminology of Galt'sov [84] (see also [85] for a clear presentation of basis modes), the $R^-_{\ell mn}(r)$ solution is computed by setting a unit normalized "in" wave boundary condition of

$$\hat{R}^-_{\ell mn}(r_* \to -\infty) = e^{-i\omega_{mn}r_*}, \tag{4.2.19}$$

near the horizon. Similarly, the $R^+_{\ell mn}(r)$ solution arises from setting a unit normalized "up" boundary condition of

$$\hat{R}^+_{\ell mn}(r_* \to +\infty) = e^{i\omega_{mn}r_*}, \tag{4.2.20}$$

at large r_*. Formally, these homogeneous solutions are both valid in the entire range $2M < r < \infty$. The standard method of integrating the Green function and source (the method of

variation of parameters) gives the solution to the inhomogeneous equation (4.2.16),

$$R_{\ell mn}(r) = c^{+}_{\ell mn}(r)\hat{R}^{+}_{\ell mn}(r) + c^{-}_{\ell mn}(r)\hat{R}^{-}_{\ell mn}(r), \tag{4.2.21}$$

where

$$\begin{aligned} c^{+}_{\ell mn}(r) &\equiv \frac{1}{W_{\ell mn}} \int_{r_{\rm min}}^{r} dr' \frac{\hat{R}^{-}_{\ell mn}(r') Z_{\ell mn}(r')}{f(r')}, \\ c^{-}_{\ell mn}(r) &\equiv \frac{1}{W_{\ell mn}} \int_{r}^{r_{\rm max}} dr' \frac{\hat{R}^{+}_{\ell mn}(r') Z_{\ell mn}(r')}{f(r')}, \end{aligned} \tag{4.2.22}$$

and

$$W_{\ell mn} \equiv \hat{R}^{-}_{\ell mn} \frac{d\hat{R}^{+}_{\ell mn}}{dr_*} - \hat{R}^{+}_{\ell mn} \frac{d\hat{R}^{-}_{\ell mn}}{dr_*}, \tag{4.2.23}$$

is the Wronskian. Outside the source libration region, Eq. (4.2.21) reduces to the normalized homogeneous solutions that are properly connected through the source region,

$$\begin{aligned} R^{+}_{\ell mn}(r) &= C^{+}_{\ell mn}\hat{R}^{+}_{\ell mn}(r), \quad r \geq r_{\rm max}, \\ R^{-}_{\ell mn}(r) &= C^{-}_{\ell mn}\hat{R}^{-}_{\ell mn}(r), \quad r \leq r_{\rm min}, \end{aligned} \tag{4.2.24}$$

where $C^{\pm}_{\ell mn}$ are the values of $c^{\pm}_{\ell mn}(r)$ evaluated at the ends of the range of the source,

$$C^{+}_{\ell mn} \equiv c^{+}_{\ell mn}\left(r_{\rm max}\right), \qquad C^{-}_{\ell mn} \equiv c^{-}_{\ell mn}\left(r_{\rm min}\right). \tag{4.2.25}$$

4.3 The method of extended homogeneous solutions in the gravitational case

4.3.1 Brief review of Barack, Ori, and Sago's method of extended homogeneous solutions

As a model problem, Barack, Ori, and Sago (BOS) considered the scalar field Φ produced by a scalar point charge in an eccentric orbit on a Schwarzschild background. The spherical harmonic amplitudes $\phi_{\ell m}(t,r) = r\Phi_{\ell m}(t,r)$ of the scalar field satisfy RWZ-like equations fully analogous to Eq. (4.2.13) but with source functions that only depend upon a Dirac

delta function,

$$S^{\rm scalar}_{\ell m} = C_{\ell m}(t,r)\,\delta[r - r_p(t)]. \tag{4.3.1}$$

Here $C_{\ell m}(t,r)$ is a smooth function that is derived from the particle's point-like charge density ρ.

With a delta function source the amplitudes $\phi_{\ell m}(t,r)$ are left piecewise continuous (C^0) at the instantaneous particle location $r_p(t)$ but lose all differentiability there. BOS argued that this behavior, while surmountable in TD calculations, would cause difficulties for Fourier synthesis in FD calculations. As they convincingly demonstrated with their first two figures, while $\phi_{\ell m}(t,r)$ converges exponentially fast outside the radial libration region, the Gibbs phenomenon is responsible for a very slow convergence of $\phi_{\ell m}(t,r)$ between $r_{\rm min}$ and $r_{\rm max}$. Furthermore, the radial derivative $\partial_r\phi_{\ell m}$ is discontinuous at $r_p(t)$ and suffers the full effects of the Gibbs phenomenon–the Fourier series converges to the mean value at the discontinuity and partial sums ($-N \le n \le N$) overshoot in the limit as both $N \to \infty$ and $r \to r_p(t)^{\pm}$. This behavior is a serious obstacle to straightforward use of FD calculations in SF regularization.

As a solution to this problem, BOS developed the method of extended homogeneous solutions (EHS). Their method involves using the Fourier-harmonic modes of the homogeneous equation in the FD to synthesize homogeneous solutions $\phi^-_{\ell m}(t,r)$ and $\phi^+_{\ell m}(t,r)$ to the TD wave equation. The Fourier convergence of these homogeneous solutions is exponentially rapid. While these solutions exist in the entire radial domain ($2M < r < \infty$), ordinarily $\phi^-_{\ell m}(t,r)$ and $\phi^+_{\ell m}(t,r)$ would be viewed as meaningful in their respective source-free regions, $r < r_{\rm min}$ and $r > r_{\rm max}$. The heart of the BOS method lies in extending both of these solutions into the region of radial libration up to the instantaneous position of the particle.

BOS demonstrated the method numerically using the monopole term of Φ. A key condition for success of the method is that, as $N \to \infty$ in the partial sums, one finds

$$\lim_{r\to r_p(t)} \phi^-_{\ell m}(t,r) = \lim_{r\to r_p(t)} \phi^+_{\ell m}(t,r), \tag{4.3.2}$$

as expected analytically. This was observed numerically and the method as a whole converges rapidly since the FD solution of the inhomogeneous equation is never summed. BOS went on to argue that the method could be extended to any ℓ and m for scalar, electromagnetic, or gravitational fields.

4.3.2 Application to gravitational perturbations

In this section we detail our application of the method to the gravitational case in RWZ gauge. It is worth first observing the magnitude of the problem to be circumvented. Given the gravitational source (4.2.14), and the solution to Eq. (4.2.16) afforded by Eq. (4.2.21), the standard approach would represent the inhomogeneous solution to the master equation (4.2.13) by

$$\Psi_{\ell m}(t,r) \sim \Psi^{\rm std}_{\ell m}(t,r) = \sum_{n=-N}^{+N} R_{\ell mn}(r)\, e^{-i\omega_{mn}t}, \qquad N \to \infty, \tag{4.3.3}$$

where we use the $\sim$ to indicate that the equality between the actual solution $\Psi_{\ell m}$ and $\Psi^{\rm std}_{\ell m}$ holds *almost everywhere* for $N \to \infty$.

Looking ahead somewhat, we use our numerical code to obtain a particular spherical harmonic amplitude, $\Psi_{22}(t,r)$ ($\ell = 2$, $m = 2$), and its radial derivative, $\partial_r \Psi_{22}(t,r)$. We can also use the code to assemble the standard partial Fourier sums (see FIGs. 4.1 and 4.2). *We find that the Gibbs problem with the standard approach is significantly worse in the gravitational case (in Regge-Wheeler gauge) than it is for the scalar field.* In the present case the field itself has a discontinuity and the radial derivative is both discontinuous as $r \to r_p(t)$ and also has a delta function singularity at $r_p(t)$. The left panels of FIGs. 4.1 and 4.2 are familiar; the partial sums have difficulty representing the jump discontinuity and overshoot the exact solution (solid curve). In the right panels, the singularity at $r_p(t)$ wreaks havoc on the ability of the Fourier synthesis to represent the exact solution.

On a bright note, outside the range of the source, the standard solution converges exponentially fast. Nevertheless, in the source region between $r_{\rm min}$ and $r_{\rm max}$ the convergence will be algebraic in general and disastrous at the location of the particle. A discontinuous (or worse, singular) function cannot be accurately represented by a finite sum of smooth

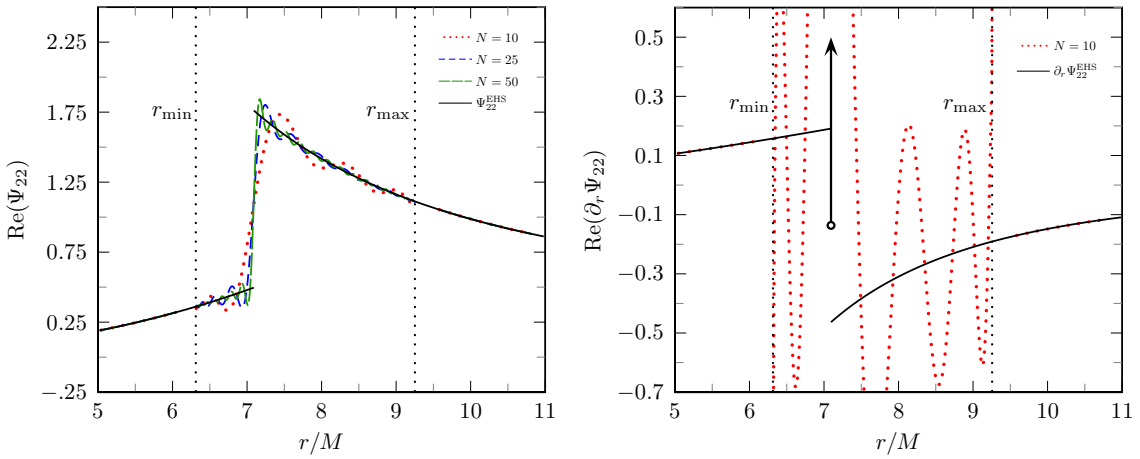

Figure 4.1: The standard FD approach to reconstructing the TD master function and its r derivative. The left panel shows $\Psi_{22}^{\rm std}$ and the right shows $\partial_r \Psi_{22}^{\rm std}$ at $t = 51.78M$ for a particle orbiting with $p = 7.50478$ and $e = 0.188917$. This figure is analogous to FIG. 1 of BOS [1]. Partial sums are computed with Eq. (4.3.3) and shown for different N. For contrast we plot the converged solution from the new method with a solid curve (see FIG. 4.3). The arrow in the right panel gives a notional representation of the delta function singularity present in $\partial_r \Psi_{22}$; the amplitude of this singular term is related to the jump in Ψ_{22} seen in the left panel.

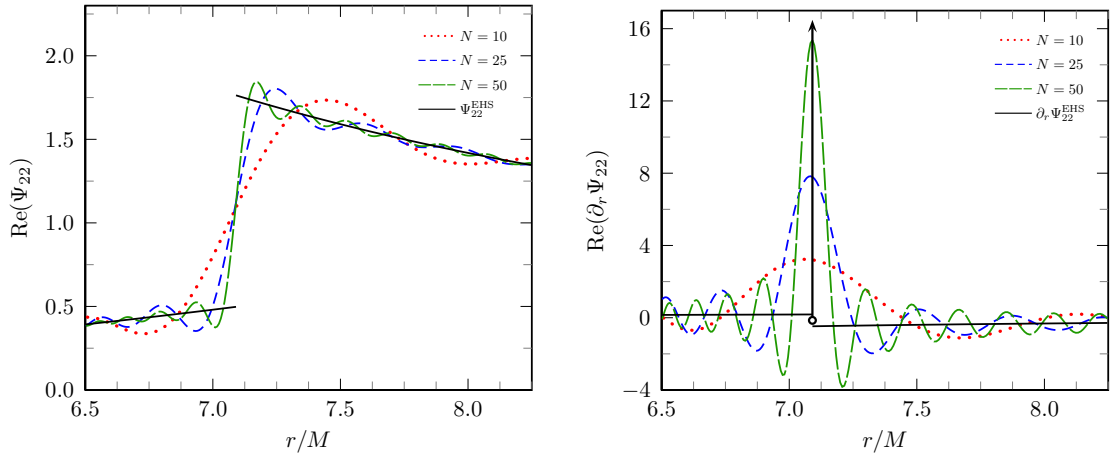

Figure 4.2: An alternate view of the behavior presented in FIG. 4.1. A change in the scale in the left panel emphasizes the Gibbs overshoots in Ψ_{22}. On the right, a zoom-out of the vertical scale more clearly indicates the attempt of the Fourier synthesis to capture the delta function at $r_p(t)$.

functions.

We now generalize the EHS method to the gravitational case. We start by recognizing

that $R^{\pm}_{\ell mn}$ from Eq. (4.2.24) are valid solutions to the homogeneous version of Eq. (4.2.16) throughout the entire domain outside the black hole,

$$R^{\pm}_{\ell mn}(r) = C^{\pm}_{\ell mn}\hat{R}^{\pm}_{\ell mn}(r), \qquad r > 2M. \tag{4.3.4}$$

Next, we use these to define the *time-domain extended homogeneous solutions*,

$$\Psi^{\pm}_{\ell m}(t,r) \equiv \sum_n R^{\pm}_{\ell mn}(r)\, e^{-i\omega_{mn}t}, \qquad r > 2M, \tag{4.3.5}$$

which result from inserting $R^{\pm}_{\ell mn}$ into Eq. (4.2.18). The central claim is then that for any t and r the actual solution to the inhomogeneous wave equation (4.2.13) is given by

$$\Psi_{\ell m}(t,r) = \Psi^{\rm EHS}_{\ell m}(t,r) \equiv \Psi^{+}_{\ell m}(t,r)\,\theta\left[r - r_p(t)\right] + \Psi^{-}_{\ell m}(t,r)\,\theta\left[r_p(t) - r\right]. \tag{4.3.6}$$

The argument made by BOS can be extended to the gravitational case and goes as follows:

- We denote the desired true solution of the inhomogeneous wave equation as $\Psi_{\ell m}$. Outside the domain of the source ($r < r_{\rm min}, r_{\rm max} < r$) $\Psi_{\ell m} = \Psi^{\rm std}_{\ell m} = \Psi^{\rm EHS}_{\ell m}$ because there $R_{\ell mn} = R^{\pm}_{\ell mn}$.

- It is assumed that $\Psi_{\ell m}(t,r)$ is analytic in the entirety of the two regions $2M < r < r_p(t)$ and $r_p(t) < r$ (excluding only a neighborhood of $r_p(t)$).

- Because the homogeneous solutions $\Psi^{\pm}_{\ell m}$ are expected to be analytic everywhere, $\Psi^{\rm EHS}_{\ell m}(t,r)$ will be analytic in the two regions discussed above (excluding only a neighborhood of $r_p(t)$). (See the extended discussion BOS have about this.)

- Because $\Psi_{\ell m}$ and $\Psi^{\rm EHS}_{\ell m}$ are identical outside the region of libration, and they are both analytic everywhere up to the location of the source, they must be equal over that entire domain.

Here we provide an additional justification for the assumed form of the solution given in Eq. (4.3.6). The source term of the wave equation is a distribution, or generalized

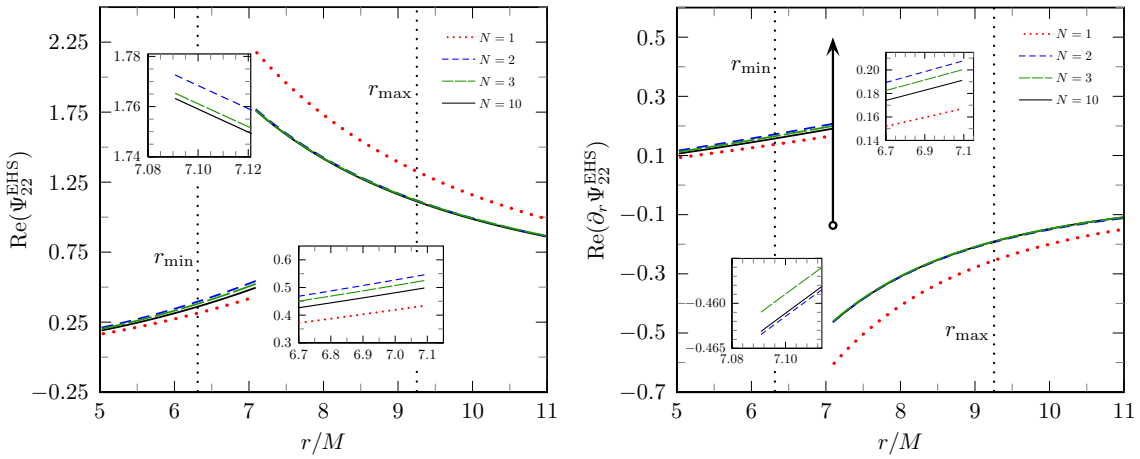

Figure 4.3: The EHS approach to reconstructing the TD master function and its radial derivative. As in FIG. 4.1, we give Ψ_{22}^{EHS} and $\partial_r \Psi_{22}^{\mathrm{EHS}}$ at $t = 51.78M$ for a particle orbiting with $p = 7.50478$ and $e = 0.188917$. Partial sums of Ψ_{22}^{EHS} are computed from Eq. (4.3.5), with a range of $-N \leq n \leq N$. The full Ψ_{22}^{EHS} and its r derivative result from $N = 10$, which gives agreement in the jumps in Ψ_{22}^{EHS} and $\partial_r \Psi_{22}^{\mathrm{EHS}}$ to a relative error of 10^{-10}. On the right, the presence of a delta function singularity is notionally depicted with an arrow. The time dependent amplitude of this singularity is separately computable from the jump in Ψ_{22}.

function [79]. Accordingly, any solution of Eq. (4.2.13) will be a weak solution–a generalized function itself–with loss of (classic) differentiability at the singular point $r_p(t)$. To determine the suitability of Eq. (4.3.6) as a solution of Eq. (4.2.13), we generalize the concept of differentiation to encompass distributions. Thus, for example, $d\theta(z)/dz = \delta(z)$. We can then take Eq. (4.3.6) as an ansatz, substitute in Eq. (4.2.13), and determine what conditions are required that it be a (weak) solution. For clarity, in the rest of this section we suppress the ℓ and m indices.

Rather than use the RWZ equation as it stands, we introduce a coordinate transformation to fix the position of the singularity. Defining $z \equiv r - r_p(t), \bar{t} \equiv t$, the derivatives transform as $\partial_{r_*} = f(r)\partial_z$ and $\partial_t = \partial_{\bar{t}} - \dot{r}_p \partial_z$, and the wave equation (4.2.13) becomes

$$L(\Psi) = -\partial_{\bar{t}}^2 \Psi + \left(f^2 - \dot{r}_p^2\right) \partial_z^2 \Psi + 2\dot{r}_p \partial_{\bar{t}} \partial_z \Psi + \left(\ddot{r}_p + (f \partial_z f)\right) \partial_z \Psi - V\Psi = \tilde{G}\,\delta(z) + \tilde{F}\,\delta'(z). \quad (4.3.7)$$

Now we assume that Ψ has the form given in Eq. (4.3.6) and substitute it into Eq. (4.3.7). The functions Ψ^+ and Ψ^- are differentiable and satisfy the homogeneous equation, $L(\Psi^\pm) = 0$. A term of the form $L(\Psi^+)\,\theta(z) + L(\Psi^-)\,\theta(-z)$ appears in (4.3.7) and drops out. Other singular terms remain, created by derivatives of the Heaviside function, and we are left with

$$\begin{aligned}\left(f^2 - \dot{r}_p^2\right)\Big(\llbracket\partial_r\Psi\rrbracket_p\,\delta(z) + \llbracket\Psi\rrbracket_p\,\delta'(z)\Big) + 2\dot{r}_p\partial_{\bar{t}}\Big(\llbracket\Psi\rrbracket_p\,\delta(z)\Big) \\ + \Big(\ddot{r}_p + (f\partial_z f)\Big)\llbracket\Psi\rrbracket_p\,\delta(z) = \tilde{G}\,\delta(z) + \tilde{F}\,\delta'(z). \quad (4.3.8)\end{aligned}$$

where

$$\begin{aligned}\llbracket\Psi\rrbracket_p(t) &\equiv \Psi^+\left(t, r_p(t)\right) - \Psi^-\left(t, r_p(t)\right), \\ \llbracket\partial_r\Psi\rrbracket_p(t) &\equiv \partial_r\Psi^+\left(t, r_p(t)\right) - \partial_r\Psi^-\left(t, r_p(t)\right)\end{aligned} \quad (4.3.9)$$

are the jumps in Ψ and $\partial_r\Psi$ at $z = 0$. Naïvely, we might expect that we can simply equate the coefficients of δ on the two sides of Eq. 4.3.8, while doing the same with the δ' coefficients. However, the δ' term on the left hand side must first be fully evaluated (as a function of time) at the location of the particle. To do this, we use the identities in Eqs. (4.A.1) and (4.A.5), which leaves

$$\begin{aligned}\left(f_p^2 - \dot{r}_p^2\right)\llbracket\partial_r\Psi\rrbracket_p\,\delta(z) + \left(f_p^2 - \dot{r}_p^2\right)\llbracket\Psi\rrbracket_p\,\delta'(z) - 2\left(f_p\partial_z f_p\right)\llbracket\Psi\rrbracket_p\,\delta(z) \\ + 2\dot{r}_p\partial_{\bar{t}}\Big(\llbracket\Psi\rrbracket_p\Big)\,\delta(z) + \Big(\ddot{r}_p + (f_p\partial_z f_p)\Big)\llbracket\Psi\rrbracket_p\,\delta(z) = \tilde{G}\,\delta(z) + \tilde{F}\,\delta'(z), \quad (4.3.10)\end{aligned}$$

where $f_p \equiv f(r_p(t))$. Note that there is no comparable expansion on the right side from the $\tilde{F}\,\delta'(z)$ term because $\tilde{F}$ is already fully evaluated at $r = r_p(t)$, by design. From here, we read off the jumps in Ψ and its r derivative at $r_p(t)$ from the coefficients of δ' and δ, respectively. Returning to Schwarzschild coordinates and using Eqs. (4.2.12) to remove $\ddot{r}_p$

and $\dot{r}_p^2$ terms, we find

$$\begin{aligned}
[\![\Psi]\!]_p(t) &= \frac{\mathcal{E}^2}{f_p^2 U_p^2}\tilde{F}(t), \\
[\![\partial_r\Psi]\!]_p(t) &= \frac{\mathcal{E}^2}{f_p^2 U_p^2}\left[\tilde{G}(t) + \frac{1}{U_p^2 r_p^2}\left(3M - \frac{\mathcal{L}^2}{r_p} + \frac{5M\mathcal{L}^2}{r_p^2}\right)\tilde{F}(t) - 2\dot{r}_p\frac{d}{dt}\Big([\![\Psi]\!]_p\Big)\right].
\end{aligned} \tag{4.3.11}$$

From the standpoint of the original coordinates, the partial time derivative $\partial_{\bar{t}}$ becomes the convective, or total, time derivative along the particle worldline.

These jump conditions amount to internal boundary conditions that are necessary conditions on a solution to the inhomogeneous wave equation in the TD. They were discussed by Sopuerta and Laguna [75] and also later, with corrections, by Field et al. [82]. In our FD-based calculations, they provide a powerful check on our transformation of the solutions back to the TD. Given the indirect way in which the Fourier transform of the source $S_{\ell m}$ determines the Fourier coefficients of the extended homogeneous solutions, considerable credence is lent to the method in seeing the partial sums of $\Psi^{\rm EHS}_{\ell m}$ converge toward satisfying these jump conditions. Secondarily, the jump conditions provide useful stopping criteria in the numerical method (see Sec. 4.4.3).

While not a focus of this chapter, we consider briefly TD simulations. There, to find a unique solution the internal boundary conditions must be augmented with initial data on a Cauchy surface and, potentially, outer boundary conditions. Care must be exercised to switch on the source smoothly in the (near) future of the initial value surface [82] (also Lau, private communication). Additionally, imposed initial data will not typically match long term periodic behavior induced by the source, and transients will sweep through the system for several dynamical times. In contrast, in the FD approach, the proper outgoing and downgoing behavior at the outer boundaries is built in from the outset and only the steady state, periodic behavior is obtained.

4.3.3 Computing normalization coefficients in the gravitational case

Finally, we provide some details on how the singular source is integrated to provide the matching normalization coefficients $C^+_{\ell mn}$ and $C^-_{\ell mn}$ that are used in Eq. (4.3.4). BOS

detail the calculation of normalization coefficients for the scalar monopole in their App. C. The gravitational case follows the same general idea, but involves some technical differences and challenges. We start by combining Eqs. (4.2.25) and (4.2.22), giving

$$C^{\pm}_{\ell mn} = \frac{1}{W_{\ell mn}} \int_{r_{\rm min}}^{r_{\rm max}} dr \; \frac{\hat{R}^{\mp}_{\ell mn}(r) Z_{\ell mn}(r)}{f(r)}. \tag{4.3.12}$$

The FD source term $Z_{\ell mn}(r)$ comes from plugging Eq. (4.2.14) into Eq. (4.2.17), yielding

$$Z_{\ell mn}(r) = \frac{1}{T_r} \int_0^{T_r} dt \; \Big(\tilde{G}_{\ell m}(t)\, \delta[r - r_p(t)] + \tilde{F}_{\ell m}(t)\, \delta'[r - r_p(t)] \Big) e^{i\omega_{mn} t}. \tag{4.3.13}$$

The equivalent integral BOS present for the scalar monopole is their Eq. (C2), which they evaluate immediately by changing the integration variable from t to r_p. Here, with a derivative-of-the-delta function present (in RWZ gauge), the immediate evaluation of this integral produces terms that are singular at the turning points ($\dot{r}_p = 0$). These terms are no problem analytically, but they are troublesome when performing the final numerical integration. We therefore find it is advantageous to delay this integration. Plugging our expression for $Z_{\ell mn}$ in above, we have

$$C^{\pm}_{\ell mn} = \frac{1}{W_{\ell mn} T_r} \int_{r_{\rm min}}^{r_{\rm max}} \Bigg[dr \; \frac{\hat{R}^{\mp}_{\ell mn}(r)}{f(r)} \int_0^{T_r} dt \; \Big(\tilde{G}_{\ell m}(t)\, \delta[r - r_p(t)] + \tilde{F}_{\ell m}(t)\, \delta'[r - r_p(t)] \Big) e^{i\omega_{mn} t} \Bigg]. \tag{4.3.14}$$

In order to avoid the singularity at the turning points, we switch the order of integration. The integration of the delta function itself is then straightforward. The derivative of δ term requires an integration by parts. Because of the compact support of the source term, we can extend the range of integration and no surface terms appear. We are left with

$$C^{\pm}_{\ell mn} = \frac{1}{W_{\ell mn} T_r} \int_0^{T_r} \Bigg[\frac{1}{f_p} \hat{R}^{\mp}_{\ell mn}(r_p) \tilde{G}_{\ell m}(t) + \left(\frac{2M}{r_p^2 f_p^2} \hat{R}^{\mp}_{\ell mn}(r_p) - \frac{1}{f_p} \frac{d\hat{R}^{\mp}_{\ell mn}(r_p)}{dr} \right) \tilde{F}_{\ell m}(t) \Bigg] e^{i\omega_{mn} t}\, dt, \tag{4.3.15}$$

where we use a p subscript to indicate evaluation of a quantity at $r = r_p(t)$. Our final integral is analogous to Eq. (C7) in BOS.

Here is a summary of key details of the application of the method in the gravitational case:

- The EHS method, applied to the gravitational case, gives exponentially converging solutions to Eq. (4.2.13) everywhere, including the location of the particle. (See FIG. 4.4.)

- Working in Regge-Wheeler gauge, the gravitational TD source term contains a delta function and a derivative-of-the-delta function, which cause $\Psi_{\ell m}$ to exhibit a jump and $\partial_r \Psi_{\ell m}$ to exhibit both a jump and a delta function singularity at the particle's location. (See FIG. 4.3.) In the scalar case, the field is piecewise continuous at the particle, with a jump in the r derivative. (See FIG. 3 in BOS.)

- Eq. (4.3.15) is valid for all radiative multipoles ($\ell \geq 2$). The $\ell = 0, 1$, modes must be handled separately.

- Martel's [50] $G_{\ell m}(t, r)$ and $F_{\ell m}(t, r)$ from Eq. (4.1.1) are not in fully evaluated form. As discussed in App. 4.A, for a given multipole, unique functions of time $\tilde{F}_{\ell m}(t) \equiv F_{\ell m}\left(t, r_p(t)\right)$ and $\tilde{G}_{\ell m}(t) \equiv G_{\ell m}\left(t, r_p(t)\right) - \partial_r F_{\ell m}\left(t, r_p(t)\right)$ emerge after fully applying the delta function constraint. We use the tilde to distinguish fully evaluated coefficients.

- In practice, we take advantage of the fact that some of the functions in the integrand of Eq. (4.3.15) are even over the period of radial libration, while others are odd. Then, rather than integrating over t from $0 \to T_r$, we can limit the range of integration to $0 \to T_r/2$. Further, we change variables to χ, as shown in Sec. 4.2.1 and integrate from $0 \to \pi$.

- For $\Psi^{\text{even}}_{\ell m}$ we use the Zerilli-Moncrief master function, and for $\Psi^{\text{odd}}_{\ell m}$ we use the Cunningham-Price-Moncrief master function. This formulation works for any master

function that obeys a Regge-Wheeler-like equation and has a source term that can be written in the form of Eq. (4.2.14).

4.4 Numerical method and results from mode integrations

4.4.1 Algorithmic roadmap

Here, we explain the specific steps our code takes to solve the inhomogeneous wave equation (4.2.13). There are several stages to the process, and at each step we compute at least one more order of magnitude accuracy than is needed at the subsequent step. The code is written in C, and we use the Numerical Recipes adaptive step size fourth order Runge-Kutta integrator [86].

1. Specify an orbit through a choice of the semi-latus rectum p and eccentricity e.

2. Numerically integrate Eqs. (4.2.10) and (4.2.11) to get the fundamental frequencies of the system, Ω_r and Ω_φ, and hence $\omega_{mn} = m\Omega_\varphi + n\Omega_r$.

3. Choose a specific ℓ and m. If $\ell + m$ is even (odd), use even (odd) parity potential and source terms. Choose starting n. (See Sec. 4.4.3.)

4. Solve the homogeneous version of Eq. (4.2.16) to get unit normalized radial mode functions, $\hat{R}^{\pm}_{\ell mn}$, in the source-free region:

   - Use the asymptotic expansion (see App. 4.D) to set an "up" plane wave boundary condition at $r_* \to +\infty$, as in Eq. (4.2.20). Numerically integrate up to the region of the source at $r_*^{\rm max}$ to get $\hat{R}^{+}_{\ell mn}$. (We let $r_*^{\rm min/max}$ be the r_* value corresponding to $r_{\rm min/max}$.)
   - Use a convergent Taylor expansion to set an "in" plane wave boundary condition (Eq. (4.2.19)) at modestly negative r_*. Numerically integrate up to the region of the source at $r_*^{\rm min}$ to get $\hat{R}^{-}_{\ell mn}$.

5. Solve the homogeneous version of Eq. (4.2.16) to continue the unit normalized radial mode functions, $\hat{R}^{\pm}_{\ell mn}$, into the source region, while also computing the normalization

coefficients $C^{\pm}_{\ell mn}$:

- Simultaneously integrate Eqs. (4.2.16) and (4.3.15) from $\chi = 0 \to \pi$ (equivalently $t = 0 \to T_r/2$ and $r = r_{\rm min} \to r_{\rm max}$). This gives $\hat{R}^{-}_{\ell mn}$ in the region of the source and $C^{+}_{\ell mn}$.
- Simultaneously integrate Eqs. (4.2.16) and (4.3.15) from $\chi = -\pi \to 0$ (equivalently $t = -T_r/2 \to 0$ and $r = r_{\rm max} \to r_{\rm min}$). This gives $\hat{R}^{+}_{\ell mn}$ in the region of the source and $C^{-}_{\ell mn}$.

As discussed in Sec. 4.3.3, the integrand in Eq. (4.3.15) contains parts which are even and parts which are odd over the radial period. By keeping the correct terms, we can get away with efficiently integrating over only half the period.

6. Use the coefficients to normalize the homogeneous solutions outside *and inside* the range of the source, as in Eq. (4.3.4).

7. Assess whether there is convergence of the partial sum over n. (Again, see Sec. 4.4.3.)

   - If yes, we are finished with this ℓ, m mode.
   - If no, return to Step 4 with the next n.

4.4.2 Energy and angular momentum fluxes at $r_* = \pm\infty$

To evaluate the energy and angular momentum fluxes at $r_* = \pm\infty$ we use the Isaacson stress-energy tensor. The energy and angular momentum fluxes, for each ℓ, m mode, can be written as [87]

$$\dot{E}^{\pm}_{\ell m} = \frac{1}{64\pi}\frac{(\ell+2)!}{(\ell-2)!}\left|\dot{\Psi}^{\pm}_{\ell m}(t,r)\right|^2, \qquad \dot{L}^{\pm}_{\ell m} = \frac{im}{64\pi}\frac{(\ell+2)!}{(\ell-2)!}\dot{\Psi}^{\pm}_{\ell m}(t,r)\Psi^{\pm *}_{\ell m}(t,r). \tag{4.4.1}$$

Here, an asterisk signifies complex conjugation. (We use $\Psi^{\rm even}_{\ell m}$ when $\ell + m$ is even and $\Psi^{\rm odd}_{\ell m}$ when $\ell + m$ is odd. In general there would be contributions from both $\Psi^{\rm even}_{\ell m}$ and $\Psi^{\rm odd}_{\ell m}$ for each mode, but our choice of $\theta_p = \pi/2$ leads to one of these functions vanishing for each ℓ

and m combination.) In terms of FD amplitudes the expressions become

$$\begin{aligned}\dot{E}^{\pm}_{\ell m} &= \frac{1}{64\pi}\frac{(\ell+2)!}{(\ell-2)!}\sum_{n,n'}\omega_{mn}\omega_{mn'}R^{\pm}_{\ell mn}R^{\pm\,*}_{\ell mn'}e^{-i(\omega_{mn}-\omega_{mn'})t},\\ \dot{L}^{\pm}_{\ell m} &= \frac{m}{64\pi}\frac{(\ell+2)!}{(\ell-2)!}\sum_{n,n'}\omega_{mn}R^{\pm}_{\ell mn}R^{\pm\,*}_{\ell mn'}e^{-i(\omega_{mn}-\omega_{mn'})t}.\end{aligned} \tag{4.4.2}$$

As is well known, the fluxes must be suitably averaged over time or space to obtain meaningful, invariant results. We average these quantities in time over one radial oscillation, which yields

$$\begin{aligned}\left\langle \dot{E}^{\pm}_{\ell m}\right\rangle &= \frac{1}{64\pi}\frac{(\ell+2)!}{(\ell-2)!}\sum_{n}\omega^2_{mn}\left|C^{\pm}_{\ell mn}\hat{R}^{\pm}_{\ell mn}\right|^2,\\ \left\langle \dot{L}^{\pm}_{\ell m}\right\rangle &= \frac{m}{64\pi}\frac{(\ell+2)!}{(\ell-2)!}\sum_{n}\omega_{mn}\left|C^{\pm}_{\ell mn}\hat{R}^{\pm}_{\ell mn}\right|^2.\end{aligned} \tag{4.4.3}$$

Here, we have also introduced $R^{\pm}_{\ell mn} = C^{\pm}_{\ell mn}\hat{R}^{\pm}_{\ell mn}$. As discussed in App. 4.D, we can write the radial function as $\hat{R}^{\pm}_{\ell mn}(r) = J^{\pm}_{\ell mn}(r)e^{\pm i\omega_{mn}r_*}$, where $J^{\pm}_{\ell mn}(r)\to 1$ as $r_*\to\pm\infty$. Therefore, if we set $J^{\pm}_{\ell mn}=1$, we can evaluate the fluxes at $r_*=\pm\infty$, leaving

$$\begin{aligned}\left\langle \dot{E}^{\pm\infty}_{\ell m}\right\rangle &= \frac{1}{64\pi}\frac{(\ell+2)!}{(\ell-2)!}\sum_{n}\omega^2_{mn}\left|C^{\pm}_{\ell mn}\right|^2,\\ \left\langle \dot{L}^{\pm\infty}_{\ell m}\right\rangle &= \frac{m}{64\pi}\frac{(\ell+2)!}{(\ell-2)!}\sum_{n}\omega_{mn}\left|C^{\pm}_{\ell mn}\right|^2.\end{aligned} \tag{4.4.4}$$

4.4.3 Code validation

To compute the total energy and angular momentum fluxes, we must sum Eqs. (4.4.4) over ℓ and m. The resulting expressions are formally over the ranges $2\le\ell\le\infty$, $-\ell\le m\le\ell$, $-\infty\le n\le\infty$. When computing $\dot{E}$ and $\dot{L}$ numerically, we put limits on each of these sums. To begin with, the low ℓ modes matter more than the high ones. But, the more eccentric an orbit, the more ℓ's must be computed to achieve the same precision in our final values. For the orbits we considered in Table 4.1, in order to achieve a relative precision of 10^{-12} in our final flux values, the highest ℓ necessary was $\ell=29$. (See Sec. 4.4.4.) In Table 4.2 we truncate the ℓ modes at $\ell=20$, as done by Fujita et al. [3].

Because of the symmetry of the spherical harmonics, the fluxes from any given $-m$ mode are equal to those from the corresponding $+m$ mode. Therefore, we fold the negative m modes over onto the positive ones, and simply multiply each positive m mode by two. Additionally, as ℓ gets larger, it is no longer necessary to compute all m values. As can be seen in Table 4.3, for a given ℓ, the largest $\dot{E}^{\infty/H}_{\ell m}$ and $\dot{L}^{\infty/H}_{\ell m}$ contributions come from the $m = \ell$ mode. We start at $m = \ell$ and decrement m until the fluxes are no longer significant. For low ℓ values we still wind up computing all $0 \leq m \leq \ell$, but as ℓ increases, we need progressively fewer m modes.

Determining the necessary n's is a bit more involved. For a given ℓ and m, there is a range, $n_{\rm min}$ to $n_{\rm max}$, over which we sum in order to achieve our desired precision. Looking at Table 4.3, it is evident that when $m = 0$, the range of n is essentially centered on 0. For these modes, we start with $n = 0$, and compute fluxes for all positive modes. When we have seen no change to any of the flux values (at a pre-specified level of precision) for several consecutive modes, we stop and repeat the process for the negative n's. As m increases, this range of n's shifts more and more into the positive. For any ℓ, the $m = \ell$ mode has far more positive n modes than negative. Eventually, ℓ becomes so large that $n_{\rm min} > 0$ for the $m = \ell$ mode. For modes where we suspect that $n_{\rm min} > 0$, we find it advantageous to start with a rough sweep of a large range of possible n values. We calculate $\dot{E}^{\infty}_{\ell mn}$ (the energy flux at $r = +\infty$ from one n mode) to low precision for a small number of n, spaced out over this range. The n for which we find the largest $\dot{E}_{\ell mn}$ will be near the center of the $n_{\rm min}$ to $n_{\rm max}$ range. We then perform our high precision mode integrations for all significant n values above and below this n.

If we are interested in a local calculation (as one would perform for a SF evaluation), we have a different method for determining which n's are significant. We still use the energy fluxes to find the approximate center of the significant n range, but for the "breaking condition" we compute n's until the jumps in $\Psi_{\ell m}$ and $\partial_r \Psi_{\ell m}$ converge properly, as follows:

- Use Eq. (4.3.5) to compute a partial mode sum approximation of both $\Psi^{\pm}_{\ell m}(t, r_p)$ and $\partial_r \Psi^{\pm}_{\ell m}(t, r_p)$ for a large number of times t_k throughout the orbit.

- Numerically evaluate the jumps in those partial sums

$$\begin{aligned}\left[\!\left[\Psi^N_{\ell m}\right]\!\right]_p &\equiv \Psi^+_{\ell m}(t, r_p) - \Psi^-_{\ell m}(t, r_p)\,, \\ \left[\!\left[\partial_r \Psi^N_{\ell m}\right]\!\right]_p &\equiv \partial_r \Psi^+_{\ell m}(t, r_p) - \partial_r \Psi^-_{\ell m}(t, r_p)\,,\end{aligned} \tag{4.4.5}$$

  for those times t_k.

- Compute the analytical values of $\left[\!\left[\Psi^A_{\ell m}\right]\!\right]_p$ and $\left[\!\left[\partial_r \Psi^A_{\ell m}\right]\!\right]_p$ derived in Sec. 4.3.2 for those times t_k.

- If $\left[\!\left[\Psi^N_{\ell m}\right]\!\right]_p = \left[\!\left[\Psi^A_{\ell m}\right]\!\right]_p$ and $\left[\!\left[\partial_r \Psi^N_{\ell m}\right]\!\right]_p = \left[\!\left[\partial_r \Psi^A_{\ell m}\right]\!\right]_p$ at all times t_k, to a chosen precision, we have computed enough n modes.

- Otherwise more n modes are needed. As in the flux computation case above, we perform the mode calculations for the n values above our starting n, and once that partial sum has converged to our desired precision, we solve for the n's below our starting n until the jump values agree.

4.4.4 Results

One of our most important results is the exponential convergence of $\Psi^{\rm EHS}_{\ell m}$ and its r derivative at the location of the particle. FIG. 4.3 shows a partial sum of these two quantities converging after only a few modes. Compare this to FIGs. 4.1 and 4.2, which shows the standard FD approach. In particular, note in those figures the failure of the standard approach to accurately represent $\partial_r \Psi_{\ell m}$, even after a large number of modes. This function is particularly badly behaved in the standard approach as smooth functions attempt to capture a delta function.

Also of note is FIG. 4.4, which shows that the convergence from the method of extended homogeneous solutions is indeed exponential, all the way up to the location of the particle. Fast and accurate computation of $\Psi_{\ell m}$ and $\partial_r \Psi_{\ell m}$ at $r_p(t)$ will eventually be critical for reliable local SF calculations.

In order to check our code's accuracy, we computed energy and angular momentum fluxes for circular and eccentric orbits. Our circular orbit fluxes agree, mode-by-mode, with

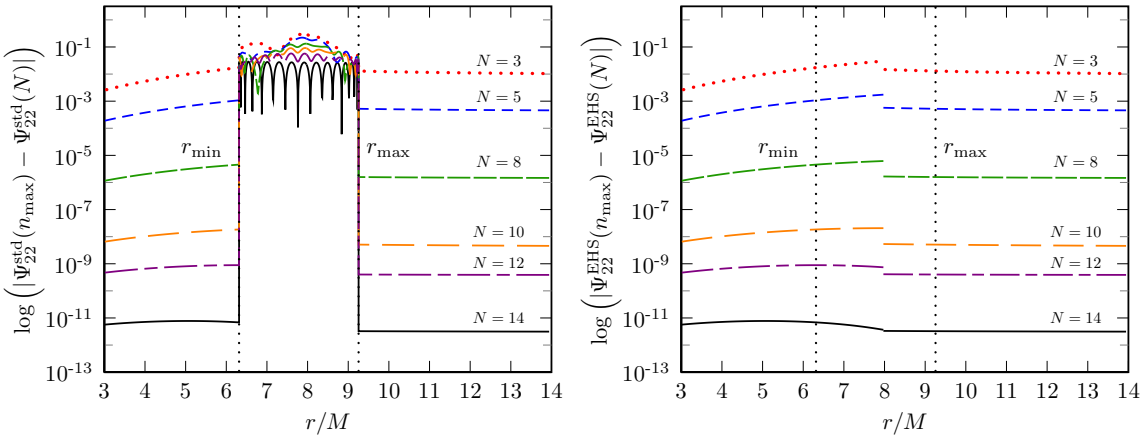

Figure 4.4: A plot of the convergence of the master function using the two methods. For a particle orbiting with $p = 7.50478$ and $e = 0.188917$ at $t = 51.78M$ we compute the master function $\Psi_{22}(n_{\rm max})$ by summing over modes ranging from $-n_{\rm max} \leq n \leq n_{\rm max}$ for $n_{\rm max} = 15$. We plot the log of the difference between $\Psi_{22}(n_{\rm max})$ and the partial sum $\Psi_{22}(N)$, for different $N < n_{\rm max}$. For the standard approach (left), we see exponential convergence in the homogeneous region, but only algebraic convergence in the region of the source. The method of extended homogeneous solutions (right) yields exponentially converging results at all points outside *and inside* the region of the source. The method of extended homogeneous solutions gives exponential convergence for $\partial_r \Psi_{\ell m}^{\rm EHS}$ as well.

published results (e.g. Cutler et al. [88]) to high precision. For eccentric orbits, we are only aware that total energy and angular momentum fluxes have been published. Our FD results agree with the fluxes at $r \to \infty$ of Fujita et al., published in [2] to at least 10^{-9}. These are included in Table 4.1. Fujita et al. have also published horizon energy fluxes [3], which we agree with, to at least 10^{-9} for a range of eccentricities. These are given in Table 4.2.

For those wishing to reproduce our results, in Table 4.3 we give mode-by-mode fluxes up to $\ell = 5$ at $r = \infty$ and down the black hole at $r = 2M$ for a particle in orbit with $p = 8.75455$ and $e = 0.764124$. Included are the ranges of n modes summed over to achieve these results.

As expected, our code is more efficient for low eccentricities. The first orbit in Table 4.1 ($p = 7.50478$, $e = 0.188917$), runs in under a half hour on a single processor machine, giving the total flux for all $2 \leq \ell \leq 23$ (although note the limits on m and n mentioned in the previous subsection) to a fractional error of 10^{-12}. As e increases, though, run times

increase greatly. The second orbit in that table ($p = 8.75455$, $e = 0.764124$) takes six hours to achieve the same accuracy for all necessary $2 \leq \ell \leq 29$. And, when $e = 0.9$ for $2 \leq \ell \leq 20$ in the last row of Table 4.2, we had to raise our fractional error to 10^{-10} in order to get a run time of eighteen hours.

Clearly, as e gets close to 1, FD methods will lose out to TD codes, which handle high eccentricities with more ease. Still for $0 \leq e \lesssim 0.9$, our run times are not unreasonable when considering the high accuracy we achieve.

4.5 Reconstruction of the metric perturbation amplitudes

The full benefit of having complete and highly converged solutions for the master functions lies in using them to reconstruct the metric. Ultimately, one wants to use the information, along with an appropriate regularization scheme, to compute the self force. A developed approach to doing this is the mode-sum regularization method [89], which makes use of Lorenz gauge. Here we use the information encoded in the master functions to compute accurately the spherical harmonic amplitudes of the metric perturbation in Regge-Wheeler gauge. The ability to determine the metric at all locations, including at the particle location, should serve as a useful starting point for computing the SF, either via a gauge transformation or an alternative regularization technique.

We summarize the metric perturbation (MP) formalism in App. 4.C, where the definitions of the master functions, $\Psi^{\rm even}_{\ell m}$ and $\Psi^{\rm odd}_{\ell m}$, are given in terms of spherical harmonic amplitudes of the metric and their radial derivatives. We reserve for this section giving the equations, (4.5.5) and (4.5.15), for reconstructing the metric amplitudes in Regge-Wheeler gauge from the master functions. These equations involve first derivatives, and in some cases second derivatives, of the master functions. They also involve spherical harmonic projections of the stress-energy tensor. Based on the form (4.1.2) anticipated in a master function, both of the abovementioned facts contribute to an expectation that the MP amplitudes might have point-singular behavior at $r_p(t)$ in the form of both δ and δ' terms. We show that all potential δ' terms cancel out. However, in general a MP amplitude might

have a functional form

$$M(t,r) = M^+(t,r)\,\theta(z) + M^-(t,r)\,\theta(-z) + M^S(t)\,\delta(z), \qquad z \equiv r - r_p(t), \tag{4.5.1}$$

where M^+ (M^-) represents a smooth function in the region $r > r_p$ ($r < r_p$), and M^S is a smooth function of t alone, giving the magnitude of the singularity. We examine M^S for all six non-zero MP amplitudes in the Regge-Wheeler gauge, and find three such terms to be nonvanishing. Throughout the rest of this section we again suppress spherical harmonic labels ℓ and m.

As mentioned the metric reconstruction equations, of each parity, require spherical harmonic projections of the stress-energy tensor. For a particle of mass μ, traveling on a geodesic of the background spacetime, with four-velocity u^μ, it is

$$T^{\mu\nu}\left(x^\alpha\right) = \mu \int \frac{d\tau}{\sqrt{-g}} u^\mu(\tau) u^\nu(\tau)\, \delta^4\left[x - x_p(\tau)\right]. \tag{4.5.2}$$

In Schwarzschild coordinates the determinant of the metric is $g = -r^4 \sin^2\theta$. After changing the variable of integration to coordinate time t, we have

$$T^{\mu\nu}\left(x^\alpha\right) = \frac{\mu\, u^\mu(t) u^\nu(t)}{u^t(t)\; r_p(t)^2}\, \delta[r - r_p(t)]\, \delta[\varphi - \varphi_p(t)]\, \delta[\theta - \pi/2]. \tag{4.5.3}$$

Spherical harmonic projections of $T^{\mu\nu}$ appear as source terms in the decomposed Einstein equations (App. 4.C) and these are in turn combined to produce the source terms for the master equations (App. 4.B). In the subsections that follow, we evaluate the time dependence of all of the stress-energy tensor projections. We use the definitions

$$\Lambda(r) \equiv \lambda + \frac{3M}{r}, \qquad \lambda \equiv \frac{(\ell+2)\,(\ell-1)}{2}. \tag{4.5.4}$$

4.5.1 Even parity

The even parity MP amplitudes are expressed in terms of $\Psi_{\rm even}$ and the source terms by (see [50])

$$\begin{aligned}
K(t,r) &= f\partial_r\Psi_{\rm even} + A\,\Psi_{\rm even} - \frac{r^2 f^2}{(\lambda+1)\Lambda}Q^{tt},\\
h_{rr}(t,r) &= \frac{\Lambda}{f^2}\left[\frac{\lambda+1}{r}\Psi_{\rm even} - K\right] + \frac{r}{f}\partial_r K,\\
h_{tr}(t,r) &= r\partial_t\partial_r\Psi_{\rm even} + rB\,\partial_t\Psi_{\rm even} - \frac{r^2}{\lambda+1}\left[Q^{tr} + \frac{rf}{\Lambda}\partial_t Q^{tt}\right],\\
h_{tt}(t,r) &= f^2 h_{rr} + fQ^{\sharp},
\end{aligned} \tag{4.5.5}$$

where

$$A(r) \equiv \frac{1}{r\Lambda}\left[\lambda(\lambda+1) + \frac{3M}{r}\left(\lambda + \frac{2M}{r}\right)\right], \quad B(r) \equiv \frac{1}{rf\Lambda}\left[\lambda\left(1 - \frac{3M}{r}\right) - \frac{3M^2}{r^2}\right]. \tag{4.5.6}$$

These equations result from the definition (4.C.6) of $\Psi_{\rm even}$ and its substitution into the even-parity field equations (4.C.3). The even-parity projections of the stress-energy tensor that appear in the equations above are defined by Eqs. (4.C.4). By enforcing the delta function constraints, they can be written in fully evaluated form (see App. 4.B), with each having a time dependent magnitude multiplying the radial delta function

$$\begin{aligned}
Q^{ab}(t,r) &\equiv q^{ab}(t)\,\delta[r - r_p(t)], \qquad Q^{a}(t,r) \equiv q^{a}(t)\,\delta[r - r_p(t)],\\
Q^{\flat}(t,r) &\equiv q^{\flat}(t)\,\delta[r - r_p(t)], \qquad Q^{\sharp}(t,r) \equiv q^{\sharp}(t)\,\delta[r - r_p(t)],
\end{aligned} \tag{4.5.7}$$

where we use a lowercase q as the base symbol of the corresponding magnitude. With Eq. (4.2.4) giving the four-velocity u^μ, the stress-energy tensor and Eqs. (4.C.4) can be

used to find

$$
\begin{aligned}
q^{tt}(t) &= 8\pi\mu\frac{\mathcal{E}}{r_p^2 f_p}Y^*, \qquad q^{rr}(t) = 8\pi\mu\frac{f_p}{\mathcal{E}r_p^2}\left(\mathcal{E}^2 - U_p^2\right)Y^*, \qquad q^{tr}(t) = 8\pi\mu\frac{u^r}{r_p^2}Y^*, \\
q^{t}(t) &= \frac{16\pi\mu}{\ell(\ell+1)}\frac{\mathcal{L}}{r_p^2}Y^*_{\varphi}, \qquad q^{r}(t) = \frac{16\pi\mu}{\ell(\ell+1)}\frac{\mathcal{L}}{\mathcal{E}}\frac{f_p}{r_p^2}u^r Y^*_{\varphi}, \\
q^{\flat}(t) &= 8\pi\mu\frac{\mathcal{L}^2}{\mathcal{E}}\frac{f_p}{r_p^4}Y^*, \qquad q^{\sharp}(t) = 32\pi\mu\frac{(\ell-2)!}{(\ell+2)!}\frac{\mathcal{L}^2}{\mathcal{E}}\frac{f_p}{r_p^2}Y^*_{\varphi\varphi}.
\end{aligned}
\tag{4.5.8}
$$

Here, Y, Y_φ, and $Y_{\varphi\varphi}$ are shorthand for the even-parity scalar, vector, and tensor spherical harmonics, respectively, evaluated along the worldline at $\theta = \pi/2$ and $\varphi = \varphi_p(t)$.

Now consider the reconstruction of the MP amplitude K, given in Eq. (4.5.5). Using the expected functional form of Ψ given in Eq. (4.1.2), K obviously does fit the general form (4.5.1) claimed above. In fact, we find

$$
K^{\pm}(t,r) = f\partial_r\Psi^{\pm} + A\Psi^{\pm}, \qquad K^S(t) = f_p[\![\Psi]\!]_p - \frac{r_p^2 f_p^2}{(\lambda+1)\Lambda_p}q^{tt} = 0, \tag{4.5.9}
$$

where the vanishing of K^S follows from use of Eq. (4.3.11) for $[\![\Psi]\!]_p$, and q^{tt} from Eq. (4.5.8). Therefore, we see that the even-parity metric function K in Regge-Wheeler gauge is (only) a C^{-1} function at the location of the particle.

Using the same approach to evaluate h_{rr} in Eq. (4.5.5) we have

$$
\begin{aligned}
h^{\pm}_{rr}(t,r) &= \frac{\Lambda}{f^2}\left[\frac{\lambda+1}{r}\Psi^{\pm} - K^{\pm}\right] + \frac{r}{f}\partial_r K^{\pm}, \\
h^{S}_{rr}(t) &= \frac{r_p}{f_p}[\![K]\!]_p = r_p[\![\partial_r\Psi]\!]_p + \frac{r_p A_p}{f_p}[\![\Psi]\!]_p.
\end{aligned}
\tag{4.5.10}
$$

Here, we have extended in a natural way the use of the $[\![\ \ ]\!]_p$ notation to let $[\![K]\!]_p$ represent the jump in K at $z = 0$. We find that the Regge-Wheeler metric function h_{rr} is not only discontinuous across $r_p(t)$ but also has a point-singular term, which is an artifact of Regge-Wheeler gauge.

The h_{tr} function is more subtle than the previous two. Looking at Eq. (4.5.5), we need

the following terms involving Ψ,

$$
\begin{aligned}
rB\,\partial_t\Psi &= rB\,\partial_t\Psi^+\,\theta(z) + rB\,\partial_t\Psi^-\,\theta(-z) - r_pB_p\dot{r}_p[\![\Psi]\!]_p\,\delta(z),\\
r\partial_t\partial_r\Psi &= r\partial_t\partial_r\Psi^+\theta(z) + r\partial_t\partial_r\Psi^-\theta(-z)\\
&\quad + \left[r_p\frac{d}{dt}\Big([\![\Psi]\!]_p\Big) + \dot{r}_p[\![\Psi]\!]_p - r_p\dot{r}_p[\![\partial_r\Psi]\!]_p\right]\delta(z) - r_p\dot{r}_p[\![\Psi]\!]_p\,\delta'(z).
\end{aligned}
\tag{4.5.11}
$$

On the right side of these equations we have evaluated all the δ and δ' coefficients at $z=0$ with Eqs. (4.A.1) and (4.A.5) (fully evaluated form). The singular terms that arise in these expressions can be grouped with the similarly singular contributions from the source terms,

$$
\begin{aligned}
\frac{r^2}{\lambda+1}Q^{tr} &= \frac{r_p^2}{\lambda+1}q^{tr}\delta(z),\\
\frac{r^3 f}{(\lambda+1)\Lambda}\partial_t Q^{tt} &= \frac{1}{(\lambda+1)\Lambda_p}\left[r_p^3 f_p\frac{dq^{tt}}{dt} + \frac{3\lambda r_p^2 + 12Mr_p - 4\lambda Mr_p - 18M^2}{\Lambda_p}\dot{r}_p q^{tt}\right]\delta(z)\\
&\quad - \frac{r_p^3 f_p}{(\lambda+1)\Lambda_p}\dot{r}_p q^{tt}\,\delta'(z).
\end{aligned}
\tag{4.5.12}
$$

Upon carefully checking the time dependence of q^{tt} and the jump in Ψ, we find that the δ' terms cancel out. There are multiple δ terms, but after using the expressions for $[\![\Psi]\!]_p$, $[\![\partial_r\Psi]\!]_p$ in (4.3.11) and the relevant q's in (4.5.8), most of the terms cancel and we are left with

$$
h^{\pm}_{tr}(t,r) = r\partial_t\partial_r\Psi^{\pm} + rB\,\partial_t\Psi^{\pm}, \qquad h^S_{tr}(t) = \mathcal{E}^2\frac{\dot{r}_p}{f_pU_p^2}q^\sharp. \tag{4.5.13}
$$

Finally, the h_{tt} term is simple. We insert Eq. (4.5.10) into the field equation for h_{tt} and get

$$
h^{\pm}_{tt}(t,r) = f^2h^{\pm}_{rr}, \qquad h^S_{tt}(t) = f_p^2h^S_{rr} + f_pq^\sharp. \tag{4.5.14}
$$

So, we see that in Regge-Wheeler gauge K is C^{-1} with no singularity along the worldline of the particle, but the three even-parity MP amplitudes in the "t,r sector" have point-singular

artifacts given by Eqs. (4.5.10), (4.5.13), (4.5.14).

4.5.2 Odd parity

Once $\Psi_{\rm odd}$ has been computed, the odd-parity MP amplitudes can be reconstructed via

$$h_t(t,r) = \frac{f}{2}\partial_r\left(r\Psi_{\rm odd}\right) - \frac{r^2 f}{2\lambda}P^t, \qquad h_r(t,r) = \frac{r}{2f}\partial_t\Psi_{\rm odd} + \frac{r^2}{2\lambda f}P^r, \tag{4.5.15}$$

(see [73]). These equations follow from the definition (4.C.14) and its substitution into the odd-parity field equations (4.C.11). Similar to before, we define the lowercase p's to be the time-dependent magnitudes of the radial delta function after fully evaluating the odd-parity projections of the stress-energy tensor

$$P^a(t,r) \equiv p^a(t)\,\delta[r - r_p(t)], \qquad P(t,r) \equiv p(t)\,\delta[r - r_p(t)]. \tag{4.5.16}$$

Also as before, we use the time dependence of the four-velocity and the stress-energy tensor to determine these magnitudes for eccentric motion on Schwarzschild,

$$p^t(t) = \frac{16\pi\mu}{\ell(\ell+1)}\frac{\mathcal{L}}{r_p^2}X^*_\varphi, \quad p^r(t) = \frac{16\pi\mu}{\ell(\ell+1)}\frac{\mathcal{L}}{\mathcal{E}}\frac{f_p}{r_p^2}u^r X^*_\varphi, \quad p(t) = 16\pi\mu\frac{(\ell-2)!}{(\ell+2)!}\frac{\mathcal{L}^2}{\mathcal{E}}\frac{f_p}{r_p^2}X^*_{\varphi\varphi}. \tag{4.5.17}$$

Here, X_φ and $X_{\varphi\varphi}$ are shorthand for the odd-parity vector and tensor spherical harmonics evaluated along the worldline at $\theta = \pi/2$ and $\varphi = \varphi_p(t)$.

Now, as in the even-parity case we can analyze the local structure of the MP amplitudes. We again assume Ψ to have the form Eq. (4.1.2). Plugging the relevant expressions into Eq. (4.5.15) for the odd-parity MP amplitude reconstruction, we find that all the point-singular parts cancel out exactly, leaving

$$\begin{aligned} h_t^\pm(t,r) &= \frac{f}{2}\partial_r\left(r\Psi^\pm\right), \qquad & h_t^{\rm S}(t) &= 0, \\ h_r^\pm(t,r) &= \frac{r}{2f}\partial_t\Psi^\pm, \qquad & h_r^{\rm S}(t) &= 0. \end{aligned} \tag{4.5.18}$$

So, we see that the odd-parity MP functions in Regge-Wheeler gauge are smooth as they

approach $r_p(t)$ with only a finite jump at that point.

FIG. 4.5 summarizes these findings graphically, for both even and odd parity, using several specific spherical harmonic modes.

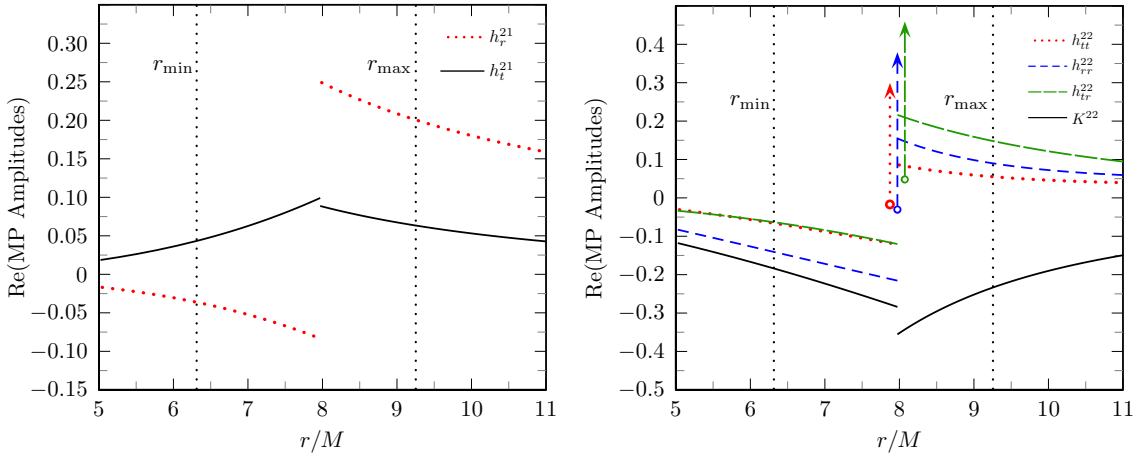

Figure 4.5: The EHS approach to reconstructing the TD MP amplitudes. We consider a particle orbiting with $p = 7.50478$ and $e = 0.188917$ at $t = 80.62M$. The left plot shows the odd-parity MP amplitudes h_r^{21} and h_t^{21}. The right shows the even-parity h_{tt}^{22}, h_{rr}^{22}, h_{tr}^{22}, and K^{22}. Note that the amplitudes h_{tt}^{22}, h_{rr}^{22}, and h_{tr}^{22} are singular along the particle's worldline, as indicated by arrows in the plot on the right. The magnitude of these singularities are given in Eqs. (4.5.10), (4.5.13), (4.5.14). The remaining three MP amplitudes approach the particle location smoothly, and have only a finite jump at that point.

4.6 Conclusion

We have achieved two main results in this chapter. First, we have shown successful application of the method of extended homogeneous solutions to gravitational perturbations from a small mass in eccentric orbit about a massive Schwarzschild black hole. In doing so, we accurately computed the master functions in the Regge-Wheeler-Zerilli formalism in the frequency domain and transformed these fields back to the time domain. With this method we achieved exponential convergence of the master functions and their derivatives for all r including the instantaneous particle location $r = r_p(t)$.

Our second important result is the reconstruction of the metric perturbation amplitudes in Regge-Wheeler gauge for arbitrary radiative modes. In addition to computing

the smooth parts of these amplitudes, we have derived the time dependent magnitudes of point-singular terms that reside at $r_p(t)$ in some components of the metric. This full and accurate knowledge of the spherical harmonic amplitudes of the metric at, and near, $r_p(t)$ lays the groundwork for one or more subsequent approaches to local computation of the self-force.

4.A The fully evaluated form of distributional source terms

In the RWZ formalism for perturbations generated by an orbiting point mass, the master equations have distributional sources with both delta function and derivative-of-delta function terms. Reduced by spherical harmonic decomposition, these distributions have support only along a one-dimensional timelike worldline $r = r_p(t)$ within a two dimensional domain. The delta function's behavior is still elementary,

$$\alpha(t,r)\,\delta[r-r_p(t)] = \alpha\left(t,r_p(t)\right)\,\delta[r-r_p(t)] \equiv \tilde{\alpha}(t)\,\delta[r-r_p(t)], \tag{4.A.1}$$

where $\alpha(t,r)$ is assumed to be a smooth function and we use the notation $\tilde{\alpha}(t)$ to indicate the one-dimensional function that results from restricting (or fully evaluating) $\alpha(t,r)$ with the delta function. At any stage in a calculation a delta function can be used to fully evaluate all smooth functions that multiply it. Under an integral the result is obvious

$$\int \alpha(t,r)\,\delta[r-r_p(t)]\,dr = \tilde{\alpha}(t), \tag{4.A.2}$$

with the resulting function of time being unique. Occasionally, there is need to differentiate such a function. The total derivative is related to derivatives of the original function by

$$\frac{d\tilde{\alpha}}{dt} = \Big[\partial_t\alpha(t,r) + \dot{r}_p\partial_r\alpha(t,r)\Big]_{r=r_p(t)}, \tag{4.A.3}$$

where on the right hand side we differentiate first and evaluate second.

Of more interest is the behavior of δ' [79]. Differentiating Eq. (4.A.1) with respect to r,

we obtain

$$\alpha(t,r)\,\delta'[r-r_p(t)] + \partial_r\alpha(t,r)\,\delta[r-r_p(t)] = \tilde{\alpha}(t)\,\delta'[r-r_p(t)]. \tag{4.A.4}$$

Rearranging terms and using the rule of fully evaluating whenever possible, we find

$$\alpha(t,r)\,\delta'[r-r_p(t)] = \tilde{\alpha}(t)\,\delta'[r-r_p(t)] - \tilde{\beta}(t)\,\delta[r-r_p(t)], \tag{4.A.5}$$

where

$$\tilde{\beta}(t) \equiv \partial_r\alpha(t,r_p(t)) = \Big[\partial_r\alpha(t,r)\Big]_{r=r_p(t)}, \tag{4.A.6}$$

which is the analogous fully evaluated form. Upon integration,

$$\int \alpha(t,r)\,\delta'[r-r_p(t)]\,dr = -\tilde{\beta}(t) = -\partial_r\alpha(t,r_p(t)). \tag{4.A.7}$$

Since the first term on the right of Eq. (4.A.5) disappears upon integration, why retain it? The answer is that we may multiply Eq. (4.A.5) by another smooth (test) function, $\gamma(t,r)$. We can then proceed to thew fully evaluated form by reducing the smooth function $\gamma(t,r)\,\alpha(t,r)$ on the left or use the same reduction on the first term on the right. In either case the result is

$$\begin{aligned}\gamma(t,r)\,\alpha(t,r)\,\delta'[r-r_p(t)] = \tilde{\gamma}(t)\,\tilde{\alpha}(t)\,\delta'[r-r_p(t)] - \tilde{\alpha}(t)\,\partial_r\gamma(t,r_p(t))\,\delta[r-r_p(t)] \\ - \tilde{\gamma}(t)\,\partial_r\alpha(t,r_p(t))\,\delta[r-r_p(t)].\end{aligned} \tag{4.A.8}$$

From this it is evident that we can *partially* evaluate a coefficient of δ' in a number of different ways.

Martel [50] introduced the notation found in Eq. (4.1.1) for gravitational master function source terms, with two-dimensional functions $G_{\ell m}(t,r)$ and $F_{\ell m}(t,r)$ multiplying δ and δ', respectively. In examining the Zerilli-Moncrief master function, he left these coefficients partially evaluated. Sopuerta and Laguna [75] started with the same notation for $G_{\ell m}(t,r)$ and $F_{\ell m}(t,r)$ in the case of the Cunningham-Price-Moncrief master function, and fully evaluated these coefficients at $r = r_p(t)$. A difficulty with the $G_{\ell m}(t,r)$ and $F_{\ell m}(t,r)$

notation is that there is no unique form of these functions if partially evaluated. Any solution of the RWZ wave equation will require a full evaluation of the source. The procedure should not matter but we prefer the clarity afforded by using the identities found in Eqs. (4.A.1) and (4.A.5) to write Eq. (4.1.1) in fully evaluated form from the outset

$$S_{\ell m}(t,r) = \tilde{G}_{\ell m}(t)\ \delta[r - r_p(t)] + \tilde{F}_{\ell m}(t)\ \delta'[r - r_p(t)], \tag{4.A.9}$$

where

$$\tilde{G}_{\ell m}(t) \equiv \Big[G_{\ell m}(t,r) - \partial_r F_{\ell m}(t,r)\Big]_{r=r_p(t)}, \qquad \tilde{F}_{\ell m}(t) \equiv \Big[F_{\ell m}(t,r)\Big]_{r=r_p(t)}. \tag{4.A.10}$$

4.B Source terms for eccentric motion on Schwarzschild

Here we give the unambiguous expressions for $\tilde{G}_{\ell m}$ and $\tilde{F}_{\ell m}$ for the even-parity Zerilli-Moncrief and odd-parity Cunningham-Price-Moncrief master functions fully evaluated at $r = r_p(t)$. We introduce new notation for constituent parts of $\tilde{G}_{\ell m}$ and $\tilde{F}_{\ell m}$ based upon the projections of the stress-energy tensor defined in App. 4.C and the fully evaluated time-dependent magnitudes of $\delta[r - r_p(t)]$ given by Eqs. (4.5.8) and (4.5.17). Note that we use $\mathcal{G}$ and $\mathcal{F}$ to denote additional time-dependent factors that multiply the various stress-energy magnitudes. The indices on these $\mathcal{G}$ and $\mathcal{F}$ factors are not tensor indices.

4.B.1 Even parity

In the even-parity case, we examine the terms first published by Martel [50], but now fully evaluate them at $r = r_p(t)$. We find,

$$\begin{aligned}
\tilde{G}_{\ell m}(t) &= \mathcal{G}^{rr}_{\ell}\, q^{rr}_{\ell m} + \mathcal{G}^{tt}_{\ell}\, q^{tt}_{\ell m} + \mathcal{G}^{r}_{\ell}\, q^{r}_{\ell m} + \mathcal{G}^{\flat}_{\ell}\, q^{\flat}_{\ell m} + \mathcal{G}^{\sharp}_{\ell}\, q^{\sharp}_{\ell m} \\
\tilde{F}_{\ell m}(t) &= \mathcal{F}^{rr}_{\ell}\, q^{rr}_{\ell m} + \mathcal{F}^{tt}_{\ell}\, q^{tt}_{\ell m},
\end{aligned} \tag{4.B.1}$$

where

$$
\begin{aligned}
\mathcal{G}^{rr}_{\ell}(t) &\equiv \frac{1}{(\lambda+1)\,r_p\Lambda_p^2}\Big[\,(\lambda+1)\,(\lambda r_p+6M)\,r_p+3M^2\Big],\\
\mathcal{G}^{tt}_{\ell}(t) &\equiv -\frac{f_p^2}{(\lambda+1)r_p\Lambda_p^2}\Big[\lambda\,(\lambda+1)\,r_p^2+6\lambda M r_p+15M^2\Big],\\
\mathcal{G}^{r}_{\ell}(t) &\equiv \frac{2f_p}{\Lambda_p}, \qquad \mathcal{G}^{\flat}_{\ell}(t) \equiv \frac{r_p f_p^2}{(\lambda+1)\Lambda_p}, \qquad \mathcal{G}^{\sharp}_{\ell}(t) \equiv -\frac{f_p}{r_p},\\
\mathcal{F}^{rr}_{\ell}(t) &\equiv -\frac{r_p^2 f_p}{(\lambda+1)\,\Lambda_p}, \qquad \mathcal{F}^{tt}_{\ell}(t) \equiv \frac{r_p^2 f_p^3}{(\lambda+1)\,\Lambda_p},
\end{aligned}
\tag{4.B.2}
$$

with the q's given in Eq. (4.5.8).

4.B.2 Odd parity

In the odd-parity case, the fully evaluated source magnitudes are equivalent to those first published by Sopuerta and Laguna [75] and later with more detail by Field, Hesthaven, and Lau [82]. We find,

$$
\tilde{G}_{\ell m}(t) = \mathcal{G}^{r_1}_{\ell}\,p^{r}_{\ell m} + \mathcal{G}^{r_2}_{\ell}\,\frac{dp^{r}_{\ell m}}{dt} + \mathcal{G}^{t}_{\ell}\,p^{t}_{\ell m}, \qquad \tilde{F}_{\ell m}(t) = \mathcal{F}^{r}_{\ell}\,p^{r}_{\ell m} + \mathcal{F}^{t}_{\ell}\,p^{t}_{\ell m}, \tag{4.B.3}
$$

where

$$
\mathcal{G}^{r_1}_{\ell}(t) \equiv \frac{\dot{r}_p}{\lambda}, \quad \mathcal{G}^{r_2}_{\ell}(t) \equiv \frac{r_p}{\lambda}, \quad \mathcal{G}^{t}_{\ell}(t) \equiv -\frac{f_p}{\lambda}, \quad \mathcal{F}^{r}_{\ell}(t) \equiv -\frac{r_p\dot{r}_p}{\lambda}, \quad \mathcal{F}^{t}_{\ell}(t) \equiv \frac{r_p f_p^2}{\lambda}, \tag{4.B.4}
$$

and the p's are given by Eq. (4.5.17).

4.C Metric perturbation formalism in the Regge-Wheeler gauge

Here we briefly summarize the definitions of metric perturbation (MP) amplitudes (on a common tensor spherical harmonic basis) for both even and odd parities. The field equations and Bianchi identities are given in terms of the MP amplitudes and spherical harmonic projected source terms. The specific gauge-invariant master functions we use in our simulations are expressed in terms of the MP amplitudes and their associated master equations,

potentials, and source terms are summarized. In what follows, lowercase Latin indices will run over (t, r), while uppercase Latin indices will run over (θ, φ). This section draws heavily from Martel and Poisson [55]. The material here serves as a basis for discussing in Sec. 4.5 how the MP can be numerically reconstructed from the master functions.

4.C.1 Even parity

Of the ten MP amplitudes, seven are in the even-parity sector. Using the decomposition of Martel and Poisson [55], they are

$$\begin{aligned} p_{ab}\left(x^{\mu}\right) &= \sum_{\ell,m} h_{ab}^{\ell m} Y^{\ell m}, \\ p_{aB}\left(x^{\mu}\right) &= \sum_{\ell,m} j_{a}^{\ell m} Y_{B}^{\ell m}, \\ p_{AB}\left(x^{\mu}\right) &= r^{2} \sum_{\ell,m} \Big(K^{\ell m} \Omega_{AB} Y^{\ell m} + G^{\ell m} Y_{AB}^{\ell m} \Big). \end{aligned} \tag{4.C.1}$$

The tensor Ω_{AB} is the metric on the unit two-sphere,

$$ds^{2} = \Omega_{AB} dx^{A} dx^{B} = d\theta^{2} + \sin^{2}\theta \, d\varphi^{2}. \tag{4.C.2}$$

The even-parity scalar ($Y^{\ell m}$), vector ($Y_{A}^{\ell m}$), and tensor ($Y_{AB}^{\ell m}$ and $\Omega_{AB} Y^{\ell m}$) spherical harmonics are defined in [55]. Note that $Y_{AB}^{\ell m}$ is the trace-free tensor spherical harmonic, which differs from what Regge and Wheeler used in their original work [14]. For the remainder of this section, we drop ℓ and m indices for the sake of brevity.

In Schwarzschild coordinates, the amplitudes defined here are related to Regge and Wheeler's original quantities. In the "t, r sector," $h_{tt} = f H_0$, $h_{tr} = H_1$, and $h_{rr} = H_2 / f$. For the off-diagonal elements, $j_t = h_0$ and $j_r = h_1$. Finally, on the two-sphere $G_{\text{here}} = G_{\text{RW}}$, while $K_{\text{here}} = K_{\text{RW}} - \ell(\ell+1) G/2$. We use the Regge-Wheeler gauge, where $j_a = G = 0$.

In this gauge and in Schwarzschild coordinates, the even-parity field equations are

$$\begin{aligned}
-\partial_r^2 K - \frac{3r-5M}{r^2 f}\partial_r K + \frac{f}{r}\partial_r h_{rr} + \frac{(\lambda+2)\,r+2M}{r^3}h_{rr} + \frac{\lambda}{r^2 f}K &= Q^{tt},\\
\partial_t\partial_r K + \frac{r-3M}{r^2 f}\partial_t K - \frac{f}{r}\partial_t h_{rr} - \frac{\lambda+1}{r^2}h_{tr} &= Q^{tr},\\
-\partial_t^2 K + \frac{(r-M)f}{r^2}\partial_r K + \frac{2f}{r}\partial_t h_{tr} - \frac{f}{r}\partial_r h_{tt} & \\
+\frac{(\lambda+1)r+2M}{r^3}h_{tt} - \frac{f^2}{r^2}h_{rr} - \frac{\lambda f}{r^2}K &= Q^{rr},\\
\partial_t h_{rr} - \partial_r h_{tr} + \frac{1}{f}\partial_t K - \frac{2M}{r^2 f}h_{tr} &= Q^{t},\\
-\partial_t h_{tr} + \partial_r h_{tt} - f\partial_r K - \frac{r-M}{r^2 f}h_{tt} + \frac{(r-M)f}{r^2}h_{rr} &= Q^{r},\\
-\partial_t^2 h_{rr} + 2\partial_t\partial_r h_{tr} - \partial_r^2 h_{tt} - \frac{1}{f}\partial_t^2 K + f\partial_r^2 K + \frac{2(r-M)}{r^2 f}\partial_t h_{tr} & \\
-\frac{r-3M}{r^2 f}\partial_r h_{tt} - \frac{(r-M)f}{r^2}\partial_r h_{rr} + \frac{2(r-M)}{r^2}\partial_r K & \\
+\frac{(\lambda+1)r^2 - 2(\lambda+2)Mr + 2M^2}{r^4 f^2}h_{tt} - \frac{(\lambda+1)r^2 - 2\lambda Mr - 2M^2}{r^4}h_{rr} &= Q^{\flat},\\
\frac{1}{f}h_{tt} - f h_{rr} &= Q^{\sharp},
\end{aligned} \tag{4.C.3}$$

which rely upon the following source terms

$$\begin{aligned}
Q^{ab}(t,r) &\equiv 8\pi\int T^{ab}Y^*\,d\Omega, \qquad Q^{a}(t,r) \equiv \frac{16\pi r^2}{\ell(\ell+1)}\int T^{aB}Y^*_B\,d\Omega,\\
Q^{\flat}(t,r) &\equiv 8\pi r^2\int T^{AB}\Omega_{AB}Y^*\,d\Omega, \qquad Q^{\sharp}(t,r) \equiv 32\pi r^4\frac{(\ell-2)!}{(\ell+2)!}\int T^{AB}Y^*_{AB}\,d\Omega.
\end{aligned} \tag{4.C.4}$$

The conservation (Bianchi) identities are

$$\begin{aligned}
\partial_t Q^{tt} + \partial_r Q^{tr} + 2\frac{(r-M)}{r^2 f}Q^{tr} - \frac{\lambda+1}{r^2}Q^{t} &= 0,\\
\partial_t Q^{tr} + \partial_r Q^{rr} + \frac{Mf}{r^2}Q^{tt} + \frac{2r-5M}{r^2 f}Q^{rr} - \frac{\lambda+1}{r^2}Q^{r} - \frac{f}{r}Q^{\flat} &= 0,\\
\partial_t Q^{t} + \partial_r Q^{r} + \frac{2}{r}Q^{r} + Q^{\flat} - \frac{\lambda}{r^2}Q^{\sharp} &= 0.
\end{aligned} \tag{4.C.5}$$

We use the gauge-invariant *Zerilli-Moncrief* master function (see [16, 18], modifying the

approach of [15]), which is

$$\Psi_{\rm even}(t,r) \equiv \frac{2r}{\ell(\ell+1)}\left[K + \frac{1}{\Lambda}\left(f^2 h_{rr} - r f \partial_r K\right)\right], \tag{4.C.6}$$

in Schwarzschild coordinates. It satisfies the wave equation

$$\left[-\frac{\partial^2}{\partial t^2} + \frac{\partial^2}{\partial r_*^2} - V_{\rm even}\right]\Psi_{\rm even} = S_{\rm even}, \tag{4.C.7}$$

with source term

$$\begin{aligned} S_{\rm even}(t,r) \equiv \frac{1}{(\lambda+1)\,\Lambda}\Bigg[& r^2 f\left(f^2\partial_r Q^{tt} - \partial_r Q^{rr}\right) + r(\Lambda - f)Q^{rr} + r f^2 Q^\flat \\ & - \frac{f^2}{r\Lambda}\Big(\lambda(\lambda-1)r^2 + (4\lambda-9)\,Mr + 15M^2\Big)Q^{tt}\Bigg] + \frac{2f}{\Lambda}Q^r - \frac{f}{r}Q^\sharp, \end{aligned} \tag{4.C.8}$$

and standard Zerilli potential

$$V_{\rm even}(r) \equiv \frac{f}{r^2\Lambda^2}\left[2\lambda^2\left(\lambda + 1 + \frac{3M}{r}\right) + \frac{18M^2}{r^2}\left(\lambda + \frac{M}{r}\right)\right]. \tag{4.C.9}$$

4.C.2 Odd parity

The remaining three MP amplitudes belong to the odd-parity sector,

$$p_{ab}\,(x^\mu) = 0, \qquad p_{aB}\,(x^\mu) = \sum_{\ell,m} h_a^{\ell m} X_B^{\ell m}, \qquad p_{AB}\,(x^\mu) = \sum_{\ell,m} h_2^{\ell m} X_{AB}^{\ell m}. \tag{4.C.10}$$

The vector ($X_B^{\ell m}$) and tensor ($X_{AB}^{\ell m}$) spherical harmonics are those defined in [55]. Note that the tensor spherical harmonics differ from those used by Regge and Wheeler by a minus sign. For the remainder of this section, we again drop ℓ and m indices.

These MP amplitudes are related to Regge and Wheeler's quantities through $h_t = h_0$, $h_r = h_1$, and $h_2^{\rm here} = -h_2^{\rm RW}$. We use Regge-Wheeler gauge, in which $h_2 = 0$. In this gauge

and in Schwarzschild coordinates, the odd-parity field equations are

$$\begin{aligned} -\partial_t\partial_r h_r + \partial_r^2 h_t - \frac{2}{r}\partial_t h_r - \frac{2(\lambda+1)r - 4M}{r^3 f} h_t &= P^t, \\ \partial_t^2 h_r - \partial_t\partial_r h_t + \frac{2}{r}\partial_t h_t + \frac{2\lambda f}{r^2} h_r &= P^r, \\ -\frac{1}{f}\partial_t h_t + f\partial_r h_r + \frac{2M}{r^2} h_r &= P, \end{aligned} \tag{4.C.11}$$

with source terms given by

$$P^a(t,r) \equiv \frac{16\pi r^2}{\ell(\ell+1)} \int T^{aB} X_B^* \, d\Omega, \qquad P(t,r) \equiv 16\pi r^4 \frac{(\ell-2)!}{(\ell+2)!} \int T^{AB} X_{AB}^* \, d\Omega. \tag{4.C.12}$$

The conservation (Bianchi) identity is

$$\partial_t P^t + \partial_r P^r + \frac{2}{r} P^r - \frac{2\lambda}{r^2} P = 0. \tag{4.C.13}$$

In the odd-parity sector, we use the gauge-invariant *Cunningham-Price-Moncrief* master function [17], which in Schwarzschild coordinates is

$$\Psi_{\rm odd}(t,r) \equiv \frac{r}{\lambda}\left[\partial_r h_t - \partial_t h_r - \frac{2}{r} h_t\right]. \tag{4.C.14}$$

It satisfies the wave equation

$$\left[-\frac{\partial^2}{\partial t^2} + \frac{\partial^2}{\partial r_*^2} - V_{\rm odd}\right] \Psi_{\rm odd} = S_{\rm odd}, \tag{4.C.15}$$

with source term

$$S_{\rm odd}(t,r) \equiv \frac{rf}{\lambda}\left[\frac{1}{f}\partial_t P^r + f\partial_r P^t + \frac{2M}{r^2} P^t\right], \tag{4.C.16}$$

and standard Regge-Wheeler potential

$$V_{\rm odd}(r) \equiv \frac{f}{r^2}\left[\ell\,(\ell+1) - \frac{6M}{r}\right]. \tag{4.C.17}$$

4.D Asymptotic expansions for Jost functions at $r_* \to \infty$

We examine here the asymptotic expansions that we use to set boundary conditions far from the black hole. The unit normalized solution to Eq. (4.2.16) is factored into the form

$$\hat{R}^+_{\ell mn}(r) = J^+_{\ell mn}(r) e^{i\omega_{mn} r_*}, \tag{4.D.1}$$

where $J^+_{\ell mn}$ is the "Jost function" [71], which goes to 1 as $r_* \to +\infty$. (We can similarly define the horizon side Jost function through $\hat{R}^-_{\ell mn} = J^-_{\ell mn} e^{-i\omega_{mn} r_*}$, which goes to 1 as $r_* \to -\infty$.) Plugging this into the source free version of Eq. (4.2.16) and changing to r derivatives, we have

$$f \frac{d^2 J^+_{\ell mn}}{dr^2} + \left[\frac{2M}{r^2} + 2i\omega_{mn} \right] \frac{dJ^+_{\ell mn}}{dr} - \frac{V_\ell}{f} J^+_{\ell mn} = 0. \tag{4.D.2}$$

From here we assume an asymptotic series solution of $J^+_{\ell mn}$ of the form

$$J^+_{\ell mn}(r) = \sum_{j=0}^{\infty} \frac{a_j}{(\omega_{mn} r)^j} \tag{4.D.3}$$

Note that contrary to a Taylor expansion which converges for fixed r with increasing j, this series converges for fixed j with increasing r. When a specific potential is chosen, the method of Frobenius can be used to find the coefficients a_j. Plugging in the even-parity potential from Eq. (4.C.9) a recurrence relation for the a_j is

$$\begin{aligned} 2i\lambda^2 j\, a_j = {} & \lambda \Big[\lambda (j-1) j - 12i\sigma (j-1) - 2\lambda (\lambda+1) \Big] a_{j-1} \\ & + 2\sigma \Big[\lambda (3-\lambda) (j-2) (j-1) - \left(\lambda^2 + 9i\sigma\right) (j-2) - 3\lambda^2 \Big] a_{j-2} \\ & + 3\sigma^2 \Big[(3-4\lambda) (j-3) (j-2) - 4\lambda (j-3) - 6\lambda \Big] a_{j-3} - 18\sigma^3 (j-3)^2\, a_{j-4} \end{aligned} \tag{4.D.4}$$

where $\sigma \equiv M\omega_{mn}$. For the odd-parity expansion, we plug in the potential in Eq. (4.C.17). The resulting recurrence relation is

$$2ij\,a_j = -2\sigma\Big[\,(j+1)\,(j-3)\,\Big]\,a_{j-2} - \Big[\ell\,(\ell+1) - j\,(j-1)\,\Big]\,a_{j-1}. \tag{4.D.5}$$

In order to use these recurrence relations, the first few terms $a_0,\ a_1, \ldots$ are needed. The recurrence relations actually provides them if one assumes that $a_j = 0$ for all negative j.

	$\dot{E}^{\infty}_{\ell m}$ (M^2/μ^2)	$\dot{E}^{H}_{\ell m}$ (M^2/μ^2)	$\dot{L}^{\infty}_{\ell m}$ (M/μ^2)	$\dot{L}^{H}_{\ell m}$ (M/μ^2)
$p = 7.50478$, $e = 0.188917$				
This Chapter, $\ell_{\max} = 23$	3.16899989185 $\times 10^{-4}$	5.23247295625 $\times 10^{-7}$	5.96755215609 $\times 10^{-3}$	8.71943028067 $\times 10^{-6}$
Fujita et al.	3.16899989184 $\times 10^{-4}$	N/A	5.96755215608 $\times 10^{-3}$	N/A
$p = 8.75455$, $e = 0.764124$				
This Chapter, $\ell_{\max} = 29$	2.12360313360 $\times 10^{-4}$	2.27177440621 $\times 10^{-6}$	2.77735939025 $\times 10^{-3}$	2.22781961809 $\times 10^{-5}$
Fujita et al.	2.12360313326 $\times 10^{-4}$	N/A	2.77735938996 $\times 10^{-3}$	N/A

Table 4.1: Total energy and angular momentum fluxes for eccentric orbits, compared with those from Fujita et al., published in [2].

	$\dot{E}^{\infty}_{\ell m}$ (M^2/μ^2)	$\dot{E}^{H}_{\ell m}$ (M^2/μ^2)	$\dot{L}^{\infty}_{\ell m}$ (M/μ^2)	$\dot{L}^{H}_{\ell m}$ (M/μ^2)
$p = 10$, $e = 0.1$				
This Chapter	6.31752474718 $\times 10^{-5}$	1.53365819446 $\times 10^{-8}$	1.95274165241 $\times 10^{-3}$	4.48832141611 $\times 10^{-7}$
Fujita et al.	6.31752474720 $\times 10^{-5}$	1.53365819445 $\times 10^{-8}$	N/A	N/A
$p = 10$, $e = 0.5$				
This Chapter	9.27335011599 $\times 10^{-5}$	1.41298859263 $\times 10^{-7}$	1.97465149446 $\times 10^{-3}$	2.15617302381 $\times 10^{-6}$
Fujita et al.	9.27335011503 $\times 10^{-5}$	1.41298859260 $\times 10^{-7}$	N/A	N/A
$p = 10$, $e = 0.7$				
This Chapter	9.46979134556 $\times 10^{-5}$	3.55415030147 $\times 10^{-7}$	1.63064691133 $\times 10^{-3}$	4.20771917244 $\times 10^{-6}$
Fujita et al.	9.46979134409 $\times 10^{-5}$	3.55415030114 $\times 10^{-7}$	N/A	N/A
$p = 10$, $e = 0.9$				
This Chapter	4.194264692 $\times 10^{-5}$	3.652142848 $\times 10^{-7}$	5.982866119 $\times 10^{-3}$	3.518978461 $\times 10^{-6}$
Fujita et al.	4.19426469206 $\times 10^{-5}$	3.65214284306 $\times 10^{-7}$	N/A	N/A

Table 4.2: Energy and angular momentum fluxes for eccentric orbits, compared with those from Fujita et al. [3]. Partial sums for all four orbits are truncated at $\ell_{\max} = 20$ for both papers. Fujita et al. obtained their numbers from integrating the Teukolsky equation. We include this table to show the agreement of our horizon energy flux values.

ℓ	m	$\dot{E}^{\infty}_{\ell m}$ (M^2/μ^2)	$\dot{E}^{H}_{\ell m}$ (M^2/μ^2)	$\dot{L}^{\infty}_{\ell m}$ (M/μ^2)	$\dot{L}^{H}_{\ell m}$ (M/μ^2)	$n_{\min}$	$n_{\max}$
2	0	1.27486196317 $\times 10^{-8}$	1.66171571270 $\times 10^{-8}$	0	0	-74	76
	1	1.15338054092 $\times 10^{-6}$	3.08063328605 $\times 10^{-7}$	1.44066000650 $\times 10^{-5}$	2.77518962557 $\times 10^{-6}$	-62	78
	2	1.55967717209 $\times 10^{-4}$	1.84497995136 $\times 10^{-6}$	2.07778922470 $\times 10^{-3}$	1.85014840343 $\times 10^{-5}$	-47	82
3	0	2.53527063853 $\times 10^{-11}$	1.23159713946 $\times 10^{-10}$	0	0	-84	85
	1	9.66848921204 $\times 10^{-10}$	2.47099909183 $\times 10^{-9}$	1.93528074730 $\times 10^{-8}$	2.10622579957 $\times 10^{-8}$	-66	87
	2	6.17859627641 $\times 10^{-7}$	1.29412677182 $\times 10^{-8}$	7.54192378736 $\times 10^{-6}$	1.23105502765 $\times 10^{-7}$	-48	93
	3	3.71507683858 $\times 10^{-5}$	8.07017762262 $\times 10^{-8}$	4.67102471030 $\times 10^{-4}$	7.99808068724 $\times 10^{-7}$	-34	99
4	0	1.14820411420 $\times 10^{-12}$	1.50591364139 $\times 10^{-12}$	0	0	-80	80
	1	4.58377338924 $\times 10^{-12}$	2.04365875527 $\times 10^{-11}$	4.50183584238 $\times 10^{-11}$	1.63314060565 $\times 10^{-10}$	-77	94
	2	1.59253324588 $\times 10^{-9}$	1.62313574547 $\times 10^{-10}$	2.40079049220 $\times 10^{-8}$	1.51029853345 $\times 10^{-9}$	-51	93
	3	2.44084848389 $\times 10^{-7}$	6.50157912447 $\times 10^{-10}$	2.91633622588 $\times 10^{-6}$	6.23354901544 $\times 10^{-9}$	-34	106
	4	1.12530626433 $\times 10^{-5}$	4.66621235553 $\times 10^{-9}$	1.37037638198 $\times 10^{-4}$	4.59633939401 $\times 10^{-8}$	-31	114
5	0	2.93546198223 $\times 10^{-15}$	1.68762144246 $\times 10^{-14}$	0	0	-94	94
	1	1.66341467681 $\times 10^{-13}$	2.73842758121 $\times 10^{-13}$	1.99357707469 $\times 10^{-12}$	2.10992243393 $\times 10^{-12}$	-77	92
	2	1.72172010497 $\times 10^{-12}$	1.49178217605 $\times 10^{-12}$	2.59625132235 $\times 10^{-11}$	1.34307539131 $\times 10^{-11}$	-63	100
	3	1.73935003471 $\times 10^{-9}$	1.01021973779 $\times 10^{-11}$	2.26258058740 $\times 10^{-8}$	9.56603438989 $\times 10^{-11}$	-46	109
	4	9.01787571564 $\times 10^{-8}$	3.64807139949 $\times 10^{-11}$	1.06079902733 $\times 10^{-6}$	3.50623060712 $\times 10^{-10}$	-29	121
	5	3.74854353561 $\times 10^{-6}$	3.02291684853 $\times 10^{-10}$	4.47051998131 $\times 10^{-5}$	2.96568439531 $\times 10^{-9}$	-19	130
Total		2.10242675876 $\times 10^{-4}$	2.27174892328 $\times 10^{-6}$	2.75262625234 $\times 10^{-3}$	2.22779475534 $\times 10^{-5}$		

Table 4.3: Energy and angular momentum fluxes for an eccentric orbit with $p = 8.75455$, $e = 0.764124$. Note that we have folded the negative m modes onto the corresponding positive m modes and doubled the flux values in this table for $m > 0$.

Chapter 5

Eccentric EMRI orbits on a Schwarzschild black hole: Transformation of the Regge-Wheeler gauge solutions to Lorenz gauge using new frequency domain based methods

In Chapter 4 we considered a point mass in an eccentric orbit about a Schwarzschild black hole. The particle pulls up a first-order gravitational field which can be found by solving the perturbed Einstein equations. We showed how we solved those equations in Regge-Wheeler (RW) gauge using the Regge-Wheeler-Zerilli (RWZ) formalism. Working in the frequency domain (FD), we obtained high accuracy solutions to the field equations and transformed the fields back to the time domain (TD). Our FD code is very efficient, largely thanks to the exponentially convergent method of extended homogeneous solutions (EHS), which we applied to radiative gravitational modes for the first time. We reconstructed the metric perturbation at all locations, including the location of the particle itself. We presented, for the first time, a detailed analysis of the singular nature of the metric in RW gauge, showing that the perturbation amplitudes are discontinuous (C^{-1}) in all cases and sometimes singular ($\sim\delta(z)$).

Having solved for the metric perturbation, we would like to correct the particle's motion. Though there are alternatives (see below), the most common technique is to calculate the self-force in Lorenz gauge. Hence, we now present work in progress on how to transform the metric perturbation from RW to Lorenz gauge.

5.1 Introduction

Attempts to evolve EMRI orbits have been made for many years. The primary method for performing these evolutions has been to use adiabatic approximations (e.g. [90]). The adiabatic approximation entails computing the energy and angular momentum fluxes of the gravitational radiation over a sufficiently long time scale, and then using those values to evolve the orbital parameters. The adiabatic approximation is based on the assumption of two fundamental timescales. The first is the orbital timescale T, or how long it takes the particle to orbit the black hole. The second is the radiation reaction timescale τ, the time it takes the orbital separation to make a fractional change of order unity. If the mass-ratio of the particle to the SMBH is μ/M, then ratio of the the radiation reaction timescale to the orbital period will be its inverse, $\tau/T \sim M/\mu$. The adiabatic approximation fails when we no longer have $\tau \gg T$. Whenever the particle is deep in the gravitational well of the SMBH it will radiate more strongly. This can happen when it is in a highly eccentric zoom-whirl orbit. It will also occur toward the end of any orbit. In the late stages of orbit evolution, the particle will spiral quickly toward the event horizon and the assumption of two, disparate timescales will be broken.

Another problem with the traditional adiabatic approximation is that it cannot incorporate the conservative effects of the self-force. As shown by Pound, Poisson and Nickel [91], neglecting the conservative piece of the self-force can lead to significant measurable differences in the particle's evolution.

Due largely to the inherent limitations of the adiabatic approximation, much research on EMRIs has focused on performing self-consistent orbit evolutions. In order to perform such a calculation, one needs to solve first for the metric at first-order, which we showed in Chapter 4 can be done to high accuracy in RW gauge. In principle one then has an entire knowledge of the first-order gravitational field. Evolution of the orbit comes down to examining how this perturbation affects zeroth-order motion. This becomes quite subtle in practice, largely because the divergent field must be regularized and some gauges are more convenient than others. Although it may be possible to evolve an orbit self-consistently in

RW gauge, the vast majority of work on self-consistent orbit evolution has been done in Lorenz gauge.

Lorenz gauge is appealing for several reasons. The field equations simplify greatly when the gauge condition $\bar{p}^{\mu\nu}{}_{|\nu} = 0$ is imposed. For those wishing to solve the field equations through time domain (TD) methods (e.g. [45]), Lorenz gauge has the benefit that one can put all ten field equations in hyperbolic form. From the point of view of computing the self-force, the Lorenz gauge metric perturbation amplitudes are much better behaved that those of RW gauge. Locally, the amplitudes are C^0, as opposed to C^{-1}, or singular, in RW gauge. Asymptotically, the metric in Lorenz gauge is flat, as opposed to non-asymptotically flat in RW gauge. We will discuss this more in detail below. Finally, the metric perturbation in Lorenz gauge is locally isotropic, which is why the mode-sum regularization scheme [41] and the MiSaTaQuWa equations of motion (1.4.7) were formulated there.

Given these benefits of Lorenz gauge, and that we possess the metric perturbation in RW gauge, we have begun the process of transforming between the two. We follow largely the work of Sago, Nakano, and Sasaki (SNS) [54], who presented one possible method for doing this exact gauge transformation. Below we show how the gauge transformation equations decouple and explain the benefit of the SNS decomposition.

Our work thus far has led to some noteworthy developments. Primary among these are two new solution techniques we have used to solve the types of equations encountered in this gauge transformation. The transformation equations decouple in harmonics into a set of wave equations at every mode. These equations have source terms with local singular parts at the particle's location. These source terms are precisely of the form we handled in Chapter 4, and present no trouble. But, in addition to these point singular sources, there are extended sources which are nonzero everywhere, and discontinuous at the particle's location. To find solutions to differential equations with source terms of this type, we developed the *method of partial annihilators* and the *method of extended particular solutions*. Each of these methods is discussed at length in what follows.

At this point we have completed numerical solutions for the odd-parity transformation and the scalar part of the even-parity transformation. Work in the near future will entail

computation of the remaining vector part of the even-parity gauge transformation. With these results in hand, we will be able to compute the self-force and compare with other similar work [47].

5.2 Benefits and drawbacks of Regge-Wheeler gauge

We previously considered bound geodesic motion on a Schwarzschild background. As described in Sec. 4.2.1, an eccentric orbit can be specified by a pair of parameters. Where useful we use either the energy $\mathcal{E}$ and angular momentum $\mathcal{L}$ per unit mass, the dimensionless semi-latus rectum p and eccentricity e, or the periapsis $r_{\min}$ and apapsis $r_{\max}$.

Using the RWZ formalism (see Sec. 4.2.2), we solved the first-order field equations. This formalism has the benefit of reducing the perturbed Einstein equations to one wave equation for each ℓ, m mode. When $\ell + m$ is even we solve for the Zerilli-Moncrief master function ($\Psi^{\ell m}_{\text{even}}$), and when $\ell+m$ is odd we solve for the Cunningham-Price-Moncrief master function ($\Psi^{\ell m}_{\text{odd}}$). We used a FD approach to find the Fourier harmonic modes (the Fourier transforms of $\Psi^{\ell m}_{\text{even}}$ and $\Psi^{\ell m}_{\text{odd}}$) and transformed back to the TD using the method of extended homogeneous solutions (EHS). This produced a weak solution form of the master functions, $\Psi_{\ell m}(t,r) = \Psi^{+}_{\ell m}(t,r)\theta\left[r - r_p(t)\right] + \Psi^{-}_{\ell m}(t,r)\theta\left[r_p(t) - r\right]$. From there we reconstructed the metric perturbation amplitudes in RW gauge, as described in Sec. 4.5.

The troubling local nature of the RW gauge metric perturbation amplitudes was covered in detail in Sec. 4.5. Even beyond these discontinuities and singularities, RW gauge exhibits undesirable features asymptotically as well. For example, consider the odd-parity amplitudes $h^{\ell m}_t$ and $h^{\ell m}_r$ (note that the remaining odd-parity amplitude $h^{\ell m}_2$ is set to zero in RW gauge). By looking at the expressions in Eq. (4.5.15) we can see how the amplitudes behave at large r. Given that $\Psi^{\ell m}_{\text{odd}} \sim F(t - r_*)$ (where $F(t - r_*)$ is any constant amplitude outgoing wave), we see that

$$h^{\ell m}_t \sim r \cdot F(t - r_*), \qquad h^{\ell m}_r \sim r \cdot F(t - r_*). \tag{5.2.1}$$

Figs. 5.1 and 5.2 demonstrate both of these problems graphically for the $\ell = 2, m = 1$

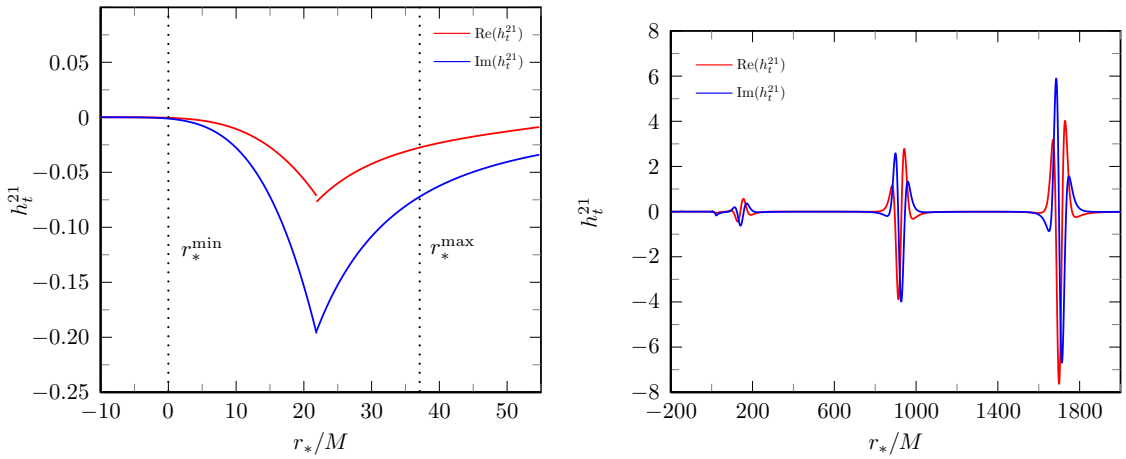

Figure 5.1: The Regge-Wheeler gauge metric perturbation amplitude h_t^{21}. As the particle orbits between periapsis and apapsis, we examine the real and imaginary parts of this amplitude at a moment in time. In the left panel, note the (very slight) discontinuity at the location of the particle. In the right panel, note the lack of asymptotic flatness.

mode. The left panels of those figures show a discontinuous field at the particle's location, $r = r_p(t)$, while the right panels show a lack of asymptotic flatness.

These problems with RW gauge can be circumvented by transforming to Lorenz gauge. Because the Lorenz gauge condition is differential (as opposed to the algebraic RW condition), we must solve a set of differential equations to perform the transformation. We examine this transformation in detail in the remainder of this chapter.

5.3 Transformation from RW to Lorenz gauge

The gauge transformation from Regge-Wheeler (RW) to Lorenz (L) involves a coordinate change of the form

$$x^\mu_{\rm RW} \to x^\mu_{\rm L} = x^\mu_{\rm RW} + \Xi^\mu, \tag{5.3.1}$$

where the gauge generator Ξ^μ is of the same order of magnitude as the metric perturbation $p_{\mu\nu}$, that is $|\Xi_\mu| \sim |p_{\mu\nu}| \ll 1$. Given Eq. (5.3.1), the metric perturbation transforms as

$$p^{\rm RW}_{\mu\nu} \to p^{\rm L}_{\mu\nu} = p^{\rm RW}_{\mu\nu} - \Xi_{\mu|\nu} - \Xi_{\nu|\mu}, \tag{5.3.2}$$

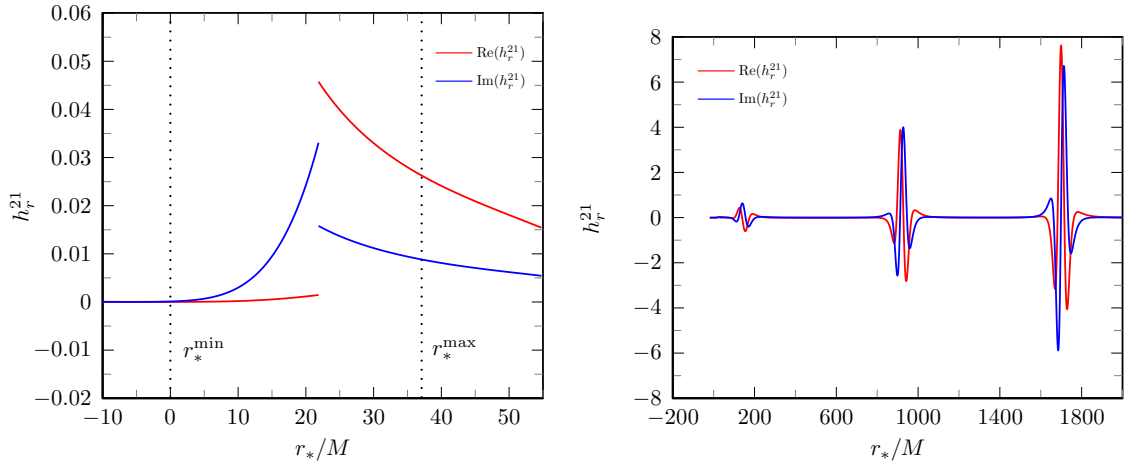

Figure 5.2: The Regge-Wheeler gauge metric perturbation amplitude h_r^{21}. As the particle orbits between periapsis and apapsis, we examine the real and imaginary parts of this amplitude at a moment in time. In the left panel, note the discontinuity at the location of the particle. In the right panel, note the lack of asymptotic flatness.

where we are using a stroke $_{|\mu}$ or ${}^4\nabla_\mu$ to indicate covariant differentiation with respect to the background metric. Now, we plug Eq. (5.3.2) into the Lorenz gauge condition (as introduced in Chapter 2), $\bar{p}^{\mu\nu}{}_{|\nu} = 0$, which gives

$$ {}^4\Box\Xi_\mu = \Xi_{\mu|\nu}{}^{\nu} = \bar{p}_{\mu\nu|}{}^{\nu} = p_{\mu\nu|}{}^{\nu} - \frac{1}{2}g^{\alpha\beta}p_{\alpha\beta|\mu}. \tag{5.3.3} $$

On the spherically symmetric Schwarzschild background, we make use of the $\mathcal{M}^2 \times \mathcal{S}^2$ decomposition of Martel and Poisson [55]. We perform a harmonic decomposition of the gauge vector in these two sectors as

$$ \Xi_a = \sum_{\ell,m} \xi_a^{\ell m} Y_{\ell m}, \qquad \Xi_A = \sum_{\ell,m} \left[\xi^{\ell m}_{\text{even}} Y_A^{\ell m} + \xi^{\ell m}_{\text{odd}} X_A^{\ell m} \right]. \tag{5.3.4} $$

There are four scalar amplitudes here which depend only on t and r; they are ξ_t, ξ_r, ξ_{even}, and ξ_{odd}.

Recall that lower case latin indices $a, b, \ldots$ are on the sector $\mathcal{M}^2 = \{t, r\}$, and upper case latin indices $A, B, \ldots$ are on the two sphere, or sector $\mathcal{S}^2 = \{\theta, \phi\}$. The line element can be written in terms of the two metrics of these sub-manifolds, $ds^2 = g_{ab}dx^a dx^b + g_{AB}dx^A dx^B$.

The covariant derivative on $\mathcal{M}^2$ is ∇_a and on $\mathcal{S}^2$ is D_A. They are defined by demanding that $\nabla_a g_{bc} = 0$ and $D_A g_{BC} = 0$. For more details on the $\mathcal{M}^2 \times \mathcal{S}^2$ decomposition, see Chapter 2.

5.3.1 Gauge transformations on the $\mathcal{M}^2$ sector

First we consider the gauge transformation equation on the $\mathcal{M}^2$ sector. The four dimensional wave operator can be written in terms of ∇_a and D_A as

$$ {}^4\Box \Xi_a = \Box \Xi_a + g^{BC} D_C D_B \Xi_a - \frac{2}{r} r_a g^{AB} D_B \Xi_A + \frac{2}{r} r^b \nabla_b \Xi_a - \frac{2}{r^2} r_a r^b \Xi_b. \tag{5.3.5} $$

Here ${}^4\Box \equiv {}^4\nabla_\mu {}^4\nabla^\mu$ and $\Box \equiv \nabla_a \nabla^a$. We plug in the expanded forms of Ξ_a and Ξ_A from Eq. (5.3.4) and this simplifies to

$$ {}^4\Box \Xi_a = \Box \xi_a Y - \frac{2\,(\lambda+1)}{r^2} \xi_a Y + \frac{2}{r} r^b \nabla_b \xi_a Y - \frac{2f}{r^2} r_a \xi_r Y + 4 r_a \frac{\lambda+1}{r^3} \xi_{\text{even}} Y, \tag{5.3.6} $$

where $\lambda \equiv (\ell+2)(\ell-1)/2$. Note that in this equation we have suppressed ℓ, m indices on the spherical harmonics Y, and on the scalar amplitudes. Also, there is an implied sum over these indices, as shown explicitly in Eq. (5.3.4). Now, this is set equal to $\bar{p}_{a\mu}{}^{|\mu}$, which, as we saw in Eq. (2.4.24) is

$$ \bar{p}_{a\mu}{}^{|\mu} = \nabla^b \bar{p}_{ab} + g^{BC} D_B \bar{p}_{aC} - r_a \frac{1}{r} g^{DE} \bar{p}_{DE} + \frac{2}{r} r^b \bar{p}_{ab}. \tag{5.3.7} $$

Plugging in for the metric from Eq. (2.4.1)

$$ \bar{p}_{a\mu}{}^{|\mu} = \left[g^{bc} \nabla_c \left(h_{ab} - \frac{1}{2} g_{ab} \left(h^d{}_d + 2K \right) \right) - \frac{j_a}{r^2} \ell(\ell+1) \right. $$
$$ \left. + r_a \frac{1}{r} h^d{}_d + \frac{2}{r} r^b \left(h_{ab} - \frac{1}{2} g_{ab} \left(h^d{}_d + 2K \right) \right) \right] Y. \tag{5.3.8} $$

In RW gauge we set $j_a = 0$, so after simplifying we find

$$ \bar{p}_{a\nu}{}^{|\nu} = \left[g^{bc} \nabla_c \left(h_{ab} - \frac{1}{2} g_{ab} \left(h^d{}_d + 2K \right) \right) + \frac{2}{r} r^b \left(h_{ab} - g_{ab} K \right) \right] Y. \tag{5.3.9} $$

Furthermore, we know from the field equations in RW gauge (4.C.3) that $h^d{}_d = -Q^\sharp$, so equating Eqs. (5.3.9) and (5.3.6) and using the completeness of the scalar harmonics, we get

$$\Box\xi_a - \frac{2(\lambda+1)}{r^2}\xi_a + \frac{2}{r}r^b\left(\partial_b\xi_a - \Gamma^c{}_{ab}\xi_c\right) - \frac{2f}{r^2}r_a\xi_r + 4r_a\frac{\lambda+1}{r^3}\xi_{\text{even}} = g^{cb}\nabla_c h_{ab} - \partial_a K + \frac{2}{r}r^b h_{ab} - \frac{2}{r}r_a K + \frac{1}{2}\partial_a Q^\sharp. \quad (5.3.10)$$

Note that the implied summation has vanished with the use of the orthogonality of the spherical harmonics. Therefore, there is one of these equations for each ℓ and m. After some lengthy algebra (in which we must expand the $\mathcal{M}^2$ box operator), this reduces to two coupled partial differential equations involving the gauge generator amplitudes ξ_t, ξ_r, and ξ_{even}. They are

$$-\frac{1}{f}\partial_t^2\xi_t + f\partial_r^2\xi_t + \frac{2f}{r}\partial_r\xi_t - \frac{2(\lambda+1)}{r^2}\xi_t + \frac{2M}{r^2}\partial_t\xi_r = -\frac{1}{f}\partial_t h_{tt} + f\partial_r h_{tr} - \partial_t K + \frac{2}{r^2}(r-M)h_{tr} + \frac{1}{2}\partial_t Q^\sharp, \quad (5.3.11)$$

and

$$-\frac{1}{f}\partial_t^2\xi_r + f\partial_r^2\xi_r + \frac{2}{r}\partial_r\xi_r - \frac{2f}{r^2}\xi_r + \frac{2}{f^2}\frac{M}{r^2}\partial_t\xi_t - \frac{2(\lambda+1)}{r^2}\xi_r + 4\frac{\lambda+1}{r^3}\xi_{\text{even}} = -\frac{1}{f}\partial_t h_{rt} + f\partial_r h_{rr} - \partial_r K + \frac{1}{f^2}\frac{M}{r^2}h_{tt} + \frac{2r-M}{r^2}h_{rr} - \frac{2}{r}K + \frac{1}{2}\partial_r Q^\sharp. \quad (5.3.12)$$

5.3.2 Gauge transformations on the $\mathcal{S}^2$ sector

On the $\mathcal{S}^2$ sector we can write the four dimensional box operator as

$${}^4\Box\Xi_A = \Box\Xi_A + g^{BC}D_C D_B\Xi_A - \frac{1}{r^2}\Xi_A + \frac{2}{r}r^b\Xi_{b,A} \quad (5.3.13)$$

Plugging in our expressions for Ξ_A and Ξ_a from Eq. (5.3.4), we find

$$
\begin{aligned}
{}^4\Box\Xi_A = \left(-\frac{1}{f}\partial_t^2 + \partial_r\left(f\partial_r\right)\right)\xi_{\text{even}}Y_A + \left(-\frac{1}{f}\partial_t^2 + \partial_r\left(f\partial_r\right)\right)\xi_{\text{odd}}X_A \\
- \xi_{\text{even}}\frac{2\left(\lambda+1\right)}{r^2}Y_A - \xi_{\text{odd}}\frac{2\left(\lambda+1\right)}{r^2}X_A + \frac{2f}{r}\xi_r Y_A
\end{aligned}
\tag{5.3.14}
$$

As we saw in Eq. (2.4.40) (recall the suppressed ℓ, m indices which we sum over)

$$
\bar{p}^{A\nu}{}_{|\nu} = \left(\nabla_b + \frac{4}{r}r_b\right)\left(j^b Y^A + h^b X^A\right) - \frac{1}{2}g^{ab}h_{ab}Y^A - \lambda G Y^A - \frac{\lambda}{r^2}h_2 X^A. \tag{5.3.15}
$$

This simplifies dramatically in RW gauge since $h_2 = j_a = G = 0$. Then, after lowering the A index (which creates a counter term) we equate this with ${}^4\Box\Xi_A$ from Eq. (5.3.14), giving

$$
\begin{aligned}
\left(-\frac{1}{f}\partial_t^2 + \partial_r\left(f\partial_r\right)\right)\xi_{\text{even}}Y_A + \left(-\frac{1}{f}\partial_t^2 + \partial_r\left(f\partial_r\right)\right)\xi_{\text{odd}}X_A - \frac{2}{r^2}\left(\lambda+1\right)\xi_{\text{even}}Y_A \\
- \frac{2}{r^2}\left(\lambda+1\right)\xi_{\text{odd}}X_A + \frac{2f}{r}\xi_r Y_A = \nabla_b h^b X_A + \frac{2}{r}h^r X_A - \frac{1}{2}g^{ab}h_{ab}Y_A.
\end{aligned}
\tag{5.3.16}
$$

Note that from the field equations (4.C.3) we have $g^{ab}h_{ab} = -Q^\sharp$, and $\nabla_b h^b = P$. Now, we multiply through by Y^A (with implied indices $\ell' m'$) and integrate over the two-sphere. The orthogonality picks out the even-parity terms and we are left with the even-parity equation

$$
\left(-\frac{1}{f}\partial_t^2 + \partial_r\left(f\partial_r\right)\right)\xi_{\text{even}} - \frac{2}{r^2}\left(\lambda+1\right)\xi_{\text{even}} + \frac{2f}{r}\xi_r = -\frac{1}{2}Q^\sharp. \tag{5.3.17}
$$

Likewise, we use the orthogonality of the odd-parity harmonics X_A, which leaves us with the odd-parity equation

$$
\left(-\frac{1}{f}\partial_t^2 + \partial_r\left(f\partial_r\right)\right)\xi_{\text{odd}} - \frac{2}{r^2}\left(\lambda+1\right)\xi_{\text{odd}} = P + \frac{2}{r}h^r. \tag{5.3.18}
$$

Note that the odd-parity equation (5.3.18) decouples entirely, but the even-parity equation (5.3.17) is coupled with Eqs. (5.3.11) and (5.3.12). Finally, note that Eqs. (5.3.18) and (5.3.17) have implied indices ℓ and m.

5.3.3 The Sago, Nakano, Sasaki decomposition

Rather than using the decomposition derived in the previous subsections, Sago, Nakano, and Sasaki (SNS) [54] take a different approach which leads to a full separation of the even-parity equations. They start by splitting the gauge vector into even- and odd-parity parts

$$\Xi^{\mu} = \Xi^{\mu}_{\text{even}} + \Xi^{\mu}_{\text{odd}}. \tag{5.3.19}$$

There is a single harmonic amplitude $\xi^{\ell m}_{\text{odd}}$ that represents Ξ^{μ}_{odd}, as can be seen in Eq. (5.3.4). Our odd-parity equation (5.3.18) is entirely equivalent to that of SNS.

The difference lies in the treatment of the even-parity part, Ξ^{μ}_{even}. As before, three spherical harmonic amplitudes represent the four components of Ξ^{μ}_{even}. SNS use a four dimensional generalization of the Helmholtz decomposition (the Hodge decomposition [92]) and choose to express these three degrees of freedom through a scalar $\Xi_{\text{even}(s)}$ (which contains one degree of freedom) and a divergence-free vector $\Xi^{\mu}_{\text{even}(v)}$ (which contains the other two). The even-parity gauge vector is then

$$\Xi^{\mu}_{\text{even}} = \Xi^{\mu}_{\text{even}(v)} + {}^4\nabla^{\mu}\Xi_{\text{even}(s)}. \tag{5.3.20}$$

Taking Eq. (5.3.3) and inserting this expression gives

$${}^4\Box\left(\Xi^{\mu}_{\text{even}(v)} + {}^4\nabla^{\mu}\Xi_{\text{even}(s)}\right) = {}^4\nabla_{\nu}\bar{p}^{\mu\nu}_{\text{even}}. \tag{5.3.21}$$

Taking the divergence, the divergence-*free* vector part vanishes, so

$${}^4\Box\left({}^4\Box\Xi_{\text{even}(s)}\right) = {}^4\nabla_{\mu}{}^4\nabla_{\nu}\bar{p}^{\mu\nu}_{\text{even}}. \tag{5.3.22}$$

Note that we are able to move the covariant derivatives past one another because they are traced out and $R_{\mu\nu} = 0$ on the background spacetime. Now, we make the implicit definition of $J_{\text{even}(s)}$ through

$${}^4\Box\Xi_{\text{even}(s)} = J_{\text{even}(s)}. \tag{5.3.23}$$

Then Eq. (5.3.22) reduces to

$$ {}^4\Box J_{\text{even}(s)} = {}^4\nabla_\mu {}^4\nabla_\nu \bar{p}^{\mu\nu}_{\text{even}}. \tag{5.3.24} $$

This latter equation is a second-order inhomogeneous wave equation, which can be solved to find the source $J_{\text{even}(s)}$ for Eq. (5.3.23). Then, solving Eq. (5.3.23) yields the even-parity scalar part $\Xi_{\text{even}(s)}$. Returning to Eq. (5.3.21), and using Eq. (5.3.23), we see that we can write

$$ {}^4\Box \Xi^\mu_{\text{even}(v)} + {}^4\nabla^\mu J_{\text{even}(s)} = {}^4\nabla_\nu \bar{p}^{\mu\nu}_{\text{even}}. \tag{5.3.25} $$

We combine the two source terms to define

$$ J^\mu_{\text{even}(v)} \equiv {}^4\nabla_\nu \bar{p}^{\mu\nu}_{\text{even}} - {}^4\nabla^\mu J_{\text{even}(s)}. \tag{5.3.26} $$

Then, we have a wave equation for the divergence-free vector piece of the even-parity gauge generator,

$$ {}^4\Box \Xi^\mu_{\text{even}(v)} = J^\mu_{\text{even}(v)}. \tag{5.3.27} $$

This summarizes the SNS decomposition in terms of tensor components. We next turn to examining two new solution techniques for equations of the type we encounter here. We will then return to the specifics of solving the equations of the SNS formalism in Secs. 5.5 and 5.6, where these equations are further decomposed into spherical harmonics.

5.4 Solution techniques for extended sources

Here we present two new FD methods for solving the types of PDEs we are presented with during the gauge transformation.

5.4.1 Partial annihilators and higher order EHS: general considerations

Consider a PDE of the form

$$\mathcal{W}^a_{\ell m}\psi_{\ell m}(t,r) = S^{\ell m}_{\rm ext}(t,r), \tag{5.4.1}$$

where $\mathcal{W}^a_{\ell m}$ is an $a^{\rm th}$ order partial differential operator in t and r, which is acting on a scalar field $\psi_{\ell m}$. The source $S^{\ell m}_{\rm ext}(t,r)$ is non-compact, and therefore not amenable to the EHS method. The annihilator method is a standard technique [60] for solving differential equations, wherein we search for a differential operator for which $S^{\ell m}_{\rm ext}$ is a homogeneous solution. Then, we could act on both sides of Eq. (5.4.1) and produce a homogeneous differential equation, albeit of a higher order. Given the singular nature of the source in our problem, it is unlikely that we will be able to find such an operator. However, it turns out in practice with such sources to be possible to find an operator that *nearly* annihilates $S^{\ell m}_{\rm ext}$, e.g.

$$\mathcal{W}^b_{\ell m}S^{\ell m}_{\rm ext}(t,r) = S^{\ell m}_{\rm sing}(t,r_p(t)). \tag{5.4.2}$$

Here $\mathcal{W}^b_{\ell m}$ is an $b^{\rm th}$ order partial differential operator in t and r, and $S^{\ell m}_{\rm sing}(t,r_p(t))$ only has support at the location of the particle. We refer to this as a *partial annihilator*. Therefore, acting with $\mathcal{W}^b_{\ell m}$ on Eq. (5.4.1) we have

$$\mathcal{W}^b_{\ell m}\mathcal{W}^a_{\ell m}\psi_{\ell m}(t,r) = S^{\ell m}_{\rm sing}(t,r_p(t)). \tag{5.4.3}$$

We now have an equation with a point-singular source, which we can solve using the EHS method, but at the price of having raised it from order a to order $a+b$.

Moving into the FD, we Fourier transform Eq. (5.4.3) to get

$$\mathcal{L}^b_{\ell mn}\mathcal{L}^a_{\ell mn}\tilde{\psi}_{\ell mn}(r) = Z^{\ell mn}_{\rm sing}(r). \tag{5.4.4}$$

The effect of the partial annihilator in the FD, $\mathcal{L}^b_{\ell mn}$, is to make a non-compact source $Z^{\ell m}_{\rm ext}(r)$ into a compact source $Z^{\ell mn}_{\rm sing}(r)$, confined between $r_{\rm min}$ and $r_{\rm max}$. Through the end

of this subsection we will suppress the mode indices. Recall that the tilde over a symbol indicates a quantity which has been Fourier transformed into the FD.

The ODE (5.4.4) in r will have $a+b$ linearly independent homogeneous solutions. (We have in mind systems where a and b are even integers.) We can specify them by demanding that half of them are purely down-going at the event horizon and the other half are purely out-going at spatial infinity. We denote the former by $\tilde{\psi}_j^-$ and the latter by $\tilde{\psi}_j^+$, where j runs from 1 to $(a+b)/2$. Now, the causally appropriate particular solution to Eq. (5.4.4) will be a linear combination of the homogeneous solutions,

$$\tilde{\psi}_p(r) = c_1^-(r)\tilde{\psi}_1^-(r) + \cdots c_{(a+b)/2}^-(r)\tilde{\psi}_{(a+b)/2}^-(r) + c_1^+(r)\tilde{\psi}_1^+(r) + \cdots c_{(a+b)/2}^+(r)\tilde{\psi}_{(a+b)/2}^+(r). \quad (5.4.5)$$

We get the various normalization functions $c_j^\pm(r)$ by the general method of variation of parameters [60]. This entails solving the equations

$$\frac{dc_j^\pm}{dr_*}(r) = Z_{\text{sing}}(r)\frac{W_j^\pm(r)}{W(r)} \quad (5.4.6)$$

where $W(r)$ is the Wronskian and $W_j^\pm(r)$ is the "modified Wronskian," which is the Wronskian with the column corresponding to the $\psi_j^\pm$ homogeneous solution replaced by the column vector $(0, 0, \ldots, 1)$. Having solved Eq. (5.4.6) for the normalization functions, we can return to the TD via the standard Fourier synthesis (recall that we have suppressed ℓ, m, n indices on $\tilde{\psi}_p$)

$$\psi_p(t, r) = \sum_n \tilde{\psi}_p(r)e^{-i\omega_{mn}t}. \quad (5.4.7)$$

This will yield a causally appropriate solution to Eq. (5.4.1).

In our system though, the source S_{sing} will have some degree of lack of differentiability, and the sum above will converge in the TD only algebraically (if at all) at the location of the particle, due to the Gibbs phenomenon. Therefore, we seek to use the EHS method to

find exponentially-convergent solutions. To that end, we define

$$C_j^- \equiv c_j^-(r_{\min}), \qquad C_j^+ \equiv c_j^+(r_{\max}), \tag{5.4.8}$$

which are referred to as the *normalization coefficients* and are the result of integrating Eq. (5.4.6) through the entire source region. Then, we define the EHS in the FD to be

$$\tilde{\psi}^{\pm}(r) \equiv \sum_{j}^{(a+b)/2} C_j^{\pm} \tilde{\psi}_j^{\pm}(r), \tag{5.4.9}$$

and the EHS in the TD are defined as

$$\psi^{\pm}(t,r) \equiv \sum_{n} \tilde{\psi}^{\pm}(r) e^{-i\omega_{mn}t}. \tag{5.4.10}$$

Then, as before with the original EHS method [1], the weak solution representation

$$\psi^{\rm EHS} \equiv \psi^{+}(t,r)\,\theta\left[r - r_p(t)\right] + \psi^{-}(t,r)\,\theta\left[r_p(t) - r\right] \tag{5.4.11}$$

expresses the solution to Eq. (5.4.1).

5.4.2 Extended particular solutions method

As an alternative to the partial annihilator method we consider solving Eq. (5.4.1) without promoting it to a higher-order equation. We start by moving Eq. (5.4.1) to the FD, yielding

$$\mathcal{L}^a_{\ell mn}\tilde{\psi}_{\ell mn}(r) = Z^{\ell mn}_{\rm ext}(r). \tag{5.4.12}$$

With its non-compact source, the EHS method is not immediately applicable to solve Eq. (5.4.12). As usual, we expect $\tilde{\psi}_{\ell mn}$ to consist of both a particular solution and homogeneous solutions. We inspect the asymptotic nature of $Z^{\ell mn}_{\rm ext}(r)$ at infinity and the event horizon. Between this and our differential operator $\mathcal{L}^a_{\ell mn}$ we should be able to find the leading order nature of the causal particular solution. On the large r side, we denote this solution as $\tilde{\psi}^{\infty}_p(r)$, and near the horizon we express it as $\tilde{\psi}^{H}_p(r)$. Here we have suppressed

the ℓ, m, n indices, and will continue to do so for the remainder of this subsection.

We first take $\tilde{\psi}_p^{\infty}(r)$, (though the opposite choice would work as well) as a boundary condition at infinity to begin our ODE integration of Eq. (5.4.12). We integrate this differential equation inward, through the region of the source and on to the horizon. At this point, in addition to having obtained a particular solution, we will have excited all a homogeneous solutions, which will be evident in the behavior near the horizon. Half of these homogeneous terms will be causal waves traveling down into the black hole, and the other $a/2$ will be acausal waves coming up from the black hole. We eliminate this acausal behavior by solving the homogeneous version of Eq. (5.4.12) for the $a/2$ acausal pieces and subtracting them off. The homogeneous solutions on the infinity side are $\tilde{\psi}_{h,j}^{+}$ where j runs from 1 to $a/2$. Likewise, there are $a/2$ homogeneous solutions on the horizon side, which we denote $\tilde{\psi}_{h,j}^{-}$. We sum up the scaled homogeneous solutions and return to the TD via

$$\psi_h^{\pm}(t,r) = \sum_{n=-\infty}^{\infty} \left[\sum_{j=1}^{a/2} \tilde{\psi}_{h,j}^{\pm}(r) \right] e^{-i\omega_{mn}t}. \tag{5.4.13}$$

This is a fairly straightforward process if Eq. (5.4.1) has a source term which is differentiable everywhere. Unfortunately, the system we work with does not have such a source, and we must be careful. The source $S_{\rm ext}$ will be a linear combination of singular pieces (δ, δ', etc.) and the master function Ψ (either $\Psi_{\rm even}$ or $\Psi_{\rm odd}$) and its derivatives. Since we are working with linear equations, we can always solve for the singular parts with the EHS method, and we therefore consider only the extended source pieces which come from Ψ. When we Fourier transform Eq. (5.4.1) to get Eq. (5.4.12) there is an ambiguity that arises. Because the TD source of Eq. (5.4.1) contains Ψ, the FD source of Eq. (5.4.12) will contain R, which has two forms,

$$R^{\rm std}(r) = c^{+}(r)\hat{R}^{+}(r) + c^{-}(r)\hat{R}^{-}(r), \qquad \text{and} \qquad R^{\pm}(r) = C^{\pm}\hat{R}^{\pm}(r). \tag{5.4.14}$$

The particular solution that we get from using $R^{\rm std}$ as the source we call the *standard particular solution* and denote as $\tilde{\psi}_p^{\infty/H}$. The superscript $^{\infty/H}$ is to distinguish between

whether the integration starts at infinity or the horizon. On the other hand, when using using $R^{\pm}$ as the source we compute the *extended particular solution* (EPS) which we denote as $\tilde{\psi}_p^{\pm}$. The superscript $^{\pm}$ is to distinguish between whether the integration starts at infinity or the horizon.

Because $R^{\rm std}$ is the Fourier transform of Ψ, it must be used when solving for the correct homogeneous solutions, as described above. Returning $\tilde{\psi}_p^{\infty/H}$ to the TD produces $\psi_p^{\infty/H}$, which will exhibit the usual Gibbs phenomenon that is always present when the source is singular. The convergence will be algebraic at best. The way around this rests on generalizing the EHS method and using the extended particular solutions (EPS).

Having computed the EPS, we have in hand what it takes to form the true solution to Eq. (5.4.1). We use the Fourier synthesis to take the EPS to the TD,

$$\psi_p^{\pm}(t,r) = \sum_n \tilde{\psi}_p^{\pm}(r) e^{-i\omega_{mn}t}. \tag{5.4.15}$$

By the same continuity arguments that apply to the EHS method, we claim that the causally appropriate solution to the inhomogeneous equation with non-compact source (5.4.1) is

$$\psi(t,r) = \Big(\psi_p^{+}(t,r) + \psi_h^{+}(t,r)\Big)\theta\left[r - r_p(t)\right] + \Big(\psi_p^{-}(t,r) + \psi_h^{-}(t,r)\Big)\theta\left[r_p(t) - r\right]. \tag{5.4.16}$$

We have verified this claim by demonstrating numerically that this approach is entirely equivalent to the partial annihilator method. The new higher-order homogeneous solutions introduced by the annihilator are precisely the same as the particular solutions found here. Note that those homogeneous solutions come in standard and EHS form, just as the particular solutions here come in standard and EPS form.

5.5 Odd-parity gauge generator

As seen in Eq. (5.3.18), the odd-parity gauge generator satisfies the equation

$$\left[-\frac{\partial^2}{\partial t^2} + \frac{\partial^2}{\partial r_*^2} - V_1(r)\right]\xi_{\rm odd}(t,r) = 2f(r)\Psi_{\rm RW} + f_p p(t)\delta\left[r - r_p(t)\right]. \tag{5.5.1}$$

In this expression, on the left we have introduced the tortoise coordinate and the spin-1 odd-parity potential $V_1 = 2f(\lambda+1)/r^2$. On the right we have noted that $fh_r/r = \Psi_{\rm RW}$ and factored the delta function out of the P term as in Sec. 4.5.2. Now we discuss the application of the two methods introduced in the previous section to this equation.

5.5.1 Partial annihilator method

Equation (5.5.1) is linear, so we can split off the singular part and define two functions, $\xi^{\rm ext}_{\rm odd}$ and $\xi^{\rm sing}_{\rm odd}$ that satisfy two separate equations,

$$\left[-\frac{\partial^2}{\partial t^2}+\frac{\partial^2}{\partial r_*^2}-V_1(r)\right]\xi^{\rm sing}_{\rm odd}(t,r) = f_p p(t)\delta\left[r-r_p(t)\right], \tag{5.5.2}$$

$$\left[-\frac{\partial^2}{\partial t^2}+\frac{\partial^2}{\partial r_*^2}-V_1(r)\right]\xi^{\rm ext}_{\rm odd}(t,r) = 2f(r)\Psi_{\rm RW}. \tag{5.5.3}$$

The equation for $\xi^{\rm sing}_{\rm odd}$ can be solved using the standard EHS approach. We are then left with finding a partial annihilator for the $\xi^{\rm ext}_{\rm odd}$ equation. Naturally, the Regge-Wheeler variable satisfies its own wave equation with a point singular source. Therefore, dividing by f and acting with the Regge-Wheeler operator, we have (where, for the remainder of this section we will drop the $^{\rm ext}_{\rm odd}$ tags for notational simplicity)

$$\left[-\frac{\partial^2}{\partial t^2}+\frac{\partial^2}{\partial r_*^2}-V_2(r)\right]\frac{1}{f}\left[-\frac{\partial^2}{\partial t^2}+\frac{\partial^2}{\partial r_*^2}-V_1(r)\right]\xi = 2S_{\rm RW}(t,r_p(t)), \tag{5.5.4}$$

where $V_2 = f\left(2(\lambda+1)/r^2-6M/r^3\right)$ is the spin-2 odd-parity RW potential and $S_{\rm RW}$ is the fully evaluated source term for the master function $\Psi_{\rm RW}$, which can be found (though not in fully evaluated form) in Martel [50]. Now we have a source which is point-singular. The trade off is that the differential equation (5.5.4) is now fourth order.

We Fourier transform Eq. (5.5.4) to obtain the FD equation

$$\left[\frac{d^2}{dr_*^2}+\omega_{mn}^2-V_2(r)\right]\frac{1}{f}\left[\frac{d^2}{dr_*^2}+\omega_{mn}^2-V_1(r)\right]\tilde{\xi}(r) = 2Z_{\rm RW}(r), \tag{5.5.5}$$

The Fourier transformed source $Z_{\rm RW}$ is no longer in general point singular, but it is compact (confined to the region $r_{\rm min}-r_{\rm max}$). There are four linearly independent homogeneous

solutions to Eq. (5.5.5). Two of these are the solutions to the second order equation, which behave asymptotically like running waves going out to spatial infinity and down the black hole,

$$\tilde{\xi}^{-}_{h2} \sim e^{-i\omega_{mn}r_*} \quad (r \to 2M), \qquad \tilde{\xi}^{+}_{h2} \sim e^{i\omega_{mn}r_*} \quad (r \to \infty). \tag{5.5.6}$$

Then, there are solutions that are only homogeneous solutions to full the fourth-order equation,

$$\tilde{\xi}^{-}_{h4} \sim f(r)e^{-i\omega_{mn}r_*} \quad (r \to 2M), \qquad \tilde{\xi}^{+}_{h4} \sim re^{i\omega_{mn}r_*} \quad (r \to \infty). \tag{5.5.7}$$

These four solutions form a fundamental set, spanning the space of homogeneous solutions of Eq. (5.5.5). The particular solution will be a linear combination of these,

$$\tilde{\xi}_p(r) = c^{-}_{h2}(r)\tilde{\xi}^{-}_{h2}(r) + c^{+}_{h2}(r)\tilde{\xi}^{+}_{h2}(r) + c^{-}_{h4}(r)\tilde{\xi}^{-}_{h4}(r) + c^{+}_{h4}(r)\tilde{\xi}^{+}_{h4}(r). \tag{5.5.8}$$

The four normalization functions $c^{\pm}_{h2/h4}(r)$ come from the method of variation of parameters, which entails solving the equations

$$\frac{dc^{\pm}_{h2/h4}}{dr_*} = 2Z_{\rm RW}(r)\frac{W^{\pm}_{h2/h4}(r)}{W(r)}, \tag{5.5.9}$$

as described in Sec. 5.4.1. For the two "+" equations, the integral form of Eq. (5.5.9) is

$$c^{+}_{h2/h4}(r) = \int_{r_{\rm min}}^{r} \left[\frac{1}{T_r}\int_0^{T_r} \Big(\tilde{G}_{\rm RW}(t)\delta\left[r' - r_p(t)\right] + \tilde{F}_{\rm RW}(t)\delta'\left[r' - r_p(t)\right]\Big)e^{i\omega_{mn}t}dt\right]\frac{W^{+}_{h2/h4}(r')}{W(r')}dr'. \tag{5.5.10}$$

Likewise, for the two "−" equations,

$$c^{-}_{h2/h4}(r) = \int_{r}^{r_{\rm max}} \left[\frac{1}{T_r}\int_0^{T_r} \Big(\tilde{G}_{\rm RW}(t)\delta\left[r' - r_p(t)\right] + \tilde{F}_{\rm RW}(t)\delta'\left[r' - r_p(t)\right]\Big)e^{i\omega_{mn}t}dt\right]\frac{W^{-}_{h2/h4}(r')}{W(r')}dr'. \tag{5.5.11}$$

The EHS method requires knowing the values of the four functions $c^{\pm}_{h2/h4}(r)$ only at the

turning points of the particle's motion $r_{\rm min}$ and $r_{\rm max}$. Therefore, switching the order of integration and integrating by parts, we find

$$C^{\pm}_{h2/h4} = \frac{1}{T_r}\int_0^{T_r}\left\{\tilde{G}_{\rm RW}(t)\frac{W^{\pm}_{h2/h4}(r_p)}{W(r_p)} - \tilde{F}_{\rm RW}(t)\left[-\frac{W^{\pm}_{h2/h4}(r_p)}{W(r_p)^2}\partial_r W(r_p) + \frac{\partial_r W^{\pm}_{h2/h4}(r_p)}{W(r_p)}\right]\right\}e^{i\omega_{mn}t}dt. \quad (5.5.12)$$

At this point we define the EHS in the FD to be

$$\tilde{\xi}^{-}_h(r) \equiv C^{-}_{h2}\tilde{\xi}^{-}_{h2}(r) + C^{-}_{h4}\tilde{\xi}^{-}_{h4}(r), \qquad \tilde{\xi}^{+}_h(r) \equiv C^{+}_{h2}\tilde{\xi}^{+}_{h2}(r) + C^{+}_{h4}\tilde{\xi}^{+}_{h4}(r), \quad (5.5.13)$$

and the EHS in the TD are defined are defined by the Fourier sums

$$\xi^{\pm}(t,r) \equiv \sum_n \tilde{\xi}^{\pm}_h(r)e^{-i\omega_{mn}t}. \quad (5.5.14)$$

The extension of these solutions to $r = r_p(t)$ then gives the desired solution to Eq. (5.5.3),

$$\xi^{\rm ext}_{\rm odd}(t,r) = \xi^{+}(t,r)\theta\left[r - r_p(t)\right] + \xi^{-}(t,r)\theta\left[r_p(t) - r\right]. \quad (5.5.15)$$

5.5.2 Second order approach, using the method of extended particular solutions

Now we look for a solution for $\xi^{\rm ext}_{\rm odd}$ that does not require a partial annihilator. In the FD its equation transforms to

$$\left[\frac{d^2}{dr_*^2} + \omega_{mn}^2 - V_1(r)\right]\tilde{\xi}^{\rm ext}_{\rm odd} = 2fR_{\rm RW}. \quad (5.5.16)$$

Again, for notational simplicity we drop the $^{\rm ext}_{\rm odd}$ tags for the remainder of this section. Asymptotically the RW function goes like $R^{\pm}_{\rm RW} \sim e^{\pm i\omega_{mn}r_*}$ as $r_* \to \pm\infty$. The potential dies away at large positive and negative r_*. We make the ansatz that $\tilde{\xi}^{+}_p \sim re^{i\omega_{mn}r_*}$ as $r \to +\infty$ We can plug this into Eq. (5.5.16) above and find a constant factor that will tell

us the scaling between $\tilde{\xi}_p^{\infty}$ and $R_{\rm RW}$ at large r,

$$\left(\frac{d^2}{dr_*^2}+\omega_{mn}^2\right)\left(A^+ re^{i\omega_{mn}r_*}\right)=2e^{i\omega_{mn}r_*}\qquad\Rightarrow\qquad A^+=\frac{1}{i\omega_{mn}}. \tag{5.5.17}$$

Therefore, the asymptotic form of $\tilde{\xi}_p^{\infty}$ is (assuming we take a unit amplitude on $R_{\rm RW}^+$)

$$\tilde{\xi}_p^{\infty}=-\frac{i}{\omega_{mn}}re^{i\omega_{mn}r_*},\qquad r\to+\infty. \tag{5.5.18}$$

Similarly, on the horizon side, by analyzing the source we assume a form of $\tilde{\xi}_p^{H}\sim f(r)e^{-i\omega_{mn}r_*}$ as $r\to 2M$, which implies

$$\left(\frac{d^2}{dr_*^2}+\omega_{mn}^2\right)\left(A^- fe^{i\omega_{mn}r_*}\right)=2fe^{-i\omega_{mn}r_*}\quad\Rightarrow\quad A^-=2\left(\frac{1}{4M^2}-\frac{i\omega_{mn}}{M}\right)^{-1}. \tag{5.5.19}$$

Therefore, the asymptotic form of $\tilde{\xi}_p^{H}$ is (assuming we take a unit amplitude on $R_{\rm RW}^-$)

$$\tilde{\xi}_p^{H}=2\left(\frac{1}{4M^2}-\frac{i\omega_{mn}}{M}\right)^{-1}fe^{-i\omega_{mn}r_*},\qquad r\to 2M. \tag{5.5.20}$$

The source term $R_{\rm RW}$ is itself the solution to the differential equation

$$\left[\frac{d^2}{dr_*^2}+\omega_{mn}^2-V_2\right]R_{\rm RW}(r)=Z_{\rm RW}(r). \tag{5.5.21}$$

We find it from the method of variation of parameters, which yields

$$R_{\rm RW}^{\rm std}(r)=c^+(r)\hat{R}^+(r)+c^-(r)\hat{R}^-(r), \tag{5.5.22}$$

where $R^{\pm}(r)$ are homogeneous solutions to Eq. (5.5.21). It is key in what follows that we use $R_{\rm RW}^{\rm std}(r)$ in the source term to Eq. (5.5.16), as opposed to

$$R_{\rm RW}^{{\rm EHS},\pm}(r)\equiv C^{\pm}\hat{R}^{\pm}(r), \tag{5.5.23}$$

which we will use later for a separate purpose.

We solve Eq. (5.5.16) in a series of steps. We start by computing the particular solutions.

- Set a boundary condition at large, positive r_* of [noting Eq. (5.5.17)] $\tilde{\xi}_p^{\infty} = A^+ r e^{i\omega_{mn} r_*}$. Integrate the inhomogeneous equation (5.5.16), through the source libration region [using Eq. (5.5.22) in the source] to large, negative r_*. At this point it will be of the form [noting Eq. (5.5.19)] $\tilde{\xi}_p^{\infty} = A^- f e^{-i\omega_{mn} r_*} - \kappa^+ e^{i\omega_{mn} r_*} - \kappa^- e^{-i\omega_{mn} r_*}$.

- Set a boundary condition at large, negative r_* of $\tilde{\xi}_p^{H} = A^- f e^{-i\omega_{mn} r_*}$. Integrate the inhomogeneous equation (5.5.16), through the source libration region [using Eq. (5.5.22) in the source] to large, positive r_*. At this point it will be of the form $\tilde{\xi}_p^{H} = A^+ r e^{i\omega_{mn} r_*} - \lambda^- e^{-i\omega_{mn} r_*} - \lambda^+ e^{i\omega_{mn} r_*}$.

In order to find a solution with the correct causal behavior, we must add homogeneous solutions to these particular solutions.

- Set a boundary condition at large, positive r_* of $\tilde{\xi}_h^{+} \approx T e^{i\omega_{mn} r_*}$. Integrate the homogeneous version of Eq. (5.5.16) to large, negative r_*. At this point it will be of the form $\tilde{\xi}_h^{+} \approx R e^{-i\omega_{mn} r_*} + e^{i\omega_{mn} r_*}$. Note that if we set the boundary condition with unit amplitude we have on the large r_* side $\tilde{\xi}_h^{+} \approx e^{i\omega_{mn} r_*}$, and on the horizon side $\tilde{\xi}_h^{+} \approx (R/T) e^{-i\omega_{mn} r_*} + (1/T) e^{i\omega_{mn} r_*}$. Here R and T are reflection and transmission amplitudes, respectively [71].

- Set a boundary condition at large, negative r_* of $\tilde{\xi}_h^{-} \approx T^* e^{-i\omega_{mn} r_*}$. Integrate the homogeneous version of Eq. (5.5.16) to large, positive r_*. At this point it will be of the form $\tilde{\xi}_h^{-} \approx R^* e^{i\omega_{mn} r_*} + e^{-i\omega_{mn} r_*}$. Note that if we set the boundary condition with unit amplitude we have on the horizon side $\tilde{\xi}_h^{-} \approx e^{-i\omega_{mn} r_*}$, and on the large r_* side $\tilde{\xi}_h^{-} \approx (R^*/T^*) e^{i\omega_{mn} r_*} + (1/T^*) e^{-i\omega_{mn} r_*}$.

Now, we wish to cancel out the acausal pieces of the particular solutions. Therefore, we form $\tilde{\xi}^{\infty} = \tilde{\xi}_p^{\infty} + \kappa^+ \tilde{\xi}_h^{+}$. In the two asymptotic regions this is

$$\tilde{\xi}^{+} \approx C^+ r e^{i\omega_{mn} r_*} + \kappa^+ T e^{i\omega_{mn} r_*} \qquad r_* \to +\infty, \tag{5.5.24}$$

$$\tilde{\xi}^{+} \approx C^- f e^{-i\omega_{mn} r_*} - \kappa^- e^{-i\omega_{mn} r_*} + R e^{-i\omega_{mn} r_*} \qquad r_* \to -\infty. \tag{5.5.25}$$

On the horizon side, we form $\tilde{\xi}^H = \tilde{\xi}_p^H + \lambda^- \tilde{\xi}_h^-$. In the two asymptotic regions this is

$$\tilde{\xi}^- \approx C^- f e^{-i\omega_{mn} r_*} + \lambda^- T^* e^{-i\omega_{mn} r_*} \qquad r_* \to -\infty, \tag{5.5.26}$$

$$\tilde{\xi}^- \approx C^+ r e^{i\omega_{mn} r_*} - \lambda^+ e^{i\omega_{mn} r_*} + R^* e^{i\omega_{mn} r_*} \qquad r_* \to +\infty. \tag{5.5.27}$$

Now, we have two solutions to the differential equation that both satisfy the causal nature of the problem. Therefore they must be equal, so we set them, with their derivatives, equal at any point,

$$\tilde{\xi}_p^H + \lambda^- \tilde{\xi}_h^- = \tilde{\xi}_p^\infty + \kappa^+ \tilde{\xi}_h^+ \tag{5.5.28}$$

$$\partial_{r_*} \tilde{\xi}_p^H + \lambda^- \partial_{r_*} \tilde{\xi}_h^- = \partial_{r_*} \tilde{\xi}_p^\infty + \kappa^+ \partial_{r_*} \tilde{\xi}_h^+. \tag{5.5.29}$$

Solving these equations for κ^+ and λ^- we find

$$\kappa^+ = -\frac{1}{W_h} \left[\left(\partial_{r_*} \tilde{\xi}_p^\infty - \partial_{r_*} \tilde{\xi}_p^H \right) \tilde{\xi}_h^- + \left(\tilde{\xi}_p^H - \tilde{\xi}_p^\infty \right) \partial_{r_*} \tilde{\xi}_h^- \right], \tag{5.5.30}$$

$$\lambda^- = -\frac{1}{W_h} \left[\left(\partial_{r_*} \tilde{\xi}_p^\infty - \partial_{r_*} \tilde{\xi}_p^H \right) \tilde{\xi}_h^+ + \left(\tilde{\xi}_p^H - \tilde{\xi}_p^\infty \right) \partial_{r_*} \tilde{\xi}_h^+ \right], \tag{5.5.31}$$

where

$$W_h \equiv \tilde{\xi}_h^- \partial_{r_*} \tilde{\xi}_h^+ - \tilde{\xi}_h^+ \partial_{r_*} \tilde{\xi}_h^-. \tag{5.5.32}$$

The constants κ^+ and λ^- tell us how to scale our homogeneous solutions so we can enforce causality. The functions $\tilde{\xi}_p^H + \lambda^- \tilde{\xi}_h^-$ and $\tilde{\xi}_p^\infty + \kappa^+ \tilde{\xi}_h^+$ (which are entirely equivalent), represent the standard solution to Eq. (5.5.16). If our TD source were differentiable everywhere, we would be able to take this solution back to the TD with an exponentially converging Fourier synthesis. However, given our source's lack of differentiability, we must use a different method to obtain exponential convergence in the transition to the TD.

We define the FD EPS of Eq. (5.5.16) to be $\tilde{\xi}_p^\pm$. They are found by integrating Eq. (5.5.16) the source term $R_{\mathrm{RW}}^{\mathrm{EHS}}$, given in Eq. (5.5.23). The EPS are made causally

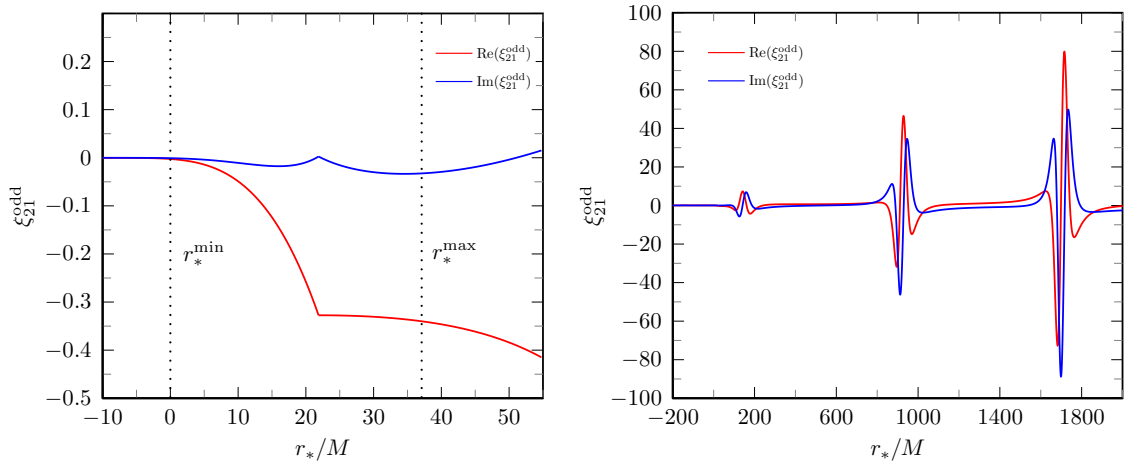

Figure 5.3: The odd-parity RW $\rightarrow$ Lorenz gauge generator amplitude $\xi^{\rm odd}_{21}$. This differs from the Lorenz gauge metric amplitude h_2^{21} (where the ^{21} are ℓ, m indices on the amplitude h_2) by a factor of -2. Note that the field h_2^{21} grows asymptotically because it is a metric perturbation amplitude on the two-sphere, where an extra factor of r^2 is present in spherical coordinates. Transforming to an orthonormal frame would produce a field which falls off like $1/r$, as radiation.

correct by adding the correctly scaled homogeneous solutions, which define

$$\tilde{\xi}^{+} \equiv \tilde{\xi}^{+}_{p} + \kappa^{+}\tilde{\xi}^{+}_{h} \qquad \tilde{\xi}^{-} \equiv \tilde{\xi}^{-}_{p} + \lambda^{-}\tilde{\xi}^{-}_{h}. \tag{5.5.33}$$

When we return to the TD, we define

$$\xi^{\pm} \equiv \sum_{n} \tilde{\xi}^{\pm} e^{-i\omega_{mn}t}. \tag{5.5.34}$$

And we claim the true solution to Eq. (5.5.3) is the weak solution,

$$\xi(t,r) = \xi^{+}\theta\left[r - r_p(t)\right] + \xi^{-}\theta\left[r_p(t) - r\right]. \tag{5.5.35}$$

We have used this solution to obtain the exact same solutions as those given by the partial annihilator method. These results are shown in Figs. 5.3, 5.4, and 5.5.

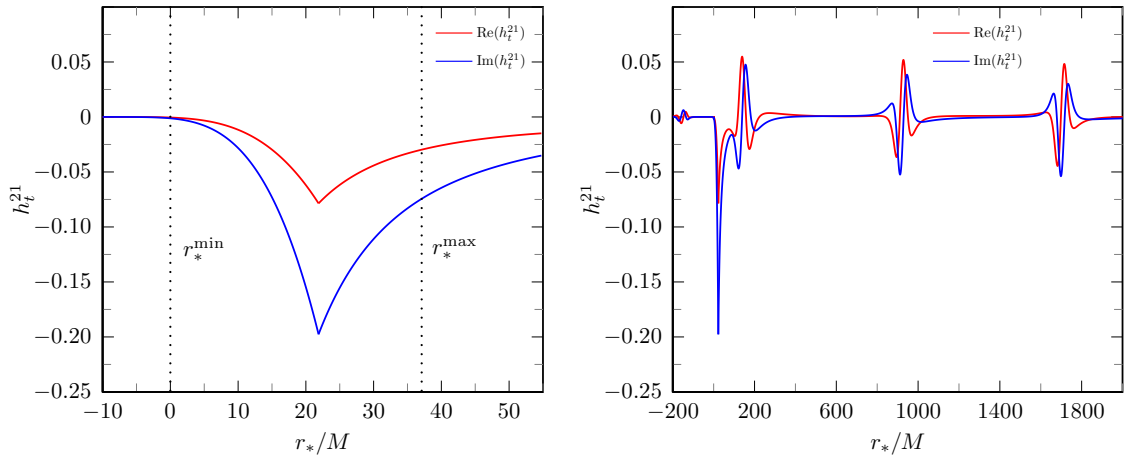

Figure 5.4: The Lorenz gauge metric perturbation amplitude h_t^{21}. Note (comparing to Fig. 5.1) the discontinuity at the location of the particle has vanished and the wave is not asymptotically flat. Note that the amplitude h_t^{21} is an off-diagonal element of the metric perturbation, which introduces an extra factor of r in Schwarzschild coordinates. Transforming to an orthonormal frame would produce a field which falls off like $1/r$, as radiation.

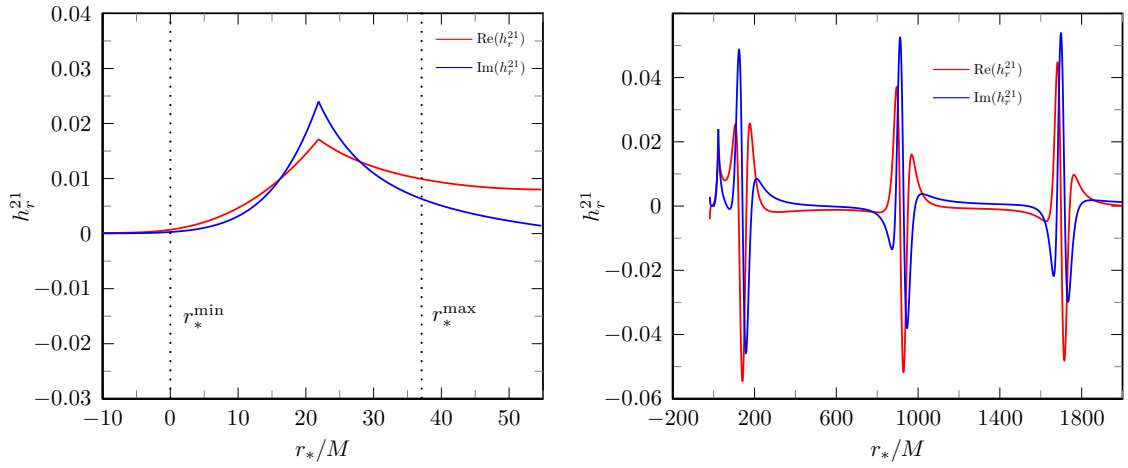

Figure 5.5: The Lorenz gauge metric perturbation amplitude h_r^{21}. Note (comparing to Fig. 5.2) the discontinuity at the location of the particle has vanished and the wave is not asymptotically flat. Note that the amplitude h_r^{21} is an off-diagonal element of the metric perturbation, which introduces an extra factor of r in Schwarzschild coordinates. Transforming to an orthonormal frame would produce a field which falls off like $1/r$, as radiation.

5.6 Even-parity gauge generator

5.6.1 Scalar part

The pair of equations (5.3.23) and (5.3.24) each have a curved space wave operator acting on a scalar. This yields the Regge-Wheeler spin-0 operator, which gives

$$\left[-\frac{1}{f}\partial_t^2+\frac{1}{r^2}\partial_r\left(r^2 f\partial_r\right)+\frac{1}{r^2\sin\theta}\partial_\theta\left(\sin\theta\ \partial_\theta\right)+\frac{1}{r^2\sin^2\theta}\partial_\phi^2\right]\Xi_{\text{even}(s)}=J_{\text{even}(s)}, \tag{5.6.1}$$

$$\left[-\frac{1}{f}\partial_t^2+\frac{1}{r^2}\partial_r\left(r^2 f\partial_r\right)+\frac{1}{r^2\sin\theta}\partial_\theta\left(\sin\theta\ \partial_\theta\right)+\frac{1}{r^2\sin^2\theta}\partial_\phi^2\right]J_{\text{even}(s)}={}^4\nabla_\mu\,{}^4\nabla_\nu\bar{p}^{\mu\nu}_{\text{even}}. \tag{5.6.2}$$

We decompose $\Xi_{\text{even}(s)}$ and $J_{\text{even}(s)}$ in scalar spherical harmonics,

$$\Xi_{\text{even}(s)}=\sum_{\ell,m}\frac{1}{r}\xi^{\ell m}_{\text{even}(s)}(t,r)Y_{\ell m}\left(\theta,\phi\right), \qquad J_{\text{even}(s)}=\sum_{\ell,m}\frac{1}{r}j^{\ell m}_{\text{even}(s)}(t,r)Y_{\ell m}\left(\theta,\phi\right). \tag{5.6.3}$$

We have already computed one divergence of $\bar{p}^{\mu\nu}$. To take the second, we need the divergence of a vector V^μ,

$${}^4\nabla^\mu V_\mu=g^{ab}V_{b|a}+g^{AB}V_{B|A}, \tag{5.6.4}$$

where the stroke (|) is the full, four dimensional covariant derivative on the background manifold. The connection terms it creates sum over all four spacetime indices. In the Martel and Poisson [55] formalism the expression expands to

$${}^4\nabla^\mu V_\mu=g^{ab}\nabla_a V_b+g^{AB}\left(D_A V_B+\frac{1}{r}r^b V_b g_{AB}\right), \tag{5.6.5}$$

Using this, the second divergence of $\bar{p}^{\mu\nu}$ is (with implied ℓ, m and a summation)

$$\begin{aligned}{}^4\nabla_\mu\,{}^4\nabla_\nu\bar{p}^{\mu\nu}=\Bigg[&-\frac{1}{2}\Box Q^\sharp-\frac{2}{r}\partial_t h_{tr}+2\frac{f^2}{r}\partial_r h_{rr}-f\partial_r K\\&+\frac{2}{f}\frac{M}{r^3}h_{tt}+\left(6f\frac{M}{r^3}+\frac{2f^2}{r^2}\right)h_{rr}-\left(\frac{4}{r^2}f+\frac{2M}{r^2}\right)K-\frac{2M}{r^3}Q^\sharp-Q^\flat\Bigg]Y\equiv S.\end{aligned} \tag{5.6.6}$$

Plugging in these expansions, we use the orthonormality of the spherical harmonics to write

$$\left[-\frac{1}{f}\frac{\partial^2}{\partial t^2}+\frac{\partial}{\partial r}\left(f\frac{\partial}{\partial r}\right)-\left(\frac{2(\lambda+1)}{r^2}+\frac{2M}{r^3}\right)\right]\xi_{\text{even}(s)}=j_{\text{even}(s)}, \tag{5.6.7}$$

$$\frac{1}{r}\left[-\frac{1}{f}\frac{\partial^2}{\partial t^2}+\frac{\partial}{\partial r}\left(f\frac{\partial}{\partial r}\right)-\left(\frac{2(\lambda+1)}{r^2}+\frac{2M}{r^3}\right)\right]j_{\text{even}(s)}=S. \tag{5.6.8}$$

After further simplification, the source term becomes

$$S=f\mathcal{W}_0K+S_{\text{sing}},\qquad \mathcal{W}_0\equiv-\frac{\partial^2}{\partial t^2}+\frac{\partial^2}{\partial r_*^2}-V_0,\qquad V_0\equiv f\left(\frac{2(\lambda+1)}{r^2}+\frac{2M}{r^3}\right), \tag{5.6.9}$$

where we have combined all the singular terms together into S_{sing}. Then we can combine the two differential equations into one fourth-order expression,

$$\mathcal{W}_0\left(\frac{1}{rf}\mathcal{W}_0\xi_{\text{even}(s)}\right)=f\mathcal{W}_0K+S_{\text{sing}}, \tag{5.6.10}$$

Given our definition of K in terms of the master function, we get

$$\mathcal{W}_0K(t,r)=\alpha(r)\Psi(t,r)+\beta(r)\frac{d\Psi(t,r)}{dr_*}+\tilde{G}_K(t)\delta(z)+\tilde{F}_K(t)\delta'(z), \tag{5.6.11}$$

where

$$\begin{aligned}\alpha(r)&=-2\frac{f}{r^6\Lambda}\Big(\lambda(\lambda+1)r^3+\lambda M\left(\lambda+1\right)r^2+3M^2\left(3\lambda-1\right)r+24M^3\Big),\\ \beta(r)&=-2\frac{f^2}{r^3}\Big(r\left(\lambda+1\right)+4M\Big),\end{aligned} \tag{5.6.12}$$

and $\tilde{G}_K\delta(z)+\tilde{F}_K\delta'(z)$ get absorbed into S_{sing}.

The S_{sing} term can be found by using fourth order EHS. For the remainder of this section we focus on solving the part of the equation with the extended source. Additionally, for the remainder of this section we will suppress the $_{\text{even},s}$ tags.

At this point we are ready to solve Eq. (5.6.10) using the EPS method. Neglecting the singular terms and moving to the FD gives

$$\mathcal{L}_0\frac{1}{rf}\mathcal{L}_0\tilde{\xi}=\alpha(r)R+\beta(r)\frac{dR}{dr_*},\qquad \mathcal{L}_0\equiv\frac{d^2}{dr_*^2}+\omega_{mn}^2-V_0. \tag{5.6.13}$$

We first need the particular solutions to this equation. The boundary conditions for these particular solutions are given in App. 5.B.2. On the right side of Eq. (5.6.13) there are two different forms of R which we consider. The first is the standard solution, which we denote as

$$R_{\rm ZM}(r) = c^+(r)\hat{R}^+(r) + c^-(r)\hat{R}^-(r), \tag{5.6.14}$$

and the second is the pair of EHS

$$R^\pm(r) = C^\pm \hat{R}^\pm(r). \tag{5.6.15}$$

Therefore, there will be two different particular solutions we can compute. We denote them by

$$\tilde{\xi}_p^H, \tilde{\xi}_p^\infty \Longleftrightarrow R_{\rm ZM}, \qquad \tilde{\xi}_p^-, \tilde{\xi}_p^+ \Longleftrightarrow R^\pm. \tag{5.6.16}$$

To simplify solving the fourth-order equation (5.6.13), we make the following definitions

$$u \equiv \frac{1}{\omega_{mn}}\frac{d\tilde{\xi}}{dr_*}, \qquad v \equiv \frac{1}{\omega_{mn}^3}\frac{1}{rf}\left[\omega_{mn}\frac{du}{dr_*} + \left(\omega_{mn}^2 - V_0\right)\tilde{\xi}\right], \qquad w \equiv \frac{1}{\omega_{mn}}\frac{dv}{dr_*}. \tag{5.6.17}$$

In addition to the particular solutions to Eq. (5.6.13), there are the homogeneous solutions as well. There are two on the horizon side; one is annihilated by the second order operator, and the other is annihilated by the full fourth-order operator. Respectively, these are $\tilde{\xi}_{h2}^-$ and $\tilde{\xi}_{h4}^-$. Similarly, there are two on the infinity side, which we denote as $\tilde{\xi}_{h2}^+$ and $\tilde{\xi}_{h4}^+$. Now, in order to get the causally appropriate solution, we must add homogeneous solutions. On the two sides we have

$$\tilde{\xi}^H = \tilde{\xi}_p^H + \lambda_{h2}^-\tilde{\xi}_{h2}^- + \lambda_{h4}^-\tilde{\xi}_{h4}^-, \qquad \tilde{\xi}^\infty = \tilde{\xi}_p^\infty + \kappa_{h2}^+\tilde{\xi}_{h2}^+ + \kappa_{h4}^+\tilde{\xi}_{h4}^+. \tag{5.6.18}$$

Removing the acausal pieces is equivalent to demanding these two solutions and their three

derivatives be identical. The four conditions are

$$\tilde{\xi}_p^H + \lambda_{h2}^- \tilde{\xi}_{h2}^- + \lambda_{h4}^- \tilde{\xi}_{h4}^- = \tilde{\xi}_p^\infty + \kappa_{h2}^+ \tilde{\xi}_{h2}^+ + \kappa_{h4}^+ \tilde{\xi}_{h4}^+, \tag{5.6.19}$$

$$\frac{1}{\omega_{mn}} \frac{d}{dr_*} \left(\tilde{\xi}_p^{s,H} + \lambda_{h2}^- \tilde{\xi}_{h2}^- + \lambda_{h4}^- \tilde{\xi}_{h4}^- \right) = \frac{1}{\omega_{mn}} \frac{d}{dr_*} \left(\tilde{\xi}_p^{s,\infty} + \kappa_{h2}^+ \tilde{\xi}_{h2}^+ + \kappa_{h4}^+ \tilde{\xi}_{h4}^+ \right), \tag{5.6.20}$$

and

$$v_p^H + \lambda_{h2}^- v_{h2}^- + \lambda_{h4}^- v_{h4}^- = v_p^\infty + \kappa_{h2}^+ v_{h2}^+ + \kappa_{h4}^+ v_{h4}^+, \tag{5.6.21}$$

$$\frac{1}{\omega_{mn}} \frac{d}{dr_*} \left(v_p^H + \lambda_{h2}^- v_{h2}^- + \lambda_{h4}^- v_{h4}^- \right) = \frac{1}{\omega_{mn}} \frac{d}{dr_*} \left(v_p^\infty + \kappa_{h2}^+ v_{h2}^+ + \kappa_{h4}^+ v_{h4}^+ \right). \tag{5.6.22}$$

Note that for the second-order equations $v_{h4}^\pm = w_{h4}^\pm = 0$, so in matrix form

$$\begin{bmatrix} v_{h4}^- & -v_{h4}^+ \\ w_{h4}^- & -w_{h4}^+ \end{bmatrix} \begin{bmatrix} \lambda_{h4}^- \\ \kappa_{h4}^+ \end{bmatrix} = \begin{bmatrix} v_p^\infty - v_p^H \\ w_p^\infty - w_p^H \end{bmatrix}, \tag{5.6.23}$$

$$\begin{bmatrix} \tilde{\xi}_{h2}^- & -\tilde{\xi}_{h2}^+ \\ u_{h2}^- & -u_{h2}^+ \end{bmatrix} \begin{bmatrix} \lambda_{h2}^- \\ \kappa_{h2}^+ \end{bmatrix} = \begin{bmatrix} \tilde{\xi}_p^{s,\infty} - \tilde{\xi}_p^{s,H} \\ u_p^\infty - u_p^H \end{bmatrix} - \begin{bmatrix} \tilde{\xi}_{h4}^- & -\tilde{\xi}_{h4}^+ \\ u_{h4}^- & -u_{h4}^+ \end{bmatrix} \begin{bmatrix} \lambda_{h4}^- \\ \kappa_{h4}^+ \end{bmatrix}. \tag{5.6.24}$$

We use Cramer's rule to solve Eq. (5.6.23) for λ_{h4}^- and κ_{h4}^+. Then, the right side of Eq. (5.6.24) boils down to one column vector, and we solve for the remaining two unknowns λ_{h2}^- and κ_{h2}^+.

At this point we have the coefficients to scale the homogeneous solutions properly. Then, the standard solution to Eq. (5.6.13) is either of the (equivalent) expressions in Eq. (5.6.18). This solution can be returned to the TD by using the standard Fourier synthesis. However, as expected, it will exhibit Gibbs behavior. This can be circumvented by using the EPS method, wherein we form

$$\tilde{\xi}^- = \tilde{\xi}_p^- + \lambda_{h2}^- \tilde{\xi}_{h2}^- + \lambda_{h4}^- \tilde{\xi}_{h4}^-, \qquad \tilde{\xi}^+ = \tilde{\xi}_p^+ + \kappa_{h2}^+ \tilde{\xi}_{h2}^+ + \kappa_{h4}^+ \tilde{\xi}_{h4}^+, \tag{5.6.25}$$

which we return to the TD through the Fourier sum,

$$\xi^{\pm}_{\text{even}(s)}(t,r) = \sum_n \tilde{\xi}^{\pm}(r) e^{-i\omega_{mn}t}. \tag{5.6.26}$$

Then, the weak form of the solution to Eq. (5.6.10) (without the singular term) is

$$\xi_{\text{even}(s)}(t,r) = \xi^{+}_{\text{even}(s)}(t,r)\ \theta\left[r - r_p(t)\right] + \xi^{-}_{\text{even}(s)}(t,r)\ \theta\left[r_p(t) - r\right]. \tag{5.6.27}$$

5.6.2 Divergence-free vector part

We briefly provide here an outline of the remaining task of solving for the divergence-free part of the even-parity gauge generator. We start by defining the antisymmetric gradient

$$F^{\mu\nu} \equiv {}^4\nabla^{\mu}\xi^{\nu}_{\text{even}(v)} - {}^4\nabla^{\nu}\xi^{\mu}_{\text{even}(v)}. \tag{5.6.28}$$

Then, taking the divergence we have

$$F^{\mu\nu}{}_{|\nu} = -{}^4\nabla_{\nu}\,{}^4\nabla^{\nu}\xi^{\mu}_{\text{even}(v)} = -J^{\mu}_{\text{even}(v)}, \tag{5.6.29}$$

where we have used the vanishing of $R_{\mu\nu}$ on the background to commute the covariant derivatives and applied the divergence-free property of $\Xi^{\mu}_{\text{even}(v)}$. The source term $J_{\text{even}(v)}$ is given previously in Eq. (5.3.26). Now, we recognize Eq. (5.6.29) as analogous to the Maxwell equations. The approach of SNS [54] is to apply the Newman-Penrose formalism to decompose Eq. (5.6.29) to find two separate equations for the tetrad scalars ϕ_0 and ϕ_2. Then a final second-order wave equation must be solved to find the spherical harmonic amplitudes of $\Xi^{\mu}_{\text{even}(v)}$. The equations all decouple, and the price we have to pay is more equations to solve. We see no outstanding issues with being able to straightforwardly apply our new methods to solve these remaining equations numerically.

5.7 Conclusion

At this point, we have finished the gauge transformation for the odd-parity sector and for the even-parity scalar part. Results for the odd-parity can be seen in Figs. 5.3, 5.4 and 5.5. Note that the gauge transformation removes the jump at the particle's location and corrects the asymptotic behavior, leaving it flat. In solving these equations we developed two new techniques, the method of partial annihilators, and the method of extended particular solutions, which are entirely equivalent. Results for the even-parity divergent-free vector part are forthcoming.

Following completion of the gauge transformation, the stage will be set for self-force calculations. We will be able to compute conservative shifts in gauge-invariant quantities such as the energy, angular momentum and generalized redshift invariant. Some of these have already been computed in the time domain. We should be able to add significantly more accuracy with our frequency domain based approach.

5.A Gauge transformation of metric perturbation amplitudes

Once the gauge vector is found by solving the equations laid out in this chapter, the metric perturbation is pushed to a new gauge via Eq. (5.3.2). This equation can be decomposed into spherical harmonics, at which point it reveals how the metric perturbation amplitudes are pushed under a gauge transformation. The even-parity amplitudes change as (e.g.

$h^{\rm L}_{tt} = h^{\rm RW}_{tt} + \Delta h_{tt}$)

$$
\begin{aligned}
\Delta h_{tt} &= -2\partial_t \xi_t + f\frac{2M}{r^2}\xi_r, \\
\Delta h_{tr} &= -\partial_r \xi_t - \partial_t \xi_r + \frac{2M}{fr^2}\xi_t, \\
\Delta h_{rr} &= -2\partial_r \xi_r - \frac{2M}{fr^2}\xi_r, \\
\Delta j_t &= -\partial_t \xi_{\rm even} - \xi_t, \\
\Delta j_r &= -\partial_r \xi_{\rm even} - \xi_r + \frac{2}{r}\xi_{\rm even}, \\
\Delta K &= -\frac{2f}{r}\xi_r + \frac{2(\lambda+1)}{r^2}\xi_{\rm even}, \\
\Delta G &= -\frac{2}{r^2}\xi_{\rm even}.
\end{aligned}
\tag{5.A.1}
$$

The odd-parity amplitudes change as (e.g. $h^{\rm L}_t = h^{\rm RW}_t + \Delta h_t$)

$$
\begin{aligned}
\Delta h_t &= -\frac{\partial \xi_{\rm odd}}{\partial t}, \\
\Delta h_r &= -\frac{\partial \xi_{\rm odd}}{\partial r} + \frac{2}{r}\xi_{\rm odd}, \\
\Delta h_2 &= -2\xi_{\rm odd}.
\end{aligned}
\tag{5.A.2}
$$

Note that ℓ, m indices are suppressed in these expressions.

5.B Asymptotic expansions and boundary conditions

In this appendix we present boundary conditions necessary for starting numerical integrations. On the large r side this involves asymptotic expansions. On the horizon side we can perform a convergent Taylor expansion, but because the potential falls off exponentially, in practice it is only necessary go to a moderately large and negative r_* and find an appropriate scaling factor.

5.B.1 Boundary conditions for the odd-parity gauge generator amplitude

We need an asymptotic expansion in order to set the appropriate boundary conditions for $\tilde{\xi}_{\rm odd}$. For the particular solution, we start by writing the asymptotic form of $\tilde{\xi}_{\rm odd}$

as $rJ_\xi(r)e^{i\omega_{mn}r_*}$. Given that we expect $R_{\rm CPM}$ (note that $R_{\rm CPM}$ and $R_{\rm RW}$ are related asymptotically by a factor of $-i\omega_{mn}/2$) to go like $J_R(r)e^{i\omega_{mn}r_*}$, we plug in to Eq. (5.5.16) and obtain

$$rf\frac{d^2}{dr^2}J_\xi + 2\left[1 + i\omega_{mn}r - \frac{M}{r}\right]\frac{d}{dr}J_\xi + \left[2i\omega_{mn} + \frac{2M}{r^2} - \frac{\ell(\ell+1)}{r}\right]J_\xi = -i\omega_{mn}J_R \quad \text{(5.B.1)}$$

Now, we change to the dimensionless variables, $z \equiv \omega_{mn}r$ and $\sigma \equiv M\omega_{mn}$, which changes the differential equation to

$$(z-2\sigma)\frac{d^2}{dz^2}J_\xi + 2\left(iz + 1 - \frac{\sigma}{z}\right)\frac{d}{dz}J_\xi + \left(2i + \frac{2\sigma}{z^2} - \frac{\ell(\ell+1)}{z}\right)J_\xi = -iJ_R \qquad \text{(5.B.2)}$$

Now, we assume the following forms of J_ξ, and J_R,

$$J_\xi(r) = \sum_{j=0}^{\infty}\frac{a_j^\xi}{z^j}, \qquad J_R(r) = \sum_{j=0}^{\infty}\frac{a_j^R}{z^j}. \qquad \text{(5.B.3)}$$

Plugging these in and assuming the equation is satisfied order-by-order gives the inhomogeneous recurrence formula

$$2i(j-1)a_j^\xi = \Big[(j-2)(j-1) - \ell(\ell+1)\Big]a_{j-1}^\xi + 2\sigma\Big[1-(j-2)^2\Big]a_{j-2}^\xi + ia_j^R. \qquad \text{(5.B.4)}$$

Note that the coefficients a_j^R are found in Eq. (4.D.5).

On the horizon side, where the potential falls away exponentially, it is enough to use the expression in Eq. (5.5.19) and a sufficiently negative r_* starting location for integration.

5.B.2 Boundary conditions for the even-parity scalar gauge generator amplitude

We need boundary conditions for the particular solution as well as the two homogeneous solutions.

Second-order homogeneous solutions

For the second-order homogeneous solutions, at large r we assume a form of $\tilde{\xi}_{\text{even}(s)}$ of $J_\xi(r)e^{i\omega_{mn}r_*}$. Then we get (in terms of the dimensionless variables defined above)

$$\left(1-\frac{2\sigma}{z}\right)\frac{d^2J_\xi}{dz^2}+\left(\frac{2\sigma}{z^2}+2i\right)\frac{dJ_\xi}{dz}-\left(2\frac{\lambda+1}{z^2}+\frac{2\sigma}{z^3}\right)J_\xi=0. \tag{5.B.5}$$

Assuming a form of

$$J_\xi(r)=\sum_{j=0}^{\infty}\frac{a_j^\xi}{z^j}, \tag{5.B.6}$$

we find

$$2ija_j^\xi=\Big[j(j-1)-2(\lambda+1)\Big]a_{j-1}^\xi-2\sigma(j-1)^2a_{j-2}^\xi. \tag{5.B.7}$$

On the horizon side, the boundary condition is the typical $\tilde{\xi}_{\text{even}(s)}=e^{-i\omega_{mn}r_*}$, and an expansion is not necessary.

Fourth-order homogeneous solutions

For the fourth-order homogeneous solutions, we make the assumptions $\xi_{\text{even}(s)}=J_\xi(r)e^{i\omega_{mn}r_*}$ and $v=J_v(r)e^{i\omega_{mn}r_*}$. These satisfy the two equations,

$$\left(1-\frac{2\sigma}{z}\right)\frac{d^2J_\xi}{dz^2}+\left(\frac{2\sigma}{z^2}+2i\right)\frac{dJ_\xi}{dz}-\left(2\frac{\lambda+1}{z^2}+\frac{2\sigma}{z^3}\right)J_\xi=zJ_v, \tag{5.B.8}$$

$$\left(1-\frac{2\sigma}{z}\right)\frac{d^2J_v}{dz^2}+\left(\frac{2\sigma}{z^2}+2i\right)\frac{dJ_v}{dz}-\left(2\frac{\lambda+1}{z^2}+\frac{2\sigma}{z^3}\right)J_v=0 \tag{5.B.9}$$

The equation for J_v is exactly the same as that for J_ξ Eq. (5.B.5). Therefore, it will have the same expansion,

$$J_v(r)=\sum_{j=0}^{\infty}\frac{a_j^v}{z^j},\qquad 2ija_j^v=\Big[j(j-1)-2(\lambda+1)\Big]a_{j-1}^v-2\sigma(j-1)^2a_{j-2}^v. \tag{5.B.10}$$

This serves as a source to the J_ξ equation, (5.B.8). Assuming a form of

$$J_\xi = \sum_{j=0} \frac{a_j^\xi}{z^{j-2}} + \sum_{j=0} \frac{b_j^\xi}{z^{j-2}} \ln(z), \tag{5.B.11}$$

we find the coupled recurrences

$$2i(j-2)b_j^\xi - \Big[(j-2)(j-3) - 2(\lambda+1)\Big] b_{j-1}^\xi + 2\sigma(j-3)^2 b_{j-2}^\xi = 0, \tag{5.B.12}$$

and

$$\begin{aligned} 2i(j-2)a_j^\xi - \Big[(j-2)(j-3) - 2(\lambda+1)\Big] a_{j-1}^\xi + 2\sigma(j-3)^2 a_{j-2}^\xi \\ - 2ib_j^\xi - (-2j+5)\, b_{j-1}^\xi - 4\sigma(j-3) b_{j-2}^\xi + a_j^v = 0. \end{aligned} \tag{5.B.13}$$

Note that the $\ln(z)$ term is necessary as the indicial equation for this asymptotic expansion has two roots, with the indicial exponents differing by an integer. In these circumstances [93] a single expansion of the Frobenius type is insufficient.

On the horizon side we do not need to perform an expansion because the potential falls off exponentially. There, we set

$$\xi_{\text{even}(s)} = \frac{8M^3\omega_{mn}^3}{1-4i\omega_{mn}M} f e^{-i\omega_{mn}r_*}, \qquad v = e^{-i\omega_{mn}r_*}. \tag{5.B.14}$$

Particular solutions

For the particular solutions we make the assumptions $\xi_{\text{even}(s)} = J_\xi(r)e^{i\omega_{mn}r_*}$, and $v = J_v(r)e^{i\omega_{mn}r_*}$ and we have the equations

$$\left(1-\frac{2\sigma}{z}\right)\frac{d^2J_\xi}{dz^2} + \left(\frac{2\sigma}{z^2}+2i\right)\frac{dJ_\xi}{dz} - \left(2\frac{\lambda+1}{z^2}+\frac{2\sigma}{z^3}\right)J_\xi = zJ_v, \tag{5.B.15}$$

$$\begin{aligned} \left(1-\frac{2\sigma}{z}\right)\frac{d^2J_v}{dz^2} + \left(\frac{2\sigma}{z^2}+2i\right)\frac{dJ_v}{dz} - \left(2\frac{\lambda+1}{z^2}+\frac{2\sigma}{z^3}\right)J_v \\ = \frac{1}{\omega_{mn}^5 f(z)}\Big(\alpha + i\omega_{mn}\beta\Big)J_R + \frac{\beta}{\omega_{mn}^4}\frac{dJ_R}{dz}, \end{aligned} \tag{5.B.16}$$

where α and β are given in Eq. (5.6.12). We assume the following forms for the three unknowns

$$J_R = \sum_{j=0} \frac{a_j^R}{z^j}, \qquad J_\xi = \sum_{j=0} \frac{a_j^\xi}{z^{j-1}} + \sum_{j=0} \frac{b_j^\xi}{z^{j-1}} \ln(z), \qquad J_v = \sum_{j=0} \frac{a_j^v}{z^{j+1}}. \tag{5.B.17}$$

The recurrence for the coefficients a_j^R is given in Eq. (4.D.4). Plugging in these summations leads to the coupled recurrences

$$2i(j-1)b_j^\xi - \Big[(j-1)(j-2) - 2(\lambda+1)\Big] b_{j-1}^\xi + 2\sigma(j-2)^2 b_{j-2}^\xi = 0, \tag{5.B.18}$$

$$\begin{aligned} 2i(j-1)a_j^\xi - \Big[(j-1)(j-2) - 2(\lambda+1)\Big] a_{j-1}^\xi + 2\sigma(j-2)^2 a_{j-2}^\xi \\ - 2ib_j^\xi - (-2j+3)\, b_{j-1}^\xi - 4\sigma(j-2) + a_j^v = 0, \end{aligned} \tag{5.B.19}$$

and

$$\begin{aligned} &2i\lambda(j+1)a_j^v - \Big(\lambda j(j+1) - 6i\sigma j - 2\lambda(\lambda+1)\Big) a_{j-1}^v \\ &\quad - \Big((3-2\lambda)\sigma j(j-1) - 2\sigma\lambda(j-1) - (8\lambda+6)\sigma\Big) a_{j-2}^v + 6\sigma^2(j-1)^2 a_{j-3}^v \\ &\quad + \Big[-2i\lambda(\lambda+1)a_j^R + \Big(-2\lambda(\lambda+1) + 2i(2\lambda+1)(\lambda-3)\sigma + 2\lambda(\lambda+1)(j-1)\Big) a_{j-1}^R \\ &\qquad + \Big(-2\lambda\,(\lambda+1)\,\sigma + 4i\,(7\lambda-3)\,\sigma^2 + 2(-4\lambda^2+3\lambda+3)\sigma(j-2)\Big) a_{j-2}^R \\ &\qquad\quad + \Big(-6\,(3\lambda-1)\,\sigma^2 + 48i\sigma^3 + 8\lambda(\lambda-6)\sigma^2(j-3)\Big) a_{j-3}^R \\ &\qquad + \Big(-48\sigma^3 + 8(7\lambda-9)\sigma^3(j-4)\Big) a_{j-4}^R + 96\sigma^4(j-5)a_{j-5}^R \Big] \frac{1}{\omega_{mn}^2} = 0. \end{aligned} \tag{5.B.20}$$

Note that a $\ln(z)$ term is again necessary.

On the horizon side we do not need to perform an expansion because the potential falls off exponentially. By analyzing the horizon side nature of the source, we see that the

particular solution has leading order behavior

$$\xi_{\text{even}(s)} = -\frac{3\left(\lambda+1\right)}{\left(1-4Mi\omega_{mn}\right)}\frac{M^2}{\left(1-2Mi\omega_{mn}\right)}f^2 e^{-i\omega_{mn}r_*}, \tag{5.B.21}$$

$$v = -\frac{3\left(\lambda+1\right)}{2M\omega_{mn}^3\left(1-4Mi\omega_{mn}\right)}f e^{-i\omega_{mn}r_*}. \tag{5.B.22}$$

Chapter 6

Conclusions and future directions

In this thesis I have given a brief summary of the current state of EMRI research. With the increasing prospects of detecting gravity waves, this already active field is growing quickly. Though in the introduction I have sketched out the work done by others in the broader problem of general orbits on a Kerr background, for the bulk of this thesis I have focused on eccentric orbits around a Schwarzschild black hole. Chapter 2 presents a review of black hole perturbation theory and associated mathematical formalism. Chapter 3 introduces some new ideas, but applied to a scalar field model problem. It is Chapters 4 and 5 that present my original research on gravitational perturbations and metric reconstruction.

6.1 Summary of original contributions

Chapter 4, which is taken from Ref. [52] contains two significant new results. The first of these is that we applied the method of extended homogeneous solutions to all radiative gravitational modes. This was an extension of the method originally introduced by Barack, Ori, and Sago [1], who used it for the monopole term of a field pulled up by a scalar charge in eccentric orbit in the Schwarzschild spacetime. Working in the frequency domain, in Regge-Wheeler (RW) gauge, the method of extended homogeneous solutions allows us to compute an exponentially convergent Fourier synthesis to obtain time domain solutions to the Regge-Wheeler and Zerilli equations at all locations, including the position of the particle. Our code allows us to compute energy and angular momentum fluxes to a high accuracy (fractional errors $\sim 10^{-12}$). Its efficiency is such that our results rival time domain

codes for orbital eccentricities approaching $e \sim 0.9$.

The second noteworthy result from Chapter 4 concerns the reconstruction of the metric perturbation from the master functions. We present the exact singular nature of the metric perturbation in RW gauge, finding that the metric perturbation amplitudes at the location of the particle are discontinuous and, in the case of some components, point-wise singular. The singular nature of the metric amplitudes apparently was not widely understood before our work. The time dependence of the singularities, of the discontinuities, and of the derivatives of the metric amplitudes are now readily computable with our code. The singularities present in RW gauge may be a challenge to attempts to compute the self-force directly in this gauge.

In Chapter 5 I address the question of how to transform the metric perturbation in RW gauge to Lorenz gauge. This is desirable because the first-order corrected equations of motion are formulated only in Lorenz gauge. Additionally, the standard mode-sum regularization procedure is designed to be used in Lorenz gauge. Lorenz gauge was chosen for these formulations because it has many nice features. (As in electrodynamics, Lorenz gauge simplifies the field equations dramatically.) For those wishing to perform time domain calculations, the Lorenz gauge field equations can be put into a fully hyperbolic form [45]. Additionally, regularization (removal of the Coulomb part of the field) is more straightforward in Lorenz gauge because it is locally isotropic. As opposed to RW gauge, the metric perturbation amplitudes are C^0 at the location of the particle and they are asymptotically flat.

Our approach to transforming the metric perturbation to Lorenz gauge follows work by Sago, Nakano, and Sasaki [54]. An elegant aspect of their approach to transforming between the two gauges is that the system of partial differential equations fully separates. Though their formulation has existed for some time, no one before this work had *actually performed* the gauge transformation. In Chapter 5, I give the current state of our work on implementing their technique. We have developed two new techniques for solving the types of equations one encounters while doing these transformations. The first is the method of partial annihilators, which entails an application of the method of extended homogeneous

solutions to higher-order differential equations. Our second new technique is the method of extended particular solutions. This is entirely equivalent to the former, but allows one to solve the types of differential equations one encounters during the gauge transformation without promoting those differential equations to higher-order. Thus far, we have fully completed the odd-parity transformation. Our results show that, as expected the Lorenz gauge amplitudes at C^0 and asymptotically flat. We have also completed part of the even-parity transformation, specifically the even-parity scalar piece. We are currently working on the even-parity divergence-free vector part of the gauge transformation.

6.2 Future directions

Following the completion of the numerical method to make the gauge transformation from RW to Lorenz, we will be capable of finding the metric to a high degree of accuracy at all locations, including the very position of the particle. Our code will be able to make such transformations for nearly arbitrarily eccentric orbits about a Schwarzschild black hole. At that point there will be several different next steps we can take.

The first step will be to compute the self-force and compare it with the results of Barack and Sago [2], derived from their time domain code. We should be able to compute conservative shifts to gauge-invariant quantities. Two such quantities are the energy and angular momentum of the particle, as functions of the observable orbital frequency. An additional observable is the eccentric orbit generalization of Detweiler's redshift invariant [46, 47]. Once the observable first-order self-force corrections have been computed in Lorenz gauge, we can examine whether any or all of these effects can be computed directly in RW gauge. This provides a powerful check on the accuracy of the transformation.

Next, we can compare first-order black hole perturbation theory calculations with post-Newtonian theory. Our work rests on an expansion in the mass-ratio between the particle and the SMBH. Post-Newtonian theory relies on an expansion in the small quantity v/c, for slowly moving bodies. In the region where these two expansions overlap, we can compare results. Further, following the work of Blanchet, Detweiler, Le Tiec, and Whiting [94] (who

worked on circular orbits), we should be able to use our results to find previously unknown post-Newtonian coefficients.

With the computation of the conservative and dissipative pieces of the self-force, one would like to evolve orbits away from their background geodesic. This is subtle task, and has not been performed in a self-consistent manner at this time. In principle, with the self-force in hand, one ought to be able to simply solve the MiSaTaQuWa equations and compute a geodesic of the perturbed spacetime. In practice, this is not straightforward.

First, Eq. (1.4.7) depends on the "tail" of the metric perturbation. The tail field is defined in Eq. (1.4.6) as an integration over the entire past history of the particle's worldline. It is not clear a priori how far back one must go in order to compute an accurate deviation from background motion.

Second, the MiSaTaQuWa equations are Lorenz gauge dependent. At first-order their gauge condition $\nabla^\nu \bar{p}_{\mu\nu} = 0$ is self-consistent with the vanishing of the divergence of the zeroth-order stress energy tensor $\nabla^\nu T_{\mu\nu} = 0$. Once the particle leaves the background geodesic, the zeroth order stress energy tensor will not be divergence free and the Lorenz gauge condition will not be satisfied. One must therefore find a way to "relax" the Lorenz gauge condition in a way consistent with the current order of perturbation theory.

Another natural extension of this work is to move to higher orders in perturbation theory. There is a practical need to go to at least second order in the mass-ratio parameter. For concreteness, consider a mass-ratio of $\mu/M = 10^{-6}$. If we evolve the particle through one orbit, the error in the phase of the particle's motion will be of order 10^{-6}. If we wish to model 10^6 orbits, which we suspect may be necessary for a LISA detection, the error in the accumulated phase will be on the order of unity. Therefore, we need to go to at least second-order in perturbation theory if we wish to have sufficiently accurate waveforms.

Astrophysical EMRI sources are expected to come from small bodies orbiting high spinning Kerr black holes. Therefore, both the long-term orbit evolution and higher-order perturbation theory discussed here will eventually have to be applied to particles moving on the Kerr background. There is much progress being made there already (e.g. [95, 26]), but the prospect of generic orbital evolution on Kerr is even more daunting than it is for

Schwarzschild. Because of this we feel that Schwarzschild will remain a worthwhile first testing-ground for some time.

Eventually, though we would like to apply our techniques to the Kerr spacetime. The traditional approach to working on Kerr (the Teukolsky formalism) is best used in the frequency domain. Additionally, given our experience with singular source terms, we feel that we should be able to solve the Teukolsky equation with a high degree of accuracy. With new features of the spacetime still being discovered [96], it promises to be a fertile area for research for some time.

Bibliography

[1] L. Barack, A. Ori, and N. Sago. Frequency-domain calculation of the self-force: The high-frequency problem and its resolution. *Phys. Rev. D*, 78(8):084021–+, October 2008.

[2] Leor Barack and Norichika Sago. Gravitational self-force on a particle in eccentric orbit around a Schwarzschild black hole. *Phys. Rev.*, D81:084021, 2010.

[3] Ryuichi Fujita, Wataru Hikida, and Hideyuki Tagoshi. An Efficient Numerical Method for Computing Gravitational Waves Induced by a Particle Moving on Eccentric Inclined Orbits around a Kerr Black Hole. *Prog. Theor. Phys.*, 121:843–874, 2009.

[4] A. Einstein, L. Infeld, and B. Hoffmann. The gravitational equations and the problem of motion. *The Annals of Mathematics*, 39(1):pp. 65–100, 1938.

[5] Susan G. Hahn and Richard W. Lindquist. The two-body problem in geometrodynamics. *Annals of Physics*, 29(2):304 – 331, 1964.

[6] B.F. Schutz. *A first course in general relativity.* Cambridge University Press, 2nd edition, 2009.

[7] Ligo home page. `http://www.ligo.caltech.edu/`.

[8] Virgo homepage. `https://wwwcascina.virgo.infn.it/`.

[9] Geo600 homepage. `http://www.geo600.org/`.

[10] M. Maggiore. *Gravitational Waves: Theory and experiments.* Gravitational Waves. Oxford University Press, 2007.

[11] C. O. Lousto and Y. Zlochower. Orbital Evolution of Extreme-Mass-Ratio Black-Hole Binaries with Numerical Relativity. *Physical Review Letters*, 106(4):041101–+, January 2011.

[12] NASA. Lisa - laser interferometer space antenna, January 2010. `http://lisa.nasa.gov`.

[13] Lisa and changes in the cosmic vision programme. `http://lisa.gsfc.nasa.gov/cosmic_vision_changes.html`.

[14] T. Regge and J.A. Wheeler. Stability of a schwarzschild singularity. *Phys. Rev.*, 108:1063–1069, 1957.

[15] F.J. Zerilli. Gravitational field of a particle falling in a schwarzschild geometry analyzed in tensor harmonics. *Phys. Rev. D*, 2:2141–2160, 1970.

[16] V. Moncrief. Gravitational perturbations of spherically symmetric systems. I. The exterior problem. *Ann. Phys.*, 88:323–342, 1974.

[17] C.T. Cunningham, R.H. Price, and V. Moncrief. Radiation from collapsing relativistic stars. i. linearized odd-parity radiation. *Astrophys. J.*, 224:643–667, 1978.

[18] C.T. Cunningham, R.H. Price, and V. Moncrief. Radiation from collapsing relativistic stars. i. linearized even-parity radiation. *Astrophys. J.*, 230:870–892, 1979.

[19] S. Chandrasekhar and S. Detweiler. The quasi-normal modes of the Schwarzschild black hole. *Royal Society of London Proceedings Series A*, 344:441–452, August 1975.

[20] S.A. Teukolsky. Perturbations of a rotating black hole. i. fundamental equations for gravitational, electromagnetic, and neutrino-field perturbations. *Astrophys. J.*, 185:635–647, 1973.

[21] Paul L. Chrzanowski. Vector potential and metric perturbations of a rotating black hole. *Phys. Rev. D*, 11(8):2042–2062, Apr 1975.

[22] Jeffrey M. Cohen and Lawrence S. Kegeles. Electromagnetic fields in curved spaces: A constructive procedure. *Phys. Rev. D*, 10(4):1070–1084, Aug 1974.

[23] Lawrence S. Kegeles and Jeffrey M. Cohen. Constructive procedure for perturbations of spacetimes. *Phys. Rev. D*, 19(6):1641–1664, Mar 1979.

[24] John M. Stewart. Hertz-Bromwich-Debye-Whittaker-Penrose Potentials In General Relativity. *Proc. Roy. Soc. Lond.*, A367:527–538, 1979.

[25] Robert M. Wald. Construction of solutions of gravitational, electromagnetic, or other perturbation equations from solutions of decoupled equations. *Phys. Rev. Lett.*, 41(4):203–206, Jul 1978.

[26] Tobias S. Keidl, John L. Friedman, and Alan G. Wiseman. Finding fields and self-force in a gauge appropriate to separable wave equations. *Phys. Rev. D*, 75(12):124009, Jun 2007.

[27] A. G. Shah, T. S. Keidl, J. L. Friedman, D.-H. Kim, and L. R. Price. Conservative, gravitational self-force for a particle in circular orbit around a Schwarzschild black hole in a radiation gauge. *Phys. Rev. D*, 83(6):064018–+, March 2011.

[28] T. S. Keidl, A. G. Shah, J. L. Friedman, D.-H. Kim, and L. R. Price. Gravitational self-force in a radiation gauge. *Phys. Rev. D*, 82(12):124012–+, December 2010.

[29] S. Detweiler. Perspective on gravitational self-force analyses. *Classical and Quantum Gravity*, 22:681–+, August 2005.

[30] Steven L. Detweiler and Eric Poisson. Low multipole contributions to the gravitational self- force. *Phys. Rev.*, D69:084019, 2004.

[31] John David Jackson. *Classical Electrodynamics*. Wiley, 1998.

[32] P.A.M. Dirac. Classical theory of radiating electrons. *Proc. R. Soc. London, Ser. A*, 167:148, 1938.

[33] E. Poisson. An introduction to the Lorentz-Dirac equation. *ArXiv General Relativity and Quantum Cosmology e-prints*, December 1999.

[34] Bryce S. DeWitt and Robert W. Brehme. Radiation damping in a gravitational field. *Annals of Physics*, 9(2):220 – 259, 1960.

[35] Steven L. Detweiler and Bernard F. Whiting. Self-force via a Green's function decomposition. *Phys. Rev.*, D67:024025, 2003.

[36] E. Poisson, A. Pound, and I. Vega. The motion of point particles in curved spacetime. *ArXiv e-prints*, February 2011.

[37] Y. Mino, M. Sasaki, and T. Tanaka. Gravitational radiation reaction to a particle motion. *Phys. Rev. D*, 55:3457–3476, 1997.

[38] Theodore C. Quinn and Robert M. Wald. Axiomatic approach to electromagnetic and gravitational radiation reaction of particles in curved spacetime. *Phys. Rev. D*, 56(6):3381–3394, Sep 1997.

[39] Leor Barack and Amos Ori. Gravitational self force and gauge transformations. *Phys. Rev.*, D64:124003, 2001.

[40] E. Rosenthal. Construction of the second-order gravitational perturbations produced by a compact object. *Phys. Rev. D*, 73(4):044034–+, February 2006.

[41] L. Barack and A. Ori. Mode sum regularization approach for the self-force in black hole spacetime. *Phys. Rev. D*, 61(6):061502–+, March 2000.

[42] I. Vega and S. Detweiler. Regularization of fields for self-force problems in curved spacetime: Foundations and a time-domain application. *Physical Review D*, 77(8):084008–+, April 2008.

[43] L. Barack and D.A. Golbourn. Scalar-field perturbations from a particle orbiting a black hole using numerical evolution in 2+1 dimensions. *Physical Review D*, 76(4):044020–+, August 2007.

[44] I. Vega, B. Wardell, and P. Diener. Effective source approach to self-force calculations. *Classical and Quantum Gravity*, 28(13):134010–+, July 2011.

[45] Leor Barack and Carlos O. Lousto. Perturbations of Schwarzschild black holes in the Lorenz gauge: Formulation and numerical implementation. *Phys. Rev.*, D72:104026, 2005.

[46] Steven Detweiler. A consequence of the gravitational self-force for circular orbits of the Schwarzschild geometry. *Phys. Rev.*, D77:124026, 2008.

[47] L. Barack and N. Sago. Beyond the geodesic approximation: Conservative effects of the gravitational self-force in eccentric orbits around a Schwarzschild black hole. *Phys. Rev. D*, 83(8):084023–+, April 2011.

[48] T. Tanaka, M. Shibata, M. Sasaki, H. Tagoshi, and T. Nakamura. Gravitational Wave Induced by a Particle Orbiting around a Schwarzschild Black Hole. *Progress of Theoretical Physics*, 90:65–83, July 1993.

[49] Curt Cutler, Daniel Kennefick, and Eric Poisson. Gravitational radiation reaction for bound motion around a schwarzschild black hole. *Phys. Rev. D*, 50(6):3816–3835, Sep 1994.

[50] Karl Martel. Gravitational waveforms from a point particle orbiting a schwarzschild black hole. *Physical Review D*, 69:044025, 2004.

[51] Roland Haas. Scalar self-force on eccentric geodesics in Schwarzschild spacetime: a time-domain computation. *Phys. Rev.*, D75:124011, 2007.

[52] Seth Hopper and Charles R. Evans. Gravitational perturbations and metric reconstruction: Method of extended homogeneous solutions applied to eccentric orbits on a Schwarzschild black hole. *Phys. Rev.*, D82:084010, 2010.

[53] C.W. Misner, K.S. Thorne, and J.A. Wheeler. *Gravitation*. Freeman, San Francisco, CA, U.S.A., 1973.

[54] N. Sago, H. Nakano, and M. Sasaki. Gauge problem in the gravitational self-force: Harmonic gauge approach in the Schwarzschild background. *Phys. Rev.*, 67(10):104017–+, May 2003.

[55] K. Martel and E. Poisson. Gravitational perturbations of the Schwarzschild spacetime: A practical covariant and gauge-invariant formalism. *Phys. Rev. D*, 71(10):104003–+, May 2005.

[56] Clifford M. Will. The confrontation between general relativity and experiment. *Living Reviews in Relativity*, 9(3), 2006.

[57] Ingrid H. Stairs. Testing general relativity with pulsar timing. *Living Reviews in Relativity*, 6(5), 2003.

[58] Ray d'Inverno. *Introducing Einstein's Relativity*. Oxford University Press, 1992.

[59] Steven Weinberg. *Gravitation and Cosmology: Principles and Applications of the General Theory of Relativity*. John Wiley & Sons, Inc, 1972.

[60] W.E. Boyce and R.C. DiPrima. *Elementary differential equations and boundary value problems*. Wiley, 2008.

[61] ESA. Esa science & technology: Lisa, January 2010. `http://sci.esa.int/science-e/www/area/index.cfm?fareaid=27`.

[62] Leor Barack. Gravitational self force in extreme mass-ratio inspirals. *Class. Quant. Grav.*, 26:213001, 2009.

[63] Adam Pound. Self-consistent gravitational self-force. *Phys. Rev.*, D81:024023, 2010.

[64] Leor Barack and Carlos O. Lousto. Computing the gravitational self-force on a compact object plunging into a schwarzschild black hole. *Phys. Rev. D*, 66(6):061502, Sep 2002.

[65] Leor Barack and Norichika Sago. Gravitational self force on a particle in circular orbit around a Schwarzschild black hole. *Phys. Rev.*, D75:064021, 2007.

[66] Leor Barack and Norichika Sago. Gravitational self-force correction to the innermost stable circular orbit of a Schwarzschild black hole. *Phys. Rev. Lett.*, 102:191101, 2009.

[67] Kostas Glampedakis, Scott A. Hughes, and Daniel Kennefick. Approximating the inspiral of test bodies into Kerr black holes. *Phys. Rev.*, D66:064005, 2002.

[68] Scott A. Hughes, Steve Drasco, Eanna E. Flanagan, and Joel Franklin. Gravitational radiation reaction and inspiral waveforms in the adiabatic limit. *Phys. Rev. Lett.*, 94:221101, 2005.

[69] Yasushi Mino. Perturbative Approach to an orbital evolution around a Supermassive black hole. *Phys. Rev.*, D67:084027, 2003.

[70] C.V. Vishveshwara. Stability of the schwarzschild metric. *Phys. Rev. D*, 1:2870–2879, 1970.

[71] S. Chandrasekhar. *The Mathematical Theory of Black Holes*, volume 69 of *The International Series of Monographs on Physics*. Clarendon, Oxford, 1983.

[72] Misao Sasaki and Hideyuki Tagoshi. Analytic black hole perturbation approach to gravitational radiation. *Living Reviews in Relativity*, 6(6):7, 2003.

[73] Carlos O. Lousto. Reconstruction of black hole metric perturbations from weyl curvature ii: The regge-wheeler gauge. *Classical and Quantum Gravity*, 22:S569, 2005.

[74] Leor Barack and Lior M. Burko. Radiation-reaction force on a particle plunging into a black hole. *Phys. Rev.*, D62:084040, 2000.

[75] Carlos F. Sopuerta and Pablo Laguna. A finite element computation of the gravitational radiation emitted by a point-like object orbiting a non-rotating black hole. *Physical Review D*, 73:044028, 2006.

[76] Lior M. Burko. Self force on particle in orbit around a black hole. *Phys. Rev. Lett.*, 84:4529, 2000.

[77] Steven Detweiler, Eirini Messaritaki, and Bernard F. Whiting. Self-force of a scalar field for circular orbits about a Schwarzschild black hole. *Phys. Rev.*, D67:104016, 2003.

[78] D. C. Champeney. *A Handbook of Fourier Theorems*. Cambridge University Press, 1989.

[79] M. J. Lighthill. *Fourier Analysis and Generalised Functions*. Cambridge University Press, 1958.

[80] C. Darwin. The Gravity Field of a Particle. *Proc. R. Soc. Lond. A*, 249(1257):180–194, January 1959.

[81] Wolfram Schmidt. Celestial mechanics in Kerr spacetime. *Class. Quant. Grav.*, 19:2743, 2002.

[82] Scott E. Field, Jan S. Hesthaven, and Stephen R. Lau. Discontinuous Galerkin method for computing gravitational waveforms from extreme mass ratio binaries. *Class. Quant. Grav.*, 26:165010, 2009.

[83] Jonathan L. Barton, David J. Lazar, Daniel J. Kennefick, Gaurav Khanna, and Lior M. Burko. Computational Efficiency of Frequency– and Time–Domain Calculations of Extreme Mass–Ratio Binaries: Equatorial Orbits. *Phys. Rev.*, D78:064042, 2008.

[84] D V Gal'tsov. Radiation reaction in the kerr gravitational field. *Journal of Physics A: Mathematical and General*, 15(12):3737–3749, 1982.

[85] Steve Drasco, Eanna E. Flanagan, and Scott A. Hughes. Computing inspirals in kerr in the adiabatic regime. i. the scalar case. *Classical and Quantum Gravity*, 22:S801, 2005.

[86] William H. Press, Saul A. Teukolsky, William T. Vetterling, and Brian P. Flannery. *Numerical Recipes in C: The Art of Scientific Computing*. Cambridge University Press, Cambridge, UK, 2nd edition edition, 1993.

[87] Kip S. Thorne. Multipole expansions of gravitational radiation. *Rev. Mod. Phys.*, 52(2):299–339, Apr 1980.

[88] Curt Cutler, Lee Samuel Finn, Eric Poisson, and Gerald Jay Sussman. Gravitational radiation from a particle in circular orbit around a black hole. ii. numerical results for the nonrotating case. *Phys. Rev. D*, 47(4):1511–1518, Feb 1993.

[89] Leor Barack and Amos Ori. Mode sum regularization approach for the self force in black hole spacetime. *Phys. Rev.*, D61:061502, 2000.

[90] P. A. Sundararajan, G. Khanna, S. A. Hughes, and S. Drasco. Towards adiabatic waveforms for inspiral into Kerr black holes. II. Dynamical sources and generic orbits. *Phys. Rev. D*, 78(2):024022–+, July 2008.

[91] A. Pound, E. Poisson, and B. G. Nickel. Limitations of the adiabatic approximation to the gravitational self-force. *Phys. Rev. D*, 72(12):124001–+, December 2005.

[92] H. Flanders. *Differential forms: with applications to the physical sciences*. Mathematics in science and engineering. Academic Press, 1963.

[93] C.M. Bender and S.A. Orszag. *Advanced mathematical methods for scientists and engineers: Asymptotic methods and perturbation theory*. Advanced Mathematical Methods for Scientists and Engineers. Springer, 1978.

[94] L. Blanchet, S. Detweiler, A. Le Tiec, and B. F. Whiting. *High-Accuracy Comparison Between the Post-Newtonian and Self-Force Dynamics of Black-Hole Binaries*, pages 415–442. Springer, 2011, 2011.

[95] S. R. Dolan, B. Wardell, and L. Barack. Self force via m-mode regularization and 2+1D evolution: II. Scalar-field implementation on Kerr spacetime. *ArXiv e-prints*, June 2011.

[96] E. E. Flanagan and T. Hinderer. Transient resonances in the inspirals of point particles into black holes. *ArXiv e-prints*, September 2010.